

PRIFYSGOL BANGOR
BANGOR UNIVERSITY

**VIRTUAL DISSECTION OF SUBCORTICAL NON-IMAGE FORMING
VISUAL PATHWAYS IN THE HUMAN BRAIN WITH DTI
TRACTOGRAPHY**

Kristin Koller

Thesis submitted to the School of Psychology, Bangor University, in partial fulfilment of the requirements for the degree of Doctor of Philosophy

September 2016
Declaration and Consent

Details of the Work

I hereby agree to deposit the following item in the digital repository maintained by Bangor University and/or in any other repository authorized for use by Bangor University.

Author Name:
Title:
Supervisor/Department:
Funding body (if any):
Qualification/Degree obtained:.....

This item is a product of my own research endeavours and is covered by the agreement below in which the item is referred to as “the Work”. It is identical in content to that deposited in the Library, subject to point 4 below.

Non-exclusive Rights

Rights granted to the digital repository through this agreement are entirely non-exclusive. I am free to publish the Work in its present version or future versions elsewhere.
I agree that Bangor University may electronically store, copy or translate the Work to any approved medium or format for the purpose of future preservation and accessibility. Bangor University is not under any obligation to reproduce or display the Work in the same formats or resolutions in which it was originally deposited.

Bangor University Digital Repository

I understand that work deposited in the digital repository will be accessible to a wide variety of people and institutions, including automated agents and search engines via the World Wide Web.

I understand that once the Work is deposited, the item and its metadata may be incorporated into public access catalogues or services, national databases of electronic theses and dissertations such as the British Library’s EThOS or any service provided by the National Library of Wales.

I understand that the Work may be made available via the National Library of Wales Online Electronic Theses Service under the declared terms and conditions of use (<http://www.llgc.org.uk/index.php?id=4676>). I agree that as part of this service the National Library of Wales may electronically store, copy or convert the Work to any approved medium or format for the purpose of future preservation and accessibility. The National Library of Wales is not under any obligation to reproduce or display the Work in the same formats or resolutions in which it was originally deposited.

Statement 1:

This work has not previously been accepted in substance for any degree and is not being concurrently submitted in candidature for any degree unless as agreed by the University for approved dual awards.

Signed (candidate)

Date

Statement 2:

This thesis is the result of my own investigations, except where otherwise stated. Where correction services have been used, the extent and nature of the correction is clearly marked in a footnote(s).

All other sources are acknowledged by footnotes and/or a bibliography.

Signed (candidate)

Date

Statement 3:

I hereby give consent for my thesis, if accepted, to be available for photocopying, for inter-library loan and for electronic repositories, and for the title and summary to be made available to outside organisations.

Signed (candidate)

Date

Statement 4:

Choose **one** of the following options

a) I agree to deposit an electronic copy of my thesis (the Work) in the Bangor University (BU) Institutional Digital Repository, the British Library ETHOS system, and/or in any other repository authorized for use by Bangor University and where necessary have gained the required permissions for the use of third party material.	
b) I agree to deposit an electronic copy of my thesis (the Work) in the Bangor University (BU) Institutional Digital Repository, the British Library ETHOS system, and/or in any other repository authorized for use by Bangor University when the approved bar on access has been lifted.	
c) I agree to submit my thesis (the Work) electronically via Bangor University's e-submission system, however I opt-out of the electronic deposit to the Bangor University (BU) Institutional Digital Repository, the British Library ETHOS system, and/or in any other repository authorized for use by Bangor University, due to lack of permissions for use of third party material.	

Options B should only be used if a bar on access has been approved by the University.

In addition to the above I also agree to the following:

1. That I am the author or have the authority of the author(s) to make this agreement and do hereby give Bangor University the right to make available the Work in the way described above.
2. That the electronic copy of the Work deposited in the digital repository and covered by this agreement, is identical in content to the paper copy of the Work deposited in the Bangor University Library, subject to point 4 below.
3. That I have exercised reasonable care to ensure that the Work is original and, to the best of my knowledge, does not breach any laws – including those relating to defamation, libel and copyright.
4. That I have, in instances where the intellectual property of other authors or copyright holders is included in the Work, and where appropriate, gained explicit permission for the inclusion of that material in the Work, and in the electronic form of the Work as accessed through the open access digital repository, *or* that I have identified and removed that material for which adequate and appropriate permission has not been obtained and which will be inaccessible via the digital repository.
5. That Bangor University does not hold any obligation to take legal action on behalf of the Depositor, or other rights holders, in the event of a breach of intellectual property rights, or any other right, in the material deposited.
6. That I will indemnify and keep indemnified Bangor University and the National Library of Wales from and against any loss, liability, claim or damage, including without limitation any related legal fees and court costs (on a full indemnity bases), related to any breach by myself of any term of this agreement.

Signature:

Date.....

Acknowledgements

Firstly, I'd like to thank my supervisor, Prof. Bob Rafal, for giving me this opportunity to obtain a PhD. Thank you for your unconditional support, particularly during the lead up to thesis submission, and for all the laughs over the years – there's never been a dull moment. Words can't express my gratitude for how much you have taught me – thanks for being a mentor, colleague and friend.

I also want to say a special thank you to members of my PhD committee, especially for sitting through a lot of committee meetings. Thanks to Dr. Paul Mullins for all the imaging support, and to Dr. Patricia Bestelmeyer, I knew your door was always open – thank you. Thanks also to Caroline and Becca who always offered a helping hand.

Thanks to Andrew Fischer and Dr. Nia Goulden for offering good company and help during MRI scanning sessions.

This research would not have been possible without the dedication of the participants that took part; your participation is very much appreciated.

A big thank you to all the MSc students that I've gotten to work with over the last few years - David, Nick, Caoife, Callam, Mike, Kevin and Chris, you will be remembered.

To all my office friends, Karolina, Therese, Alex, Maria, Oren, and Aygul – thanks for all the support and good times. I will miss you!

A big thanks to Neil – I really appreciate all your support, especially during the final weeks. Thanks also to my sister Justé, and brother in law, Graham, for your unconditional support – thank you.

Finally, I want to dedicate this thesis to my parents, Mark and Marlette. Thanks for your support and for always believing in me.

List of abbreviations

BNST	Bed nucleus of the stria terminalis
COG	Centre of gravity
CSF	Cerebrospinal fluid
DTI	Diffusion tensor imaging
FA	Fractional anisotropy
fMRI	Functional magnetic resonance imaging
LGB	Lateral geniculate body
MEG	Magnetoencephalography
MRI	Magnetic resonance imaging
OT	Optic tract
RTT	Retinotectal tract
SC	Superior colliculus
SOA	Stimulus onset asynchrony
TOJ	Temporal order judgement
VC	Visual cortex
V1	Primary visual cortex

List of tables and figures

Tables

Table 2.1. Fractional anisotropy (FA) values for RTT and isolated RTT.....	53
Table 3.1. Temporal hemifield as predictor of threat bias	78
Table 4.1. Centre of gravity (COG) of SC-amygdala	103
Table 4.2. Centre of gravity (COG) of stria terminalis	106
Table 5.1. SC-amygdala in left and right hemispheres as predictors of threat	119
Table 5.2. SC-amygdala as predictor of threat bias	119
Table 6.1. Stria terminalis as predictor of threat bias.....	129
Supplementary Table 6.1. Individual participant stria terminalis FA and threat bias scores	130
Table 7.1. Summary of main findings.....	136

Figures

Figure 1.1 The visual system: retino-geniculo-striate and extrageniculate projections.....	5
Figure 2.1. Region of interest masks for dissection of RTT and retino-geniculo-striate...	47
Figure 2.2. Sequence of stimuli presented during each trial on gap paradigm	49
Figure 2.3. Bilateral retinotectal tracts virtually dissected with DTI tractography (N=19)	50
Figure 2.4. Bilateral isolated retinotectal tract (red), retinotectal tracts (green) and retino- geniculo-striate tracts (blue) dissected with DTI tractography (N=19)	51
Figure 2.5. Composite streamlines for the retinotectal tract (RTT, red) and the isolated retinotectal voxels common to 100% of participants (yellow) virtually dissected with DTI tractography (N=19)	52
Figure 2.6. Distribution of saccade latency peaks for Participant 5 and Participant 12. ...	54
Figure 2.7. Average saccade latency measured on gap paradigm	55
Figure 2.8. Short latency saccades measured on gap paradigm.....	55
Figure 2.9. RTT FA as predictor of short latency saccades.....	56
Figure 2.10. RTT FA as predictor of short latency saccades in temporal and nasal hemifields.....	57
Figure 3.1. Examples of threatening (top) and pleasant (bottom) pictures selected from the IAPS database used for this experiment	73
Figure 3.2. Illustration of the order of events during each trial on saccade decision paradigm	74
Figure 3.3 Saccade choices to threatening and non-threatening stimuli on saccade decision paradigm.....	77
Figure 3.4. Saccade choices to temporal and nasal hemifield on saccade decision paradigm	77
Figure 3.5. Saccade latency to threatening and non-threatening stimuli on saccade decision paradigm	79

Figure 3.6. Saccades to threat with repeated stimulus exposure.....	80
Figure 3.7. Saccade latency to threat with repeated stimulus exposure.....	81
Figure 3.8. Stimulus pairs presented to participants during saccade decision task.	82
Figure 3.9. Brachium SC FA as predictor of threat bias.....	83
Figure 3.10. Brachium SC as predictor of saccade latency	84
Figure 4.1. Masks used for the virtual dissection of connectivity between the superior colliculus (SC) and the amygdala	98
Figure 4.2. Masks used for the virtual dissection of connectivity of the stria terminalis connecting the bed nucleus of the stria terminalis with the amygdala	100
Figure 4.3. Example of exclusion mask used during dissection of stria terminalis.....	100
Figure 4.4. Probabilistic tractography between the amygdala and superior colliculus in the healthy human brain (N=19)	102
Figure 4.5. Probabilistic tractography of the stria terminalis in the healthy human brain (N=19)	105
Figure 4.6. Probabilistic tractography of the stria terminalis and connection between the superior colliculus and the amygdala in the healthy human brain (N=19).....	107
Figure 5.1. Virtual dissection with DTI tractography of connections between the superior colliculus and amygdala in 19 healthy humans	118
Figure 5.2. SC-Amygdala as predictor of threat bias.....	120
Figure 5.3. Strength in connectivity of SC-Amygdala as predictors of threat bias in temporal and nasal visual hemifields.....	121
Figure 5.4. Anatomical relation between SC-amygdala and RTT pathways.....	122
Figure 6.1. Stria terminalis FA as predictor of threat bias.....	128
Supplementary Figure 6.1. Masks employed for virtual dissection with DTI tractography of the stria terminalis	131
Supplementary Figure 6.2. Threatening and pleasant stimulus pairs selected from IAPS (Lang, Bradley & Cuthbert, 1997) employed during the saccade decision task.....	132
Supplementary Figure 6.3. Stimulus presentation sequence during saccade decision task.....	133
Figure 7.1. Virtual dissection with probabilistic tractography between SC-pulvinar- amygdala of patient DG	141

Thesis Summary

This thesis presents novel evidence in support of a functional role for the anatomy of subcortical non-image forming white matter connections in the human brain. Observations of preserved ability to process threat in the absence of visual awareness in cortically blind patients suggest the existence of an older, primitive and phylogenetically conserved visual circuit that processes orientation to threat. Three pathways including the retinotectal tract, the stria terminalis and a putative pathway for processing visual threat connecting the superior colliculus and the amygdala via the pulvinar were virtually dissected with DTI tractography in healthy participants *in vivo*. Additionally, connectivity strength of dissected pathways were tested as predictors of performance on behavioural eye-tracking paradigms designed to optimise reflexive orienting responses to salient peripheral visual stimuli including abrupt onsets and threat.

Behavioural findings demonstrated a temporal hemifield advantage for short latency reflexive saccades performed within a ‘gap’ paradigm, supporting the prediction that the superior colliculus receives retinal afferents *via* the retinotectal pathway that summon reflexive saccades. Saccadic bias to orient to threatening stimuli on a temporal order saccade decision task also demonstrated an advantage in the temporal hemifield, consistent with predictions that retinal afferents to the superior colliculus contribute to a subcortical threat mediating circuit connecting the superior colliculus, pulvinar and amygdala.

Connectivity strength of anatomical demonstrations of a putative threat mediating connection between the superior colliculus, pulvinar and amygdala predicted a bias to orient to visual threat, thereby validating anatomical dissections presented here with functional evidence. Topography of the SC-amygdala pathway demonstrated a trajectory from the pulvinar to the lateral amygdala. The anatomy of the outflow of the amygdala connecting to the bed nucleus of the stria terminalis was also considered, demonstrating anatomically distinct trajectories of the two pathways despite occupying topographies in close proximity. Stria terminalis connectivity strength also predicted a bias to threat, providing novel evidence for a functional role in selective orienting to threat, potentially driven by superior-colliculus afferents to amygdala nuclei.

Table of Contents

List of abbreviations	vi
List of tables and figures	vii
Thesis Summary	ix
Chapter 1 – General Introduction.....	1
<i>Anatomy of the visual system</i>	<i>2</i>
<i>Non-image forming vision</i>	<i>6</i>
<i>Preserved reflexive properties after visual cortex destruction.....</i>	<i>7</i>
<i>Residual visual function in monkeys</i>	<i>8</i>
<i>Residual visual function in humans after V1 destruction</i>	<i>10</i>
<i>Further questions on blindsight phenomena.....</i>	<i>16</i>
<i>Implicit processing.....</i>	<i>17</i>
<i>Conscious phenomena in blindsight?</i>	<i>20</i>
<i>Affective blindsight – an unexpected finding?</i>	<i>21</i>
<i>Simulating non-conscious perception in healthy humans.....</i>	<i>22</i>
<i>Alternative perspectives: is non-conscious processing of emotion exclusive to a subcortical route?.....</i>	<i>24</i>
<i>Anatomical basis for a subcortical visual system.....</i>	<i>28</i>
<i>Diffusion tensor imaging as tool for studying anatomy.....</i>	<i>34</i>
<i>Structure of the thesis.....</i>	<i>35</i>
Chapter 2 - Saccade latency bias to temporal hemifield: evidence for role of superior colliculus in mediating reflexive saccades.....	37
<i>Abstract.....</i>	<i>38</i>
<i>Introduction.....</i>	<i>39</i>
<i>Method</i>	<i>44</i>
<i>Results</i>	<i>50</i>
<i>Discussion.....</i>	<i>57</i>
Chapter 3 - Saccade bias toward threat in a saccade decision paradigm: Connectivity evidence for a role of the superior colliculus	62
<i>Abstract.....</i>	<i>63</i>
<i>Introduction.....</i>	<i>64</i>
<i>Method</i>	<i>72</i>
<i>Results</i>	<i>76</i>
<i>Discussion.....</i>	<i>85</i>

Chapter 4 - Anatomical relationship between the stria terminalis and a pathway connecting the superior colliculus and the amygdala in humans: virtual dissection with DTI tractography	92
<i>Abstract</i>	93
<i>Introduction</i>	94
<i>Method</i>	96
<i>Results</i>	101
<i>Discussion</i>	108
Chapter 5 - Structural connectivity of connection between the superior colliculus and amygdala in humans predicts bias in orienting toward threat	114
<i>Abstract</i>	115
<i>Introduction</i>	115
<i>Method</i>	116
<i>Results</i>	117
<i>Discussion</i>	122
Chapter 6 - Stria terminalis structural connectivity in humans predicts bias in orienting toward threat	124
<i>Abstract</i>	125
<i>Introduction</i>	126
<i>Methods and Results</i>	127
<i>Conclusion</i>	129
<i>Supplementary information</i>	130
Chapter 7 – General Discussion.....	134
<i>Role of retinal projection to SC in mediation of reflexive saccades</i>	135
<i>Role of SC in predicting saccade bias to threat</i>	138
<i>Anatomical relationship between SC-amygdala and BNST-amygdala connections</i>	139
<i>Linking SC-amygdala pathway function with anatomy in the healthy brain</i>	142
<i>Consideration of stimuli used in saccade decision task</i>	143
<i>A novel role of the stria terminalis in selective orienting to threat</i>	144
<i>Directions for future research</i>	145
<i>Concluding remarks</i>	146
References.....	147
Appendix	
<i>Appendix A. Participant study information sheet</i>	163
<i>Appendix B. Participant consent form</i>	167
<i>Appendix C. Bangor Imaging Unit MR safety screening questionnaire</i>	169
<i>Appendix D. State-Trait Anxiety Inventory (STAI)</i>	171

CHAPTER 1

GENERAL INTRODUCTION

This thesis investigates the anatomy of white matter circuits that have been implicated in processing visual stimuli not consciously perceived. Conscious visual experience is predominantly mediated by visual neocortex from retinal ganglion cell input processed in the lateral geniculate nucleus of the thalamus. However, primitive animals with little forebrain such as amphibians rely more heavily on retinal ganglion projections to subcortical structures such as the optic tectum, homologue to the superior colliculus in humans, for visual orienting. Evidence of orienting to unseen visual stimuli, in particular threatening stimuli, in cortically blind humans and monkeys has suggested that a subcortical processing system may mediate visually triggered responses in absence of the primary visual cortex. This may suggest that a subcortical route in humans is phylogenetically conserved to optimise rapid orienting in challenging environments, given a bold evolutionary assumption that vision in man is analogous to vision in monkey. Undoubtedly controversial, and certainly not without unresolved criticism, the literature presents a strong and provocative case for a subcortical route of visual processing.

In my examination of this complex phenomenon, the anatomy of the visual system will be reviewed briefly first. The concept of non-image forming vision and blindsight will be introduced next, and the literature on residual visual function in humans and monkeys post damage to the primary visual cortex will be reviewed. Next, the measurement of ‘unseen’ visual stimuli through the manipulation of sensory or attentional awareness in healthy humans will be reviewed briefly. The following section will review the anatomy of proposed subcortical visual circuits, followed by an introduction of diffusion tensor imaging tractography as a tool to study anatomy of the brain that is employed in this thesis research. Finally, the introduction will conclude with an outline of the structure of the thesis.

Anatomy of the visual system

The eye receives visual information through cells in the retina; retinal ganglion rod and cone cells which are receptive to high intensity wavelengths and low intensity illumination of light, respectively. Additionally, some ganglion cells are themselves sensitive photoreceptor cells containing the photo-pigment melanopsin, serving a non-image forming role in setting the circadian sleep-wake rhythm via projections to the suprachiasmatic nucleus of the hypothalamus (Lucas, Douglas & Foster, 2001; Morin, Blanchard & Provencio, 2003; Neuenhuys, Voogd & van Huijzen, 2008), commonly referred to as the circadian ‘body clock’. Axons from retinal ganglion cells form a myelinated nerve bundle exiting the posterior pole of the eye towards the brain by forming the optic nerve. The optic nerve axons

partially decussate in the optic chiasm, with fibres from the nasal half of the retina crossing to the opposite hemisphere, and the fibres from the temporal half of the retina remaining uncrossed (Van Essen, Newsome, & Maunsell, 1984). After crossing at the chiasm, the myelinated ganglion nerve bundles form the optic tracts, predominantly projecting fibres that terminate at the lateral geniculate nucleus (LGN) in the thalamus.

The LGN is a laminated concave cellular nucleus in the thalamus, consisting of six layers. Magnocellular (M) layers form the first two layers consisting of large cells at the origin of the LGN concave centre, and parvocellular layers (P) form the remaining third to sixth layers consisting of small cells. Intercalated small cell koniocellular (K1-K6) layers exist below each of the main LGN layers (see Figure 1.1). Retinal fibres project to the contralateral LGN layers M1, P4 and P6 and ipsilateral LGN layers M2, P3 and P5. Similarly, koniocellular layers receive projections from the retina that projects to its overlying M or P layer (Neuwenhuys et al., 2008). After termination of retinal fibres at the LGN, efferent projections form the optic radiations, terminating at the primary visual cortex (V1).

The primary visual cortex is often described in the literature using interchangeable terms including calcarine cortex, due to its position relative to the calcarine fissure that separates its upper and lower banks on the medial surface of the occipital lobe, and striate cortex, due to its highly characteristic micro-layer of myelinated fibres (the line of Gennari) situated in the layer of cortical layer IV. In addition to retinal projections via the LGN, several extra-geniculate subcortical routes exist. Instead of terminating at LGN, some fibres project to the superior colliculus, pulvinar nucleus of the thalamus, pretectal nuclei and the hypothalamus. This thesis focuses on the anatomy and function of extrageniculate visual pathways, which will be discussed in greater detail later.

The projections from the retina to primary visual cortex follow fixed termination points, some of which are presented in Figure 1 below (reviewed in Neuwenhuys et al., 2008; Van Essen et al. 1984; Van Essen, 2004; Inouye, 1909; Inoye, 2000):

1. Due to the partial crossing of retinal fibres, taking place at the optic chiasm, each half of the visual field is represented in the opposite occipital lobe. For example, the left half of the visual field is represented in the right occipital lobe, and vice versa. Furthermore, under binocular viewing conditions, the right half of the visual field projects onto the nasal hemi-retina of the right eye and the temporal hemi-retina of the

left eye, both of which project to the left occipital lobe, and vice versa for the left visual field. Additionally, retinal projections from each eye are represented in both occipital hemispheres. For example, when the left eye is patched the right eye ‘sees’ information from both the left and right visual hemi-fields. Information in the right visual hemi-field is termed the temporal visual hemi-field and projects onto the nasal hemi-retina, and information from the left visual field is termed the nasal visual hemi-field and projects onto the temporal hemi-retina. In turn, the temporal hemi-retina projects to the contra-lateral occipital lobe, in this case the left occipital lobe, and the nasal hemi-retina projects to the ipsi-lateral occipital lobe, in this case the right occipital lobe. If viewing with the left eye, the opposite terms apply; the left visual field is the temporal visual hemi-field projecting to the nasal hemi-retina, and the right visual field is the nasal visual hemi-field projecting to the temporal hemi-retina. Thus the terms temporal and nasal are defined by viewing field of the eye.

2. For each visual field, the upper quadrant is represented in the lower banks of the contralateral calcarine sulcus, and the lower quadrant is represented in the upper bank of the calcarine sulcus.
3. Figure 1.1 illustrates how projections of the contra-lateral (red) and ipsi-lateral (black) retina remain as separate layers in the lateral geniculate body (LGB) and in the striate cortex (arrows): the central visual field is represented posteriorly in the visual cortex (1), the monocular visual field is represented anteriorly in the visual cortex (3) and the binocular peripheral visual field (2) is located intermediate between the anterior and posterior regions of the visual cortex.
4. Extrageniculate projections to the superior colliculus (SC) and pulvinar nucleus of the thalamus are shown in Figure 1.1. Additionally, koniocellular layers of LGB project to the middle temporal visual area (MT) bypassing V1. They also project to the superficial layers of the SC and layer 1 of V1, and also receive input from the SC (Hendry & Reid, 2000).

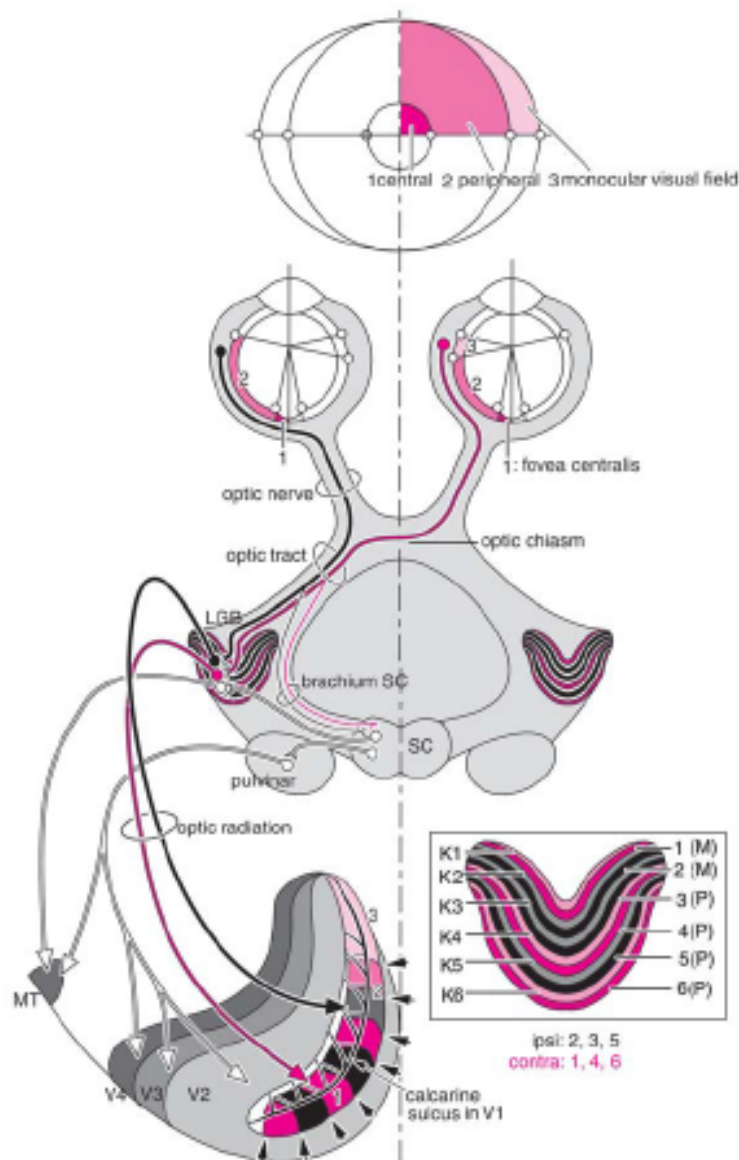


Figure 1.1 The visual system: retino-geniculo-striate and extrageniculate projections. MT, medial temporal visual area, V1-V4, visual cortical areas V1-V4, LGB, lateral geniculate body, K1-K6, koniocellular layers, M1-M2, magnocellular layers, P3-P6, parvocellular layers, (Neuwenhuys et al., 2008, pg. 758, Figure 19.3).

Retinal projections to LGN are segregated in such a way that it is possible to distinguish different functional streams based on retinal ganglion cell types in visual information processing. Parvocellular (P) layers in the LGN give rise to the parvocellular visual stream, a slow-processing system carrying both chromatic and achromatic information (Neuwenhuys et al., 2008). This system comprises of neurons that emanate from retinal ganglion cells that have small receptive fields and that are characterised by high spatial resolution and transmit nerve impulses slowly (Tamietto & de Gelder, 2010). Magnocellular

(M) layers in the LGN give rise to the magnocellular visual stream, a fast system employing cells involved with achromatic contrast detection and motion perception. The magnocellular system comprises of neurons emanating from retinal ganglion cells with large receptive fields, characterised by low spatial resolution (Tamietto & de Gelder, 2010). Once visual information has reached the primary visual cortex, two major visual processing streams emerge. The dorsal visual stream, occupying the occipito-parietal region transmits visuo-spatial information to the parietal lobe and the medial temporal lobe (MT). The ventral visual stream, occupying the occipito-temporal region, relays information about object properties to the ventral temporal lobe.

Non-image forming vision

The concept of vision that is non-image forming has been extensively reported in neuropsychological streams of research often described as ‘non-conscious’ or ‘implicit’ processing of visual stimuli. As previously mentioned, non-image forming vision involves anatomical circuits projecting from the retina to subcortical structures, instead of projecting to the primary visual cortex via the lateral geniculate nucleus of the thalamus. Subcortical structures such as the superior colliculus, the pulvinar and the amygdala nucleus have been demonstrated to play various roles in processing ‘unseen’ visual signals. Non-image forming vision refers to visual processes that are image-independent. For example, luminance signals used in circadian regulation or motion signals that mediate the optokinetic reflex (Ter Braak, Schenk and Vliet, 1971). Another example is the Riddoch effect, eliciting the phenomenal experience of motion in the absence of an image (Riddoch, 1917).

Evidence of un-seen visual processing has been provided by studies carried out in patients with lesions to the primary visual cortex. Such patients are able to discriminate between emotional and neutral facial expressions above chance, despite being unaware of what they are seeing, a phenomenon termed blindsight. The term ‘blindsight’ has been classically defined as the ability of clinically blind patients to detect, localise and discriminate visual stimuli in the absence of phenomenal visual awareness (Sanders, Warrington, Marshall, & Wieskrantz, 1974; Weiskrantz, Warrington, Sanders, & Marshall, 1974). Blindsight occurs when the primary visual cortex is partially or wholly lesioned, yet the residual parts of the visual system continue to function. Specifically, it has been suggested that some types of ‘residual vision’ are driven by a primitive, phylogenetically older subcortical visual system inherited from our early predecessors that functions independently of the newly evolved primary visual cortex.

The blindsight phenomenon has sparked much debate in the past four decades amongst scientists and philosophers with several controversies remaining unresolved. The root of the challenge in defining blindsight centers around the dependency on blind patients to report specifics about what, where and how they are ‘seeing’ objects in their blind field, that they do not experience as ‘seeing’, revealing the unavoidable oxymoronic nature attached to measuring this phenomenon. The literature reports challenges of distinguishing conscious from non-conscious vision, often pre-empted by the manipulation of forced-choice versus graded subjective measures of visual consciousness. Additionally, it highlights the ambiguity in comparing similarities between blindsight and normal vision. Despite such challenges in the study of blindsight, the blind that can ‘see’ continue to pique our scientific quest to pinpoint the neural basis and behavioural characteristics of blindsight.

Preserved reflexive properties after visual cortex destruction

Early accounts on visual function suggested that destruction of the visual cortex and optic radiations resulted in absolute blindness, with regions of destruction resulting in absolute blindness in corresponding visual field areas or visual ‘scotomas’ (Teuber, Battersby & Blender, 1960, Holmes, 1918). However, studies in soldiers with injury to the occipital lobe hinted that some form of residual visual function were possible. For example, Riddoch (1917) suggested that visual perception were possible due to the ability of patients to detect movement in their blind field. Such studies highlighted the ambiguity in determining visual function post-occipital destruction with the challenge being where absolute blindness ends and visual function begins. Despite the lack of agreement on whether ‘residual vision’ existed, the survival of reflexive responses to visual stimulation, mostly via light, remained relatively unquestioned due to evidence provided from experiments in both humans and monkeys prior to the birth of blindsight. For example, despite blindness in absence of visual cortex, patients are still able to elicit pupillary light reflexes in response to light (Magoun, 1935) and able to discriminate between sudden changes in room darkness/brightness (Brindley, Gautier-Smith, & Lewin, 1969). This is due to the survival of a brainstem reflex pathway from the eye to pretectum, mediating visual processing independent of visual cortex. This comprises a network of connections between retinal ganglion cells from the eyes and regions of the pretectal area including the olivary pretectal nucleus and the oculomotor nuclei (Neuwenhuys et al., 2008).

In addition to the preserved pupillary light reflex, similar evidence has been demonstrated for the eye blink reflex in response to bright light (Bender & Krieger, 1951)

and for the preserved ability of the eyes to track moving visual targets via brief saccades to maintain smooth visual pursuit, termed optokinetic nystagmus (Ter Braak, Schenk, & Vliet, 1971; Van Hof-Van Duin & Mohn, 1983). Ter Braak, Schenk and Vliet (1971) presented a case of a patient with complete bilateral damage to the striate cortex and lateral geniculate nuclei, demonstrating leftward OKN in response to a rightward moving cylinder, despite denying seeing any movement. However, Cowey (2010) noted that residual OKN may be controversial since, although OKN persists after unilateral brain damage (e.g. Braddick et al, 1992, Heide et al, 1990), OKN in complete cortical blindness as described by ter Braak, Schenk & Vliet (1971) has not been replicated in other studies (Brindley, Gautier-Smith & Lewin, 1969; Perenin, Ruel & Hecaen, 1980; Perenin, 1991).

Evidence for a phylogenetic subcortical network as a candidate processing system for residual visual function has been supported by evidence of increased preserved residual function post ablation of V1 in non-human primates. Similar to findings in humans, reflexive properties are also preserved in monkeys with lesion to V1. For example, Kluver (1941) demonstrated preserved visual blink and pupillary reflexes in response to bright light in monkeys with near complete destruction of V1. Furthermore, Pasik and Pasik (1982) reported intact OKN in monkeys 6 months after complete ablation of V1. Such findings in non-human primates informed our understanding of residual visual function in relation to its putative subcortical mediated network.

Residual visual function in monkeys

Before the first observations of blindsight in humans, several studies carried out in monkeys provided evidence for residual visual function after total destruction of V1. For example, preserved ability to discriminate between visual stimuli (Kluver, 1941; Pasik & Pasik, 1982), orientation (Keating, 1975), brightness (Schilder, Pasik & Pasik, 1971) and luminous flux (Kluver 1941; Schilder et al. 1971).

Several studies have provided reports of residual ability to discriminate between wavelengths. For example, Schilder et al. (1972) reported that after total ablation of V1, monkeys were able to relearn red versus green target discrimination despite substantial and randomized variation in the intensity of broadband (high-speed) stimuli. However, in contrast to this finding, Lepore, Cardu, Rasmussen and Malmo (1975) were unable to demonstrate wavelength discrimination in monkeys, criticizing Schilder, Pasik and Pasik's (1972) methodology for lacking appropriate prevention of flux cues in their wavelength discrimination task. However, Keating (1975) argued that their findings of wavelength

discrimination in monkeys trained to discriminate between blue and yellow wavelengths, *via* tasks that measured the angular velocity of moving stimuli in addition to reaching towards light, confirmed that monkeys lacking striate cortex preserved the ability to discriminate wavelengths, independent of luminance or total luminous flux. On the other hand, Cowey et al. (1998) argued that if the spectral sensitivity of monkeys lacking V1 is shifted towards scotopic levels, even a photometer would be able to register the longer-wave length stimuli (red) as dimmer than the green, and the green as dimmer than the blue, with the exception of the physically dimmest longer-wave stimulus. An early study by Malmö (1966) demonstrated that after ablation of V1, the peak spectral sensitivity under light adaptation was near identical to those under dark-adaptation. Furthermore, a study by Humphrey (1974) showed that Helen, a cortically blind monkey, was unable to discriminate between red and green wavelengths, when the brightness of the green stimuli was adjusted equivalent in luminance to the red stimulus, arguing for the inability for wavelength discrimination to exist independent of intensity. In contrast, Cowey and Stoerig (1999) demonstrated a tendency for a shift in peak wavelength luminance sensitivity at low illumination in hemianopic monkeys. However this difference in findings could be attributed to the fact that monkeys in previous studies had extensive lesion to the occipital lobes extending beyond V1 and into extra-striate areas.

In addition to evidence for wavelength discrimination, there has also been evidence for shape and pattern discrimination. For example, Weiskrantz (1963) studied a 4.5-month young monkey with bilateral removal of the striate cortex and some spared anterolateral geniculate nucleus cells. Weiskrantz (1963) reported successful discrimination between stimuli when there was a difference in the contour length of the stimuli, even when the luminance flux was equal. However, this finding has been challenged by subsequent studies demonstrating the near inability of cortically blind monkeys to perform well on shape discrimination tasks. For example, Dineen and Keating (1981) showed that only 3 out of 5 monkeys were able to discriminate at 80% correct between shapes when contour, shape of sub elements and number of corners were varied. This finding supports the finding from Weiskrantz (1963), but also presents the question of why this assumed 'shape perception' does not easily occur in all monkeys, and whether there may be hidden underlying mechanisms driving such effects. Furthermore, Pasik, Pasik and Schilder (1969) and Pasik and Pasik (1982) demonstrated that shape discrimination at 90% correct in monkeys with V1 ablation was only relearned after several 1000 trials, and only when shapes remained in the same orientation. That is, a triangle was only discriminable from a circle if it maintained the

same orientation throughout the experiment. Since the monkey studied in Weiskrantz (1963)'s study was much younger in comparison to adult monkeys from the other studies, it is possible that shape perception was more easily demonstrated in Weiskrantz's (1963) experiment due to differences between younger and older monkeys. Such findings collectively do not refute the idea that monkeys are able to perform shape discrimination in absence of V1; however the difficulties that accompany such findings do raise the question of whether this is truly a non-conscious visual response.

Studies of residual visual ability informed scientists of how powerful the visual system could be, even in absence of its assumed chief component, the visual striate cortex. However, studies demonstrating motion perception, shape perception and shape discrimination demonstrated concrete rather than abstract or subjective vision that led Humphrey (1974) to propose the idea of stimulus salience in blindsight. Humphrey's destriated monkey, Helen, was unable to discriminate between different target shapes if the discriminability of each of the shapes were matched, demonstrating that if the salience or 'eye catching' characteristic in two different shapes were the same, they were indistinguishable to Helen's destriated brain. Such studies in monkeys opened the door to hypothesising the existence of residual visual capabilities in humans, which led to the discovery of 'blindsight'.

Residual visual function in humans after V1 destruction

As aforementioned, damage to V1 classically results in loss of vision in the corresponding damaged portion of the visual field. However, since the visual cortex is not the only recipient of input from the retina via the LGN, it is surprising that even a high contrast light presented to the corresponding damaged visual field is nevertheless unseen by human patients (Richards, 1973). Furthermore, lower primates, carnivores and rodents demonstrate preserved visual function via subcortical areas such as the superior colliculus and the pretectum, rendering it questionable as to why this was not previously readily shown in humans (Richards, 1973). As mentioned previously, it was evident that some residual visual function remained after V1 removal in the form of reflexive function including pupillary responses to light, blink reflexes and optokinetic nystagmus. Even though some findings from such studies suggested that some ability to detect changes in illumination of large portions of the visual field were possible, it remained unclear whether this may in fact merely have been due to preserved reflexive properties (Richards, 1973).

In moving towards establishing residual visual abilities in humans post-ablation of V1, Richards (1973) demonstrated that blind patients were able to discriminate stereoscopic disparity of dark flashes of stimuli in their blind scotoma. Under forced-choice conditions, patients with lesion to V1 were required to choose whether a target stimulus was convergent (near) or divergent (far) in relation to a central fixation plane. As initially predicted by Richards, patients were unable to discriminate between near and far stereoscopic disparity in their blind field, with the exception of two out of nine patients, in whom lesion to V1 was the least extensive and therefore to be interpreted with caution. Interestingly, however, patients were able to perform such stereoscopic disparity discrimination between targets in front of versus behind the fixation plane reasonably above chance during monocular but not binocular viewing. Monocular viewing conditions allow for the isolation of visual function that is processed via a pathway that projects to subcortical regions, and not to V1 via LGN. Therefore, Richards (1973) argued that the finding from their study indicates the dependence on a subcortical route for processing vision when the V1 is absent. Despite the successful demonstration of residual vision, the residual stereoscopic vision in the monocular blind field reported here was not clear enough to convince sceptics, and is often not cited. Furthermore, the stimuli employed during this experiment were complex and perhaps not ideal to demonstrate residual visual function. Nonetheless, Richards' (1973) study scratched the surface on a host of experiments that defined what we now call blindsight, which followed suit. Richards (1973) concluded that some form of residual vision remains after V1 damage, and that the nature of such residual visual discrimination has the properties of a primitive stereoscopic mechanism that ignores the sign of stereoscopic stimulus disparity.

Prior to the early seventies, some forms of residual visual function had been established. For example, it was clear that after ablation of V1, reflexive responses including pupillary and blink responses to light, and OKN, in addition to some abstract forms of residual ability to detect motion via light flickering and stereoscopic disparity remained preserved in the blind field. In the monkey brain, which relies heavily on a primitive subcortical visual system, independent of the V1 equivalent area 17, several more convincing residual visual abilities had been demonstrated. Such findings provided strong motivations among researchers to investigate residual visual function in humans. Two key studies were conducted that provided evidence that the residual visual capabilities after V1 removal were greater in humans than previously thought.

The first was a study conducted by Pöppel, Held, & Frost (1973) reporting evidence for the processing of information about the locus of light stimuli presented in blind areas of

the visual field. Their experimental paradigm included a lesion-specific meridian for each individual patient's blind field, with monocular visual targets presented at angular distances from the centre of gaze. Four patients with intact foveal vision, and each with a deficit in one of the four quadrants of the visual field, were asked to saccade towards the position where the light flashed. Simultaneous with target onset, was an auditory 'click' to cue participants to saccade towards the light, since they were otherwise blind to target onset. Pöppel et al. (1973) reported that some patients found the testing experience puzzling, asking the same question that has been puzzling to researchers for centuries: "How can I look at something I haven't seen?" (Pöppel, Held, & Frost, 1973, pp. 295). Their findings showed that patients were clearly unable to identify the correct position of the targets. However, an interesting pattern of saccade magnitude was observed, with the smallest displacement of eye movements observed for targets closest to the central fixation, and larger displacement observed for targets at larger eccentricities. This effect was however limited to a 30° radius beyond which smaller saccade displacements were favoured. Rigorous combinatorial and x2 analyses demonstrated that this effect was not by chance and was seen for all four patients ($p < .0001$).

A lack of demonstration of this effect in control patients with retinal scotomata (as opposed to cortical scotomata of the initial four patients), demonstrated that the effect was not purely due to intensity discrimination of scattered light. Furthermore, in absence of the auditory 'click' cue, the effect was also absent, along with no report of patients 'sensing' the presence or absence of the target light. Consistent with prior studies, Pöppel et al. (1973) argued that the observed effect was mediated by a functional central visual mechanism driven by the midbrain. They also provided an alternative explanation, suggesting that an undetected form of dissociation of visual function exists in the damaged V1, which is not measurable by the ordinary perimetry. The findings from this study, due to its robust and clear demonstration of residual visual function provided convincing evidence to support the claim that it was possible for patients to rely on mechanisms that do not involve V1 to elicit responses to visual targets without 'seeing'.

Following the study by Pöppel et al. (1973), the second key study that coined the definition of 'blindsight' was a study published on two occasions by Weiskrantz et al. (1974) and Sanders et al. (1974), which provided evidence in favour of the idea that preserved vision post removal of V1 was greater than previously expected in man. Pöppel et al. (1973) demonstrated that 34 year-old DB, with a restricted lesion to the upper right occipital lobe causing a hemianopia in his left visual field, was able to accurately localise visual stimuli in the blind field. Through a series of tasks carried out by patient DB, this work provided key

residual visual characteristics to the working definition of blindsight. The first was a weak correlation between target position and saccade size to target fixation position for stimulus locations smaller than a 30° radius, confirming Pöppel et al. (1973)'s finding. When presented with small circles of light of 2° eccentricity for three seconds in the blind field along a horizontal meridian, patient DB did not saccade to the stimulus location accurately, however performed saccades according to their proximity of target location. For example, for targets smaller than a 30° radius, the target closest to fixation yielded the smallest saccade amplitudes and the target furthest away from fixation yielded the largest saccade amplitudes. Secondly, DB performed the same task with surprising accuracy when instead, of guessing target location with saccadic eye movements, guessed by reaching with his finger, with increased performance for larger circles of light. Thirdly, DB performed near perfect in discriminating between vertical and horizontal lines presented directly on-screen for 125 ms for line stimuli greater than 8° from fixation. For discrimination at shorter stimulus duration of 62.5 ms, DB also performed above chance. Similarly, in a fourth experiment, DB performed well in discriminating 'X' from 'O' stimuli, except for stimuli between 5° and 10° of their vertical limit. However, although still excellent, DB's performance was not as striking as discrimination between vertical and horizontal lines, performing above chance for stimuli presented for 250 ms and at chance for stimuli presented at 62.5 ms. Furthermore, in an experiment measuring what the authors termed 'minimal separable acuity', where moiré patterns allowed for presentation of grated lines varying in width, DB demonstrated a reliable performance in guessing whether lines were present or not, with increased correct responses made for lines of larger width. Finally, DB demonstrated promising residual capabilities in discriminating green from red spots. However the authors reported technical difficulties in stimulus control rendering this intriguing finding not yet conclusive.

Findings from reports by Weiskrantz et al. (1974) and Sanders et al. (1974) provided the first conclusive evidence of blindsight in humans. Their evidence demonstrated that in the absence of V1, it is possible for humans to locate visual targets with substantial accuracy, including the capacity to partly distinguish spatial distribution and orientation of stimuli, whilst denying 'seeing' said stimuli. Studies by Weiskrantz et al. (1974) and Pöppel et al. (1973) were the first to mark the transition from viewing residual visual function as merely leftover mechanical apparatus allowing spared reflexive motor properties, to blindsight, a phenomenon of 'seeing without seeing' operated by a part of the brain, that does not require an intact V1. However, these studies provided evidence from a small number of patients, with very specific lesions that represented an absence of V1. Furthermore, even though

performance on blindsight experiments were impressive, they still remained above chance for complex tasks such as determining separable acuity, discriminating simple shapes and red and green colour discrimination. Despite such breakthrough reports, many questions concerning blindsight remained unanswered, which will be reviewed shortly.

Thus far, the distinguishing features of blindsight have been that stimuli were not consciously seen and that discrimination was (at least partially) preserved when occurring under forced-choice conditions. For example, blindsight was considered to be present when a patient responded at statistically above chance under forced-choice conditions, in the absence of conscious visual awareness. The initial breakthrough blindsight defining studies by Weiskrantz et al. (1974) and Pöppel et al. (1973) ignited rapid interest in the study of blindsight. For example, Perenin and Jeannerod (1975) demonstrated that blindsight patients with post-geniculate lesions could accurately locate unseen stimuli via finger pointing, whereas pre-geniculate lesioned patients could not. Furthermore, Blythe, Kennard, and Ruddock (1987) demonstrated residual vision post damage to striate cortex in 5 patients who successfully located light targets presented in the scotoma. However, this effect was only present in 5 out of 25 patients with striate cortex damage. Weiskrantz (1987) presented a follow up case of patient DB who initially demonstrated preserved visual ability to discriminate between lines of different orientation in the frontal plane. Additionally, DB demonstrated an ability to detect stimuli in his scotoma, which could not be due to stray light falling upon the intact visual field due to the use of optic discs as control for diffusion of light into the intact visual field. DB could discriminate two forms with large cue differences more readily compared to small cued component differences, and was unable to discriminate shapes above a 75% correct threshold when cued components were eliminated by the use of Efron figures as stimuli (See Stoerig & Cowey, 1997). However, DB was unable to discriminate between two forms with different orientations when presented simultaneously in his scotoma (Weiskrantz, 1987).

Perenin and Rosetti (1996) further demonstrated that successful form orientation discrimination was specific to grasping and reaching responses in a hemianopic patient, compared to verbal and manual finger or wrist pointing. Visuo-motor grasping and reaching systematically correlated with form size and orientation, whereas verbal and manual responses performance was at chance. Perenin and Rosetti's (1996) data provided evidence for separate visual pathways in humans controlling visuomotor orientation transformation vs. visual identification, the former of which may be V1 independent.

Blindsight patients also demonstrated the ability to discriminate stationary and moving stimuli that were randomly interleaved within blank trials (Magnussen & Mathiesen, 1989; Stoerig & Pöppel, 1986; Stoerig, 1987; Stoerig & Cowey, 1989; Stoerig, Hübner, & Pöppel, 1985). Additionally, blindsight patients could discriminate target displacement (Blythe et al., 1987), wavelength (Stoerig, 1987; Stoerig & Cowey, 1992) and motion direction (Barbur, Ruddock, & Waterfield, 1980; Perenin, 1991).

The literature refers to the methods described above as direct assessment, which requires the patient to respond directly in a yes/no or some other forced choice manner, to a visual target confined to the visual defect. However, the use of such direct assessment introduces the risk of response bias. For example, if a patient is asked to respond either 'yes' or 'no' in response to a visual target, Cowey (2010) notes that the patient's response is dependent not only on the sensitivity to detect the target, but additionally on the independent tendency to select one response more than the other, thereby introducing a biased response. The use of signal detection paradigms (Green & Swets, 1966) has been used in attempt to control for such response bias whilst measuring non-conscious responses to visual stimuli presented in the patient's blind field. Signal detection analysis allows for the breakdown of responses into response proportions to the signal, including hits and misses, and response proportions to noise, including false alarms and correct rejections (Macmillan, 2002). Accordingly, the true sensitivity of observer responses is reflected not in the total correct responses to the signal, but instead in the difference between the means of the two distributions, i.e. the difference between the hit and false alarm rates (Macmillan, 2002).

Using a signal detection paradigm, Stoerig et al. (1985) showed that a patient with lesion to the visual cortex demonstrated above chance sensitivity to detect a light signal. The study was carried out on a patient with a partial left visual field hemianopia due to an infarction of the posterior, right occipital lobe, sparing parts of the primary visual pathway. Following an auditory cue, the patient made 'yes' or 'no' responses indicating whether a visual target appeared in any of five locations including 20', 30', 40' and 50' eccentricity on the 180° meridian, and 14' eccentricity on the 195° meridian, constituting the patients equivalent blind spot position in the scotoma. Receiver operating curves (ROC) for each position showed that the patient performed above chance discrimination between target and non-target trials for positions 20', 40' and 50' along the horizontal meridian. Better target discrimination at more peripheral eccentricities was not merely the result of a learning effect, since the patient showed no time-related improvement regardless of retinal position. The patient further performed poorly at detection in the blind spot. The authors noted that this is

an important finding showing that the failure to respond to targets in the blind spot whilst responding to targets in the other positions, demonstrates that performance was mediated by functions in the blind field. The absence of blindsight in the blind spot obviates the objections of Campion, Latto and Smith's (1983) that such blindsight phenomena are merely due to scattered light falling onto unimpaired parts of the visual field. Stoerig et al. (1985) confidently ruled out the light scatter hypothesis after taking into account that discrimination was best for peripheral targets requiring more eccentric retinal positions, which were the positions farthest away from the border of the functional visual field and hence the least likely to receive signal from scattered light, in addition to the use of small visual targets no larger than two log units above background luminance rendering influence from light scatter highly unlikely.

Following up from the above mentioned finding from Stoerig, Hübner & Pöppel's (1985) study showing better visual discrimination for more eccentric targets, Stoerig & Pöppel (1986) conducted a similar experiment on five patients with post-geniculate lesions to the primary visual cortex. Using a signal detection paradigm, Stoerig and Pöppel (1986) presented small visual targets to the patients at three different retinal positions; a central target, an eccentric target and a target within the natural blind spot of the scotoma. The target in the natural blind spot served as control for visual function as a result of light scatter onto the retina. Four of the patients demonstrated target detection, however exclusively at the eccentric position, and demonstrated no detection for the location in the blind spot. The fifth patient's visual cortex lesion was due to traumatic injury and was in the anterior portion of the visual cortex, as opposed to vascular injury in the remaining patients, leading to posterior primary visual cortex damage. The difference in lesion location may explain the lack of detection observed in one patient. Overall, these findings correspond with Stoerig et al.'s (1985) study, showing that the observed residual visual function is not merely due to light scatter onto the retinal field, which would be expected if detection was present in the blind spot. The authors conclude that residual target detection in such patients are dependent on target eccentricity, and is not caused by light scatter onto the retina.

Further questions on blindsight phenomena

Despite groundbreaking studies claiming that residual vision was possible in the blind, several discrepancies remained. As mentioned, Campion et al.'s (1983) experiments presented a strong case against a 'blindsight phenomenon', suggesting instead that residual visual abilities were merely the result of scattered light onto the retina, or due to intact remnants of

the striate cortex. Campion et al. (1983) showed that hemianopic patients could respond to a bright target in a scotoma in the blind peripheral hemi-field by seeing light that has been reflected from the patients nose. King, Azzopardi, Cowey, Oxbury and Oxbury (1996) controlled for light scatter by testing patients with a half-patch placed across the blind hemi-retina, thereby separating light scatter falling on the normal retina, from light falling on the blind retina. In this study, four hemispherectomized patients demonstrated blindsight that was purely as a result of light scattered onto the normal hemi-retina. However, one patient with a lesion exclusive to the occipital lobe demonstrated blindsight even when the normal hemi-retina was covered. The authors concluded that subcortical pathways that survive total hemispherectomy cannot mediate voluntary behavioural responses to visual targets in the blind field. However, this may yet be the case for patients with restricted damage to the striate cortex. Also, as mentioned earlier, several studies have similarly refuted the light scatter hypothesis by controlling for such artefact by showing that blindsight no longer occurs when presented in the natural blind spot of the scotoma in both patients and monkeys (Cowey & Weiskrantz, 1963; Cowey, 2010).

Another early criticism of the blindsight phenomenon was that residual vision may have been due to islands of surviving V1 (Fendrich, Wessinger & Gazzaniga, 1992). This arose from the inability to obtain a structural brain scan from patient DB, who first demonstrated blindsight (Weiskrantz, 1974). It was therefore, at such early stages of studying blindsight, not possible to establish whether patient DB (Weiskrantz, 1974) had spared V1 cortex accounting for blindsight like visual abilities. However it has since been shown that blindsight is not a likely result of spared V1 due to the structural scans obtained from blindsight patients, including patient GY, showing no spared islands of V1 that corresponds to his visual field defect (Barbur, Watson, Frackowiak, & Zeki, 1993; Bridge et al., 2008).

Implicit processing

As mentioned, the studies reviewed so far have involved direct measures of visual discrimination. Such measures require a direct response from the participant; a 'yes' or 'no' response to indicate the presence of a stimulus in the blind field, or a 'forced-choice' response to characterise a given stimulus from two options. Cowey (2010) notes an important distinction between forced-choice and yes/no paradigms. Where yes/no paradigms are characteristic of clinical vision tests, forced-choice paradigms are characteristic of psychophysical vision measures. Accordingly, forced-choice tests may be less prone to response-bias in comparison to yes/no paradigms since a patient's response in the latter

paradigm depends on both the target sensitivity and the patient's individual preference or 'bias' to favour one response over another, independent of the patient's sensitivity to the target. For example, if one patient's individual criteria for choosing a 'yes' response is a strict one, they may choose 'no' responses more frequently regardless of what they think the right response is.

Campion et al. (1983) argued that awareness may introduce a crucial confound when considering the validity of forced-choice methods. The manner in which awareness is defined draws attention to the question of whether blindsight is near to normal vision, or whether it is a unique visual ability exclusive to patients with lesion to the primary visual cortex. In theory, a lack of visual awareness whilst still responding correctly above chance in blindsight could suggest a qualitatively distinct ability from normal vision, supporting a subcortical extra-striate visual system. However, a patient may be aware of a visual stimulus in the blind field, yet this awareness may be contingent upon the experimenter or the patient's definition of awareness. For example, a patient may be aware of a stimulus in the blind field and respond to it, but may not respond as accurately as he/she would have if the stimulus was in the intact field. In addition to the artefact of light scatter reflected into the blind field, as previously mentioned, forced-choice paradigms that screen for conscious responses may also suffer from artefacts caused by saccades made into the blind field (Campion et al., 1983). Furthermore, Cowey (2010) notes that direct methods of assessment in blindsight may pose discomforting for patients, who are forced to judge stimuli that they deny seeing, without the option to explain the nature of experience. Such response bias confounds have posed a challenge in measuring visual discrimination in blindsight patients, who are not immune to the subjectivity of their responses.

The use of indirect measures of assessing residual visual function post damage to the primary visual cortex have attempted to offer a response bias free, more accurate measure of implicit visual discrimination. In order to demonstrate implicit processing of stimuli presented in the blind field without the use of direct, forced-choice measures, a measure of an 'unseen' stimulus, manipulated spatially and temporally is examined in the intact visual field (Stoerig & Cowey, 1997; Cowey, 2010). More simply, when a patient responds to stimuli in the sighted field, blindsight is inferred from the effects of a stimulus on performance in the blind field. If responses to stimuli in the sighted field are influenced by the unseen stimulus under such indirect testing conditions, this is a good indication that unseen stimuli are truly processed in the blind field, and are not due to an artefact of response bias often contaminating direct measures. For example, simultaneous or prior onset of an un-seen

stimulus has been shown to alter the mean reaction time of response to a seen stimulus. Furthermore, an asymmetry in responses to the temporal or nasal visual hemifield has been used as a marker to reflect subcortical visual processing, by retinal input to the superior colliculus (e.g. Tomalski, Johnson & Csibra, 2009; Johnson, 1990), which will be considered in more detail later. Rafal, Smith, Krantz, Cohen and Brennan, (1990) showed that distractor signals in the blind half of the visual field in hemianopic patients were able to influence saccades in the intact visual field. Furthermore, this effect was only present when the blind field was temporal, providing evidence in support of a subcortical visual processing route. This study provided an important contribution to the understanding of measuring residual visual function post lesion to V1, not only by showing that indirect measures allow reliable responses of implicit visual orientation, but also by demonstrating that such implicit orienting responses, in this case at least, are mediated via the retinotectal pathway, connecting the optic tract with the superior colliculus, and are not dependent on primary visual cortex function. However, in contrast, this finding has not been replicated by Walker, Mannan, Maurer, Pambakian and Kennard (2000) who demonstrated that saccade latency in the intact field of hemianopic patients were not affected by distractors in their hemianopic field.

Marzi, Tassinari, Aglioti and Lutzemberger (1986) also demonstrated blindsight using an indirect method – a redundant target effect paradigm - by testing the influence of unseen stimuli on visual responses in 20 hemianopic patients with retrochiasmatic lesions. Typically, normal participants demonstrate neural summation; faster responses to two targets presented simultaneously compared to a single stimulus in either one hemi-field, or opposite hemi-fields (ie. one target in the left and one in the right hemi-field), known as the redundant target effect. Initially, all patients demonstrated neural summation only in one hemi-field. However, after single case analyses, one patient demonstrated inter-hemispheric neural summation, like normals, and three patients demonstrated inter-hemispheric neural summation in at least one testing session. Despite the lack of this effect in the remaining 17 patients, the inter-field neural summation in a small number of hemianopic patients provide supporting evidence for blindsight in paradigms where forced-choice guessing and artefacts of direct measures are eliminated. Corbetta, Marzi, Tassinari and Aglioti (1990) demonstrated similar results, showing inter-field neural summation in two out of four patients with hemianopia as a result of posterior cerebral artery infarction.

Pöppel (1986) demonstrated blindsight using indirect measures in one hemianopic patient by showing that colour processing may be a retinal phenomenon. Similar to results typically observed in normal individuals, when the hemianopic patient fixated on a white

surface surrounded by a given colour, the resulting after-image was seen as if the colours were swapped; the white centre formed the outline, and the outer surrounding appeared inside the white boundary. This study offers an important contribution to the literature demonstrating that colour processing as a blindsight phenomenon can be measured through indirect measures of residual visual function.

Another important contribution was made by Marcel (1998), who demonstrated higher order visual function influenced by semantics in the blind field in two hemianopic patients. Patients demonstrated discrimination of upper case letters and words presented in their blind field only at chance. However, when required to provide a description of a given word presented in the intact field, patient responses were biased towards a word cued previously presented in their blind field. For example, when presented with the target word 'BANK', patient descriptions were biased according to preceding cues either 'MONEY' or 'RIVER'. This finding suggests that blindsight phenomena may also include higher order functions such as semantic processing, and provides further supporting evidence that indirect measures of residual visual processing post damage to V1 may be more sensitive in showing effects of non-conscious perception in comparison to direct measures.

Conscious phenomena in blindsight?

One of the biggest controversies in the blindsight literature has been a conflict of agreement among researchers in defining blindsight phenomena. The literature reviewed thus far were in support of three core characteristics that define blindsight phenomena: visually guided behaviour is considered blindsight if it is unconscious, subcortical and evoked by stimuli presented in the scotoma (Campion et al., 1983). However, as mentioned previously, the criteria of 'awareness' introduces a confound when measuring blindsight phenomena, since it is vulnerable to contamination by subjectivity from both experimenter and the patient completing the task. Furthermore, several studies have reported that in some cases patients report qualia in response to visual stimuli perceived non-consciously. For example, some report perceptual experiences in response to visual stimuli such as "dark shadows" (Barbur et al. 1980), "visual pin pricks" (Richards, 1973) or "white halos" (Perenin & Jeannerod, 1978), where others report "feelings" that a certain stimulus was present (Weiskrantz et al. 1974). In light of such disagreement regarding the unconscious nature of blindsight phenomena, Weiskrantz (1995) draws a distinction between two types of blindsight in humans; Type II blindsight is accompanied by a non-visual "feeling" of awareness, where Type I blindsight is not.

Affective blindsight – an unexpected finding?

De Gelder, Vroomen, Pourtois and Weiskrantz (1999) demonstrated a surprising finding suggesting that blindsight may also exist for affective stimuli such as fearful faces. Their study presented patient GY who suffered a right hemianopia as a result of damage to his left occipital lobe. Based on previous functional neuroimaging evidence demonstrating that unseen fear stimuli can evoke activation of subcortical structures (Breiter, Etcoff, & Whalen, 1996; Morris et al., 1998) and subcortical reactions occurred in response to emotional stimuli made subliminal via backward masking paradigms, De Gelder et al. (1999) found that recognition of emotional facial expressions was also present in patient GY. In a series of experiments, GY discriminated different facial expressions (e.g. fearful, happy, sad, angry) correctly at above chance level. In a two alternative forced choice paradigm, GY performed correctly overall 66% of the time in discriminating happy/fearful, angry/sad and angry/fearful facial expressions, when presented in his blind field. Importantly, GY reported to recognise a light flash during the onset and offset of stimuli presentation, but reported complete unawareness of the emotion expressed in the face. GY also demonstrated such face discrimination when presented with video clips of happy, sad, angry and fearful faces in a four alternative forced choice paradigm. GY's performance was overall 52% correct, which the authors conclude was well above the chance level of 25% correct.

Morris, DeGelder, Weiskrantz and Dolan (2001) later further demonstrated fMRI data in patient GY showing amygdala activation in response to fearful faces presented in his blind visual hemi-field. First, GY performed above chance in discriminating the gender of male and female fearful or happy facial expressions presented in both his intact (63.5% correct) and his blind field (76% correct). In comparison to happy faces, fearful faces presented in GY's blind hemifield evoked bilateral amygdala activation. In contrast, only left amygdala activation was evoked when fearful faces were presented in the healthy visual hemifield, compared to happy faces. Interestingly, activation of striate, fusiform and dorsolateral prefrontal cortices were seen only for faces presented in the healthy visual hemifield, similar to reports in normal participants (e.g. Haxby et al. 1994). Secondly, when faces were presented in combination with an auditory noise, thereby conditioning fear responses, GY responded increasingly faster throughout the course of the experiment, demonstrating a learning dependent facilitation of fear processing. Furthermore, GY demonstrated activation in the superior colliculus and bilateral amygdala activation in response to conditioned fearful faces presented in his blind visual hemi-field, which was not reported for GY's healthy visual hemi-field.

The above two studies presented strong evidence in favour of a subcortical visual system that functions in the absence of the primary visual cortex, that is responsible for processing such unseen facial expressions. However, Cowey (2010) notes that such conclusions based on evidence from De Gelder et al. (1999) and Morris et al. (1999) should be assessed with caution. Given that the stimuli were also presented in GY's normal visual field, it may have been possible that GY picked up on salient features of fearful facial expressions seen in the normal visual field (e.g. wide open eyes or teeth), and used such features as cues to choose faces as fearful when presented in his blind field. A good control for this possible confound is employing a patient with bilateral damage to the visual cortex. Pegna, Khateb, Lazeyras and Seghier (2005) reported a cortically blind patient TN, with bilateral damage to the primary visual cortex. When presented with facial expressions, TN demonstrated increased activation in the right amygdala in response to fearful facial expressions, despite reporting not being aware of the emotional valence of the faces. Furthermore, Gonzalez-Andino, Grave De Peralta Menendez, Khateb, Landis, and Pegna (2009) later showed in patient TN, that faces elicited responses in the brain at different times. All facial expressions evoked responses from 70ms onwards in the superior temporal polysensory area, whereas emotional faces occurred 120ms after onset in the right anterior areas, and with evoked responses recorded from the right amygdala occurring after 200ms. Accordingly, Gonzalez et al. (2009) concluded that, taking such timings into account, affective blindsight may be mediated by subcortical inputs to the temporal lobe, and that non-conscious higher order processing of visual stimuli may be processed at fast rates in absence of V1.

Simulating non-conscious perception in healthy humans

As mentioned previously, in order to measure non-conscious vision in the healthy brain with intact primary visual cortex, the visual stimuli need to be manipulated in order to be perceived non-consciously. The literature suggests that such non-conscious perception of visual stimuli is achievable by manipulating the presentation of the stimuli so that participants are unaware of their presence. This can be achieved either through manipulating the attention that is paid to the stimulus, or manipulating the sensory properties of the stimulus rendering it non-conscious.

Functional imaging in humans (Rees, Russell, Frith & Driver, 1999) and single cell recordings in monkeys (Chelazzi, Duncan, Miller & Desimone, 1998) have demonstrated that unattended stimuli evoke reduced neural responses in comparison to attended stimuli.

Furthermore, unattended stimuli are often perceived with reduced accuracy or not perceived at all (Mack & Rock, 1998). However, emotional stimuli have demonstrated an exception to this rule, triggering responses even in the absence of attention paid to them. Emotional stimuli, especially threatening or aversive stimuli, evoke rapid, involuntary responses in normal sighted participants (Lang, Bradley & Cuthbert, 1998). Typically, a dual task paradigm is employed to measure non-conscious responses to emotional stimuli when manipulating attentional unawareness. For example, Vuilleumier, Armony, Driver and Dolan (2001) used a dual task paradigm and functional magnetic resonance imaging to investigate neural responses to unattended fearful versus neutral facial expressions. Attentional awareness was manipulated by engaging the participant's main focus on an attention demanding task, whilst simultaneously presenting pictures of fearful or neutral stimuli at irrelevant locations. For example, participants selected whether pictures of houses that were presented on the left and right sides of the screen were identical, whilst pictures of faces appeared vertically at the top and bottom of the screen. The relevant location of primary attendance was alternated throughout the task (ie. faces were presented horizontally on some trials, and vertically on others). This resulted in the measure of responses when faces were both attended and not attended to. Results showed delayed reaction time to the task performance when fearful versus neutral stimuli were presented at irrelevant unattended locations in the task. Importantly, fMRI analyses demonstrated greater activation in the amygdala in response to fearful versus neutral faces, regardless of location.

However, Tamietto and de Gelder (2010) suggests caution in classing such attentional unawareness as non-conscious perception, since studies fail to demonstrate that unattended emotional stimuli are not consciously perceived, creating uncertainty of whether emotion stimuli are truly perceived non-consciously under attentional manipulation conditions. Instead, it may be more appropriate to class such responses as pre-attentive since they occur before and independent from attentional selection.

Typically, techniques such as backward masking or binocular rivalry are used to manipulate sensory awareness to render stimuli non-conscious. Neuroimaging studies in humans demonstrated activation in the amygdala, superior colliculus, pulvinar and basal ganglia, with responses remaining either the same or enhanced for non-consciously versus consciously perceived stimuli under sensory unawareness paradigms (Tamietto & De Gelder, 2010). For example, Whalen et al. (1998) used a backward masking paradigm and fMRI to show increased amygdala activation in response to non-consciously perceived fearful faces. In a backward masking paradigm, awareness of the target is prevented by briefly presenting a

masking stimulus immediately after the target stimulus. Whalen et al. (1998) collected fMRI data from 10 normal participants, and presented them with fearful faces, masked 33ms afterwards with neutral faces. Eight participants reported not being aware of any concealed facial expression after the experiment. Despite this unawareness of fearful faces in the majority of subjects, BOLD fMRI signal was higher in the amygdala when participants viewed fearful compared to neutral faces. Furthermore, Williams, Morris, McGlone, Abbott, and Mattingley (2004) used a binocular rivalry paradigm to show amygdala activation in response to non-consciously perceived stimuli. During binocular rivalry, each eye receives a separate image which causes monocular channels in V1 to inhibit each other, resulting in one image being perceived and dominating over the other, which is suppressed. Williams et al. (2004) used such a paradigm to present either neutral, happy or fearful faces in one eye and a picture of a house in the other eye in 12 normal participants. Bilateral amygdala activation increased for fearful versus neutral faces in both conscious and non-conscious perceived conditions, whereas, interestingly, amygdala activation increased bilaterally for fearful versus neutral faces only when the face was suppressed. The authors suggest that the amygdala may have a limited capacity when differentiating between different faces when relying on a subcortical route, possibly reflected through a trade off between specificity and speed of processing (Williams et al., 2004).

Despite such findings, the studies used small sample sizes and it cannot be certain whether the participants demonstrated non-conscious vision similar to that demonstrated by patients with damage to the primary visual cortex. In attempt to create a temporary lesion to the primary visual cortex, albeit at a much smaller scale than what is observed in blindsight patients, Jolij and Lamme (2005) and Ro, Shelton, Lee and Chang (2004) used transcranial magnetic stimulation (TMS) to temporarily block visual processing in primary visual cortex to show that participants were still able to locate happy and sad facial expressions and discriminate between them. This study showed that blocking visual processing through the visual cortex does not suppress non-conscious processing of stimuli, showing that non-conscious perception of stimuli are not only possible in patients with lesion to V1. Behavioural measures of emotion processing are reviewed in Chapter 3.

Alternative perspectives; is non-conscious processing of emotion exclusive to a subcortical route?

Although the focus of this thesis is on the anatomy and function in support of a subcortical route for processing unseen emotion, it is important to briefly consider alternative

perspectives regarding the utility of pathways connecting the amygdala that may contribute to emotion processing. Several studies have presented results in support of a role for the amygdala even in the absence of visual awareness of emotive stimuli, however the limit of such non-conscious processing, and extent to which this effect is confined to specific experimental or stimulus conditions, remains open for debate.

A distinction between sensory unawareness and attentional unawareness allows for an appreciation of non-conscious processing of emotion via two qualitatively different functional mechanisms of the amygdala. The use of dual-task, visual search, attentional blink or Stroop paradigms allow for emotional stimuli to be perceived non-consciously by deviating attention away from the stimulus (Diano, Celeghin, Bagnis & Tamietto, 2016). The consensus is that cortical activation in visual areas triggered by task-irrelevant visual stimuli are normally limited and suppressed by competing fronto-parietal top-down mechanisms that are engaged in task-relevant voluntary attention (Beck, Reese, Frith & Lavie, 2001). However, as previously mentioned, emotional stimuli may not be limited by attention to the same extent as neutral stimuli (Vuilleumier, 2005). On the other hand, sensory unawareness, tested with the use of binocular rivalry, backward masking or continuous flash suppression (Diano et al., 2017), renders stimuli to be perceived non-consciously by interfering with function in the ventral occipito-temporal cortex which is required for awareness of visual stimuli (Macknik & Livingstone, 1998; Williams & Mattingley, 2004; Tong, Meng & Blake, 2006).

Several neuroimaging studies in healthy participants have reported that unattended emotional stimuli do not suppress activity in the amygdala, cortical or subcortical structures (Vuilleumier, Armony, Driver & Dolan, 2001; Anderson, Christoff, Panitz, Rosa & Gabrieli, 2003; Bishop, Duncan & Lawrence, 2004; Williams, McGlone, Abbot & Mattingley, 2005). This has led to the assumption that the function of the amygdala in the perception of non-conscious emotion is strictly automatic, however conflicting evidence renders the current consensus divided (Pessoa, 2005; Pessoa, Padmala & Morland, 2005; Silvert et al., 2007). For example, Pessoa, McKenna, Gutierrez and Ungerleider (2002) showed that amygdala responses could be suppressed when attention is demanded elsewhere, thereby arguing that attention is required for processing emotion, whereas Vuilleumier et al. (2001) showed that activation of the amygdala in response to fearful faces is attention independent. Such inconsistencies may have resulted from potential confounds due to methodological differences, responses of the amygdala to different stimuli properties and the difficulty in a robust comparison between awareness and unawareness of identical stimuli in healthy

participants (Diano et al., 2017). As reviewed previously, studies in affective blindsight patients as a result of V1 lesion may provide an effective way to investigate the neural mechanisms of non-conscious emotion processing, since several methodological confounds that involve manipulating seen and unseen stimuli to be identical in healthy participants are eliminated.

Inconsistencies in the literature has divided the explanation for amygdala function in non-conscious perception of emotion between two extreme arguments; the amygdala is dependent on awareness vs. the amygdala's function is automatic and independent of awareness. However, a middle ground between the two opposing arguments is emerging, proposing instead that the neural networks for conscious and non-conscious emotion processing may be integrated rather than strictly segregated (Vuilleumier, 2005; Pessoa, Japee, Sturman & Ungerleider, 2006; Duncan & Barrett, 2007; Tamietto & de Gelder, 2010; Pourtois, Schettino & Vuilleumier, 2013; Diano et al., 2017). Accordingly, the response of the amygdala involves processing involving both awareness and unawareness at varying temporal dimensions. Furthermore, initial unawareness may dictate whether a stimulus will reach awareness, and subsequently modulate behaviour (Diano et al., 2017). Adopting this view may account for inconsistencies in the literature, by suggesting that the role of the amygdala in processing non-conscious emotion may be more complex and interconnected with additional cortical neural networks than previously assumed.

Consideration of the temporal dynamics of amygdala processing is critical in order to interpret its role in awareness and unawareness of emotions. The technique that has typically been used to study non-conscious emotion processing has been fMRI, which has high spatial but poor temporal resolution, often averaging temporal sections of 2 seconds (Diano et al., 2017). Recent advancements in techniques with high temporal resolution but traditionally poor signal in deep subcortical structures such as the amygdala have provided evidence in favour for a framework in which the amygdala contributes to both processes of awareness and unawareness, driven by an underlying subcortical and cortical integrated neural network. For example, Luo, Holroyd, Jones and Hendler (2007) combined MEG and MRI to show that event-related activity in response to visual stimuli occurred earlier in the amygdala (20-30 ms after stimulus onset) compared to activity in the visual cortex (40-50 ms after stimulus onset). Furthermore, a later MEG study by Luo et al. (2010) showed enhanced activity in the amygdala in response to threatening faces (30-60 ms), which occurred under attentional unawareness and was independent of task load. Furthermore, fronto-parietal activity occurred later, followed by an interaction of emotion processing and attention (280-340 ms). Similarly,

EEG recordings demonstrate that damage in the amygdala influence emotion perception at two separate time windows, an early process occurring 100-150ms post stimulus onset, and a later process at 500-600ms after stimulus onset (Rothstein et al., 2010). Intracranial electrophysiological recording studies have also suggested an early and later component of emotion processing in the amygdala. For example, Hesse et al. (2016) reported that early activity of 80-200ms exclusive to the amygdala predicted fast encoding of visual scenes with intentional harm. Furthermore, Mendez-Bertolo et al. (2016) recently demonstrated rapid amygdala responses starting at 74ms after stimulus onset, which were specific to fearful compared to neutral or happy faces. Importantly, rapid responses in the amygdala were selective to low spatial frequency components of the fearful faces, providing evidence in favour for a subcortical visual route of processing. Such findings suggest that amygdala automaticity may be a function of time, representative of a dual-stage model of an interaction between emotion and attention (Diano et al., 2017). Accordingly, early amygdala responses allows for the initial discrimination between threat and neutral stimuli, independently of awareness and attention resources, before fronto-parietal mechanisms have sufficient time to effectively suppress task irrelevant stimuli. After sufficient time, subsequent amygdala responses are modulated by attention, leading to conscious perception of emotion.

It is important to acknowledge that, although the role of a subcortical route involving the superior colliculus, pulvinar and the amygdala in processing rapid, non-conscious threat has been emphasised, it does not rule out contributions from alternative routes, alternative theoretical possibilities or cortical contributions at varying instances of emotion processing during both awareness and unawareness (Pessoa & Adolphs, 2010). Potential alternative pathways have recently been suggested as candidates that may contribute to non-conscious perception of emotion. In mice, two studies recently demonstrated disynaptic subcortical pathways originating in the superior colliculus, one that travelled via the parabigeminal nucleus (Shang et al. 2015) before connecting the amygdala, and another via the lateral posterior nucleus of the thalamus (Wei et al. 2015), that played a function in triggering innate defensive responses to visual threat. Furthermore, extrastriate visual areas including areas along the ventral visual stream receive collaterals from both the lateral geniculate nucleus and the pulvinar that bypass V1 that can relay visual information to the amygdala (Tamietto & Morrone, 2016). Therefore, the literature suggests that several potential neural routes may in fact contribute to the non-conscious perception of emotion.

The above-mentioned findings suggest that the processing of non-conscious emotion may be more complex and integrated with multiple neural networks than what has been

previously suggested. Therefore, cortical versus subcortical processing, attentional versus sensory unawareness, and fast versus slow processing of emotion may not be mutually exclusive in processing non-conscious perception of emotion. The focus of this thesis is on one potential part of the neural network, the subcortical visual processing route. However, it is important to appreciate that the subcortical pathway may indeed form part of a much more complex and larger integrated neural network, capable of dealing with both sensory and attentional unawareness, and which supports amygdala function at varying temporal stages of non-conscious emotion processing.

Anatomical basis for a subcortical visual system

The literature reviewed thus far have suggested the possibility of preserved visual function, in the absence of the visual cortex, a part of the brain that was previously regarded as the chief site of visual processing in humans. The evidence that simple visual reflexes, and even abstract vision, such as facial expression processing, is possible without the primary visual cortex in humans is intriguing as it tells us something about the development and the possible evolution of the brain. It is important to note that a more primitive visual system may be one that processes environmental visual signals for survival, in comparison to less urgent elaborate and complex visual cognition. The literature suggests a network of subcortical structures that are responsible for transmitting signals to control the orientating of attention. For example, a non-human primate may rely on reflexive functions mediated by subcortical structures to alert a warning signal for action for survival in response to seeing a threat in the environment, such as a snake or a tiger. The urgency of the necessity to survive is imperative, leaving little time for higher order processing of what the threat looks like. Thus, the brain is able to process threats at fast rates via a putative subcortical network, not possible via the highly evolved primary visual cortex. However, the case for a more primitive subcortical route for transmitting information about emotionally valenced stimuli in NHPs is still lacking sufficient evidence in humans.

Part of the difficulty in identifying the reliability in this hypothesis is how visual responses to threat are measured in healthy humans. We have seen that patients with damage to the primary visual cortex demonstrate remarkable unexpected residual visual abilities, but such effects can only be linked with anatomy of lesion sites of the individual patient. Furthermore, simulating ‘blindsight’ or responses to ‘unseen’ visual stimuli in healthy humans, may not be similar to the blindsight seen in patients with damage to V1. Due to the invasive nature of brain lesions and ethical concerns it is also not possible to recreate such

lesions invasively in aid of scientific research. Neuroimaging techniques have offered a non-invasive alternative to study brain anatomy. Diffusion tensor imaging (DTI), the imaging technique used in this thesis, is a useful non-invasive tool to map out white matter connections in the healthy human brain, in-vivo. Several fMRI studies, have also provided promising evidence in favour of a subcortical network for visual processing. The following section will review literature on the anatomy of subcortical structures and their putative connections that have been suggested to transmit and process visual signals.

A current distinction can be drawn between two sub-systems. The first system comprise of sites responsible for visual encoding which are directly connected to subcortical structures that include neurons that are visually responsive to emotional stimuli. This system involves the following structures: the superior colliculus, the amygdala, the pulvinar nucleus of the thalamus, the substantia innominata and the nucleus accumbens (Tamietto & de Gelder, 2010). The second system involves subcortical areas that contain neurons that respond to non-visual emotion, for example to carry out emotional reactions, memory consolidation, disposition tendencies and motivation. This system involves structures including the locus coeruleus, the periaqueductal grey, the nucleus of basalis of Meyenert, basal ganglia sections and the hippocampus (Tamietto & de Gelder, 2010).

As mentioned, studies in cortically blind patients have suggested a subcortical pathway connecting the amygdala and the superior colliculus, via the pulvinar nucleus of the thalamus to be a possible route for fear processing in the absence of primary visual cortex. The superior colliculus is a laminated structure in the midbrain that plays a chief role in orienting the line of sight towards important objects in the environment through the movement of the head, eyes and body (Schiller, 1998). In primitive animals with little forebrain, such as amphibians, the area of the optic tectum corresponds to the superior colliculus in humans, and is the primary visual processing centre and also converts visual signal into motor efferents (Schiller, 1998). Such animals become blind as a result of optic tectum ablation and fail to execute visually guided motor functions (Schiller, 1984). However, in humans, the chief role of the superior colliculus has been to control eye movements (Schiller, 1984; Sparks, 1986; Wurtz & Albano, 1980). Visual processing in mammals and primates with a highly developed neocortex have been mainly attributed to the geniculo-striate system. Two types of layers, superficial and deep layers, are embedded in the superior colliculus. Superficial layers, layers 1-3, contain a retinotopic map and receives direct projections from the retina and V1, projecting to the visual thalamus and pretectum to primarily serve a visual sensory function (May, 2006). Single cells in the superficial layers

respond to small visual stimuli and are not sensitive to shape, orientation, colour or direction of motion (Schiller, 1998).

In the deep layers of the superior colliculus, signals that instruct orienting behaviour such as somatosensory, auditory and visual signals, merge on premotor neurons that connect to saccade and head movement circuits. The arrangement for coding eye movements is coded topographically, i.e. a place code, in the deep layers. Schiller and Stryker (1972) demonstrated this arrangement by comparing saccade size elicited by electrically stimulating the abducens nucleus versus the superior colliculus. With a constant stimulation frequency of 500Hz, stimulation of the abducens nucleus showed increased saccade size as a function of increasing burst duration. However, in contrast, the superior colliculus demonstrated the same amplitude and size of saccade, contingent on location of stimulation. Interestingly, for long duration stimulation, saccade size proportions did not increase to account for more stimulation, but instead became additive in a staircase fashion. Therefore, saccade size and direction is dependent on location of stimulation of superior colliculus; anterior, posterior, medial and lateral stimulation generates small, large, upward and downward saccades, respectively (Schiller, 1998). Accordingly, the superior colliculus layers correspond to two zones; the superficial zone generates ascending fibres whilst receiving mostly visual inputs, whereas the deep zone receives mixed multimodal inputs, projecting both ascending and descending fibres to the thalamus, brainstem and spinal cord (Neuwenhuys et al., 2008). Retinal fibres from each eye project to the superior colliculus bilaterally, and has a contralateral dominance in primates (Neuwenhuys et al., 2008). Thus, a retinotectal pathway is formed from joint ipsi and contralateral retinal fibres in each hemisphere, with a contralateral dominance.

A retinotopic pattern represents the contralateral hemifield representation in the superior colliculus in the following manner; the horizontal meridian separates the superior colliculus into medial and lateral halves, the vertical meridian corresponds to the rostral superior colliculus, the upper and lower visual fields are represented medially and laterally, respectively, and the fovea rostromedially. The caudal superior colliculus receives predominantly contralateral retinal fibres for the monocular visual field. Only a small amount of ganglion cells, approximately 10% constitute the retinotectal pathway (Neuwenhuys et al., 2008).

The main function of the superior colliculus is to generate saccades, which are rapid eye movements that ensure that important visual targets in the visual field fall onto the fovea by controlling the focus of the line of sight. Smooth pursuit eye movements are distinct from

saccadic eye movements as they maintain fixation on the fovea during motion. For example, Schiller & Logothetis (1987) demonstrated different response latencies between the two systems, further suggesting different underlying neural mechanisms. In a step-ramp paradigm, a monkey fixated on a small target against a uniform background, and, upon offset of the fixation target, looked towards and tracked a new peripheral target, which was projected at varying speeds. Remarkably, traces of the eye movements showed that smooth pursuit of the peripheral target begins at 75 to 100 ms, prior to initiation of the saccade towards the target, taking place at 125-150 ms.

In considering the superior colliculus as a functional centre alongside the pulvinar nucleus of the thalamus and the amygdala nucleus in a putative subcortical non-conscious vision processing circuit, it is important to consider the contribution of the retinotectal pathway. Several studies have demonstrated behavioural effects thought to reflect retinotectal activity. For example, it is thought that the presence of an asymmetry in visual responses in the temporal versus nasal visual hemi-field reflects retinotectal function, based on the finding that newborns, in whom the geniculostriate pathway is not fully developed yet, orient to faces and simple face-like patterns presented in the temporal hemi-field (Johnson, 1990; Valenza, Simion, Cassia, Umiltà, 1996). Since the retino-tectal pathway is contralaterally dominant, presentation in the temporal visual hemi-field results in processing via the nasal hemi-retina, en route to the contralateral hemisphere. This effect has also been shown in adult humans. Tomalski, Johnson and Csibra (2009) showed that healthy adult humans oriented faster to simple upright versus inverted face-like patterns presented in the temporal versus nasal visual hemi-field, an effect that was present for saccades only and not perceptual key-press responses, demonstrating a specific oculomotor function. Furthermore, Dodds, Machado, Rafal and Ro (2002) demonstrated a temporal-nasal asymmetry for blindsight stimuli in a patient with a dense right hemi-anopia. In a two alternative, forced choice localisation task under monocular viewing conditions, patient MP performed localisation of stimuli presented in the contralesional temporal hemifield with extreme accuracy, whilst performing at chance for targets in the contralesional nasal hemi-field. Sylvester, Josephs, Driver and Rees (2007) demonstrated using fMRI, that under monocular viewing conditions, visual stimulation in the temporal versus nasal visual hemi-field strongly increased activation in the contralateral superior colliculus, an asymmetry that was absent for activation in the lateral geniculate nucleus and visual cortical areas.

Findings from the above mentioned studies suggest the superior colliculus plays a pivotal role, via the retinotectal pathway in mediating visual responses to unseen stimuli.

However, this finding has not been consistent throughout the literature, leaving questions regarding whether such effects are exclusive to unseen stimuli, or whether the ratio of temporal to nasal fibres are truly dominant for the temporal visual hemifield. For example, Bompas, Sterling, Rafal and Sumner (2014) demonstrated oculo-motor specific temporal-nasal asymmetries for choice saccades, when S-cone stimuli were used which were presumed invisible to the magnocellular pathway and the superior colliculus. Additionally, saccade latency did not demonstrate temporal nasal asymmetry, suggesting that temporal nasal asymmetry may not be a marker for retinotectal function, which relies on bottom up processing from low level visual pathways. Furthermore, Williams, Azzopardi and Cowey (1995) showed in four macaque monkeys that the ratio of temporal versus nasal retrograde tracers post horseradish peroxidase injection in the superior colliculus were no different when measured afterwards in the temporal and nasal hemi-retinae compared to the measures in the optic tract. This suggest that the ratio of temporal versus nasal retinal projections may not be as asymmetric as had been previously claimed (Wilson & Toyne, 1970, Hubel, Le Vay & Wiesel, 1975) in primates.

The fixation offset effect or the ‘gap’ effect is another behavioural task that has been suggested to reflect responses mediated via the retinotectal pathway. The visual grasp reflex (VGR) is a brief saccade to a target onsetting in the periphery, and is highly adaptive for survival, allowing us to foveate on an approaching potentially dangerous stimulus in preparation for action (Machado & Rafal, 2000). Cells in the rostral pole of the superior colliculus are active during fixation in the dark, with increased activation if fixation is accompanied by an additional visual signal at fixation. Cells in the caudal superior colliculus are active during movement from one fixation point to another, and inhibit rostral pole neurons (Wurtz & Munoz, 1995). The fixation offset effect (FOE), first demonstrated by Saslow (1967), occurs when the VGR becomes disinhibited as a result of the offset of the fixated target before or simultaneous with the onset of a peripheral target. This increases the speed of reaction time to initiate an eye movement to the target. A ‘gap’ paradigm is often used, which includes a 200ms temporal gap between fixation offset and target onset, resulting in extremely brief saccade latencies, sometimes seen as a bimodal distribution of saccade latencies with a separate population of express saccades (Fischer & Ramsperger, 1984). The use of the ‘gap’ effect as a possible marker for retinotectal function will be reviewed in more detail in Chapter 2.

As mentioned, other key structures involved in the mediation of unseen emotional stimuli is the pulvinar and the amygdala. The pulvinar is a nucleus in the posterior thalamus

that is active during non-conscious perception of emotional stimuli (de Gelder & Hadjikhani, 2006; de Gelder, Morris & Dolan, 2005, Tamietto & de Gelder, 2010). Retinal ganglion cells project directly to the lateral and inferior pulvinar in the thalamus, corresponding to a retinotopic representation of subnuclei (Lyon, Nassi & Callaway, 2010). A lesion in the pulvinar results in the loss of an attention capture effect that consciously perceived emotional stimuli trigger, leading to the assumption that the pulvinar involves orienting of visual attention (Ward, Danziger & Bamford, 2005). However, since the pulvinar is monosynaptically connected with the amygdala, it is not clear whether this attentional effect results due to a relay between pulvinar and amygdala, or whether the pulvinar drives visual attention independently (Romanski, Giguere & Bates, 1997). The amygdala, perhaps the most extensively studied structure thought to mediate visual perception of emotional stimuli, is a large hub of nuclei in the dorso-medial portion of the temporal lobe. The rostromedial and rostradorsal walls of the inferior horn of the lateral ventricle is partly formed by the amygdala (Neuwenhuys et al., 2008). It is thought that the amygdala is responsible for the perception of emotional stimuli in order to perform an action, for example a fearful stimulus will trigger a survival response in an organism. Unlike the superior colliculus and the pulvinar, the amygdala activates in response to both conscious and non-conscious perception of emotional stimuli (Sergeyev, Chochol & Armony, 2008).

The chief visual projections to the amygdala are from the striate and extrastriate visual cortices. However Morris and colleagues (de Gelder et al., 2005; Morris, Öhman & Dolan, 1999) proposed a second route of amygdala processing, which projects from the amygdala to the superior colliculus through the pulvinar nucleus of the thalamus. This suggestion was made based on the observation that patients with damage to the primary visual cortex demonstrated blindsight. This proposed subcortical, fast route may presumably account for fast responses to unseen emotional stimuli. Such a subcortical ‘low road’ has been suggested to be a ‘quick and dirty’ processing mechanism, processing coarse features in visual stimuli, compared to a slower geniculostriate route, mediating refined higher order visual processing (Tamietto & De Gelder, 2010). Studies on the anatomy of this pathway have been scarcely reported in the primate brain. Using diffusion tensor tractography in humans, Tamietto et al. (2012) demonstrated connections between the amygdala and superior colliculus traversing the pulvinar nucleus of the thalamus. Furthermore, they also showed in one hemianopic patient, stronger connections of this pathway in the lesioned hemisphere compared to healthy controls, suggesting a functional role for this subcortical route. Additionally, Rafal et al. (2015) demonstrated the same subcortical pathway using diffusion

tensor imaging tractography in healthy humans and macaque monkeys. Anatomical evidence in support of a subcortical route for fear processing is still scarce and anatomical findings linked with functional evidence for this pathway is required. Anatomical evidence for this route is reviewed in more detail in Chapter 4. This thesis aims to contribute to this body of research, by associating strength in connectivity of virtually dissected subcortical fear processing pathways using diffusion tensor tractography with behavioural measures of visual threat processing, presented in Chapter 4.

Diffusion tensor imaging as tool in studying anatomy

Diffusion tensor imaging (DTI) is a magnetic resonance imaging technique first proposed by Basser, Mattiello and Le Bihan (1994) which allows for the non-invasive, in-vivo imaging and measurement of white matter in the brain (Basser & Pierpaoli, 1996). DTI takes advantage of the internal geometry of axons, where diffusion occurs non-randomly, with the diffusion of water molecules being restricted such that there is more diffusion along the length of the axon (axial diffusion), compared to radial diffusion perpendicular to the length of the axon (Basser & Pierpaoli, 1996). The direction of movement of the axon in the same direction, termed anisotropic diffusion, suggests that there is a boundary or axon wall surrounding the molecules, thereby allowing white matter to be reconstructed using MRI signal, in comparison to isotropic diffusion, where molecules diffuse randomly and equally in all directions – for example in cerebrospinal fluid (CSF). A diffusion weighting (b factor) is applied through controlled gradients of magnetic fields to measure both the direction and the size of molecule diffusion. The motion of molecules over time in an anisotropic diffusion represents an ellipsoid shape, as opposed to a spherical shape representing isotropic diffusion. The anisotropic ellipsoid can be geometrically described as a collection of vector fields guided by three principal directions, representing a ‘tensor’ (Huettel, Song & McCarthy, 2004). In order to measure diffusion in the brain, signal is measured from multiple directions in order to reconstruct diffusion tensors allowing principal diffusivity directions to be quantified (Assaf & Pasternak, 2008).

Fractional anisotropy (FA) is a scalar measurement of diffusion anisotropy in each voxel, which is referred to as an indirect measure of how strongly connected a set of voxels in a given axon bundle are. It is calculated by taking into account the three principal diffusion directions (Dx, Dy, Dz) that essentially calculates a ratio of axial to radial diffusion with a value between 0 and 1. Images representing FA values can be colour coded based on the principle diffusion direction according to an RGB (red-green-blue) map, with red

representing left-right fibres, green representing anterior-posterior fibres and blue representing inferior superior fibres.

Diffusion tensor tractography is a diffusion imaging based technique which allows for the reconstructions of anatomy based on the principal eigenvectors in the living brain, non-invasively (Basser, Pajevic, Peirpaoli, Duda & Aldroubi, 2000). Previously, anatomical dissections of white matter were only possible in experimental animals using invasive histological and viral tracer techniques (Assaf & Pasternak, 2008). However, DTI has often been criticized for being error prone, for example presenting spurious fibres as part of the same fibre bundle that cannot be part of the same tract. This occurs since it is essentially a computerized reconstructed model, based on information of diffusion on a voxel by voxel basis, while it provides no information of direction of axonal transmission, or synapses. In voxel containing fibres from more than one tract, tractography can demonstrate spurious connectivity because of crossing or kissing fibres. Furthermore, several studies have suggested that the measure of FA may not be the most reliable indicator of white matter integrity, since it measures diffusion signal at a macro rather than a micro level, without taking into account signal interactions or hindrances between micro organelles in the axon cell structure (Jones, Knösche, & Turner, 2013; Jones & Nilsson, 2014). Nonetheless, diffusion tractography can be an extremely valuable anatomical tool when utilised correctly in measuring white matter axons in the injured and healthy brain. The objective for this thesis was to collect DTI images from healthy participants, and virtually dissect subcortical pathways that have been suggested to mediate non-conscious perception of visual stimuli.

Structure of the thesis

This thesis follows the structure of an introduction including review of relevant background literature, five experimental chapters, and a discussion. Adapted versions of chapters that have been published or submitted for publication are presented in journal article format.

Chapter 2 investigates whether connectivity strength measures of the retino-tectal pathway, connecting the optic tract to the superior colliculus, possibly forming the first initial starting point of the proposed subcortical visual circuit, reflects individual differences in express reflexive saccade performance and asymmetry between responses to the temporal and nasal visual hemi-field, both characteristic properties of retino-tectal function. An adaptation of the ‘gap effect’ task is used and the imaging scanning protocol is outlined for Chapters 2, 4, 5 and 6.

Chapter 3 presents a novel behavioural temporal order saccade decision task attempting to measure reflexive responses to threatening stimuli, possibly mediated by subcortical circuitry including the amygdala, pulvinar nucleus of the thalamus and the superior colliculus. Behavioural results from this experiment are correlated with the connectivity strength of the retino-tectal pathway described in Chapter 2.

Chapter 4 considers a proposed subcortical connection between the superior colliculus, the pulvinar nucleus of the thalamus and the amygdala that has been suggested to mediate subliminal responses to threat. Virtual dissection of this ‘threat-mediating’ pathway is demonstrated with DTI tractography in healthy humans. Virtual dissections of the stria terminalis, connecting the amygdala with the bed nucleus of the stria terminalis are additionally dissected to rule out spurious connectivity, due to its close proximity to the putative threat-processing pathway. Part of the anatomical findings have been published; Rafal, R. D., Koller, K., Bultitude, J. H., Mullins, P., Ward, R., Mitchell, A. S., & Bell, A. H. (2015). Connectivity between the superior colliculus and the amygdala in humans and macaque monkeys: virtual dissection with probabilistic DTI tractography. *Journal of Neurophysiology*, 114(3), 1947–62.

Chapter 5 tests for a functional association between the pathway connection strength of the SC and the amygdala and behavioural responses to visual threat measured during the saccade decision task in Chapter 3. This study aimed to provide evidence in support for the existence of a threat-mediating pathway connecting the superior colliculus with the amygdala through the pulvinar.

Chapter 6 investigates the association between responses to visual threat on the saccade responses measured in Chapter 3 and strength in connectivity of the stria terminalis, connecting the amygdala with the bed nucleus of the stria terminalis in healthy humans. This experiment tests the hypothesis that the stria terminalis plays a role in selective orienting to visual threat, in contrast to previous findings, which did not examine selective orienting, but rather arousal responses to threat. Chapter 6 is presented in the format of a brief communication ready for submission.

The thesis concludes with a general discussion in Chapter 7.

CHAPTER 2

SACCADE LATENCY BIAS TO TEMPORAL HEMIFIELD: EVIDENCE FOR ROLE OF SUPERIOR COLLICULUS IN MEDIATING REFLEXIVE SACCADES

Saccade latency bias to temporal hemifield: evidence for role of superior colliculus in mediating reflexive saccades

Abstract

The superior colliculus (SC) plays a critical role in mediating reflexive eye movements. Under optimal conditions, for example including a temporal ‘gap’ of 200ms after fixation offset and prior to target onset, it is possible to isolate a population of reflexive saccades with short latencies between 80-100ms. It has been shown that ablation of the SC disrupts express saccades in monkeys, however it remains to be established whether express saccade generation is dependent upon visual afferents transmitting direct retinal projections to SC via the retinotectal tract (RTT). This experiment combined behavioural and neuroimaging data from nineteen healthy participants to investigate whether express saccades demonstrate shorter latencies to targets in the temporal hemifield, a marker for RTT function, and whether a temporal hemifield advantage correlates with strength in connectivity measures (fractional anisotropy, FA) of virtual dissections of the RTT with diffusion tensor imaging (DTI) tractography. Saccade latency of a population of potential express, reflexive saccades that were isolated using a ‘gap’ paradigm demonstrated shorter latencies to peripheral targets in the temporal compared to the nasal visual hemifields. Strength in RTT connectivity (FA) did not demonstrate statistically reliable correlation with saccade latency, potentially due to inclusion of the brachium of the SC in the resulting streamlines. The advantages for reflexive saccades towards temporal hemifield targets suggest that visual afferents from the retina to the superior colliculus contribute to generating express saccades.

The superior colliculus plays a chief role in targeting and generating reflexive saccadic eye movements in order to orient the line of focus of salient visual signals onto the fovea (Schiller, 1998). Mean saccade latency in response to a peripheral target is typically 180-250ms (Carpenter, 1977; Wheelless, Boynton & Cohen, 1966). However, saccade latencies are considerably reduced during the ‘gap’ effect, which occurs when a temporal ‘gap’ of 200-300ms is introduced after offset of a fixated visual stimulus prior to onset of a peripheral visual saccade target (Saslow, 1967; Fischer & Ramsperger, 1986). Indeed, under these conditions, it is also possible to demonstrate a bimodal saccade latency distribution with an isolable population of very short latency (80-100ms) saccades, called ‘express saccades’.

Ablation of the SC in monkeys has been shown to abolish express saccades (Schiller, Sandell & Maunsell, 1987). However, it has not been shown in humans or non-human primates (NHP) that the visual afferents that trigger express saccades are transmitted via direct retinal projections to the SC, ie. the retinotectal tract (RTT). The goal of this experiment was to test the hypothesis that reflexive saccadic eye movements are triggered by retinal stimulation transmitted via the RTT. Toward this end I used a gap paradigm to generate reflexive saccades and used both a behavioural marker of RTT mediation, a temporo-nasal asymmetry, and diffusion imaging to examine a correlation between the latency of reflexive saccades and the connectivity strength of the RTT. For the neuroimaging component of the analyses, I introduce a novel technique for isolating voxels of the RTT on diffusion-weighted images.

Literature on the gap effect, the contributing role of the superior colliculus and the anatomical evidence for the retinotectal pathway is reviewed first, followed by a brief introduction to the current study.

The ‘gap’ effect and express saccades

Typically, saccade latency in response to a peripheral target is approximately 180ms-250ms in duration (Carpenter, 1977; Wheelless, Boynton & Cohen). However, introducing a temporal ‘gap’ of 200ms-300ms after fixation offset and prior to target onset considerably reduces saccade latency (Fischer & Ramsperger, 1984; Saslow, 1967). Saslow (1967) first showed this ‘gap’ effect in two human participants who demonstrated shorter saccade latencies with means of approximately 150ms when a 200ms ‘gap’ preceded the onset of a new peripheral target after the offset of a fixation point, compared to simultaneous target onset and fixation offset, which elicited saccade latencies with means of approximately 200ms. A gap of 200 ms was shown to be the optimal gap for producing short latency

saccades, with mean latencies increasing to approximately 250ms when the temporal gap was reduced to 100ms. Fischer and Ramsperger (1984) later replicated this experiment, showing that saccade reaction time distributions were bimodal during gap trials, with two peaks at approximately 100ms and 150ms, respectively, corresponding to a mean reaction time of approximately 125ms, closer to the fast saccade peaks reported by Salsow (1967). The first saccade latency peak in the bimodal distribution was termed express saccades, originally defined by their characteristically short latency of 70ms in the monkey, whereas the saccades in the second peak were classed as fast regular saccades (Fischer & Weber, 1993).

Fischer and Ramsperger (1986) subsequently showed that if subjects are trained on a gap paradigm for several days, the second peak of saccade latency decreases and the first increases, eventually giving rise to a single unimodal distribution of express saccades. Several studies have reported a lack of a bimodal distribution of saccades in gap paradigms, reporting unimodal distributions at peaks of 100ms with bimodal peaks inconsistently seen in independent participants (Wenban-Smith & Findlay, 1991; Reuter-Lorenz, Hughes & Fendrich, 1991). However, Fischer and Weber (1993) later demonstrated that although often observed, a bimodal distribution is not necessarily needed to produce express saccades. Accordingly, 17 naive participants demonstrated express saccades with bimodal distributions of express and slow saccades shown in 12 participants, with only 3 subjects showing only a unimodal distribution of express saccades. In contrast, in overlap trials when the fixation point remained visible simultaneous with target onset, a wide distribution peaking at approximately 200ms presented slow regular saccades.

The gap effect is therefore distinct from express saccades, and is a combination of several components. The visual grasp reflex (VGR), which occurs when the eyes fixate on a visual target, becomes disinhibited when the offset of a fixated target occurs before or simultaneous with the onset of a peripheral target (fixation offset effect, FOE), thereby reducing the latency of a saccade to the target. The fixation offset effect (FOE) likely triggers the shorter reaction time observed in gap paradigms as a result of fixation offset driven by oculomotor function (Reuter-Lorenz, Hughes, & Fendrich, 1991), combined with an alerting effect prior to target onset (Kingstone & Klein, 1993). The oculomotor specific FOE requires the offset of fixation stimuli that are at the fovea, whereas the gap effect additionally occurs for fixation stimulus offsets that are eccentric to the fovea which do not activate neurons in the rostral pole of the SC that inhibit eye movements (Fendrich, Demirel & Danzinger, 1999).

The reduction in saccade latency seen in gap paradigms has been attributed to several potential mechanisms including an alerting effect (Ross & Ross, 1980), sensory processing

(Reulen, 1984), oculomotor preparedness (Kalesnykas & Hallet, 1987; Saslow, 1967) or attentional mechanisms (Fischer, 1987). Reuter-Lorenz et al. (1991) demonstrated that the gap effect could be attributed to facilitated premotor processing in the superior colliculus. Firstly, Reuter-Lorenz, Hughes and Fendrich (1991) showed that the difference in saccade latency as a result of using the ‘gap’ paradigm was equal for bright and dim targets. Even though overall saccade latency was faster for bright compared to dim targets, the size of the gap effect remained the same between gap versus overlap trials for both bright and dim targets. This finding suggested that oculomotor processing of saccades occurs after initial sensory processing of luminance, resulting in a saccade latency that is the result of the timings of these two independent processes added together. Furthermore, their second experiment showed that the gap effect is exclusive to saccades made directly towards a peripheral target or ‘pro-saccades’, compared to ‘anti-saccades’, i.e. saccades made in the direction opposite to the target. Additionally, the reduced saccade latency caused by the gap effect was also not demonstrated for manual button press choices. Considering these findings that the gap effect is exclusive to pro-saccades and is additive with effects of luminance, Reuter-Lorenz et al. (1991) suggest that the gap effect may be driven by premotor processes initiated by the oculomotor system. Specifically, the gap effect could be attributed to processing mechanisms in the superior colliculus, since superior colliculus ablations abolish express saccades in monkeys, whilst causing only a mild reduction in latency of regular saccades (Schiller, Sandell & Maunsell, 1987).

Superior colliculus and the ‘gap’ effect

The superior colliculus is a laminated midbrain structure consisting of both superficial and deep layers. A retinotopic map is represented in the superficial layers, receiving direct projections from the retina to serve a visual sensory function (May, 2006). The superficial layers contain cells that respond to small visual targets without being sensitive to shape, orientation, colour or direction (Schiller, 1998). Cells in the deep layers of the superior colliculus respond to signals that instruct orienting behaviour such as somatosensory, visual and auditory cues. The size and direction of saccades depends on the location of superior colliculus stimulation, with the anterior, posterior, medial and lateral stimulation corresponding to small, large, upward and downward saccades, respectively (Schiller, 1998). Fixation neurons in the rostral pole of the superior colliculus (SC) are active during fixation with increased activity when a visual signal is additionally presented at fixation (Machado & Rafal, 2000). Consequently, movement cells in the caudal superior colliculus inhibit fixation

neurons. Combined, fixation and movement neurons control eye movements to locate a moving target in the periphery with the aim to fixate on it; an effect termed the visual grasp reflex (Machado & Rafal, 2000).

Anatomical investigations of the superior colliculus have suggested several potential routes of processing between the retina and oculomotor centres in the brainstem to mediate short latency saccades elicited in the gap paradigm (Fischer & Boch, 1990). Suggestions have included a projection to the superior colliculus direct from the striate cortex (Tootell, Hamilton, & Switkes, 1988) or via the frontal eye fields (Barbas & Mesulam, 1980) either through direct projection to the brainstem (Glicksten, May & Mercier, 1985) or indirectly via the superior colliculus (Künzle et al. 1976) or via the substantia nigra to the superior colliculus (Astruc, 1971). Another potential route of processing express saccades elicited during the gap paradigm is the retinotectal connection between retinal ganglion cells in the retina and the superior colliculus. It has not yet been established whether one route is exclusively responsible for the initiation of express saccades, or if several connections with the superior colliculus contribute to generating short latency saccades. By process of elimination, it is possible to infer which routes are likely contributing to mediating express saccades. For example, as previously mentioned, the ability to make express saccades is preserved after lesions of the frontal eye fields, whereas superior colliculus lesions abolish express saccades in the monkey (Schiller et al., 1987). The striate cortex cannot be ruled out as a possible processing route for express saccades, since express saccades can only be elicited with an intact visual cortex (Boch, 1989). Interestingly, lesions in the area of the pulvinar in the posterior thalamus abolished the inhibitory effect of visual stimuli at fixation for visually guided but not voluntary saccades (Rafal, McGrath, Machado & Hindle, 2004). This demonstrates that independent neural systems are likely in control of visually versus voluntary guided fixation with an important function for the pulvinar in controlling visually guided fixation. Together, these findings suggest a critical role of the superior colliculus in mediating express saccades elicited during the gap effect.

Functional role of retinotectal pathway in gap effect?

The retinotectal pathway, along with subcortical areas including the pulvinar and the amygdala, has been suggested to form part of a phylogenetically preserved older visual system thought to mediate ‘blindsight’, the ability of patients with lesion to the visual cortex to respond to visual targets in the absence of visual awareness (Weiskrantz, 1974). Kato, Takura, Ikeda, Yoshida and Isa (2011) demonstrated the role of the retinotectal pathway in

visually guided orienting by showing that monkeys with lesions to the visual cortex showed severe deficits in locating targets in their blind field (blindsight) following muscimol injections in the ipsilesional superior colliculus. The authors concluded that this effect could not have been solely as a result of a motor deficit, but rather a visual deficit created as a result of disruption in the superficial layers of the superior colliculus. Since the exact circuitry that mediates express saccades have not yet been established, and considering the prediction that the retinotectal pathway plays a role in residual visual function in the absence of striate cortex, it is important to investigate whether the afferents that activate reflexive saccades (VGR) are transmitted via the retinotectal pathway.

Several studies in animals have demonstrated the anatomy of the retinotectal pathway. For example, Leventhal, Rodieck & Dreher (1981) demonstrated that a variety of retinal ganglion cells project to the superior colliculus using retrograded horseradish peroxidase tracers injected in the retina of old world monkeys. Similarly, Perry and Cowey (1984) injected horseradish peroxidase into the superior colliculus of macaque monkeys, demonstrating retrograded tracing between cells in the retina and the superior colliculus. Approximately 10% of cells from the retina projected to the superior colliculus, of which the majority projected towards the contralateral hemisphere. A dominance of contralateral projections from the retina to the superior colliculus results in an advantage to process vision from the temporal visual hemifield. Such asymmetry has been a useful marker of retinotectal function in behavioural experiments demonstrating a bias to orient towards the temporal hemifield (e.g. Tomalski et al., 2009). In contrast, anatomical demonstrations of the retinotectal pathway in non-human primates demonstrate large projections from the retina to the superior colliculus. For example, in rats and rabbits, almost all retinal ganglion cells project to the superior colliculus (Linden & Perry, 1983; Vaney, Peichl, Wässle & Illing, 1981). Anatomical demonstrations of the retinotectal pathway with tracers are, of course, not possible in living humans. However, with the use of diffusion tensor imaging tractography it is possible to virtually dissect white matter tracts in the living human brain non-invasively. In this experiment, diffusion tensor imaging tractography was used to virtually dissect the retinotectal pathway in healthy human participants.

The current study: linking anatomy with behaviour

This experiment considered the role of the retinotectal pathway's direct projection to the superficial layers of the superior colliculus from the retina in saccade generation to peripheral targets in a gap paradigm. The goal was not to measure the 'gap' effect *per se* (i.e. fixation

present minus fixation offset reaction time (RT)). Rather, my goal was to attempt to isolate a subpopulation of short latency reflexive saccades (express saccades) that I hypothesise to be dependent upon retinotectal afferents. Toward this end, I used a gap paradigm, in which the fixation point offset 200 ms prior to target appearance, in order to provide optimal circumstances for participants to generate short latency ‘express’ saccades. If the retinotectal pathway is involved in generating short latency saccades in a gap paradigm, it was predicted that there would be a temporal hemifield advantage in measured saccade latency, especially for short latency saccades. Furthermore, strength in pathway connectivity of the retinotectal pathway may be reflected more strongly in saccade latency towards temporal versus nasal targets. Diffusion tensor imaging (DTI) tractography was used to virtually dissect the retinotectal pathway in healthy human participants. Saccadic reaction times in response to peripheral targets in a gap paradigm, along with measures of temporal and nasal saccade latency were predicted to correlate with strength in pathway connectivity of the retinotectal pathway across individuals

Method

Participants

A random sample of 19 healthy participants (9 male, age range 18-47) was recruited from the student population at Bangor University. Participants had no known neurological, psychological, psychiatric or cognitive impairments. The study was advertised on student online forums and via word of mouth. Participants were screened against exclusion criteria related to MR safety. Payment of £10/hour was provided for participation in MRI scanning and £6/hour for eye tracking. Participants had normal or corrected to normal vision. All participants were tested on three separate occasions each: MRI scanning for approximately 1 hour, in addition to two eye tracking sessions.

Virtual dissection of retinotectal pathway with probabilistic DTI tractography

Magnetic Resonance scanner. A Phillips 3 Tesla Achieva magnetic resonance (MR) scanner at the Bangor Imaging Unit at Bangor University was used to acquire T1-weighted anatomical and diffusion weighted images.

T1 anatomical scans. High resolution multi-echo T1 weighted images (0.7x0.7x0.7 mm isotropic voxel resolution) were acquired using an MPRAGE (magnetization prepared gradient echo) sequence.

DTI scans. DWI-EP (diffusion weighted imaging – echo planar) images were collected at 2x2x2mm with the following parameters: b-values = 0 (averaged four volumes) and 2000, b-directions = 61, slices = 76, section thickness = 2mm, TR = 2 s, TE = 35ms. The first 10 participants were scanned using a 16-channel head and neck coil, and 9 participants were scanned using a 32-channel head coil.

Data pre-processing. Following data acquisition, the image files for the DTI data and the structural T1 scans were manually converted from DICOM format into NIFTI with dcm2nii (<http://www.sph.sc.edu/comd/rorden/mricron/>). Subsequent data pre-processing was carried out using the FSL-FDT toolbox (Behrens et al, 2003; Behrens, Berg, Jbabdi & Rushworth, 2007; <http://fsl.fmrib.ox.ac.uk/fsl/fslwiki/>). Diffusion weighted images were corrected for eddy currents and head motion using affine registration to the first b-zero volume. This was carried out to prevent approximate stretches and shears created in the diffusion weighted images that may have been induced by eddy currents in the gradient coils (Behrens et al., 2007). After eddy current correction, diffusion tensor models were fitted at each voxel using the DTI-FIT tool in FSL. Diffusion parameters were calculated using the Markov Chain Monte Carlo sampling method. The DTI data was then prepared for probabilistic tractography via the BEDPOSTX tool in FSL's FDT toolbox. Probabilistic tracking was carried out using the PROBTRACKX tool in FSL's FDT toolbox. Prior to running the BEDPOSTX process, the non-diffusion brain image was extracted from the skull (using the FSL brain extraction tool (BET)), and a brain mask was formed. Anatomical T1-weighted scans were brain extracted using the BET-tool, and were registered with the B0 diffusion brain image, using FSL's FLIRT tool. Masks were drawn based on anatomical landmarks in each participant's individual non-diffusion T1-registered brain using FSLView.

Design. The goal of this experiment was to: 1) Achieve bilateral virtual dissection (with probabilistic DTI tractography) of the retinotectal pathway connecting the optic tract with the superior colliculus. 2) Correlate individual differences on two behavioural measures with connectivity strength of the retinotectal tract (measured with fractional anisotropy (FA)): 1: mean short saccade latency on modified 'gap' saccade task and 2: short saccade latency for temporal vs nasal hemifield saccade targets.

Procedure. Prior to MRI scanning, the participant was provided with a safety-screening questionnaire and interview. Once both the experimenter and the participant were satisfied that it was safe for the participant to be scanned, the scanning session started and lasted approximately 40 minutes.

Probabilistic tractography. For this experiment I developed a novel virtual dissection method to isolate voxels with retinotectal fibres for which FA values were computed. A streamline was generated between the optic tract just posterior to the optic chiasm (a very identifiable anatomical landmark) and the SC. This streamline contains voxels through which the RTT passes. However, most voxels in the resulting streamline also contain retino-geniculate fibres. Since only about 10% of retinal ganglion cells project to SC, most of the fibres in this streamline are not RTT fibres. It was therefore necessary to exclude, from computation of FA, those voxels that also contained retino-geniculate fibres. For this purpose, a mask was generated by virtually dissecting a second streamline that included voxels containing retino-geniculate fibres. This was achieved by using a mask on the calcarine cortex to create the streamline connecting the optic tract with visual cortex. Tractography between the optic tract and the superior colliculus was performed in both hemispheres of each subject's diffusion weighted images using the subject-specific masks 1) the superior colliculus (SC) and 2) the optic tract just posterior to the optic chiasm (*see Figure 2.1*). Masks were drawn manually on each subject's diffusion space registered T1-weighted anatomical brain image using anatomical landmarks. Streamlines were generated in both directions (ie. SC as seed and optic tract as waypoint mask, and vice versa). The common overlaps of the retinotectal tract in both directions were calculated in order to include only the voxels that would be most likely to be part of the tract. Figure 2.1 presents the SC and the optic tract region of interest masks in one representative subject. Region of interest masks used to dissect the retino-geniculo-striate pathway included masks in the optic tract and the primary visual cortex, also shown in Figure 2.1.

Measurement of FA values and statistical analyses. Each voxel of each tract represented the number of streamlines that passed through that given voxel. All voxels were thresholded so that only voxels containing at least 10% of the maximum number of traces were included as part of the final tract. As described previously, the common overlaps of the retinotectal tract in both directions for each participant were added to form a composite streamline for each participant. Composite streamlines for all participants were registered to the same brain space and added together to create one pathway demonstrating the common overlap within the sample. Additionally, after subtraction of the retino-geniculo-striate pathway from the RTT, the resulting isolated RTT streamline for each individual participant was registered to a common brain space and added together to form a composite isolated RTT streamline. This isolated composite RTT pathway was thresholded at 100% to include only the voxels that included streamlines common to all 19 participants in the sample. A

mask of these voxels was created for both left and right hemispheres. This mask was then registered to each individual participant's diffusion space and was used for computation of mean fractional anisotropy (FA) of voxels within each participant's isolated 100% overlapped RTT streamline. FA values for each hemisphere in each participant were included in the final statistical analyses.

The justification for using the 100% common overlap amongst participants, rather than individual trajectories for each participant was to exclude potential noise or spurious fibres that may have been included in certain participants' analyses. Given the possibility of inclusion of spurious connectivity when using DTI, using the common overlap of all participants ensured a higher accuracy in the dissection of pathways, whilst still allowing individual variability to be reflected through the measure of FA.

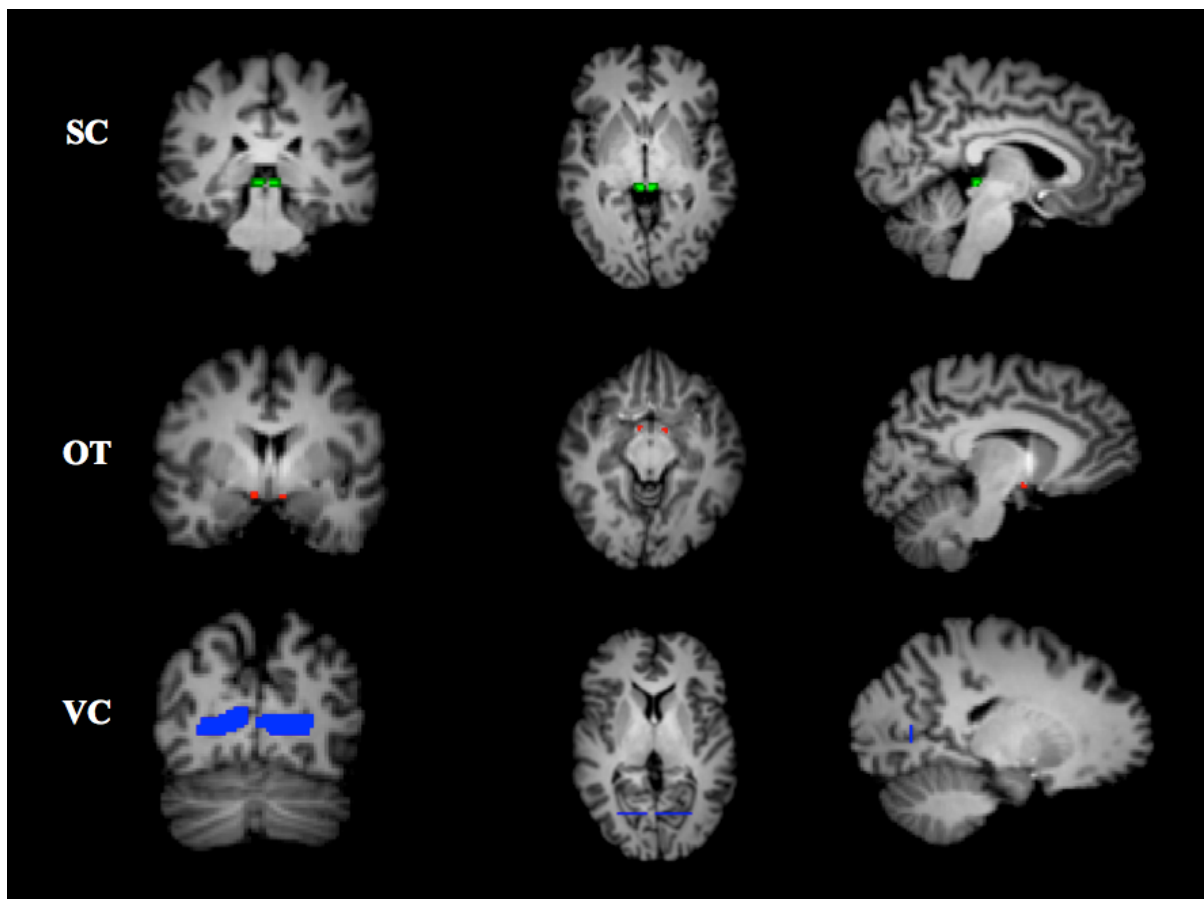


Figure 2.1. Region of interest masks for dissection of RTT and retino-geniculo-striate. Masks were drawn on coronal (left), axial (middle) and sagittal (right) slices that were used to virtually dissect retinotectal tracts and retino-geniculo-striate tracts. SC = superior colliculus (green), OT = optic tract (red), VC = visual cortex (blue).

Saccade measures on modified 'gap' paradigm

Eyetracking apparatus. An EyeLink1000® eyetracking device continuously recorded eye position and pupil diameter to an EyeLink Data File (EDF). Presentation software was used to generate visual stimuli and to output eye position data to the recorded data file. EyeLink1000® analysis software was used to measure saccade latency with the default setting of 30 degrees per second.

Experimental display set up. Presentation programming software ran the task using Microsoft Windows 7 on an iMac. A separate Dell display monitor (12.5x22inches) connected to the setup presented stimuli to the participant. This display monitor was measured to be 57 cm from the eye position of the participant, which allowed the degrees of the viewing angle to be controlled for across participants. A chin and headrest was attached to the table, which ensured that the participant was kept at 57cm away from the display monitor at all times and to reduce head movement during eye tracking. Each participant wore an eye patch to ensure monocular viewing conditions.

Stimuli. Stimuli consisted of white circles with a 3cm diameter and a white fixation cross (2cm x 2cm) presented on a black background. The fixation cross was continuously displayed between trials with an inter-trial interval (ITI) of 1000ms. At the beginning of each trial, a blank black screen replaced the fixation cross for 200 ms before presentation of the saccade target in order to provide the optimal temporal gap to enable generation of express saccades. Target stimuli were presented unilaterally and randomly in either the right or the left visual field. The eccentricity of the target stimuli was 15° between the target and the fixation cross (12° between centre of target and centre of fixation cross) in order to avoid having stimuli presented in the blind spot when it was in the temporal hemifield. Figure 2.2 presents the sequence of stimuli presented during each trial.

Design. Mean saccade latencies (dependent variable) toward temporal and nasal visual hemifield targets were compared within participants. Correlational analyses were carried out to investigate the relationship between strength in retinotectal pathway connectivity measured with fractional anisotropy and saccade latency towards peripheral targets in the temporal and nasal hemifields.

Procedure. Participants were verbally instructed to fixate on a central fixation cross and to look briefly and as accurately as possible towards a peripheral white circle which may appear either on the left or the right side of the fixation cross, and then fixate straight back again on the fixation cross. The experiment lasted approximately 5 minutes and participants were thanked upon completion of the task. Trials were presented to participants as follows:

when eye position was maintained within $\pm 2^\circ$ from the fixation cross, target stimuli appeared on-screen, preceded by a 200ms gap where a blank black screen was presented. Each block consisted of 60 trials. Stimuli were presented to participants under monocular conditions through patching of one eye during the first testing session, and patching of the other eye during the second session. Testing sessions occurred separately on consecutive days. Patching of the left or right eye first was counterbalanced across participants.

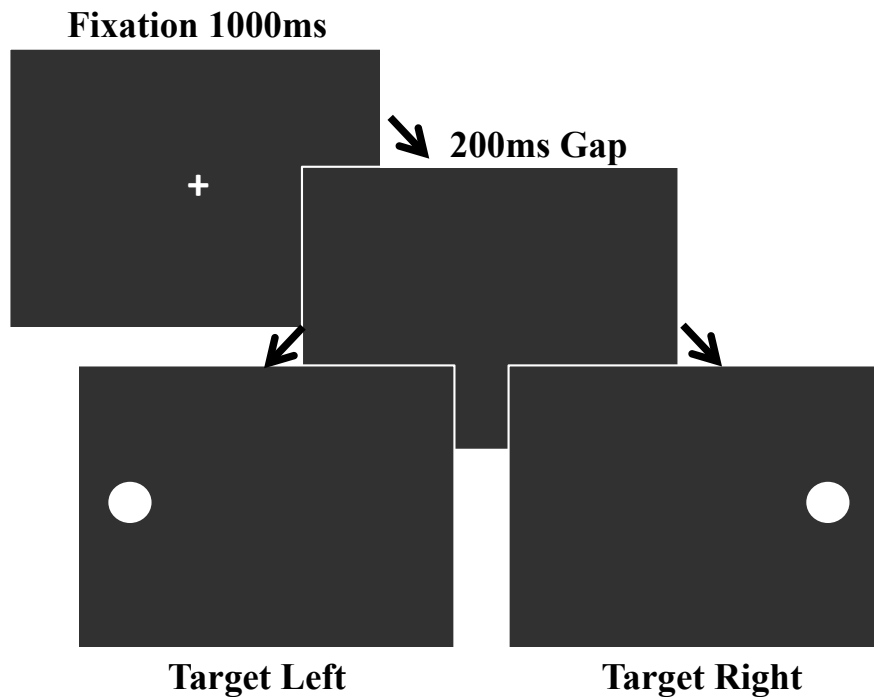


Figure 2.2. Sequence of stimuli presented during each trial on gap paradigm. Each trial was followed by an inter-trial interval of 1000ms (not shown). Under monocular viewing conditions, participants were instructed to saccade rapidly to the target appearing randomly on the left or right in equal proportions. The viewing angle between the target and fixation centres was 12° .

Ethical considerations. Prior to commencement of this study, ethical approval was received from Bangor University's Ethics Review Committee. Written consent was obtained prior to participation from all participants. This study used safe and non-invasive techniques that involved no known ethical concerns for participants. Participants were informed that their data and personal demographical information would be kept anonymous at all times. See Appendix A, B and C for copies of participant information and consent forms.

Results

Virtual dissection of retinotectal tract with diffusion tensor imaging (DTI) tractography.

Virtual dissection of the retinotectal (RTT) connection between the superior colliculus and the optic tract was demonstrated bilaterally in all 19 participants. In order to reduce noise, each tract was dissected twice: tracts were generated first using the optic tract region of interest mask as the seed mask, and the superior colliculus as the waypoint mask, and then repeated in the opposite order. All voxels in each streamline were thresholded so that only voxels containing at least 10% of the maximum number of traces were included as part of the final tract. The tracts were then added together (using FSL maths) and only voxels that ‘overlapped’, i.e. were present in both tracts, were isolated as the retinotectal tract for use in subsequent analyses. The virtually dissected streamline corresponded to the known anatomy of the RTT and ascended from the optic tract slightly dorsally, connecting to the superior colliculus laterally, via a trajectory around the posterior ventrolateral diencephalon. Figure 2.3 presents the common overlap of RTT tract voxels of all participants registered to a common brain space.

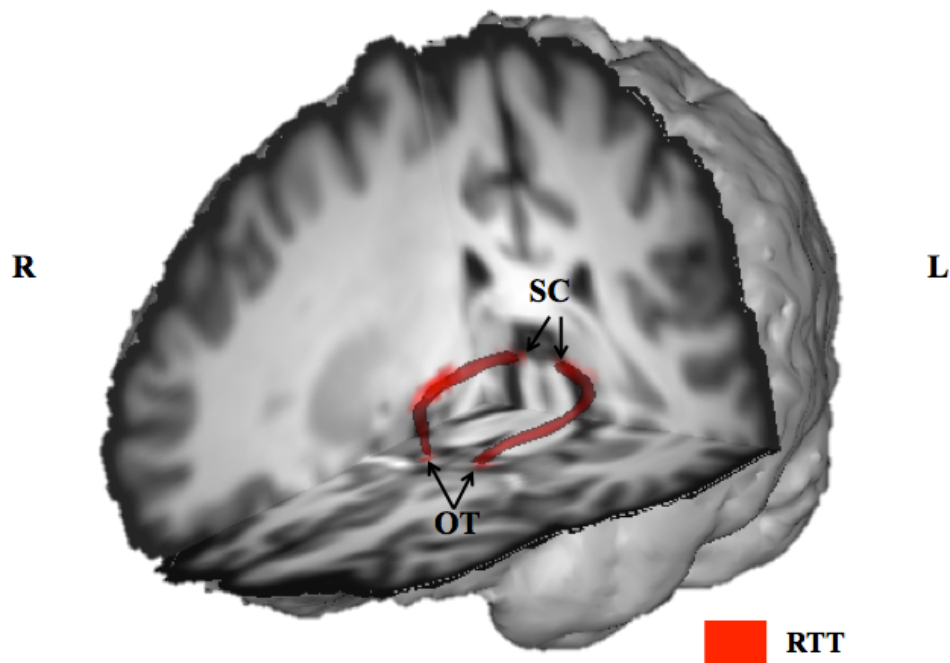


Figure 2.3. Bilateral retinotectal tracts virtually dissected with DTI tractography (N=19). Tracts (red) represent the common overlapping voxels in tracts of all participants (threshold at 66% participant overlap) registered to a common brain space. SC = superior colliculus, OT = Optic Tract, R = Right, L = Left. RTT = retinotectal tract.

In order to avoid including voxels shared with the retino-geniculate pathway in the optic tract and to isolate only voxels that were exclusive to the retinotectal tract, the retino-geniculo-striate pathways were subtracted from the RTT pathways resulting in an isolated RTT pathway remnant for each participant, presented in Figure 2.4. The isolated RTT tract represented the final part of the original RTT tract, forming a trajectory between the posterior ventrolateral diencephalon, entering the superior colliculus laterally. No anatomical differences were observed between the RTT, isolated RTT and retino-geniculo-striate tracts in the left versus the right hemispheres.

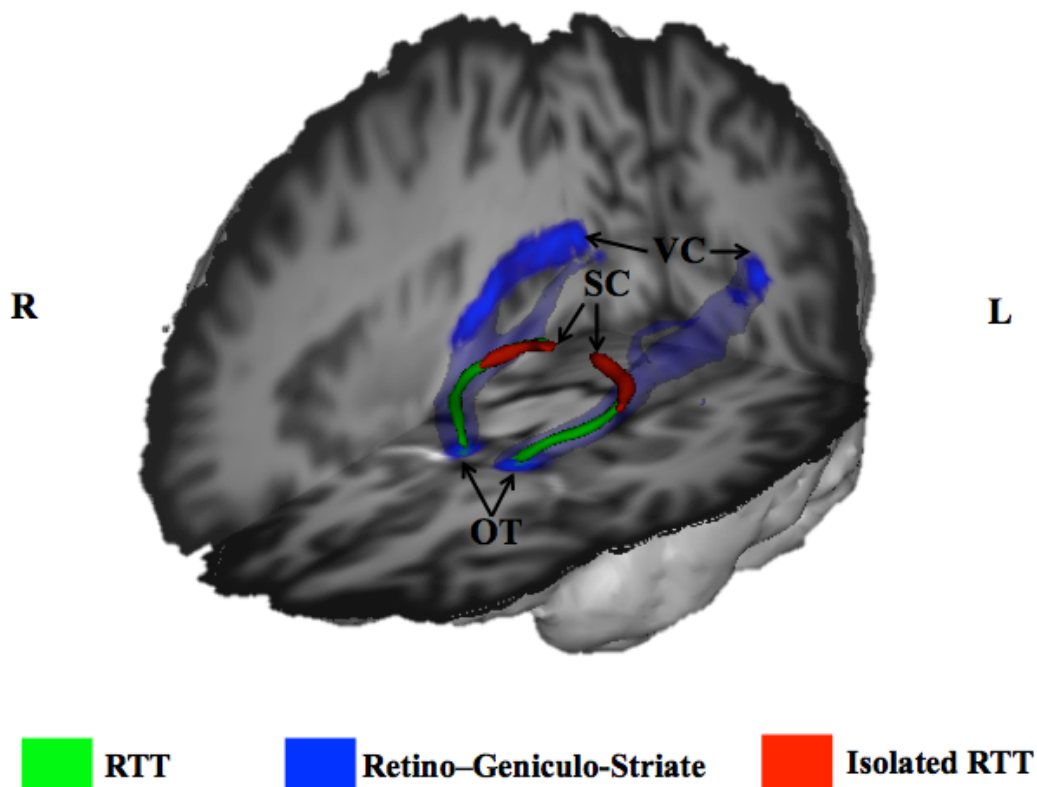


Figure 2.4. Bilateral isolated retinotectal tract (red), retinotectal tracts (green) and retino-geniculo-striate tracts (blue) dissected with DTI tractography (N=19). Isolated retinotectal tracts were created by subtracting dissected retino-geniculo-striate tracts from retinotectal tracts in each participant, in order to exclude voxels shared between retino-geniculate and retinotectal tracts. RTT = retinotectal tract.

Calculation of connectivity strength with fractional anisotropy (FA). RTT, isolated RTT and 100% overlapped isolated RTT tracts for each participant were used as masks on the fractional anisotropy (FA) image for each participant (generated with DTIFIT utility in the FTD toolbox of FSL) to calculate mean FA values for each of the three streamlines in each individual participant. Paired-samples t-tests demonstrated no significant differences in mean FA between left and right RTT pathways ($t(18) = -.39, p = .7$, two-tailed) or left and right isolated RTT pathways ($t(18) = .41, p = .69$, two-tailed). However, for the 100% overlapping voxels of the isolated RTT pathway a significant difference was observed for the left and right hemispheres across participants (mean difference = $-.03, SE = .01, t(18) = -3.12, p = .01$). Figure 5 presents the anatomical relationship between the composite isolated RTT (100% overlapped) and the composite RTT tract for all participants. Table 2.1 presents FA values of RTT and isolated RTT (100% overlap) tracts for each participant. FA values for isolated RTT tracts (100% overlap) only were used in analyses of saccade latency in the gap experiment (reported in Table 2.1 below).

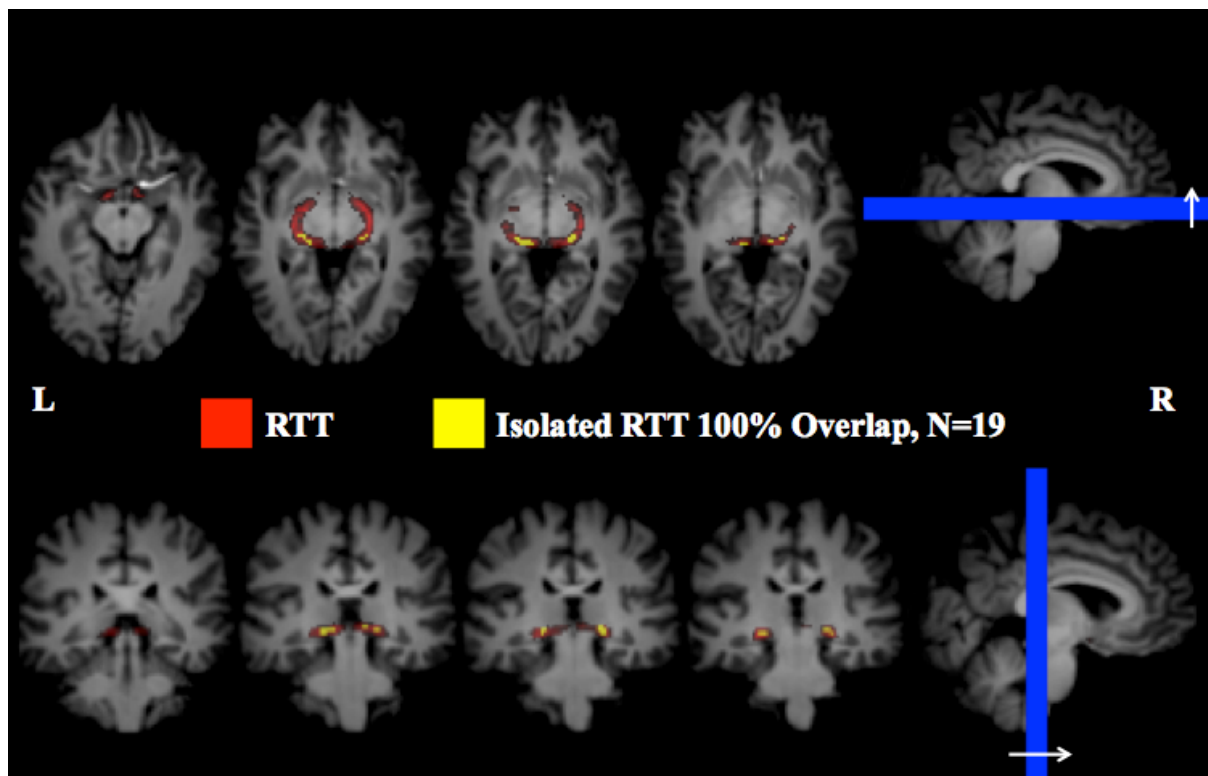


Figure 2.5. Composite streamlines for the retinotectal tract (RTT, red) and the isolated retinotectal voxels common to 100% of participants (yellow) virtually dissected with DTI tractography (N=19). Isolated retinotectal tracts (100% overlap) were created by subtracting dissected retino-geniculo-striate tracts from retinotectal tracts in each

participant, in order to exclude voxels shared between retino-geniculo-striate and retinotectal tracts. The resulting isolated retinotectal tracts were registered to common brain space and added together forming a composite streamline. This composite streamline was thresholded at 100% to include only retinotectal voxels common to all participants. RTT = retinotectal tract.

Table 2.1. Fractional anisotropy (FA) values for retinotectal and isolated retinotectal tracts.

Participant	RTT			100% Participant Overlap Isolated RTT		
	Left	Right	Average	Left	Right	Average
1	0.26	0.24	0.25	0.22	0.23	0.22
2	0.29	0.30	0.30	0.22	0.20	0.21
3	0.32	0.36	0.34	0.21	0.21	0.21
4	0.24	0.31	0.28	0.19	0.20	0.20
5	0.29	0.30	0.30	0.17	0.19	0.18
6	0.30	0.31	0.31	0.23	0.28	0.25
7	0.27	0.25	0.26	0.21	0.26	0.23
8	0.22	0.30	0.26	0.16	0.23	0.19
9	0.32	0.31	0.32	0.23	0.33	0.28
10	0.27	0.27	0.27	0.25	0.26	0.26
11	0.32	0.29	0.31	0.29	0.26	0.27
12	0.31	0.31	0.31	0.22	0.21	0.21
13	0.29	0.30	0.30	0.17	0.23	0.20
14	0.24	0.29	0.26	0.25	0.33	0.29
15	0.30	0.29	0.30	0.19	0.17	0.18
16	0.38	0.25	0.32	0.26	0.30	0.28
17	0.29	0.33	0.31	0.24	0.24	0.24
18	0.28	0.25	0.27	0.14	0.19	0.16
19	0.33	0.33	0.33	0.16	0.30	0.23
Total Average	0.29	0.29	0.29	0.21	0.24	0.23

Saccade latency measures on gap paradigm

Saccade Latency Distribution The majority of participants demonstrated normally distributed frequency histograms, however 7 participants demonstrated multiple saccade latency frequency distribution peaks, two of which demonstrated trimodal peaks. Figure 2.6 presents saccade latency distribution from 2 participants. Preliminary analyses demonstrated an overall mean saccade latency on all trials of $M = 182.75$ ($SD = 45.01$). Overall the distribution demonstrated a central peak with most saccades made between approximately 100-200ms. Trials that were regarded as probable anticipatory saccades (saccades < 70ms) were aborted and repeated during the experiment. Failures to respond (saccades > 350ms, 1.88%) and incorrect saccades towards the opposite direction of the target (7.58%) were excluded from analyses. Inclusion of these trials did not have a large effect on the overall outcome statistics.

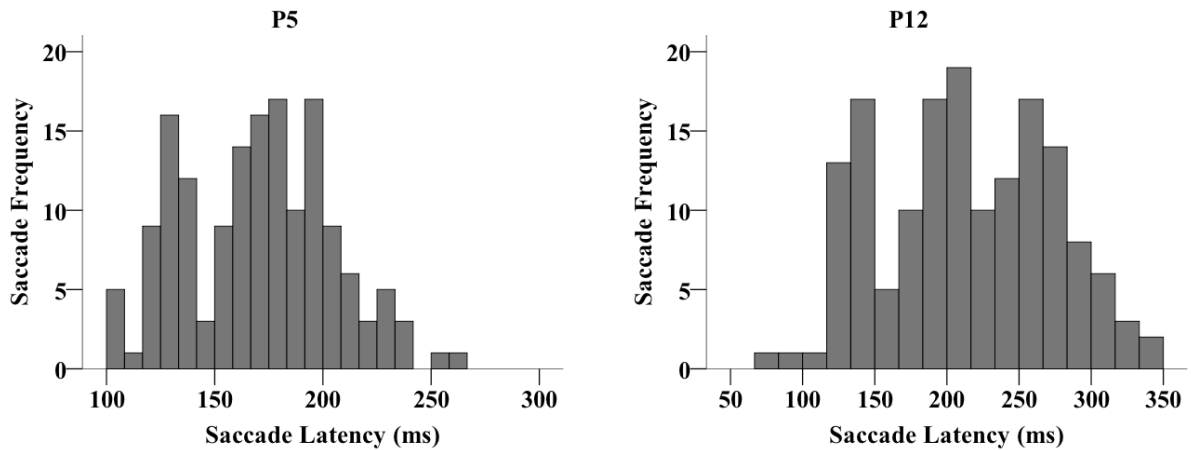


Figure 2.6. Distribution of saccade latency peaks for Participant 5 ($M = 169.74$, $SD = 58.46$) and Participant 12 ($M = 214.23$, $SD = 33.88$). Participant 5's saccade latencies demonstrated frequency peaks at 110ms, between 120-140ms, and 150-200ms. A trimodal distribution of saccade latency was observed for Participant 12, with three clear peaks between 120-150ms, 175-200ms and 250-275ms.

Effects of temporal and nasal visual hemifield on saccade latency: analysis of variance (ANOVA). A repeated measures ANOVA was conducted to test whether there was an advantage of temporal versus nasal target location on saccade latency. A 2 (eye view: left/right) x 2 (saccade response field: temporal/nasal) ANOVA showed no main effects of eye view (Wilks' lambda = .99, $F(1,18) = .19$, $p = .67$, multivariate partial eta squared = .01) or saccade response field (Wilks' lambda = .99, $F(1, 18) = .11$, $p = .74$, partial eta squared = .01) on saccade latency and no interaction between eye view and response field (Wilks' lambda = .93, $F(1,18) = 1.29$, $p = .27$, partial eta squared = .07). Figure 2.7 presents mean saccade latency of temporal and nasal saccades for left and right monocular eye view.

Since some participants demonstrated multiple saccade latency frequency distribution peaks, and some demonstrated populations of 'fast' saccade peaks at intervals earlier than others with ranges of 'fast' saccade peaks between 70-150 ms, saccades within this latency window were isolated as a separate population of 'fast' saccades or potential express saccades and was used for further analyses. Saccade latency means were averaged for left and right eyes for this analysis. A paired-samples t-test was carried out in order to test the planned prediction that 'fast' latencies were shorter in the temporal compared to the nasal visual hemifield. As expected, 'fast' saccades were shorter in the temporal compared to the nasal visual hemifield ($t(18) = -2.52$, $p = .01$ (one-tailed), mean difference = -5.31, $SD = 9.8$, Figure 2.8).

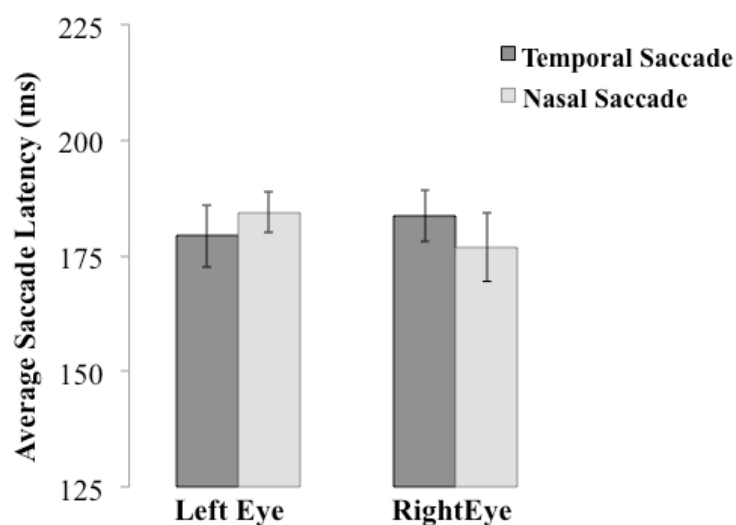
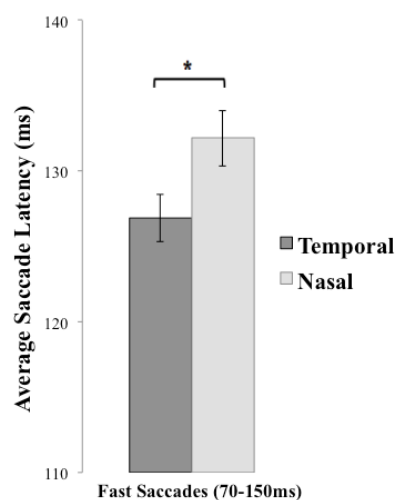


Figure 2.7. Average saccade latency measured on gap paradigm. Repeated measures ANOVA (2(eye view: left/right) x 2 (saccade: temporal/nasal)) showed no significant differences in temporal and nasal mean saccade latencies for the left or right monocular viewing eye (error bars present standard error of the mean).



* Denotes $p < .05$

Figure 2.8. Short latency saccades measured on gap paradigm. Saccade latencies for a population of short saccades (between 70-150ms) were shorter in the temporal compared to the nasal visual hemifield ($t(18) = -2.52$, $p = .01$ (one-tailed), mean difference = -5.31 , $SD = 9.8$). Error bars represent standard error of the mean.

Strength in connectivity (fractional anisotropy) of isolated RTT pathway (100% overlap) as predictor of saccade latency

Left and right hemisphere isolated RTT voxels (100% overlap) were averaged across left and right hemispheres for each participant and averaged fractional anisotropy (FA) was correlated

with saccade latency of the ‘fast’ group of saccades within the temporal and nasal visual hemifields. Mean FA of averaged isolated RTT voxels (100% overlap) for each participant did not correlate with the overall mean saccade latency of fast saccades (between 70ms – 150ms), presented in Figure 2.9 (Pearson $r = .29$, $p = .23$, two-tailed).

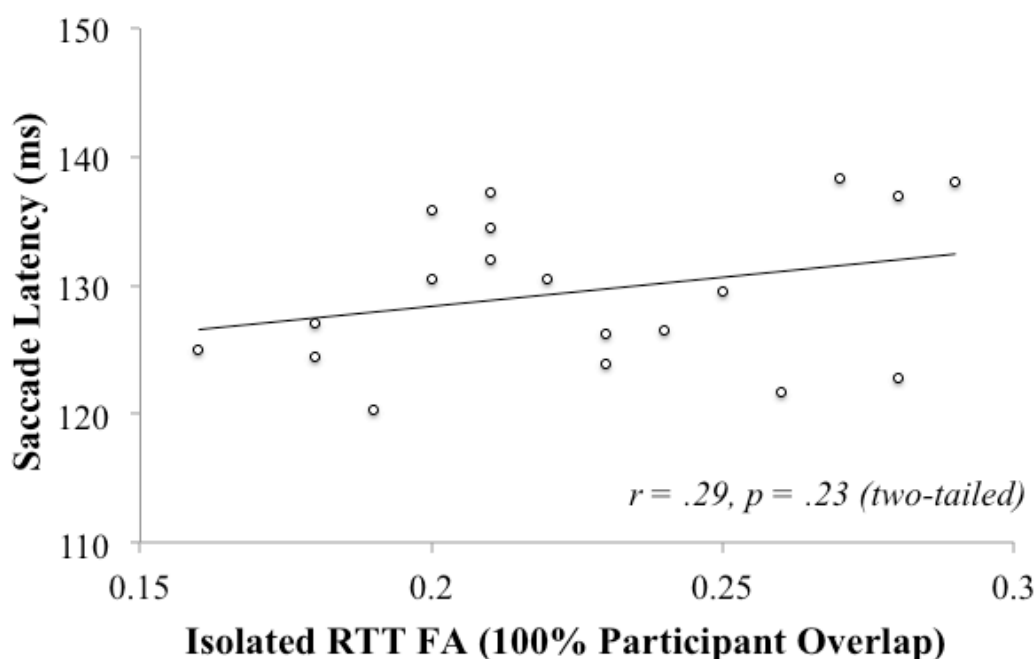


Figure 2.9. RTT FA as predictor of short latency saccades. Scatter plot demonstrating non statistically reliable correlation between strength in retinotectal pathway connectivity (FA, 100% overlap of isolated retinotectal voxels) and mean saccade latency within isolated short latency saccades (between 70-150ms). RTT = retinotectal tract.

Additionally, averaged isolated RTT voxels (100% overlap) mean fractional anisotropy (FA) values for each participant did not correlate with mean saccade latency of fast saccades (between 70ms – 150ms) in the temporal ($r = .41$, $p = .085$, two-tailed, (significance alpha set at 0.025)) or nasal ($r = .08$, $p = .75$, two-tailed) visual hemifields. Figure 2.10 presents scatter plots of correlations between mean saccade latency of fast saccades (between 70ms – 150ms) in the temporal and nasal visual hemifield with strength in connectivity (FA measures) of isolated RTT tracts (averaged across left and right hemispheres, 100% overlap) across participants. No significant correlations were observed between RTT FA (100% overlap) and overall saccade latency, or saccade latency in the temporal hemifield or nasal visual hemifields.

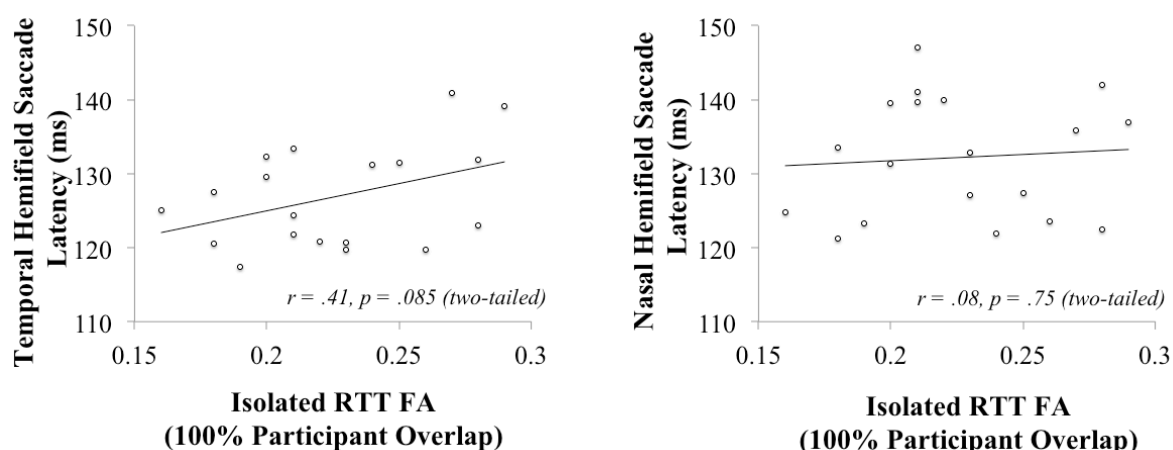


Figure 2.10. RTT FA as predictor of short latency saccades in temporal and nasal hemifields. Pearson correlation demonstrating no correlations between strength in connectivity of isolated retinotectal voxels (100% overlap across participants) with mean saccade latencies within a fast range of 70-150ms across individuals in the temporal (left figure) or the nasal (right figure) visual hemifields. RTT = retinotectal tract.

A post-hoc power analysis was conducted for the simple correlations of FA and performance carried out in this chapter and subsequent chapters throughout the thesis. Taking into account the significance level of $\alpha = .05$ and the sample size of 19 participants, the post-hoc power analysis suggested that a correlation coefficient of approximately $r = .59$ would be required to obtain statistical power at the recommended .8 level (Cohen, 1988).

Discussion

The aim of this study was to establish a functional role for the retinotectal tract (RTT) in mediating visually guided saccades on a modified gap paradigm. Virtual anatomical dissection with DTI tractography in this study confirmed bilateral RTT connecting the superior colliculus and the optic tract in 19 healthy human participants. As expected, saccade latency under gap conditions was faster than the regular saccade latency range previously reported. A smaller population of potential express saccades were observed, along with a majority of fast regular saccades. Furthermore, overall saccade latency did not show an advantage towards the temporal versus nasal visual hemi-field. However, an advantage for saccades towards the temporal visual hemifield (shorter latency) was observed in the potential population of express saccades. Based on the hypothesis that reflexive saccades are triggered by visual input through the RTT, this study included three predictions; 1) there

would be a temporal hemifield advantage for potential express saccade latencies, 2) saccade latency would correlate with strength in connectivity of the RTT, and 3) for express saccades, this correlation would be stronger for saccades in the temporal compared to the nasal visual hemifield. The demonstration of a latency advantage for short (potential express saccades) saccades in the temporal hemifield supports the first prediction. Strength in RTT connectivity measured with fractional anisotropy (FA) did not correlate with overall or short saccade latencies on the modified gap paradigm, and this effect was also not present for saccades in the temporal compared to nasal visual hemifields. These findings suggest a role for the superior colliculus in mediating visually summoned reflexive saccades.

Findings from this study demonstrated the majority of saccades below the latency of slow regular saccades, which is usually above 200ms (Fischer & Weber, 1993). The mean saccade latency reported was approximately 180ms faster than mean saccade latencies reported in non-gap paradigms (Saslow, 1967). For example, Saslow (1967) reported an average saccade latency of 150ms under gap conditions, compared to an average of 200ms during non-gap trials. The mean of the saccade latency peak reported in this study is close to saccade latencies of fast regular saccades, such as reports of 170ms by Fischer and Ramsperger (1993) and by Reuter-Lorenz, Hughes and Fendrich (1993) in some subjects. Furthermore, mean saccade latency observed here is around the same range of saccade latency in gap conditions (180ms-190ms) compared to non-gap conditions (199ms-223ms) reported by Fendrich, Demirel and Danziger (1999).

The distribution of saccade latency observed in this study demonstrated a central peak at approximately 170ms. However the majority of saccades were observed between the ranges of 120-200ms. Previous reports of bimodal distributions of saccade latencies under gap conditions reported an initial population of express saccades with mean latencies between 100ms-140ms followed by a second peak of saccade latencies between 150ms-200ms (e.g. Saslow, 1967; Fischer & Weber, 1993). Observations of saccade latency frequency distributions of participants in this experiment showed that the majority of participants (12) demonstrated distributions that were normal, with the remainder (7) demonstrating potential multi-modal distribution peaks. In two cases, participants demonstrated trimodal distributions, with clear saccade latency frequency peaks at approximately 130ms. Saccade frequency distributions reported in this study are in line with frequency distributions reported previously, showing bi- or trimodal distributions in some but not all participants (Fendrich & Weber, 1993).

An advantage to orient towards the temporal versus the nasal visual hemi-field was not observed in the overall population of saccades as has been observed previously for saccade latencies towards face-like stimuli (Johnson et al., 1990; Tomalski et al. 2009). Given the observation that ablation of the superior colliculus interrupts initiation of express saccades but not regular saccades, it was expected that, within a gap paradigm, saccade latencies towards the temporal visual hemi-field would be shorter compared to saccades towards the nasal visual hemi-field, given the dominance of contralateral fibres projecting from the retina to the superior colliculus. However, the superior colliculus is critical for initiating express but not regular saccades. Therefore, the observation of faster saccade latencies towards the temporal versus nasal visual hemifield for saccades between the range of 70-150ms, classed in this study as ‘fast saccades’, an effect not observed for regular saccades, suggest that ‘fast saccades’ observed in this study served as a proxy for reflexive, express saccades. Furthermore, the temporal-nasal asymmetry in express saccade latency under gap paradigm conditions observed in this study could potentially provide further evidence for the involvement of the superior colliculus in mediating express but not regular saccades. More critically, it shows, for the first time, that the role of the SC in generating express saccades is dependent upon afferent input to the SC via the RTT rather than solely via input from visual cortex.

Anatomical demonstration of the retinotectal pathway between the superior colliculus and the optic tract virtually dissected with diffusion tensor imaging (DTI) tractography in this study was similar to reported connections in animal studies (Leventhal et al., 1981; Perry & Cowey, 1984). The dissected RTT ascended from the optic tract dorsally, entering the superior colliculus laterally, via a trajectory around the posterior ventrolateral diencephalon. Whereas viral tracer studies in monkeys, rats and rabbits report detailed accounts of the exact internal anatomical locations where the tracers were observed, virtual dissections with DTI do not enable the same level of detail. For example, it was observed that the projection from the optic tract entered the superior colliculus dorso-laterally, with no detail with regards to the location of termination in the superficial layers of the superior colliculus.

It was expected that strength in connectivity measures (FA) for the RTT would correlate with saccade latencies on the modified gap paradigm across participants. Specifically, it was expected that, for short latency saccades, strength in pathway connectivity might correlate more strongly with saccade latency towards the temporal versus the nasal visual hemifield, reflecting the role of the superior colliculus via the RTT. Instead, both overall and short saccade latencies on the gap paradigm did not correlate with strength in

connectivity of RTT voxels (isolated from shared voxels with the retino-geniculate pathway). Furthermore, despite the advantage in saccade latency towards the temporal visual hemifield observed for short saccades, likely representing express saccades, no correlation between RTT connection strength (FA) and saccade latency for temporal or nasal visual hemifield responses were observed.

In order to interpret the lack of correlation between RTT FA and saccade latency it is important to consider a potential limitation. Upon visual inspection of the isolated RTT (Figure 2.5 in Results), it is evident that the isolated RTT shares voxels with the brachium of the superior colliculus, a region that is known to receive afferents from the primary visual cortex (V1) to the retina, also passes through the superior colliculus. Subtraction of the retino-geniculo-striate pathway from the RTT excluded retino-geniculate fibres, but not striato-collicular fibres from the RTT. Therefore, the isolated RTT in fact represent the brachium of the superior colliculus, containing both RTT and striato-collicular fibres. Therefore, this may account for a lack in correlation between RTT FA and saccade latency overall, and saccade latency to the temporal or nasal visual hemifields for short saccade latencies. One possible way to attempt to isolate the brachium from the RTT voxels may be to dissect and subtract the striato-collicular voxels from the RTT, however this approach is likely to remove all of the brachium of the superior colliculus voxels.

Furthermore, the use of a gap paradigm was chosen to isolate a potential population of express saccades that are more likely to be reflexive rather than voluntary. However, since the task used in this study required voluntary responses from participants, it is not possible to arbitrarily assume that all saccades that were isolated as short latency saccades (between 70-150ms) were exclusively reflexive. Therefore, the isolated potential population of express saccades likely comprised mostly, but not exclusively, of reflexive saccades. Similarly, overall saccades likely represented mostly, but not exclusively, voluntary saccades. It may be reasonable to expect that strength in connectivity of the geniculo-striate pathway may correlate with such a measure of voluntary saccades. Suggested future work could test this by isolating the geniculo-striate pathway from the RTT, and correlating geniculo-striate pathway connectivity with overall saccade latency on the gap paradigm.

In consideration of short saccade latencies, a small number of participants demonstrated larger differences between saccade latency towards temporal versus nasal visual hemi-fields, which could have resulted in the overall temporal bias observed. Additionally, since some participants may have made express saccades towards the temporal visual hemifield less frequently than others, this may have accounted for the advantage

observed for express saccade latency towards the temporal visual hemifield. In comparison with previous studies (e.g. Fischer & Weber, 1993; Fendrich, et al., 1999) the gap paradigm employed in this study included trials in which a temporal gap was present on every trial, compared to including both gap trials and overlap trials, where the fixation point remains visible simultaneous with peripheral target onset. Past experiments interpreted faster saccade latencies observed during gap trials, relative to slower latencies reported during overlap trials. Therefore, it is not possible to know whether saccade latency on non-gap trials would have been significantly slower compared to gap trials. However, since saccades using the gap paradigm in this study were reported to be within the same range as that of previous studies where both gap and non-gap trials were incorporated, this is a strong indication that the short saccade latency reported here was a result of inclusion of a 200ms gap after fixation offset and prior to target onset. Furthermore, contributions from the retino-pulvinar pathway would also be worth examining in the same data, given the finding that pulvinar lesion disrupts the fixation-offset effect for visually guided saccades (Rafal, McGrath, Machado & Hindle, 2004).

To conclude, contrary to what was predicted, connectivity strength of voxels in the retinotectal pathway (which included voxels shared with the brachium of the superior colliculus) virtually dissected with DTI tractography demonstrated no statistically reliable correlations with short saccade latencies in the temporal or nasal visual hemifields. This may have resulted due to a small number of RTT voxels shared with a large number of voxels of the brachium of the superior colliculus, receiving cortico-collicular afferents from the primary visual cortex to the superior colliculus. Therefore, future research could investigate whether it is possible to isolate RTT voxels, contributing to mediating reflexive saccades, from geniculostriate voxels, contributing to mediating voluntary saccades. Findings from this study demonstrated a latency advantage for saccades towards the temporal visual hemifield compared to the nasal visual hemifield for saccades between the ranges of 70-150ms, likely representing a majority of reflexive, express saccades. This effect was not present for saccades between the ranges of 70-350ms, likely representing a majority of voluntary saccades. This finding demonstrates that afferent input from the RTT to the SC contributes to generating express saccades.

CHAPTER 3

SACCADE BIAS TOWARD THREAT IN A SACCADE DECISION PARADIGM: CONNECTIVITY EVIDENCE FOR A ROLE OF THE SUPERIOR COLLICULUS

Saccade bias toward threat in a saccade decision paradigm: Connectivity evidence for a role of the superior colliculus

Abstract

Rapid orienting of attention to threat is critical for an organism to survive in a changing environment. A phylogenetically conserved subcortical visual processing route involving the superior colliculus has been suggested to mediate such rapid responses to threat. A novel temporal order saccade decision task was employed in this study to demonstrate a saccadic bias to threat when threat stimuli were presented with competing non-threatening images in nineteen participants. Additionally, an increased bias to threat in the temporal hemifield under monocular viewing conditions suggested a role for the superior colliculus (SC) in mediating responses to threat via retinal afferents of the retinotectal tract (RTT). Virtual dissection of the brachium of the superior colliculus with DTI tractography, which contained a minority of RTT streamlines, correlated with an overall saccade choice bias to threat, but not to threat in the temporal hemifield, suggesting that cortico-collicular afferents from the visual cortex to the SC additionally contribute to mediating voluntary saccadic choices to threat.

Orienting of attention is biased towards stimuli with biological relevance, such as faces that contain emotions of anger or threat (Bannerman, Milders, & Sahraie, 2010, 2009; Fecica & Stolz, 2008; Kissler & Keil, 2008; West, Anderson, & Pratt, 2009). This advantage has been argued to be a critical survival mechanism mediated by a phylogenetically conserved primitive visual system involving the superior colliculus, the amygdala and the pulvinar nucleus of the thalamus (Morris, Ohman, & Dolan, 1999). The rationale for this study was to design an experiment that would measure a bias to threat that could serve as a basis for investigating the functional relationship between proposed subcortical threat-mediating pathways virtually dissected with diffusion tensor imaging (DTI) tractography. The current chapter presents a novel temporal order judgement paradigm to test a bias to threatening compared to pleasant stimuli. The goal was to demonstrate a choice bias to threat that is larger in the temporal visual hemifield, representing a temporal-nasal asymmetry characteristic of retinotectal tract (RTT) mediation. Furthermore, the aim was to establish a functional role for the RTT in orienting attention to threat, by demonstrating that RTT strength in connectivity predicted choices to threat stimuli. Attentional mechanisms involved in measuring emotion, behavioural measures of emotion, the use of eye movements as a measure of attending to emotions and the temporal order judgment (TOJ) paradigm as a tool to study bias to emotional stimuli are reviewed in the introduction prior to the introduction of the current study.

Emotions have the ability to influence our behavioural responses to emotionally valenced stimuli, for example to approach or avoid an object in the environment. Limited attentional processing capacity means that we cannot simultaneously provide equal attention to all stimuli in the environment, and are therefore 'pre-programmed' to selectively attend to some stimuli over others for survival. Two chief processes influence such selective attention. First, exogenous attention driven by low level perceptual stimulus characteristics, occurring when a stimulus has salient physical features (e.g. abrupt onset, sudden motion, visually looming) resulting in rapid involuntary orienting of attention towards the stimulus (Pool, Brosch, Delplanque, & Sander, 2015). Secondly, endogenous attention, a much slower voluntary process (often presumed to be conscious), occurs when attention is oriented towards a stimulus relevant to a given task (Folk, Remington & Johnson, 1992). Several studies have reported that attention is biased towards emotional stimuli when several stimuli compete for attention (Yiend, 2010), which has been suggested to be a potential third influence on attention (Vuilleumier, 2005). Similar to exogenous attention, emotional attention is fast and involuntary, and has been shown to be mediated by the amygdala,

differing from structures that mediate exogenous and endogenous attention (Vuilleumier, 2005; Vuilleumier & Brosch, 2009). Investigations of the neural substrates of emotion have emphasised that automatic rather than voluntary processes are responsible for mediating fear and anxiety (Le Doux, 1996; Ohman, 1993). In line with the theory that a subcortical visual system in the brain has been phylogenetically preserved for survival, it has been suggested that neural structures sensitive to biological stimuli related to threat have unique relevance and can capture attention before conscious evaluation occurs (Bar-Haim, Lamy, Pergamin, Bakermans-Kranenburg & Van Ijzendoorn, 2007).

Attentional mechanisms in measuring emotion

The bias to orient towards stimuli with emotional content over others has been attributed to attentional mechanisms. Several components of attention have been suggested to be at play during attending to a stimulus. For example, Posner and Boies (1971) proposed three components of attention; alertness, selectivity and processing capacity. Alertness occurs during tasks in which participants are required to maintain attention for long periods of time. For example, a foreperiod of a reaction time task provides a warning signal to the participant to remain vigilant and to maintain attention to possible targets that may appear. Selective attention occurs when participants are required to maintain attention in order to select information from one source compared to another. Limited processing capacity controls attention by allowing us to understand how two processes interfere with one another when executed at the same time, allowing insight into which processes demand priority, such as noticing a snake in the environment in order to execute an escape plan.

Attention capture has been used as a term to describe when a stimulus is able to bias attention when top-down and bottom up processes are competing (Theewes, 2010). The process of attending to a new stimulus has been proposed to include components of attention that may be interpreted in three steps; initial orienting of attention towards a stimulus, engaging of attention with the stimulus and disengaging attention away from the stimulus (Posner, 1980). It is understood that the attentional capture by threat involves the first two components where the third involves disengaging from the stimulus.

Behavioural measures of emotion

Several paradigms have been used to measure behavioural responses to emotional stimuli focusing mainly on measuring manual response reaction times. Such paradigms have included visual search, emotional Stroop, dot-probe and spatial cueing tasks. Each paradigm

has measured different aspects of attentional selection (Pool, Brosch, Delplanque & Sander, 2015).

The visual search paradigm is a primary tool to test attentional preference amongst competing stimuli (Bar-Haim et al., 2007). Visual search paradigms require participants to search for a target stimulus presented amongst distractor stimuli. Attention capture is often measured as a search slope, where an increase in the number of distractors amongst a target is typically proportional to an increase in reaction time. The search slope measure provides an index of how rapidly the target can demand attention by filtering out attention to distractors. For example, Eastwood, Smilek and Merikle (2001) demonstrated that search slopes were steeper for visual search responses towards a happy face among neutral distractors, compared to an angry face among neutral distractors, since angry faces captured attention more rapidly. Alternatively, when reaction time to a target amongst distractors is independent of the amount of distractors present, the attention demand by the target represents a ‘pop out’ effect (Treisman & Gelade, 1980). Several studies have also reported shorter manual reaction times towards positively valenced target stimuli presented amongst distractor stimuli rather than to negatively valenced stimuli (Fox, Russo, Bowles, & Dutton, 2001; Lundqvist & Öhman, 2005; Öhman, Flykt & Esteves, 2001, Öhman, Lundqvist & Esteves, 2001). Furthermore, Hunt, Cooper, Hungr, & Kingstone (2007) demonstrated no difference between reaction time to search for an angry face target compared to other targets. Visual search tasks have also been used in the context of studying processing of emotional stimuli in anxious individuals (Hadwin et al., 2003; Rinck, Becker, Kellermann & Roth, 2003).

The classic Stroop task was designed to show that some stimuli automatically capture attention and that their processing cannot be fully inhibited. The classic Stroop task, for example, showed that word reading is automatic. The Stroop effect is the difference in colour-naming performance between congruent stimuli, for example a blue word presented in the colour blue, and incongruent stimuli, for example a green word presented in the colour blue. The Stroop effect is manifest as increased latencies in the incongruent naming condition, representing interference in ability to focus attention exclusively on colour. Adapted from the classic Stroop paradigm, the emotional Stroop paradigm tests for emotion-related bias by measuring colour naming in the presence of a stimulus of emotional importance. A bias to emotion-related stimuli is observed when the time for colour naming is extended in the presence of an emotion compared to a neutral stimulus (MacLeod, 1991). Despite its initial wide use, the Stroop paradigm for testing emotional bias has been critiqued for potentially allowing delayed response times as a result not due to interference by

emotional stimuli, but due to processes independent of attention (Algom, Chajut & Lev, 2004). Additionally, De Ruiter and Brosschot (1994) suggested that active avoidance, not attentional capture, is responsible for the Stroop effect initiated by threat stimuli in the emotional Stroop task.

In order to avoid such interpretive problems, the dot-probe paradigm was designed by MacLeod, Mathews, & Tata (1986), supported by the rationale that true interference from threat-related stimuli will be detected more robustly when participants perform neutral responses to a target unrelated to the valence of the stimulus, i.e. a visual dot probe. In this paradigm, the participant is required to respond via button press to the position of the dot probe, and instructed to ignore any other distractor stimuli. A distractor stimulus, typically either a neutral or emotionally valenced stimulus, appears at a time interval prior to the target dot onset. Attention capture is measured by a shorter reaction time to the target dot probe following presentation of an attention demanding distractor, thereby ‘probing’ for the influence of emotion. The effect of a distractor may also be demonstrated through a delay in reaction time, representing avoidance of attending to a distractor. For example, Macleod et al. (1986) reported that visual attention was shifted towards threat-related words in clinically anxious individuals. This effect was demonstrated through shorter reaction times when the dot-probe was presented in the same location as the threat-related compared to neutral-related word. In contrast, normal controls shifted attention away from threat-related words, demonstrating longer reaction times when the dot-probe and threat-related word appeared in the same location. Thus, reaction time latency on the dot-probe paradigm reflects an index of attention towards emotionally related stimuli.

The use of dot-probe paradigms has offered several advantages when measuring the effect of emotional stimuli on visual attention. For example, the attention advantage towards dot-probe target stimuli are strong indicators of bias driven by stimuli with emotional content since participants are responding to a neutral target, the dot-probe, and the possibility that attention is delayed due to response bias or general arousal is eliminated (Bar-Haim et al., 2007). Furthermore, the dot-probe paradigm allows for the manipulation of stimulus onset asynchrony, allowing for insight into the time-course of attentional orienting. However, the use of the dot-probe test does not allow for the separation of attention bias due to initial orienting to, or disengaging from the emotional cue. However, some dot-probe experiments have included a baseline condition with two neutral cues (Koster, Crombez, Verschuere & De Houwer, 2004). In this paradigm, initial orienting bias is reflected when faster reaction times are observed towards the dot-probe in the same location as the emotional cue, relative to this

baseline comparison. Similarly, disengagement of attention to the emotional cue is reflected when reaction times are faster towards the target dot-probe in the opposite location to the emotional cue, relative to the neutral-neutral baseline condition.

Posner's (1980) classic spatial cueing paradigm involved the presentation of a cue predicting the likely appearance of a target at one of two locations, followed by a target presented mostly at the cued location, representing the valid-cue condition. On a small proportion of trials the target appears at an alternative location, representing the invalid-cue location. Typically, performance is facilitated in processing targets at validly cued locations. The advantage for valid cue location trials has been suggested to represent the engagement component of attention, whereas slower reaction times to invalid cue trials has been attributed to result from the difficulty in disengaging from the cue location stimulus.

Stormork, Nordby and Hugdahl (1995) tested for attention bias to emotion stimuli by adapting the spatial cuing paradigm. They manipulated the spatial cue by making it a stimulus with emotional content. Using this emotional spatial cueing paradigm, Fox, Russo, Bowles and Dutton (2001) tested for threat-related attentional capture in anxious individuals. Threat related bias was shown for performances when the threat cue and the target appeared at the same locations. An attention bias on valid cue trials when the cue was threat-related, suggests that the attention advantage took place at the early orienting stage. In contrast on invalid cue trials, when the target and cue appeared at different locations, a difficulty in disengaging attention from threat is demonstrated. Similar to the dot-probe paradigm, participants are instructed to ignore the identity of the cue and the target is neutral, thereby ruling out attributing the attention advantage due to random response bias. However, unlike the dot-probe task where stimuli compete for attention, the spatial cueing paradigm involves only one target presented in the visual field.

Eye movements and attending to emotions

The majority of paradigms measuring attention bias towards emotion have measured manual responses. However, Bannerman, Milders, & Sahraie (2009) noted that both visual search and dot-probe paradigms do not provide information regarding the time-course for detection and attentional shifts directly towards the emotional target, thereby assessing attention only indirectly. Furthermore, the interval between the stimuli and dot probe allows only a rough evaluation of the time course of visual attention response latency. Early studies that used eye-movements to monitor visual attention to emotional stimuli focused on the first landing position and fixation duration on a target stimulus, providing little information on specific

temporal dynamics of visual attention to emotional stimuli (Bannerman et al., 2009). Also, manual response latencies are substantially longer compared to saccade latencies, even though both measures of response time include time taken for perceptual, motor and execution processes to take place. For example, where eye movements can be executed as fast as 120ms in categorisation tasks (Kirchner & Thorpe, 2006), average manual response latency is approximately 450ms (Thorpe, Fize, & Marlot, 1996). The stimulus asynchrony between cue presentation and target onset further influences the allocation of attention. The majority of studies used manual reaction time responses and cue durations ranging between 100ms-500ms (Bannerman et al., 2010). Delayed disengagement or sustained attention and detailed perceptual processing result from long cue durations (500ms) and not attentional capture by threat (Yiend & Mathews, 2010), whereas short cue durations (100-300ms) produce varying results (Bannerman et al., 2010). For example, Koster, Crombez, Verschuere, Van Damme and Wiersema (2006) demonstrated both attentional capture and disengagement at shorter cue durations in anxious individuals. However, Fox et al. (2002) reported only disengagement effects. Additionally, differences in cue-target asynchrony (e.g. 150-960ms) affect the time course of attentional allocation thereby altering reaction time.

For such reasons, saccade latency may be a more sensitive measure of attention bias, and as noted by Henderson (2003), saccades represent an overt behavioural demonstration of attention allocation, making saccade latency measures optimal for studying the temporal dynamics of attention in real time. Furthermore, faster orienting of attention via eye movements makes sense from an evolutionary perspective, since extracting information from the environment in one single glance is critical for survival (Bannerman et al., 2009).

Studies on measuring a bias to emotional stimuli with the use of eye movements have not been as plentiful as manual responses, however several studies have been carried out. Bannerman et al. (2010) carried out an experiment to investigate the time course of attentional orienting towards fearful faces using an adapted version of Posner's (1980) spatial cueing task described. Using both manual and saccade response measures and cue durations of 20ms and 100ms, Bannerman, Milders & Sahraie, (2010) demonstrated that attentional capture was exclusive to saccade responses at short (20ms) cue durations. Furthermore, delayed disengagement occurred for saccades at short (20ms) cue durations, whereas delayed disengagement of fear occurred at later cue durations (100ms) for manual responses. These findings suggest manual response cueing effects develop at a later time in comparison with saccadic cueing effects. This finding is consistent with emotion theories suggesting that attention is rapidly biased to environmental fear stimuli, which, as suggested by Bannerman

et al. (2010), may be revealed by saccade but not manual responses. Furthermore, in another experiment, Bannerman, Milders, and Sahraie (2009) showed that the speed of discrimination between emotional (fearful, angry and happy) and neutral faces presented simultaneously for 20ms to the left and right sides of a fixation cross was faster when the emotional face rather than the neutral face was the target to localise. Furthermore this effect occurred at both short (20ms) and long (500ms) presentation durations for saccades, but occurred only at longer durations for manual responses, further supporting the measure of eye movements as a faster measure of discrimination between neutral and emotional facial expressions.

Kissler and Keil (2008) additionally demonstrated that emotional content influences saccade latency to peripheral targets. They presented peripheral neutral, pleasant or unpleasant pictures, and participants were required to saccade towards (pro-saccade) or away (anti-saccade) from the target. Peripheral stimuli appeared either simultaneous with fixation offset, or after a 200ms gap. Interestingly, shorter saccade latencies were demonstrated for emotional versus neutral pictures in the left visual field, whereas this effect was seen only for pleasant pictures in the right visual field with slowed saccade latencies towards unpleasant pictures observed in the right visual field. Additionally, more errors were observed for anti-saccades towards emotional in comparison to neutral stimuli. Together, the above-mentioned findings suggest that saccades rather than manual reaction time responses may be better indicators of bias to emotionally relevant compared to neutral stimuli.

The temporal order judgment (TOJ) paradigm as a tool to study bias to emotional stimuli

Temporal order judgement (TOJ) paradigms typically involve the presentation of two stimuli at different time intervals, or stimulus onset asynchronies (SOAs), thereby allowing the rate at which a stimulus is processed to be assessed (Fecica & Stolz, 2008). When the participant is presented with two stimuli, their task is to judge which stimulus appeared first. The time difference between the onsets of the two stimuli allows for the manipulation of processing time of a given stimulus so that when the stimuli are presented at short SOAs, resulting in a difficult judgement of which stimulus appeared first, the participant regards the stimulus that is processed first as the stimulus that appeared first. This has been attributed to the effect of visual ‘prior entry’, the notion that a stimulus that is attended to seems as if it appears prior to an unattended stimulus (Titchener, 1908, Schneider & Bavelier, 2003).

The temporal order judgment paradigm has been used as a tool to study if stimuli with emotional content can show visual prior entry. Fecica and Stolz (2008) investigated the influence of facial expression affect on perception of order of stimulus presentation using the

temporal order judgment paradigm. They demonstrated that when participants were presented with two schematic faces to the left and right of fixation at varying stimulus onset asynchronies, facial affect influenced perception of temporal order for short (17ms) but not for long (100ms) SOAs. During short SOA's, participants chose the emotional (angry/happy) relative to neutral face as the stimulus that appeared first the majority of the time. Furthermore, during trials in which the emotional and neutral face appeared simultaneously (0ms, synchronous onset), participants chose the emotional stimulus as the face that appeared first above chance of what would be expected if two neutral stimuli were presented.

Consistent with such findings, West, Anderson & Pratt (2009) also showed that facial threat showed visual prior entry effects on the temporal order judgment paradigm. In a series of experiments using manual response measures, West et al (2009) showed that proportions of choices were higher to faces that displayed a threatening emotion (e.g. anger) compared to faces that displayed a neutral emotion for both schematic and photographic face images. Furthermore, this advantage for threat displaying faces remained when threat faces were competing with inverted threat faces, suggesting that the response bias was specifically driven by the emotion of the face, and not low level physical properties of the image. Such findings further support the idea that stimuli with emotional relevance capture attention more than neutral or biologically relevant non-threatening stimuli when presented concurrently.

The current study

The current study tested the hypothesis that saccade latency and choices are biased towards threatening compared to biologically relevant, non-threatening pleasant stimuli on a novel temporal order judgment paradigm. As reviewed in the General Introduction and in Chapter 2, the processing of threatening stimuli has been suggested to be mediated through a subcortical network transmitted through the retinotectal tract and then, from the SC, via a putative threat mediating pathway connecting the superior colliculus with the amygdala via the pulvinar nucleus of the thalamus. The goal of this experiment was to develop a paradigm to measure a bias to threat that could be employed to: 1) test the hypothesis that threat information is transmitted to the SC via the retinotectal pathway by demonstrating a temporal hemifields advantage to saccade toward threatening stimuli and; 2) test whether a bias toward threat correlates with strength of pathway connectivity (measured with FA) of subcortical pathways proposed to play a function in threat and subcortical visual processing.

This novel adaptation of a saccade decision task based on the temporal order judgement paradigm was selected over other paradigms measuring responses to threat since it

would allow for the capture of both an orienting bias to threat and a bias to the temporal versus the nasal visual hemifield, suggested to be a characteristic feature of retinotectal pathway function. Threatening and non-threatening stimuli were presented to the left and right of fixation at three stimulus onset asynchronies; threat first (53ms), simultaneous (0ms) and non-threat first (53ms). Temporal order judgements during the simultaneous condition were predicted to be biased toward threatening versus non-threatening stimuli and to be biased to the temporal visual hemi-field. It is expected that a bias to threat would be larger in the temporal compared to the nasal visual hemifields, if the expected bias to threat is indeed mediated by a subcortical network involving the retinotectal pathway (Chapter 2). Another goal of the current experiment was to establish a measure of ‘threat bias’ that could be correlated with the strength in connectivity of potential pathways that have been virtually dissected with diffusion tensor imaging (DTI) tractography in this thesis that are expected to play a role in threat processing. Therefore, it was planned to correlate the measure of saccadic threat bias of the temporal order judgment experiment with strength in connectivity (measured with fractional anisotropy, FA) of the retinotectal pathway in the current chapter, the proposed threat mediating pathway connecting the superior colliculus and the amygdala via the pulvinar nucleus of the thalamus in Chapter 5, and the stria terminalis connecting the amygdala with the bed nucleus of the stria terminalis in Chapter 6.

Method

Participants. Participant, eye tracking apparatus and experimental display set up information in addition to ethical considerations are outlined in Chapter 2 Methods.

Stimuli. Threatening and pleasant images were selected from the International Affective Picture System (IAPS) of emotional photographs that have been rated as pleasant or threatening based on 14 separate studies involving ratings of 60 pictures (Lang, Bradley & Cuthbert, 1999). Each image measured 9.5cmx9.5cm. Figure 3.1 presents examples of threatening and pleasant images used during this experiment. A full list of stimuli pairs used for this experiment is presented in Figure 3.8. In a previous experiment, selected high arousal ‘threatening’ images (e.g. shark) were matched for arousal in ‘pleasant’ images (extreme sports). However, following a pilot study in our lab, participants reported some of the pleasant images to be ‘threatening’, which resulted in the selection of lower arousal ‘pleasant’ images (e.g. bunny, flower) for this experiment. However, a paired samples t-test showed a significant difference in the mean arousal ratings for threatening ($M=6.0$, $SD=0.78$) compared to pleasant ($M=3.8$, $SD=0.61$) stimuli ($t(9) = 7.65$, $p<.001$).

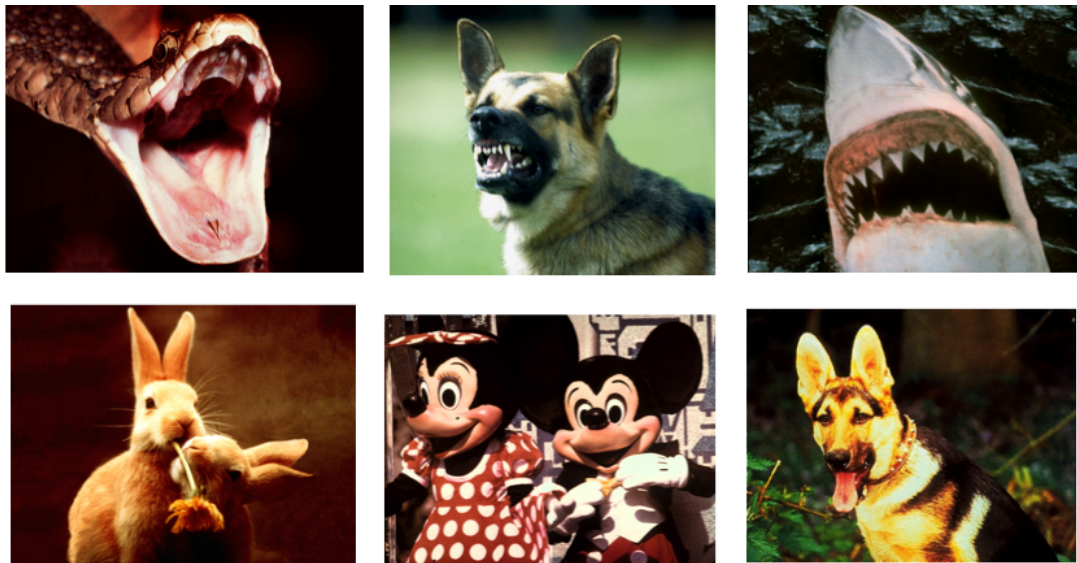


Figure 3.1. Examples of threatening (top) and pleasant (bottom) pictures selected from the IAPS database used for this experiment (Lang, Bradley & Cuthbert, 2008).

To control for the effect of luminance on orientation bias, the luminance of each picture was measured using a luminance photometer (Konica Minolta LS-110), measuring luminance in candelas per square metre (cd/m^2) in a dimly lit room with the photometer held 57cm away from the screen. ‘Pleasant’/’Threatening’ images were matched for luminance. A paired samples t-test showed no significant differences between overall luminance for ‘threatening’ ($M=18.4$, $SD=5.87$) compared to ‘pleasant’ ($M=18.5$, $SD=6.84$) pictures ($t(9) = 0.23$, $p = 0.82$).

Stimuli were presented on a black background with a white fixation cross appearing prior to stimulus onset (separated by 200ms gap). The viewing angle of the centre of the fixation cross was 12 degrees to the inner edge of the target stimuli (right and left) and 16 degrees to the centre of the target stimuli. Trials were presented to participants as follows: when eye position was maintained within ± 2 degrees from fixation, stimuli appeared on-screen, preceded by a 200ms gap where a black screen was presented. Matched pairs of threatening and pleasant stimuli were presented for 100ms on screen in three possible random stimulus onset asynchronies: 1) simultaneous onset, 2) threatening preceding pleasant stimulus onset by 53ms, 3) pleasant preceding threatening stimulus onset by 53ms. The task comprised 300 random trials, which included 100 trials of each condition. Trials were aborted and repeated randomly when a saccade occurred before the target appeared on screen and when a saccade was made out of the range of the target stimulus. Figure 3.2 represents the order of events during each trial.

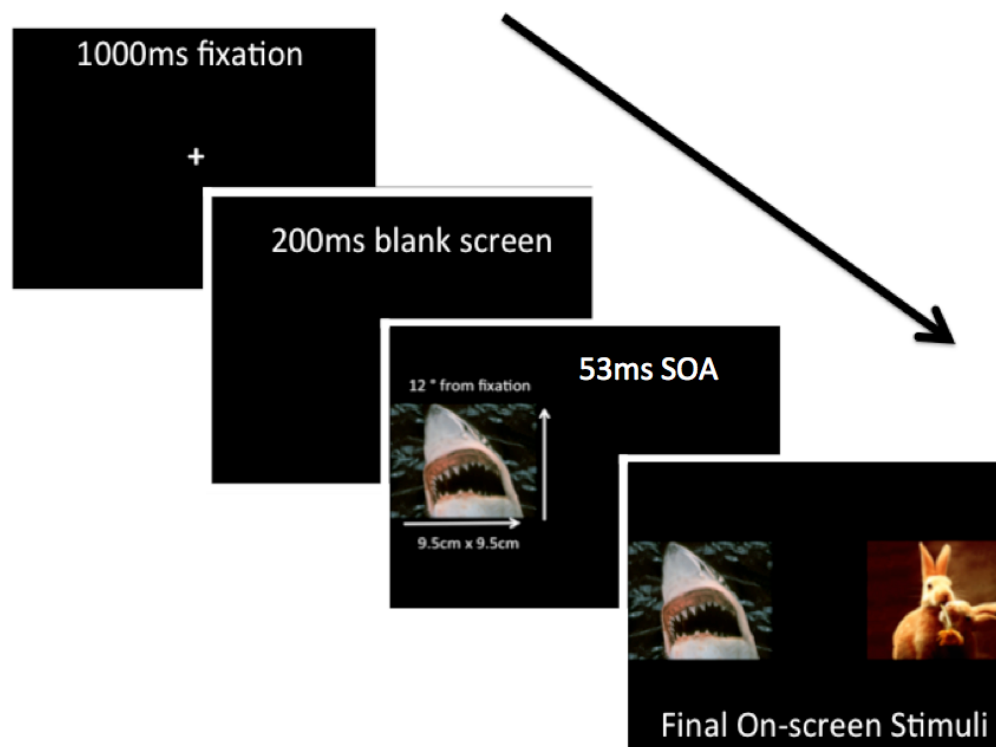


Figure 3.2. Illustration of the order of events during each trial on saccade decision paradigm. Target stimuli appeared randomly on-screen in three conditions: simultaneous onset, right target appeared 53ms before left target, or left target appeared 53ms before right target. Additionally, stimulus types (pleasant vs. threatening) appeared randomly to the left/right.

Design. This experiment comprised of two eyetracking sessions carried out under monocular eye viewing conditions; one completed with left eye viewing, and the other with the right eye viewing. Sessions were counterbalanced to control for order or habituation effects. Independent variables of interest included within subjects variables; eye view (left/right), SOA condition (simultaneous, threat presented first, pleasant presented first), visual field (temporal/nasal) in which the saccade was made and saccade choice (threat/pleasant). The percentage of frequency of saccadic choices made towards stimuli (dependent variable) was analysed with a 2 (eye view) x 3 (SOA) x 2 (threat field) x 2 (response) repeated measures analysis of variance (ANOVA). The percentage frequency of saccade choices made toward threatening versus pleasant stimuli during the simultaneous onset condition was regarded as threat bias scores for individual participants.

Procedure. Participants who responded to the study advert were contacted via e-mail and invited to take part. Prior to participation of the study, participants were provided with a

study information sheet explaining the nature of the experiment and the experimental protocol. Upon entering the experimenting room, the participant was asked to take a seat and was verbally informed once again of the nature of the study. It was explained that there would be multiple tasks to complete during the session and that one eye will be patched. The participant was then instructed to complete the first task verbally as follows: “For this task, you will first see a fixation cross on the screen. Once the fixation cross disappears, two images will appear on both the left and the right. Your task is to look at the image that you think appeared first. Sometimes this will be an easy task, and other times it will be very difficult. Try to be as fast and accurate as possible. Once you’ve looked at the target image, please fixate on the fixation cross as accurately as possible in order for the next trial to occur. Please keep your head as still as possible and remember to make only eye movements and not head movements. This experiment will be approximately 20 minutes in duration. Before we start, there will be a brief practice session for you to become familiar with the task”.

The participant was given the opportunity to ask questions and sign the written consent form. When it was clear that the participant understood the instructions, the participant was asked to take a seat at the experimental set-up. The participant was asked to patch either the left or right eye and to place their head and chin on the chin rest. The eye patch, chair and chin rest was adjusted accordingly and the experimenter ensured that the participant was as comfortable as possible. The eye-tracking camera was adjusted (i.e. moved to the left or the right) to capture the viewing eye that was being tracked. The participant was asked to look at the centre of the screen while the experimenter adjusted the focus using the knob on the camera lens, in addition to the pupil and corneal threshold by clicking on the arrows on the camera setup screen to obtain conditions for optimal accuracy during eye-tracking.

At this stage the participant was informed that the practice session would be starting after calibration has been carried out. The participant was asked to fixate on the calibration squares on the screen while the experimenter pressed the spacebar to calibrate, validate and accept the eye location with the on-screen target. Upon successful calibration, the participant was informed that the practice session would begin. Once both the participant and experimenter were satisfied with performance on the practice trials, the participant completed the saccadic choice task. Participants completed two sessions of the TOJ saccade task on separate consecutive days (under counterbalanced monocular viewing conditions). Upon completion of the experiment, the participant was thanked for their cooperation and was verbally debriefed on the nature of the experiment.

Results

Preliminary inspection of individual data. Overall more saccades were made towards threatening compared to pleasant stimuli ($M = 50.94$, $SE = 0.64$) and saccade latency towards threatening pictures was longer ($M = 301.51$, $SE = 23.41$) compared to non-threatening stimuli ($M = 299.26$, $SE = 22.98$). No response-bias towards the left or right visual field was observed in the sample for mean saccade choices (mean difference = 1.79%, $SE = 6.68$, $t(18) = .27$, $p = .79$, two-tailed) or latency (mean difference = .69, $SE = 7.1$, $t(18) = .1$, $p = .92$, two-tailed).

Saccadic choice: threatening versus non-threatening stimuli. Saccade choice bias towards stimuli were analysed by a 2 (eye view: left/right) x 3 (picture presentation SOA: threatening first/simultaneous/non-threatening first) x 2 (threat location in visual hemi-field: temporal/ nasal) x 2 (saccade choice: threatening/non-threatening) repeated measures analysis of variance (ANOVA). No main effects were observed for eye view, SOA, threat-field or response. As expected, a two-way interaction between SOA and response (Wilk's lambda = .13, $F(1,19) = 56.8$, $p < .001$, partial eta squared = .87) was shown, demonstrating that saccade choices towards threatening versus non-threatening pictures changed across SOA condition; when the threatening picture appeared first, on average 75% of saccades were made towards threat ($SE = 2.5$), when the non-threatening picture appeared first, on average 74% of saccades were made towards the non-threatening picture ($SE = 2.3$). On simultaneous trials, on average 51% of saccades were made towards the threatening versus non-threatening picture ($SE = .96$). Furthermore, a three-way interaction between SOA x threat-field x response (Wilk's lambda = .69, $F(1,19) = 3.85$, $p = .04$, partial eta squared = .31) showed that there were differences between saccades made towards threatening versus non-threatening pictures in the temporal versus nasal visual hemi-field across SOA. Figures 3.3 and 3.4 presents mean saccade choices towards threatening versus pleasant pictures in the temporal and nasal visual hemi-fields.

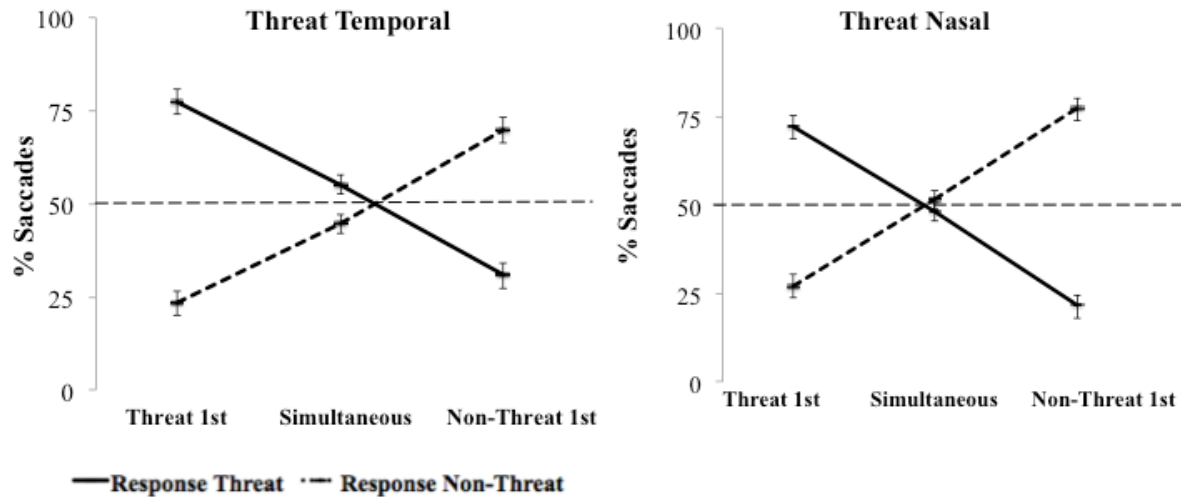


Figure 3.3 Saccade choices to threatening and non-threatening stimuli on saccade decision paradigm. Mean saccade choices towards threatening vs. non-threatening stimuli in the temporal (left) and nasal visual hemi-fields (right), across three SOA's: threat appeared first, threat and non-threat appeared simultaneously, and non-threat appeared first. For non-simultaneous SOA's, the second picture appeared 53ms after the first. Repeated measures ANOVA demonstrated a three-way interaction of SOA x threat field x response.

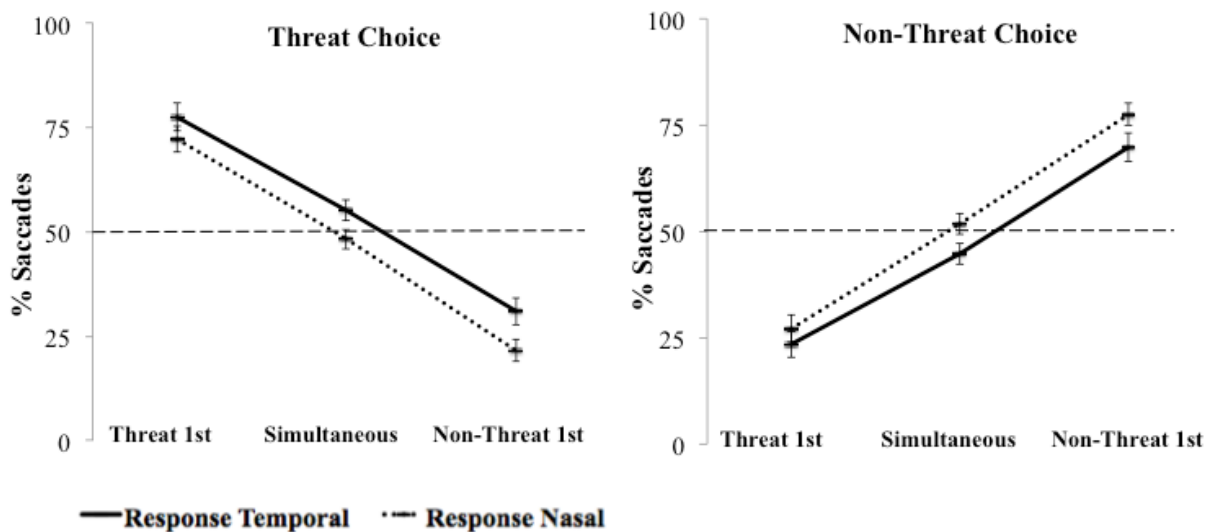


Figure 3.4. Saccade choices to temporal and nasal hemifield on saccade decision paradigm. Mean saccade choices to threatening (left) and non threatening (right) stimuli in the temporal and nasal visual hemifields across three SOA's: threat appeared first, simultaneous threat and non-threat onset, non-threat appeared first. For non-simultaneous SOA's, the second picture appeared 53ms after the first. Repeated measures ANOVA demonstrated a three-way interaction of SOA x threat field x response. In the simultaneous condition, more saccades were made toward threat compared to non-threat stimuli in the temporal but not the nasal visual hemifield. This effect was followed up with a binomial regression model below.

To interpret the interaction between visual hemi-field and response to threat, and to test whether a saccadic choice bias for threat was larger in the temporal visual hemi-field in the simultaneous condition, simultaneous trials were isolated and analysed with a hierarchical mixed-effects binomial regression model (MLWin version 2.1; Rasbash, Charlton, Browne, Healy, & Cameron, 2009). Random intercepts were fitted for each participant (no random slopes). The random effects of location of threat (temporal versus nasal) were tested as predictor of threat bias. The model followed a two-level structure, with trial number entered as level one, and participant number entered as level 2. Table 3.1 presents the effects of temporal hemifield on threat bias for simultaneous trials.

Table 3.1. Temporal hemifield as predictor of threat bias. Hierarchical mixed-effects binomial regression model with random intercepts fitted for each participant (MLWinV2.1, Rasbash et al., 2009). A bias to saccade to threatening versus non-threatening stimuli was observed overall ($p = .051$, Step 1), and an effect of threat bias when presented in the temporal versus nasal visual hemifield ($p < .001$, Step 2).

	<i>B</i>	<i>SE</i>	<i>p</i>
<i>Step 1</i>			
Threat Bias	0.072	0.034	0.051
<i>Step 2</i>			
Threat Bias	-0.07	0.05	0.19
Threat Temporal	2.67	1.02	0.01*

* Denotes $p < .05$

Saccadic latency: threatening versus non-threatening stimuli. Mean saccade latency towards threatening and non-threatening stimuli were analysed by a 3 (picture presentation SOA: threatening first/simultaneous/non-threatening first) x 2 (threat location in visual hemifield: temporal/nasal) x 2 (saccade choice: threatening/non-threatening) repeated measures analysis of variance (ANOVA). Since no significant differences in saccade latency were observed between the left and right eyes (mean difference = 4ms, $SE = 11.76$, $t(18) = .34$, $p = .74$, two-tailed) and to account for missing cases of saccade latency scores, saccade latencies for each condition were averaged across left and right eyes. The omnibus ANOVA demonstrated no statistically significant main effects of threat-field or response on saccade latency.

As expected, a main effect of SOA demonstrated overall differences in saccade latency across the three SOA's (Wilk's lambda = .7, $F(2,17) = 3.7$, $p = .047$, partial eta squared = .3). Bonferroni adjustment for multiple comparisons demonstrated significantly

longer saccade latency for the threat-first SOA compared to the simultaneous SOA (mean difference = 13.54ms, $SE = 4.9$, $p = .038$), and no significant differences between saccade latency for simultaneous SOA compared to non-threat first SOA or threat-first compared to non-threat first SOA. Furthermore, a two-way interaction between SOA and response (Wilk's lambda = .37, $F(2,17) = 14.34$, $p < .001$, partial eta squared = .995) demonstrated that saccade latency towards threatening versus non-threatening pictures where different dependent on SOA condition; when the threatening picture appeared first, saccade latency towards threat ($M = 301.29$, $SE = 24.12$) was shorter compared to non-threat pictures ($M = 332.83$, $SE = 24.34$), when threat and non-threat pictures were presented simultaneously, saccade latency towards threat was shorter ($M = 301$, $SE = 23.15$) compared to non-threat pictures ($M = 306.04$, $SE = 24.94$), and when the non-threatening picture appeared first, saccade latency was shorter for non-threat pictures ($M = 295.42$, $SE = 23.48$) compared to threat ($M = 325.35$, $SE = 24.57$). Figure 3.5 presents mean saccade latencies towards threatening versus non-threatening pictures in the temporal and nasal visual hemi-fields.

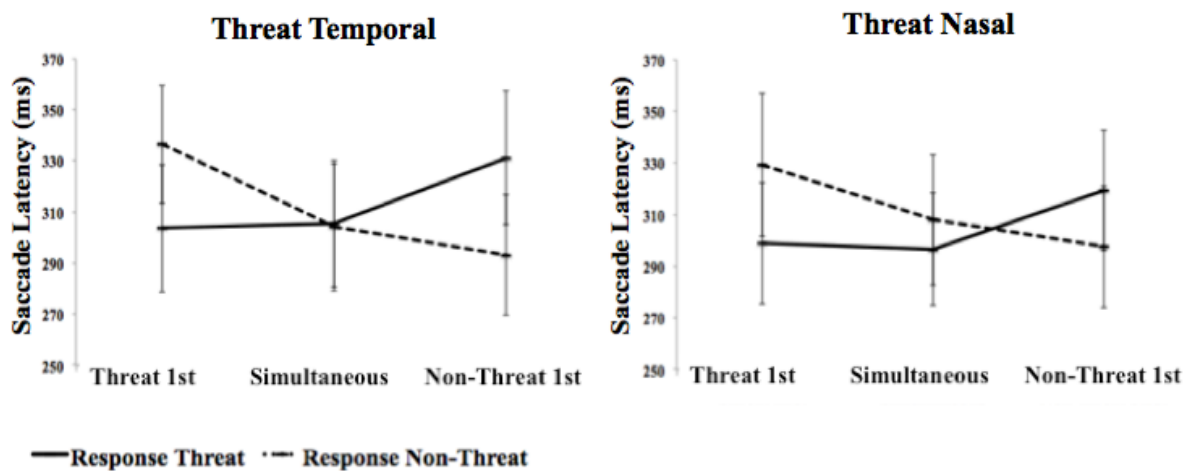


Figure 3.5. Saccade latency to threatening and non-threatening stimuli on saccade decision paradigm. Mean saccade latencies towards threatening vs. non-threatening stimuli in the temporal (left) and nasal visual hemi-fields (right), across three SOA's: threat appeared first, threat and non-threat appeared simultaneously, and non-threat appeared first. For non-simultaneous SOA's, the second picture appeared 53ms after the first. Repeated measures ANOVA demonstrated a three-way interaction of SOA x threat field x response (Wilk's lambda = .37, $F(2,17) = 14.34$, $p < .001$, partial eta squared = .995).

Planned paired samples t-tests demonstrated faster saccades to threat compared to non-threat stimuli in the nasal ($t(18) = -1.5$, $p = .16$) compared to the temporal hemifield ($t(18) = 2.5$, $p = .01$) for simultaneous trials, however these results were not statistically

reliable. Contrary to what was expected, overall saccade latencies towards the nasal visual hemi-field ($M = 295.01$, $SE = 24.52$) were faster compared to saccade latencies towards the temporal visual hemifield ($M = 295.01$, $SE = 21.87$, $t(18) = 2.48$, $p = .02$, two-tailed), showing the largest advantage for saccade latency when threat was presented in the nasal visual hemifield in the simultaneous SOA condition.

Effect of stimulus exposure repetition on saccade choices and latency. In order to investigate whether a difference in effect of threat at first stimulus exposure compared to later repeated exposures occurred during the experiment, responses between the first, fifth and tenth stimulus exposures were compared for saccade choices and latencies to threat. It was important to determine whether habituation to threat occurred, i.e. a threat bias decreased with increased time, suggesting involvement of a fast processing route involving subcortical structures, or whether a threat bias increased steadily over time, suggesting a slower processing route involving the visual cortex.

Saccadic choices to threat. In order to investigate whether saccade choices to threat increased from the first stimulus exposure compared to later repeated exposures, simultaneous SOA trials were isolated for separate analyses. Repeated measures ANOVA was carried out to compare saccades to threat at three picture pair exposures (1st/5th/10th exposure). No main effects of exposure were demonstrated. Although saccades to threat increased from 1st, 5th and 1st to 10th exposures, these effect were not statistically significant (Wilk's lambda = .89, $F(2,17) = 1.05$, $p = .37$, partial eta squared = .11), shown in Figure 3.6.

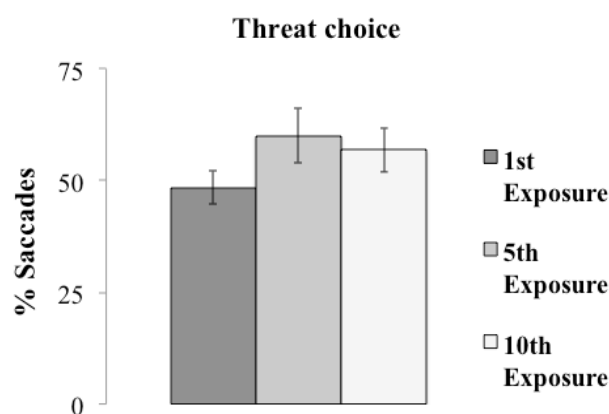


Figure 3.6. Saccades to threat with repeated stimulus exposure. Repeated measures ANOVA comparing saccades to threat at three picture pair exposures (1st/5th/10th exposure). No significant increase in threat was observed from the first, fifth and tenth exposures.

Saccade latency to threat. In order to investigate whether saccade latency demonstrated an advantage to threat (decreased latency from the first stimulus exposure compared to later repeated exposures), a repeated measures ANOVA was carried out to compare saccades to threat at three picture pair exposures (1st/5th/10th exposure). No significant main effects of exposure on saccade latency were demonstrated. Although saccade latency to threat decreased from the first stimulus exposure to the fifth and tenth exposures, this effect was not statistically reliable (Wilk's lambda = .75, $F(2,17) = 2.88$, $p = .08$). Figure 3.7 presents differences in saccadic latency to threat at the 1st, 5th and 10th repeated stimulus exposure.

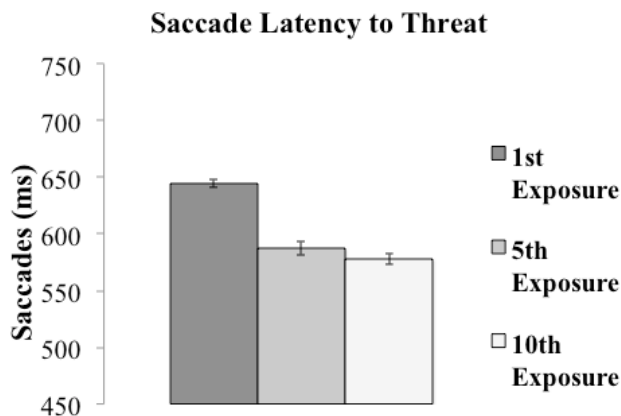


Figure 3.7. Saccade latency to threat with repeated stimulus exposure. Repeated measures ANOVA comparing saccade latencies to threat at three picture pair exposures (1st/5th/10th exposure). No significant decrease in threat was observed from the first, to the fifth and tenth exposures.

Effect of individual stimuli on saccade choices to threat. In order to inspect the characteristics of stimuli that elicited a bias to threat, the stimuli were visually inspected in order of highest to lowest percentage bias to threat. Figure 3.8 presents stimulus pairs that were presented randomly to participants during the saccade decision task (stimuli were always presented with the same pairing). Such visual inspection was needed to investigate the possibility that the bias to threat stimuli in the temporal hemifield was due to attention grabbing features unrelated to threat (e.g. face-like features,). Furthermore, although no differences in total luminance was observed between individual picture pairs, the possibility that some stimuli may have contained more central luminance compared to others, and thereby causing a bias to luminance instead of to threat, needed to be investigated.





















Picture ID	Threat	Pleasant	% Threat Bias
2			60.79
3			56.84
1			56.58
7			52.89
8			52.89
4			51.05
10			47.8
9			47.63
6			47.11
5			44.21

Figure 3.8. Stimulus pairs presented to participants during saccade decision task. The pairs are listed in order of highest to lowest percentage saccade bias to threat.

Although the stimulus pair that elicited the highest percentage of responses to threat (pair 2) included a picture of a bright shark paired with a picture of a bunny, and high percentages of threat bias were observed for picture pairs that included a threatening face, it is unlikely that this bias to threat in the temporal hemifield was purely a result of attention grabbing features unrelated to threat. This is because the picture pair containing a bright shark is paired with a picture of a bright bunny, and other stimuli that contain high luminance centrally (e.g. the non-threatening image in pair 8) still elicited a bias to threat. Furthermore, the stimulus pair that elicited the second highest percentage of bias to threat (pair 3) included a covered face with a knife paired with a non-threatening butterfly on a bright flower. Importantly, although the threatening stimulus in pair 3 could have been recognised as a face, it did not contain clear classic face-like features (e.g. eyes, teeth, mouth) and therefore it is likely that attention was biased to the threatening nature of the stimulus.

Strength of retinotectal tract connectivity as predictor of bias to threat

Saccade choice to threat. In order to investigate the effect of the strength in connectivity of the retinotectal pathway on threat bias, Pearson correlation was carried out and demonstrated a correlation between the average strength in connectivity (measured with fractional anisotropy, FA) of the isolated brachium of the SC voxels common to 100% of participants (described in Chapter 2) and the percentage bias to saccade to threat ($r = .41, p = .04$, one tailed), shown in Figure 3.9.

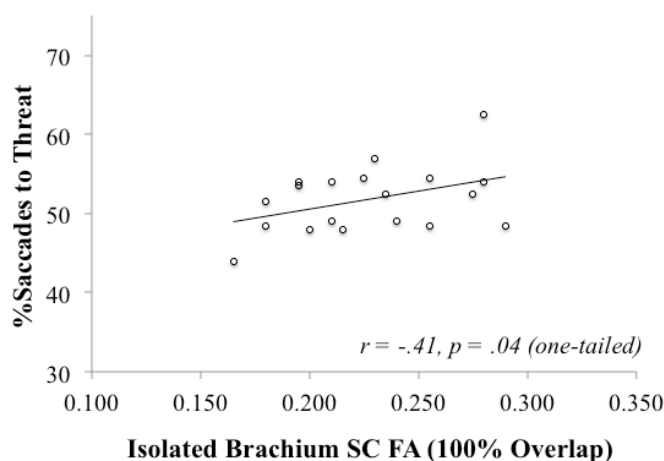


Figure 3.9. Brachium SC FA as predictor of threat bias. Correlation between strength in connectivity (mean FA) of 100% participant overlap of isolated RTT (RTT with voxels of the retino-geniculo-striate pathway subtracted) and a bias to saccade to threatening versus non-threatening stimuli on a saccade decision task.

Subsequent correlations were carried out separately to determine if the effect of FA on threat bias was mediated by afferents to the superior colliculus via the RTT, which would result in an effect of FA on threat bias driven by the saccade bias towards the temporal hemifield. A significant correlation between FA and threat bias was not observed for threat responses to the temporal visual hemifield ($r = -.07, p = .35$, one tailed, significance alpha value set at $p < .025$ to control for multiple comparisons). A significant correlation was observed between FA and responses to threat in the nasal visual hemifield, however this result did not survive the adjusted significance value cut off ($r = .41, p = .04$, one-tailed).

Saccade latency to threat. To investigate whether strength in connectivity of the isolated RTT (100% overlap, including brachium of SC voxels) predicted saccade latency to threat, similar correlational analyses carried out previously on the threat choice responses were carried out on the saccade latency to threat. No correlations were observed between FA and saccade latency to threat ($r = -.05, p = .83$, two-tailed), presented in Figure 3.10. Furthermore, subsequent correlations demonstrated no significant correlations between saccade latency to threat in the temporal ($r = -.03, p = .9$, two-tailed) or the nasal visual hemifields ($r = -.001, p = .99$, two-tailed).

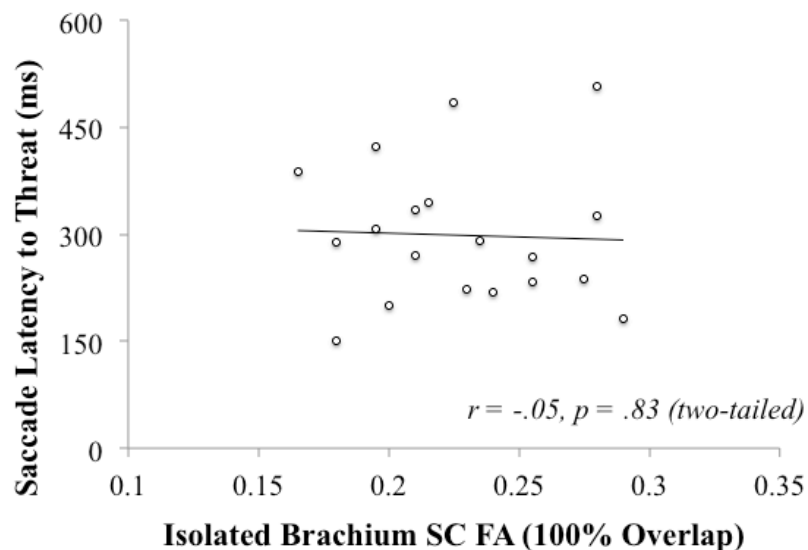


Figure 3.10. Brachium SC as predictor of saccade latency. Correlation between strength in connectivity (mean FA) of 100% participant overlap of isolated retinotectal pathway (retinotectal pathway with voxels of the retino-geniculo-striate pathway subtracted) and saccade latency to threatening stimuli on a saccade decision task.

Discussion

The two aims of the research reported in this chapter were to measure an attention orienting bias to threat and to test the hypothesis that visual afferents to the SC, via the RTT, are involved in mediating orienting responses toward threat. This behavioural measure of threat bias reported here forms the basis for achieving the overall objective of the series of experiments presented in this thesis; establishing a functional role for subcortical extrageniculate pathways thought to process rapid orienting to threat.

This study examined the influence of threat on the temporal order judgment of saccades towards picture pairs in a saccade decision paradigm. Two pictures, one threatening and one pleasant appeared to the left and right of a fixation point and appeared either simultaneously or appeared one before the other, separated by a stimulus onset asynchrony. The prediction was that saccades would be biased towards threatening pictures, and that this effect would be larger in the temporal visual hemifield. As predicted, participants performed well in choosing which picture appeared first during trials in which picture pairs were separated by a stimulus onset asynchrony, regardless of whether the picture was threatening or pleasant. The key condition of interest during this task was the simultaneous onset trials, where participants were forced to choose a stimulus as the one that appeared first, whilst being unaware that both stimuli appeared at the same time. It was predicted that a saccadic choice bias towards threatening pictures would be demonstrated, since threatening pictures may be more salient and may therefore more likely elicit rapid orienting of attention for survival compared to pleasant images. This prediction was confirmed by the results; participants demonstrated a bias to threat during simultaneous picture onset. Moreover, the results were consistent with RTT mediation: the threat orienting bias was exclusive to threatening stimuli appearing in the temporal visual hemifield.

As expected, reaction times were shortest for saccades made towards the pictures that appeared first, regardless of whether the picture was threatening or pleasant, or whether the picture appeared in the temporal or nasal visual hemifield. During the simultaneous stimulus onset condition, it was expected that a saccade latency advantage, that is shorter saccade latency, would be reflected in saccadic choices towards threatening pictures rather than pleasant pictures. Interestingly, this was not the case; when threatening stimuli were presented in the temporal hemifield, saccade latencies towards threatening and pleasant stimuli were similar, whereas saccades towards threat in the nasal visual hemifield demonstrated a trend for shorter latencies compared to saccades towards pleasant pictures, resulting in the biggest advantage for saccade latency to threat shown in the nasal visual

hemifield. Furthermore, contrary to what was expected, overall saccade latencies towards pictures in the temporal hemifield were slower compared to latencies towards the nasal visual hemifield, possibly attributed to the advantage induced by threat stimuli in the nasal visual hemifield.

Although saccadic choices to threat increased from the first, to the fifth and to the tenth stimulus exposure, these differences were not statistically significant; saccade latencies reduced overall from the first to the fifth, and from the first to the tenth repeated stimulus exposures, however no statistically significant differences in such latencies were observed between threatening and pleasant stimuli. This may suggest that perhaps participants improved in making spontaneous responses with increased repeated stimulus exposure. Therefore, contrary to the expectation that participants may demonstrate a greater bias to threat for stimuli during the early compared to later repeated stimulus exposures, with subsequent habituation to threat, no statistically significant differences were observed.

As predicted, strength in connectivity (FA) of the isolated RTT that also included the brachium of the superior colliculus (as mentioned in Chapter 2), correlated with a bias to threat. It was predicted that this effect would be stronger for threat bias in the temporal hemifield, thereby suggesting mediation of attention bias via afferents from the retina to the superior colliculus (RTT). This effect was expected since, as reviewed in the General Introduction and Chapter 2, approximately 10% of cells from the retina project to the superior colliculus, of which the majority project towards the contralateral hemisphere. Such dominance of contralateral projections from the retina to the superior colliculus results in an advantage to process vision from the temporal visual hemifield. Behavioural measures of temporal-nasal asymmetry (e.g. Tomalski, Johnson & Csibra, 2009; Johnson, 1990) have been a useful marker to test for retinotectal function. However, RTT FA demonstrated a trend to correlate with saccadic choice bias to threat in the nasal but not in the temporal visual hemifield. One potential explanation for this result, as described in Chapter 2, may be due to the presence of brachium of the SC voxels that were not isolable from the RTT in these dissections. The resulting brachium of the SC dissections may have contained few RTT fibres relative to a majority of streamlines from the visual cortex. Therefore, cortico-collicular afferents from the primary visual cortex (V1) to the brachium via the SC may account for the overall correlation between RTT FA and threat bias, the lack of demonstration of correlation between RTT FA and threat bias in the temporal visual hemifield, and the trend for a correlation between RTT FA and threat bias in the temporal visual hemifield. Furthermore, this saccade decision task presented stimuli that potentially elicited two competing collicular

activations; conditions that would optimise responding reflexively (by using the 200ms gap prior to stimulus onset) whilst simultaneously making a voluntary saccade to the target that appears first. During two competing collicular activations the competition needs to be resolved in order to select the target (see Song, Rafal & McPeck, 2011). Therefore, it may be that the anatomical RTT dissections represent streamlines from the visual cortex to the brachium that support the mediation of top-down cortically influenced voluntary rather than bottom-up, reflexive saccades, mediated through subcortical routes via afferents to the SC via the RTT. RTT strength in connectivity (FA) did not correlate with overall saccade latencies to threat, or to threat in the temporal or nasal visual hemifields. Since a saccade latency advantage (shorter latency) to threat was not observed in the behavioural results, it was not surprising that RTT FA did not correlate with saccade latencies to threat. Additionally, due to potential conflict between voxels of the brachium of the superior colliculus, mediating voluntary saccades, compared to voxels within the RTT mediating reflexive orienting saccades to threat, it may not be reasonable to expect a correlation between the resulting isolated RTT and saccade latency to threat.

Findings from this study are consistent with previous experiments reporting a bias to threatening compared to neutral stimuli. For example, Fecica & Stolz (2008) similarly reported a choice bias to faces that showed emotional rather than neutral facial expressions during trials in which stimuli onset appeared simultaneously during a temporal order judgment paradigm. Furthermore, similar to performance on non-simultaneous SOA trials, participants performed well in choosing which stimulus appeared first during long SOAs when it was easy to make the required temporal order judgment. These findings are also in line with reports by West, Anderson and Pratt (2009) who showed a bias to faces that displayed a threatening compared to neutral configuration during simultaneous onset displays on a temporal order judgment paradigm. Furthermore, this effect was also present when threat faces were compared against inverted threat faces. Accordingly, West et al. (2009) suggested that this offers evidence that the temporal order bias to threat is not due to a bias towards low-level spatial frequencies of the stimulus but is driven by the emotional content in the face. Furthermore, they argue that this finding suggests that threat stimuli also offers an advantage when compared with other stimuli with biologically relevant, non-threatening emotional content, and is not exclusive to a comparison of threat with neutral stimuli. Findings from this study offer a novel contribution to the literature by demonstrating that orienting of attention is biased towards threat, even when threatening images are compared with pleasant images.

In contrast to previous eye movement studies investigating saccade latency bias to threat, findings from this study did not demonstrate a significant advantage of saccade latency to threat compared to non-threatening pleasant stimuli. For example, Bannerman et al.'s (2010) emotional spatial cueing task demonstrated faster saccade latencies towards targets when a threat cue versus neutral cue was presented prior to the target at short cue durations. Furthermore, in another study Bannerman et al. (2010) reported shorter saccade latencies to emotional faces (angry/happy/fearful) when paired with neutral faces. Kissler and Keil (2008) reported an advantage in saccade latency towards threat in the left visual field, yet reported a saccade latency advantage for pleasant stimuli in the right visual field.

One reason for a lack of saccade latency bias to threatening pictures reported in this study could be due to the direct comparison of threatening stimuli with pleasant stimuli, rather than threatening stimuli compared with neutral stimuli as has been reported in previous experiments (e.g. Bannerman et al., 2010, Bannerman et al., 2009, West et al., 2009, Fecica & Stolz, 2008). For example, Fecica and Stolz (2008) reported that judgements of temporal order were biased towards emotional faces only when paired with a neutral and not with another emotional (happy) face. Furthermore, West et al. (2009) claimed faster saccade latencies towards threat even when competing with biologically relevant non-threatening stimuli, however the stimuli used for comparison were inverted images of the same threatening (angry) faces. Since faces are a special type of stimulus that the brain is biologically 'hard-wired' to recognise (Ohman, 1993), and since the configuration of a face plays an important factor in face recognition, the advantage of saccade latency towards threatening compared to inverted threatening schematic faces as reported by West et al. (2009) may not be sufficient to conclude that a saccade latency advantage would be clear when threatening and pleasant stimuli are competing for attention. Furthermore, West et al. (2009) reported a saccade latency advantage for neutral compared to inverted neutral faces, further demonstrating a saccade latency advantage for recognisable faces, rather than an advantage towards one affective emotional face over another.

Another reason for a lack of a saccade latency advantage for threatening compared to pleasant stimuli demonstrated in this study could be due to the temporal-nasal hemifield manipulation employed during this experiment, which was not the case in previous experiments measuring threat. It was expected that saccade latencies would be biased towards the temporal visual hemifield, and that this bias would be larger for threatening compared to pleasant stimuli, since a bias to orient towards stimuli in the temporal visual hemifield (e.g. Tomalski et al., 2009; Johnson, 1990) has been a useful marker of visual orienting controlled

by the superior colliculus. Saccade latencies were shortest during simultaneous trial responses towards threatening stimuli in the nasal visual hemifield. This finding is unexpected considering the saccadic choice bias to threat; however saccade latency and visually guided saccadic choices may reflect the influence of threat differently. The threatening stimulus in the nasal visual hemifield may have acted as a distractor from responding to the stimulus that would be easiest to saccade towards, i.e. the stimulus in the temporal hemifield, therefore accounting for slower responses to pleasant stimuli when threat was presented in the nasal visual hemifield.

Many previous studies used face stimuli to investigate the effect of threatening emotion on orienting of attention, whereas stimuli used for this study included threatening and pleasant pictures (e.g. shark versus bunny/snake versus flower). Therefore, compared to pictures of faces, a wider variety of types of threatening or pleasant pictures were used to measure threat bias in this study. The wider variety of stimuli used for this study may have contributed to variability in response bias. For example, upon visual inspection of stimulus pairs in order of highest to lowest percentage bias to threat, threatening stimuli such as sharks, threatening face-like stimuli and snakes elicited a higher percentage bias to threat compared to pictures of spiders, dogs and bears. Since a bias to threat was not exclusive to face-like stimuli, findings from this study provide evidence for a bias to threatening pictures other than face stimuli.

The current study had several important limitations to consider. The stimuli used during this study included a wide variety of pictures (e.g. snake, spider, dog, flower, bunny) compared to stimuli used in previous studies (e.g. West et al., 2009; Fecica & Stolz, 2008) such as face pictures or schematic images of faces that have carefully controlled for confounding features in the image that may capture attention that is not triggered by the emotional properties of the stimulus. Therefore, the stimulus set utilised in this study may have included features unrelated to threat that may have biased orienting of attention. However, since a bias to threat was demonstrated for a wide variety of stimuli and not exclusively to face-like or bright stimuli, it is unlikely that the bias to threat was elicited by attention grabbing stimulus features. Furthermore, the presence of a threat bias for stimuli in the temporal hemifield provides plausible evidence that the advantage towards the temporal hemifield was driven by the threatening nature of the stimuli, presumably mediated by the superior colliculus receiving afferents from the retina. Additionally, the current study did not include a control condition in the paradigm where threatening or pleasant pictures were paired with a neutral picture. Inclusion of this comparison may provide a useful indicator of

how strongly saccadic choices are biased towards threatening or pleasant pictures compared to neutral pictures, and whether this effect is larger for threat compared to pleasant pictures.

Despite the contributions offered by findings from this experiment, several questions remain unanswered. The aim of this thesis was to investigate the role of subcortical pathways in mediating orienting of attention to threat. Findings from the current experiment suggest a functional role for the superior colliculus via the retinotectal pathway in mediating threat. However, evidence for a functional role of a subcortical threat-processing pathway connecting the superior colliculus and the amygdala via the pulvinar nucleus of the thalamus in healthy human participants remains to be established. This research question will be investigated in Chapter 5. Furthermore, the relationship between retinotectal pathway strength in connectivity and saccade latency to threat bias is still unclear. Additionally, the relationship between different subcortical routes that have been suggested to mediate threat, for example the relationship between the retinotectal pathway and the pathway connecting the superior colliculus with the amygdala via the pulvinar nucleus of the thalamus, remains to be established.

To summarise, the bias to threat in the temporal visual hemifield on the saccade decision task demonstrated in this study is consistent with the hypothesis that visual signals that trigger orienting of attention to threat are transmitted via the RTT. Brachium of the SC voxels, including a small number of RTT mixed with a majority of cortico-collicular voxels correlated with a choice bias to threat. This effect was not present for the temporal hemifield, which may be due to a paucity of RTT fibres present in the brachium of SC dissection. This suggests that cortico-collicular afferents to the SC from V1 may also contribute to mediating saccade choices to threat. Saccade latency did not correlate with brachium of the SC voxels in the saccade decision task. This effect is similar to a lack of correlation observed between brachium FA and reflexive saccades made during a ‘gap’ paradigm presented in Chapter 2. Since the gap paradigm provided a measure of potential reflexive saccades that may also have included some voluntary saccades, this would suggest that afferents from V1 to SC (via brachium) did not provide a statistically reliable contribution to mediation of reflexive saccade latency. Taken together with a similar effect observed with saccades on the saccade decision paradigm, which likely contained a mix of voluntary and reflexive saccades, it may further suggest that averaged saccade latency provided a noisy measure of saccade latency from both reflexive and voluntary saccades, thereby accounting for a lack of correlation with brachium FA.

Findings from this experiment support a role for the superior colliculus in predicting saccadic choice bias to threat. These findings support theories of threat processing that argue for the existence of a subcortical visual route for threat processing involving the superior colliculus, the amygdala and the pulvinar nucleus of the thalamus.

CHAPTER 4

ANATOMICAL RELATIONSHIP BETWEEN THE STRIA TERMINALIS AND A PATHWAY CONNECTING THE SUPERIOR COLLICULUS AND THE AMYGDALA IN HUMANS: VIRTUAL DISSECTION WITH DTI TRACTOGRAPHY

Rafal, R. D., Koller, K., Bultitude, J. H., Mullins, P., Ward, R., Mitchell, A. S., & Bell, A. H. (2015). Connectivity between the superior colliculus and the amygdala in humans and macaque monkeys: virtual dissection with probabilistic DTI tractography. *Journal of Neurophysiology*, *114*(3), 1947–62. <http://doi.org/10.1152/jn.01016.2014>

Anatomical relationship between the stria terminalis and a pathway connecting the superior colliculus and the amygdala in humans: virtual dissection with DTI tractography

Abstract

A subcortical connection between the superior colliculus (SC), pulvinar and amygdala has been suggested to mediate the preserved processing of emotional valence in the absence of visual awareness demonstrated by cortically blind patients. This study provides anatomical evidence for the existence of connections between the amygdala and the SC through the pulvinar in the healthy human brain. Virtual dissections with probabilistic DTI tractography demonstrated a dorsolateral trajectory through the pulvinar that traversed above the temporal horn of the lateral ventricle, thereby connecting laterally to the amygdala. The close neighbouring topography of the stria terminalis was also dissected to obviate artifactual connectivity with crossing fibres. The two pathways were demonstrated to be anatomically distinct, demonstrating topography of the SC-amygdala streamline traversing above the temporal horn, occupying a dorso-medial position relative to the stria terminalis.

A historical view of the function of the amygdala has suggested a role in mediating responses to threat and fear. Several studies in rats and humans have also suggested a critical role of the amygdala in detection of stimuli conveying saliency or biological relevance. Accordingly, the amygdala serves the organism as critical for regulating social behaviour necessary to survive in and adapt to a changing social environment (Adolphs, 2008; Adolphs & Spezio, 2006). The main visual input to the amygdala projects via the striate and extrastriate cortex. However, the demonstration of cortically blind patients to process threat has led to the proposal for the existence of a phylogenetically conserved, older visual system playing a role in threat processing for survival (de Gelder, Morris, & Dolan, 2005; Morris, Ohman, & Dolan, 1999). Accordingly, this alternative visual processing route is presumably a subcortical connection to the amygdala from the superior colliculus (SC), which plays a role in orienting of attention, through the pulvinar nucleus of the thalamus, which plays a role in visual processing. It has been posited that this assumed subcortical connection would likely allow for the unconscious, rapid processing of emotional stimuli (Tamietto & de Gelder, 2010).

Several controversies surround the strong indications in favour of a rapid, unconscious subcortical threat-processing pathway (Beatrice de Gelder, van Honk, & Tamietto, 2011; Pessoa & Adolphs, 2010; Tamietto & de Gelder, 2010). Consideration of several outstanding questions may aid in clarification of such controversies. Firstly, considering whether anatomical evidence for a subcortical threat-processing pathway exist in the primate brain? Secondly, is the nature of the information processed by this pathway unconscious? Finally, considering whether the visual signal processed by this presumed subcortical pathway is faster in comparison to affective visual signals transmitted via the cerebral cortex?

A recent study by Tamietto, Pullens, De Gelder, Weiskrantz and Goebel (2012) demonstrated connections between the SC and the amygdala through the pulvinar in humans with the use of in-vivo diffusion tensor imaging (DTI) tractography. They additionally showed that the connections in the hemisphere of a hemianopic patient with a lesioned striate cortex were in fact stronger in comparison to neurologically intact brains of non-hemianopic controls. Thus, their study provided an important contribution by demonstrating both anatomical evidence for the existence of this subcortical visual pathway, and additionally providing evidence for a functional role of this pathway in mediating blindsight.

The current study aimed to provide further anatomical demonstration of a subcortical connection between the SC and the amygdala in the human brain, thereby providing

supporting evidence in attempt to resolve the first outstanding question outlined above. Here I demonstrate with the use of probabilistic DTI tractography anatomical evidence for connectivity between the SC and the amygdala through the pulvinar in the healthy human brain *in vivo*. These results build upon the results presented by Tamietto et al. (2012) by demonstrating for the first time in any species its trajectory between the thalamus and the amygdala. In order to demonstrate that the pathway connecting the SC with the amygdala is distinct from the stria terminalis as it projects from the amygdala above the temporal horn of the lateral ventricle, the stria terminalis was dissected in order to confirm that the two tracts are anatomically distinct and to demonstrate their topographic relationship to one another.

The stria terminalis is one of three major white matter fibre bundles that connect the amygdala to other parts of the brain. It is part of the extended amygdala system that has neurons embedded within its white matter fibres (Neuwenhuys et. al., 2008). Its main projection is to the bed nucleus of the stria terminalis in the hypothalamus as well as the septal nuclei; and it also conveys projections from the amygdala to the habenula via the stria medullaris. The stria terminalis has been speculated to play a role in the expression of anxiety in response to sustained threat (or perceived threat). The chief source of evidence has been provided by animal research; however a limited number of studies have been carried out in humans. Research in rats (De Olmos & Ingram, 1972) have shown that the stria terminalis, also referred to as the dorsal amygdalofugal pathway, emerges from the caudo-medial amygdala, arching along the medial border of the caudate nucleus and then sits in the wall of the lateral ventricle as it passes between the caudate and anterior thalamic nucleus before turning inferiorly toward the region of the anterior commissure. At this point, dorso-caudal to the anterior commissure, the stria terminalis splits into pre-, post- and commissural components. Post-commissural fibres spread to the bed nucleus of the stria terminalis (BSTN) and anterior hypothalamic nucleus (Neuwenhuys et. al., 2008).

Non-invasive imaging techniques such as diffusion imaging have suggested reconstructed anatomical models of stria terminalis with connected neighbouring structures in the human brain *in-vivo* (Avery et al., 2014; Krüger, Shiozawa, Kreifelts, Scheffler, & Ethofer, 2015). Anatomical features exclusive to the human brain have been reported to be a structural connection with the temporal pole and a functional connection with the paracingulate gyrus, in addition to structural and functional connections of BNST with several subcortical, limbic, thalamic and basal ganglia regions (Avery et al., 2014). Similar to the anatomy reported in the animal literature, *in vivo* structural diffusion-weighted imaging in

the human brain has demonstrated connections between the BNST and the amygdala, one via the stria terminalis and the other via the ansa peduncularis, and a third anterior connection emanating from the BNST that terminates in the orbitofrontal cortex (Krüger et al., 2015). Although the anatomical structure of the stria terminalis has been reported in animal studies, research on the anatomy in the human brain has been scarce and limited by less sophisticated, non-invasive reconstructed MRI imaging techniques, compared to gold standard viral tract tracing.

We recently demonstrated (Rafal, Koller, Bultitude, Mullins, Ward, Mitchell & Bell, 2015) DTI tractography dissections of the stria terminalis in healthy humans and rhesus macaques. The trajectory of the stria terminalis demonstrated a similar trajectory in both humans and monkeys. We showed that the stria terminalis emerged from the amygdala and traversed above the temporal horn of the lateral ventricle, following the lateral border of the tail of the caudate nucleus and between the border of the anterior thalamic nucleus and the body of the caudate nucleus before descending through the diencephalon to the region of the BNST. Although such imaging techniques have become increasingly sophisticated and have provided invaluable insights into the anatomical findings in humans, such structural findings are still limited by a lack of sufficient behavioural evidence in support of its function.

This chapter presents, in addition to the data in healthy humans that have been published (Rafal et al., 2015), virtual dissections with probabilistic DTI tractography of the connectivity between the SC and the amygdala via the pulvinar of an additional 7 participants. The anatomical relationship between the SC-amygdala and the connection between the BNST and the amygdala through the stria terminalis is considered by using a novel analysis of the centre of gravity of each tract.

Method

Information on participants, MRI apparatus and procedures, scanning parameters and data processing are reported in Chapter 2 Methods. All participants were neurologically healthy and screened for high levels of anxiety on psychometric measures of anxiety measured by the State-Trait Anxiety Inventory (STAI range: 23-59, Spielberger, Gorsuch, Lushene, Vagg & Jacobs, 1983).

Probabilistic tractography.

Virtual dissection of connections between the superior colliculus and the amygdala. Probabilistic tractography was implemented using ProbtrackX from the FSL-FDT toolbox

(curvature threshold = 0.2, number of samples = 5000). Tractography between the SC and the amygdala was performed in both hemispheres of each participant's diffusion weighted images using the participant-specific masks on 1) the superior colliculus (Figure 4.1) and 2) the amygdala (Figure 4.2). In order to evaluate the robustness of streamlines produced with the inclusion of a pulvinal mid-waypoint mask, as was reported for the first group of human participants in Rafal et al. (2015), the connection between the SC and the amygdala was dissected without inclusion of a pulvinal mask in the second group of human participants. Since no major differences were observed between tracts dissected with a pulvinal mask and tracts that were dissected without inclusion of a pulvinal mask in both humans and monkeys, the analyses for the additional participants added to the 'second group' of human data for this study were performed without a pulvinal mask.

Masks were drawn manually on each subject's diffusion space registered T1 anatomical brain using anatomical landmarks in 10 subjects. For the remaining 9 subjects, masks were drawn manually on the MNI-152 standard anatomical brain template (Montreal Neurological Institute) and registered to each subject's diffusion space. The amygdala masks were drawn on coronal slices at the posterior border of the amygdala, using the gray-white matter junction at the border of the amygdala in the sagittal plane as a landmark, taking care to exclude extraneous white matter beyond this border (Figure 4.2). All masks were drawn and individually visually inspected by one researcher and additionally individually inspected on each subject's brain scan by another researcher. Figure 4.1 presents examples of the superior colliculus and exclusion masks and examples of the amygdala masks are presented in Figure 4.2.

Initially, streamlines were generated in both directions (ie. amygdala as seed and SC as waypoint mask, and *vice versa*). The common overlaps of the connection between the SC and amygdala in both directions were calculated in order to include only the voxels that would be most likely to be part of the tract. The most reliable tract was demonstrated using the amygdala as the seed mask and the SC as the waypoint and termination mask in the majority of subjects. However, in a minority of participants who demonstrated reliable tracts in both directions, upon visual inspection, 'overlapping' tracts were used and in few cases tracts with the SC as the seed mask and the amygdala as the waypoint and termination masks were used. Systematic visual inspection of all tracts ensured anatomical connections consistent amongst participants.

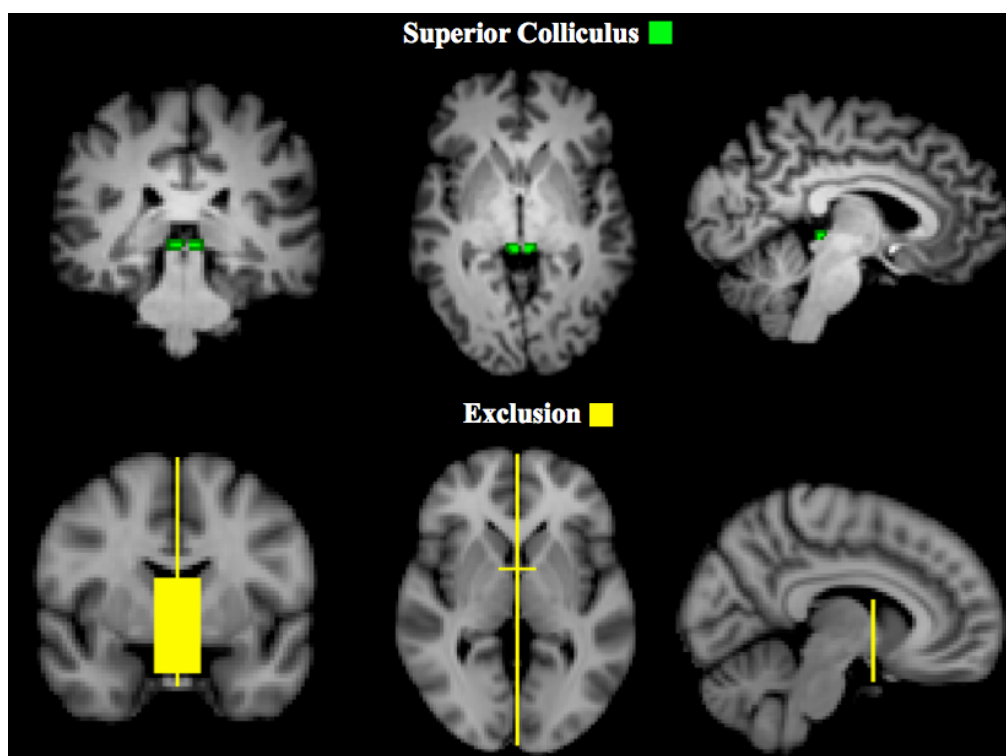


Figure 4.1. Masks used for the virtual dissection of connectivity between the superior colliculus (SC) and the amygdala. Left, coronal sections; middle, axial sections; right, sagittal sections. Superior colliculus masks are shown in green (top) in one representative participant. Exclusion masks are presented in yellow (bottom) on the Montreal Neurological Institute (MNI) T1-weighted standard atlas brain scan.

The value of each voxel of the resulting streamline represented the total number of traces passing through that voxel. Each voxel was thresholded so that only those voxels that contained at least 10% of the maximum number of traces found in any voxel remained. A recent study that directly compared diffusion tensor imaging (DTI) tractography with tracers in monkeys has reported that a threshold of 10% is optimal to most reliably reflect the anatomy of tractography compared with tracers (Azadbakht et al., 2015).

Virtual dissection of the stria terminalis. As reported in the Results section, the trajectory of the connections between the SC and the amygdala was found to traverse above the temporal horn of the lateral ventricle. The stria terminalis is the chief amygdalo-fugal projection that similarly traverses the temporal horn of the lateral ventricle. The topography of the stria terminalis has been demonstrated with DTI tractography (Avery et al. 2014; Kwon et al. 2011). Consideration of the anatomical relationship between the pathway connecting the SC and the amygdala and the stria terminalis was important since some amygdalo-fugal projections to the thalamus may potentially cross paths with the stria terminalis, as reported by Aggleton and Mishkin (1984). However, the outputs from the

amygdala to the thalamus project to the midline thalamic nuclei, and not to the pulvinar (Aggleton & Mishkin, 1984). Nonetheless, the identification of the stria terminalis trajectory was critical to demonstrate that connections found between the SC and the amygdala were not merely a result of an artefact from crossing or kissing fibres connected to the pulvinar converging with the stria terminalis.

Tractography between the BNST and the amygdala was performed in both hemispheres of each subject's diffusion weighted images using the subject-specific masks on 1) the bed nucleus of the stria terminalis (BNST) – near the anterior commissure just lateral to the fornix where it traverses the hypothalamus, 2) the amygdala and 3) along the trajectory of the stria terminalis – between the caudate and the anterior thalamic nuclei subjacent to the frontal horn of the lateral ventricle (Figure 4.2). A mid-waypoint mask in the stria terminalis was included in order to include only streamlines that follow the trajectory of the stria terminalis. The stria terminalis is most readily visualized in sagittal slices as a stripe of higher signal between the thalamus and the body of the caudate nucleus. Masks were drawn manually on each subject's diffusion space registered T1 anatomical brain using anatomical landmarks in 10 subjects. For the remaining 9 subjects, masks were drawn manually on the MNI-152 standard anatomical brain template (Montreal Neurological Institute) and registered to each subject's diffusion space. All masks were drawn and individually visually inspected by one researcher and additionally individually inspected on each subject's brain scan by another researcher. Streamlines were generated in both directions (ie. BNST as seed and amygdala as waypoint mask, and vice versa). The common overlap of the stria terminalis in both directions were calculated in order to include only the voxels that would be most likely to be part of the tract. Out of all three possible dissections, the dissections that represented the trajectory of the stria terminalis most accurately bilaterally were included in the statistical analysis for each participant. Figure 4.2 presents the BNST, stria terminalis and amygdala region of interest masks in one representative subject.

Furthermore, an exclusion mask was used in the majority of dissections in order to prevent streamlines from connecting to regions known not to be part of the stria terminalis. Such regions included a small mask in the fornix and a mid sagittal mask. Since the specific interest was in the section of the stria terminalis that projects from the amygdala and connects with the BNST, and not the anterior projection connecting the ansa peduncularis, further exclusion regions such as a single coronal slice excluding the frontal lobe and a small bilateral exclusion of where the anterior connection between the amygdala and BNST (bypassing the stria terminalis) would be located was included (presented in Figure 4.3).

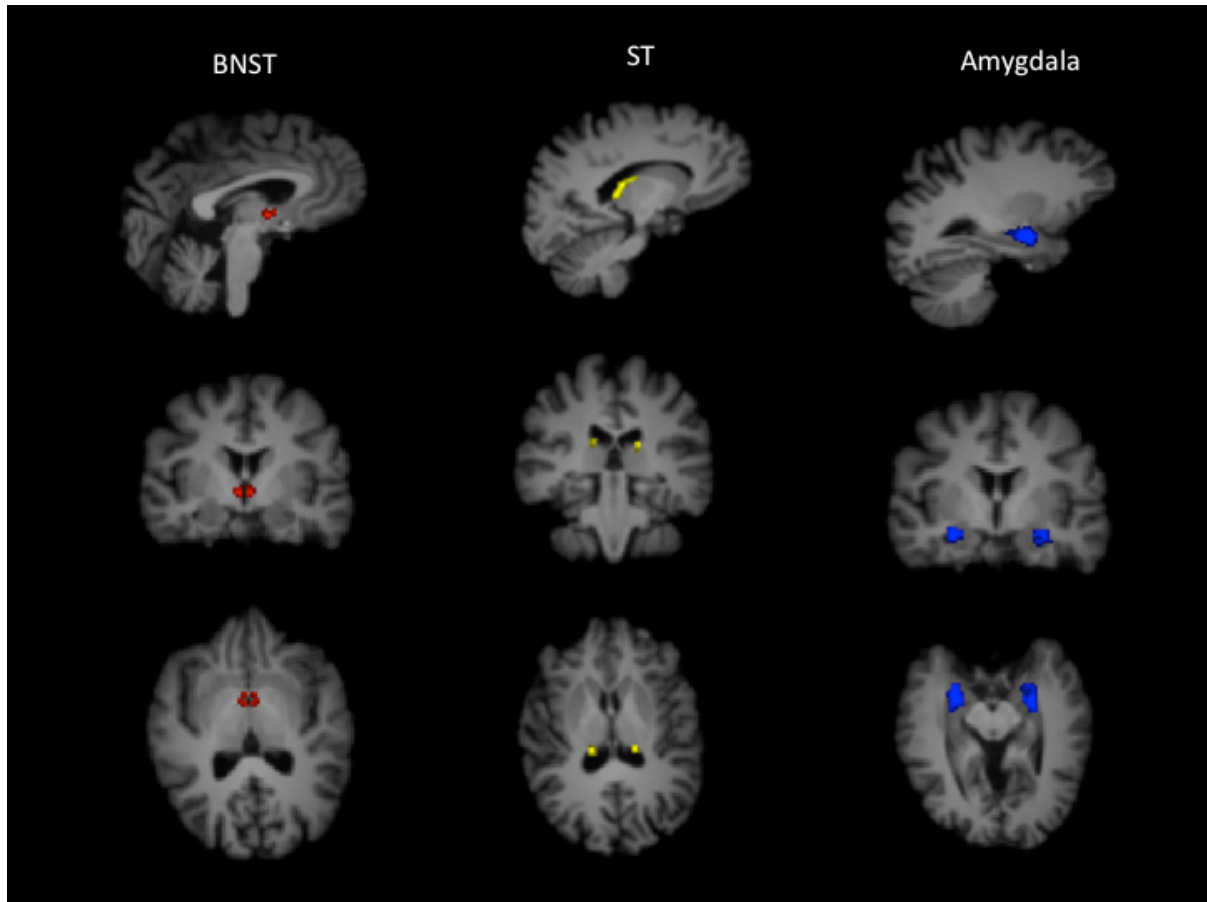


Figure 4.2. Masks used for the virtual dissection of connectivity of the stria terminalis connecting the bed nucleus of the stria terminalis with the amygdala. Middle, coronal sections; bottom, axial sections; top, sagittal sections. Bed nucleus of stria terminalis (BNST) in red (left), stria terminalis waypoint in yellow (middle) and amygdala in blue (right).

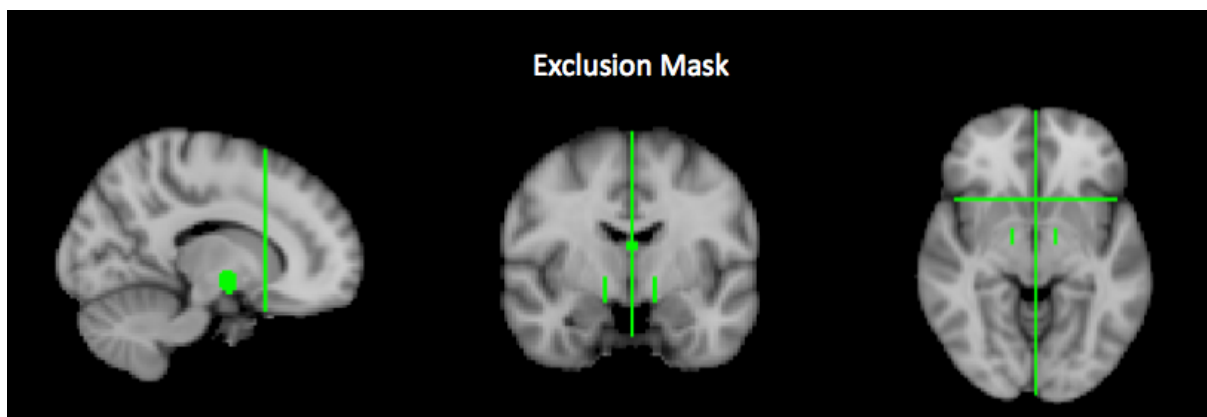


Figure 4.3. Example of exclusion mask used during dissection of stria terminalis. Regions include parts of fornix, mid sagittal slice, frontal lobe and anterior region between amygdala and BNST.

Results

Connections between the SC and the amygdala.

Connections between the SC and the amygdala were demonstrated in both hemispheres of all 19 participants. Figure 4.4 presents A 3D reconstruction of the common overlap of streamlines in all participants in addition to visualisation of the topography of the pathway and its anatomical relationships to other structures in a series of coronal and sagittal slices. Pathways were generated using masks drawn in the superior colliculus and the amygdala. A coronal exclusion mask through the diencephalon and optic tracts were used to dissect the connection in 15 participants in the left hemisphere and 13 participants in the right hemisphere. In the majority of subjects, the tract initially ascended dorsally from the SC, continuing to ascend postero-laterally to the pole of the medial pulvinar. The pathway then curved ventro-laterally to a position above the temporal horn of the lateral ventricle proceeding rostrally above the temporal horn, crossing from the medial to the lateral terminal, turning medially thereby connecting with the lateral amygdala.

Similar to analyses performed by Tamietto et al. (2012), tractography was performed twice in each hemisphere; with the amygdala used as the seed mask and superior colliculus as waypoint and termination in one direction, and the SC used as seed mask and the amygdala as waypoint and termination mask in the opposite direction. In order to isolate the voxels most probable to be part of the SC and amygdala pathway, a common ‘overlap’ of the two topographically similar streamlines was created. Overlapping streamlines were created by first adding together binarised versions of each tract and then thresholding to isolate only voxels common to both the amygdala-SC and SC-amygdala pathways. With this approach, overlapping pathways showing continuous connections between the amygdala and the SC were demonstrated in the 13 left and 14 right hemispheres out of 19 participants. In cases where overlapping streamlines did not demonstrate continuous connections between the SC and amygdala, the single streamline that corresponded most strongly to the topography demonstrated in the sample was used. In such cases, pathways that were generated with the SC as the seed mask was used in one hemisphere in the left hemisphere and in one hemisphere in the right hemisphere, and the tracts were generated in 5 hemispheres in the left and 4 hemispheres in the right using the amygdala as the seed mask. Overlapping the streamlines in this approach in each participant demonstrated pathways that were reduced in noise and the most likely topographical representation of the anatomy of the connection.

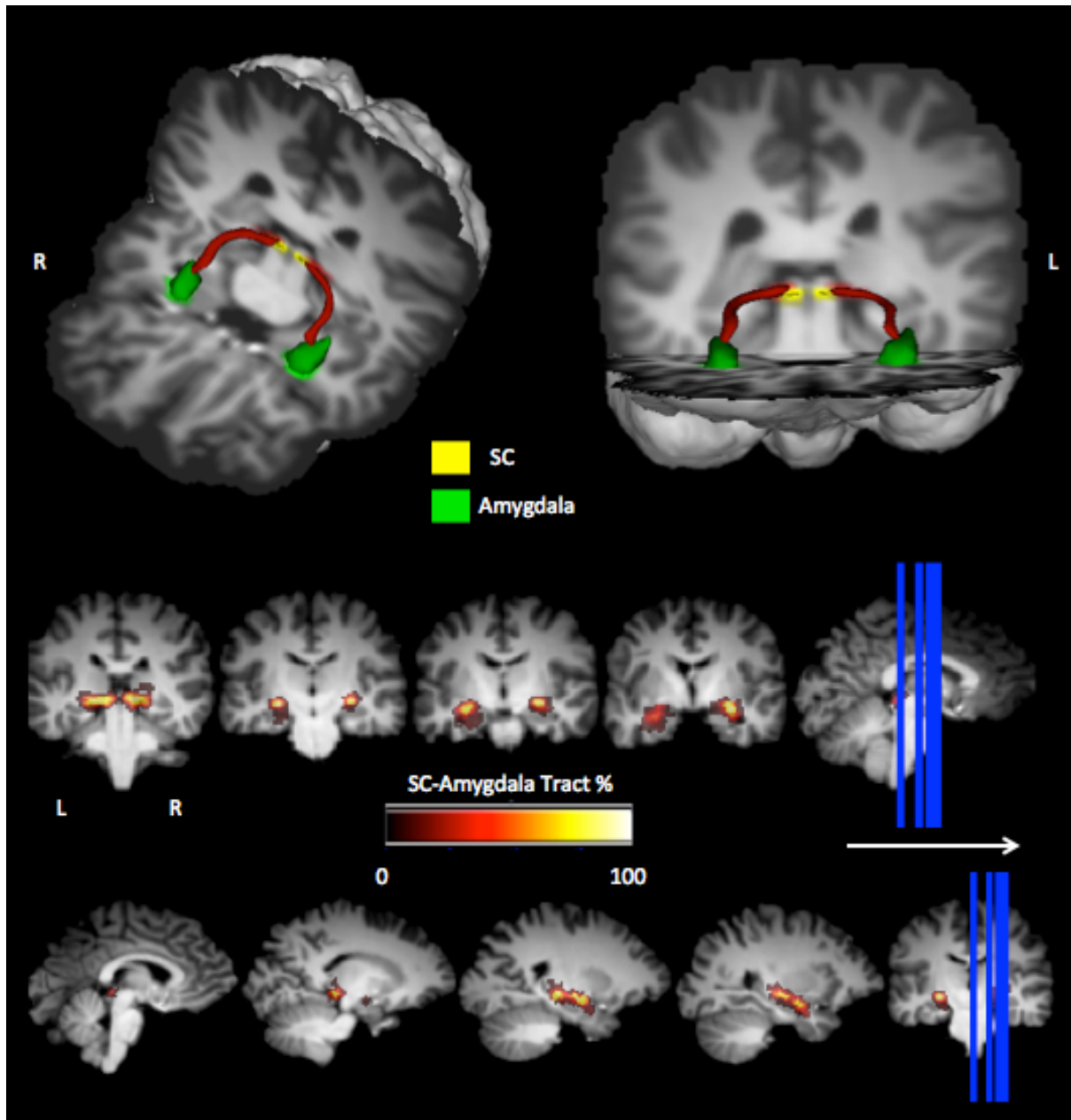


Figure 4.4. Probabilistic tractography between the amygdala and superior colliculus in the healthy human brain ($N=19$). Top: Composite 3D reconstruction (shown in red) of connection between the superior colliculus (shown in yellow) and the amygdala (shown in green) in tracts of each participant registered to a common brain space. Coronal (middle) and sagittal (bottom) slices demonstrate the unthresholded composite streamline for all participants with a colour scale indicating the proportion of participants whose streamline runs through each voxel.

Variability in connection between SC and amygdala between subjects.

The overlap between the two opposing amygdala-SC and SC-amygdala connections additionally allowed a more direct evaluation of the topographical variability in streamlines across participants. Figure 4.4 shows the averaged streamlines for all participants aligned to a

single T1-weighted image. The colour scales represent the proportion of participants through which the streamline passed in each voxel. The image reflects both the variability in the trajectory and the variability in the cross-sectional size of the streamlines across participants. To measure inter-subject variability in the trajectory of the streamlines, a ‘centre of gravity’ (COG) estimate of each streamline was computed in a series of coronal slices. This was restricted to a segment of the streamline that traversed above the temporal horn of the lateral ventricle, since this part of the pathway runs perpendicular to the coronal plane. Eight coronal slices covered this segment. A COG measure for each participant’s streamline in each hemisphere was computed in the left-right (LR) and superior-inferior (SI) (z) coordinates and averaged across all participants. There was little variability observed overall in the streamline across participants in the segment of the connections traversing the temporal horn. The mean standard deviation of the COG average across the 8 coronal slices across participants was within 1-2mm. Since the size of each voxel was 2mm, this difference in standard deviation was near the anatomical resolution of the measurement. Table 4.1 presents the COG variability (standard deviation in mm) of the in-plane (y, anterior-posterior) across all participants.

Table 4.1. Centre of gravity (COG) of SC-amygdala. Standard deviation (2mm isotropic voxels) of the COG of the amygdala - superior colliculus overlapped streamline in x and z coordinates in a series of consecutive slices in the coronal (y) plane in left and right hemispheres.

<i>Anterior/Posterior</i>	<i>Left/Right</i>		<i>Superior/Inferior</i>		<i>Mean</i>	
<i>Y-Plane Slice</i>	Left X	Right X	Left Z	Right Z	Mean X	Mean Z
51	1.49	1.58	1.07	0.98	1.53	1.03
52	0.86	1.11	1.19	1.10	0.99	1.14
53	0.72	0.65	1.05	1.19	0.69	1.12
54	0.75	0.50	0.98	1.10	0.62	1.04
55	0.71	0.64	0.89	1.03	0.68	0.96
56	0.72	0.71	0.90	0.86	0.71	0.88
57	0.87	0.76	1.10	0.89	0.82	0.99
58	1.09	0.84	1.09	0.99	0.97	1.04
Mean	0.90	0.85	1.03	1.02	0.88	1.03
SD	0.19	0.25	0.08	0.09	0.21	0.06

Connections of the stria terminalis

Virtual dissection of the stria terminalis was demonstrated in all 19 human subjects (bilaterally in 18 subjects, and unilaterally in the right hemisphere of 1 subject). The

trajectory of the stria terminalis demonstrated a streamline that emerged from the amygdala, traversing above the temporal horn of the lateral ventricle before tracing along the lateral border of the tail of the caudate nucleus and then the border of the anterior thalamic nucleus and the body of the caudate nucleus, prior to descending through the diencephalon to the region of the bed nucleus of the stria terminalis. Exclusion masks excluding parts of the fornix, mid-sagittal exclusion, frontal lobe and anterior region between amygdala and BNST were required for 8 subjects. Figure 4.5 presents the trajectory of the stria terminalis demonstrated via a composite tract of all participants' tracts, registered and added to the same brain space.

A similar 'overlap' approach of calculating the voxels most probable to represent the topography of the stria terminalis between stria terminalis dissections generated using the BNST as seed versus using the amygdala as seed mask was less successful compared to the SC-amygdala dissection. In the majority of subjects (15 subjects in left and right hemispheres), stria terminalis dissections achieved with the amygdala as the seed, the stria terminalis region of interest mask as the mid-waypoint mask, and the BNST as the final way-endpoint and termination mask demonstrated the most anatomically consistent and continuous stria terminalis connections. However, tracts obtained via the abovementioned overlapping approach were demonstrated in the left hemisphere of 2 participants, and the right hemisphere of 2 participants. In one participant's the right hemisphere, the dissection in the opposite order (BNST as seed, stria terminalis and amygdala as waypoints and amygdala as termination mask) was used.

Figure 4.5 shows the averaged streamlines for all participants aligned to a single T1-weighted image. The colour scales represent the proportion of participants through which the streamline passed in each voxel. The image represents both the variability in the trajectory and the size of the streamlines across participants.

To measure inter-subject variability in the trajectory of the stria terminalis streamlines, a 'centre of gravity' (COG) estimate was also computed in the same series of coronal slices as was used to compute the COG for the connection between the SC and the amygdala described above. A COG measure for each participant's streamline in each hemisphere was computed in the left-right (LR) and superior-inferior (SI) (z) coordinates and averaged across all participants. There was little variability observed overall in the streamline across participants in the segment of the connections traversing the temporal horn.

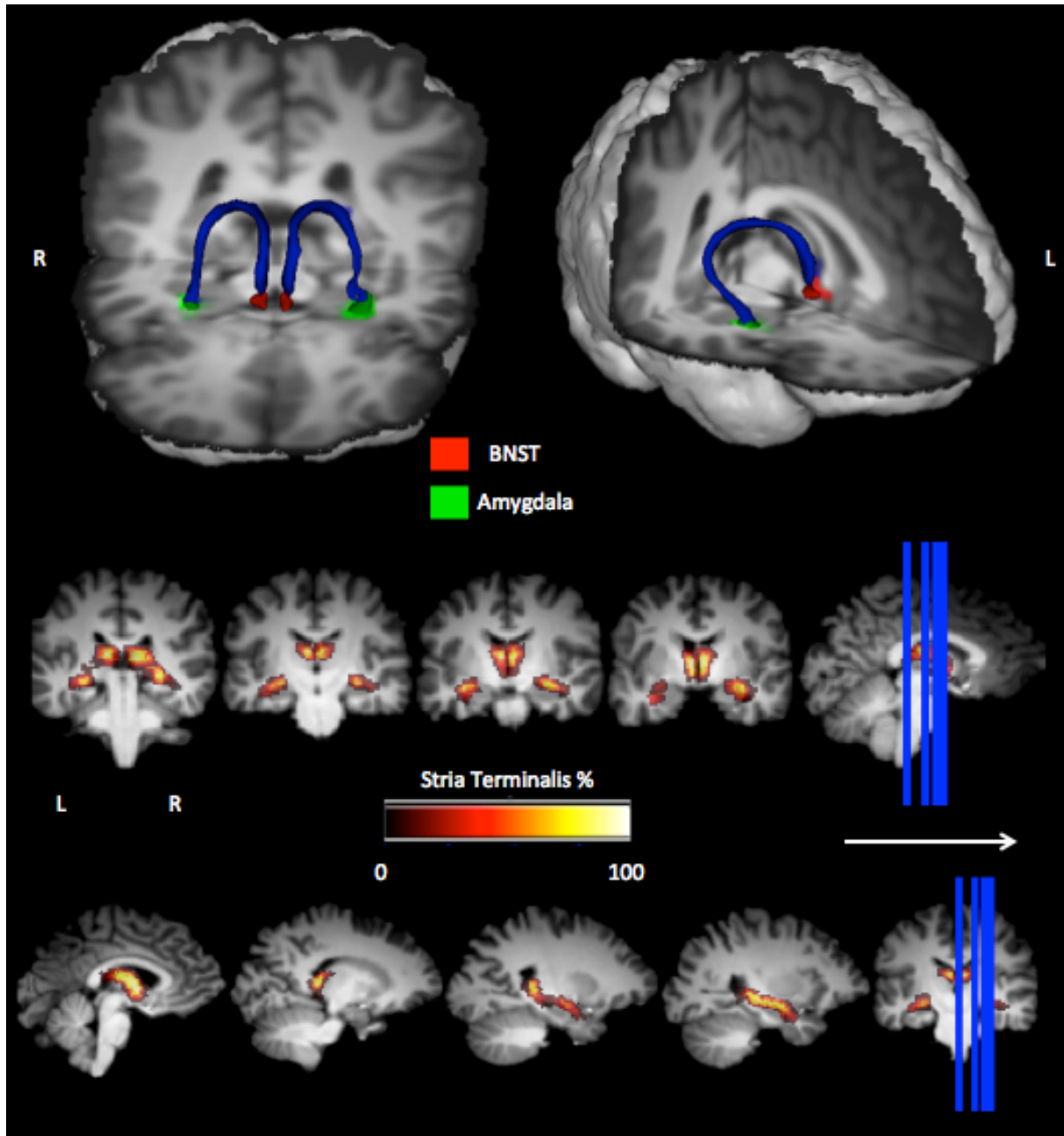


Figure 4.5. Probabilistic tractography of the stria terminalis in the healthy human brain ($N=19$). Top: Composite 3D reconstruction (shown in blue) of connection between the bed nucleus of the stria terminalis (red) and the amygdala (shown in green) in tracts of each participant registered to a common brain space. Coronal (middle) and sagittal (bottom) slices demonstrate the unthresholded composite streamline for all participants with a colour scale indicating the proportion of participants whose streamline runs through each voxel.

Variability in connection of the stria terminalis between subjects.

The mean standard deviation of the COG average across the 8 coronal slices across participants was within 3-4mm, demonstrating variability in anatomy of the stria terminalis beyond the resolution of the anatomy of the measurement across participants. Table 4.2

presents the CoG variability (standard deviation in mm) of the in-plane (y, anterior-posterior) of the stria terminalis across all participants.

Table 4.2. Centre of gravity (COG) of stria terminalis. Standard deviation (2mm isotropic voxels) of the centre of gravity of the stria terminalis overlapped streamline in x and z coordinates in a series of consecutive slices in the coronal (y) plane in left and right hemisphere and means for both hemispheres.

<i>Anterior/Posterior</i>	<i>Left/Right</i>		<i>Superior/Inferior</i>		<i>Mean</i>	
<i>Y-Plane Slice</i>	Left X	Right X	Left Z	Right Z	Mean X	Mean Z
51	1.89	2.18	1.57	1.45	2.04	1.51
52	2.00	1.98	1.61	1.00	1.99	1.31
53	2.10	1.95	1.54	0.91	2.02	1.22
54	1.99	2.29	1.45	1.25	2.14	1.35
55	2.12	2.23	1.54	1.19	2.18	1.37
56	1.93	2.22	1.21	1.37	2.07	1.29
57	1.65	2.04	1.22	1.20	1.85	1.21
58	1.92	1.89	1.58	1.14	1.91	1.36
Mean	1.95	2.10	1.46	1.19	2.02	1.33
SD	0.10	0.13	0.13	0.13	0.08	0.07

Topographic relationship between the amygdala-SC connection and the stria terminalis

In order to investigate the topographical relation between the stria terminalis relative to the amygdala-SC connection statistically, COG measures of the stria terminalis in left-right (LR) (x) and superior-inferior (SI) coordinates was similarly computed for the same 8 coronal slices in the same segment above the temporal horn of the lateral ventricle described previously that measured that variability in COG for the SC-amygdala connection. Figure 4.6 presents the projection of the stria terminalis relative to the connection between the SC and the amygdala streamline. Separate analyses of variance (ANOVA)s for left-right (LR) (x) and superior-inferior (SI) (y) were performed for COG estimates for the SC-amygdala and stria terminalis streamlines for each of the 8 coronal slices for both the left and right hemisphere tracts, entering the coronal slice mask as a between subject's factor. There was a reliable difference between the COG of the two streamlines in the SI planes in both hemispheres: left Z mean coordinate $F(1,126) = 257.16, p < 0.001$; right mean Z coordinate $F(1,131) = 1175.12, p < 0.001$. A reliable difference was demonstrated for the COG in the left-right plane in the left hemisphere ($F(1,126) = 1053.77, p < .001$) and in the right hemisphere ($F(1,131) = 653.47, p < .001$).

The SC-amygdala streamline traversed above the temporal horn just medial to the stria terminalis [left hemisphere (mean difference 2.5 mm, *SE* 0.08 mm), right hemisphere

(mean difference 2.95 mm, *SE* .12 mm)], passing dorsally to the stria terminalis [left hemisphere (mean difference 1.04 mm, *SE* 0.0 mm), right hemisphere (mean difference 1.75 mm, *SE* 0.05 mm)].

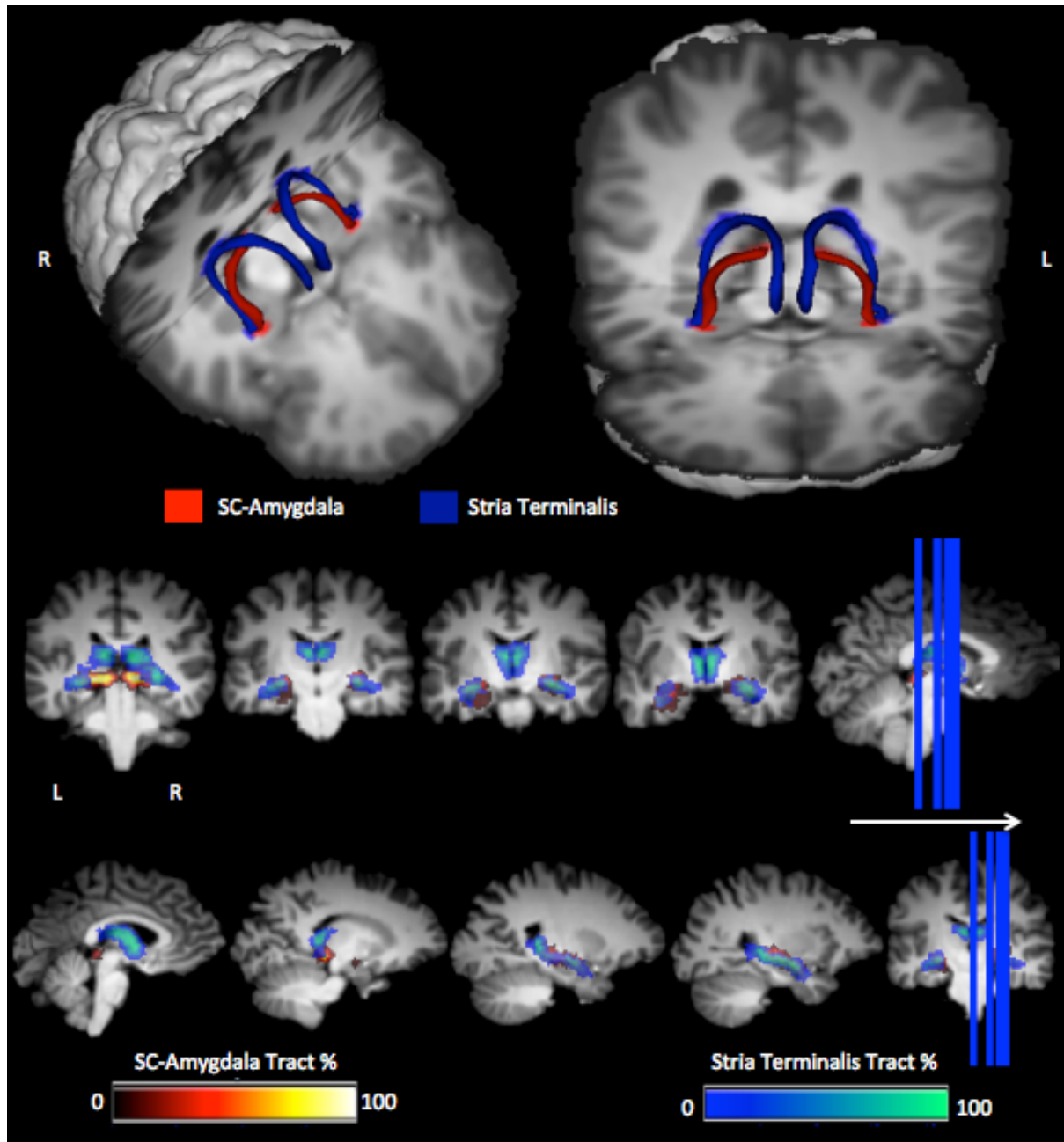


Figure 4.6. Probabilistic tractography of the stria terminalis and connection between the superior colliculus and the amygdala in the healthy human brain ($N=19$). Top: Composite 3D reconstruction of connection between the bed nucleus of the stria terminalis and the amygdala (shown in blue) and connection between the superior colliculus and the amygdala (shown in red) in hemispheres of each participant registered to a common brain space. Coronal (middle) and sagittal (bottom) slices demonstrate the unthresholded composite streamline for all participants with colour scales for the SC-amygdala (bottom left, warm) and for the stria terminalis connections (bottom right, cool) indicating the proportion of participants whose streamline runs through each voxel.

Discussion

Probabilistic DTI tractography demonstrated potential anatomical connections between the SC and the amygdala passing through the pulvinar nucleus in the thalamus. Additionally, this data demonstrates the topography of putative connections of a collo-thalamic projection between the thalamus and the amygdala, for the first time in any species. Collo-thalamic connections ascended from the SC passing through the medial pulvinar to the pole of the pulvinar. From here, the trajectory descends turning laterally and rostrally passing through the lateral pulvinar. Upon exiting the pulvinar, the pathway traverses above the temporal horn of the lateral ventricle, positioned dorsal and medial to the stria terminalis, thereby connecting the lateral amygdala laterally at the stria terminalis terminal.

The observations of the connection between the SC and the amygdala here in humans are consistent with a recent report (Tamietto et al., 2012) that demonstrated potential connectivity between the SC and the amygdala with deterministic DTI tractography. This study presented separate tracts that were generated from the SC to the pulvinar, and from the pulvinar to the amygdala. Additionally, connectivity between the SC and amygdala as an isolated streamline by using both amygdala and SC as seed masks were demonstrated.

Tamietto et al.'s (2012) did not present a description of the specific topology of the connections between the SC and the amygdala. Furthermore, the anatomical relationship between these connections in relation to other anatomical structures such as the stria terminalis were not reported. Therefore, it is not possible to confirm that the connections reported by Tamietto and colleagues were the same as the connections reported here. Supplemental Fig. S3 in their report shows a streamline that traverses over the temporal horn of the lateral ventricle, however also demonstrates clearly the stria terminalis in the same image, and therefore it is not possible to assign the streamline traversing superior to the temporal horn shown in Fig. S3 to the SC-pulvinar-amygdala pathway without ambiguity.

A novel approach to solve this problem was employed to show that connections from the pulvinar to the amygdala are independent from the stria terminalis and can therefore not be attributed to artifacts of intersection with it. A centre of gravity (COG) analyses was used to demonstrate that the segments of these pathways that traverse above the temporal horn of the lateral ventricle are anatomically distinct, at least in the inferior-superior (z) plane. Furthermore, an initial sample of human participants not reported in this chapter demonstrated SC-pulvinar-amygdala pathways that shared voxels with the stria terminalis. For this reason, the stria terminalis was used as an exclusion mask to dissect SC-pulvinar-

amygdala connections in that sample demonstrating that the resulting connections were independent connections of the stria terminalis.

The amygdala receives collaterals from colliculo-thalamic projections that project to the cortex. This collateral pathway in the rat projects from the SC to the lateral amygdala via the suprageniculate nucleus. Since rodents do not have a distinguishable pulvinar, the suprageniculate nucleus is described as a posterior thalamic nucleus. In prototypical primates such as the tree shrew (*Tupaia belangeri*) (Fan et al., 2013), the SC projects to the pulvinar. From here, topographic outputs from the SC project to the dorsal pulvinar, which in turn projects outputs to the amygdala (Day-Brown et al. 2010). Benevento and Standage (1983) demonstrated in macaque monkeys that SC efferents project to the inferior, medial and lateral nuclei of the pulvinar. In monkeys however projections to the amygdala from the pulvinar nuclei that receive inputs from the superficial layers of the superior colliculus have not yet been identified, unlike what has been demonstrated in the tree shrew. Benevento & Standage (1983) reported that the medial thalamic nucleus receives afferents only from the deep layers of the superior colliculus and only the inferior and lateral pulvinar nuclei received afferents from the superficial layers of the SC. Therefore, it is not clear how coarse visual signals conveying threat could be relayed through the pulvinar to the amygdala, since efferents from the pulvinar to the lateral amygdala have been demonstrated from the medial pulvinar nucleus in the macaque monkey, however not from the inferior or lateral pulvinar (Pessoa, 2005). Despite a lack in such anatomical evidence demonstrated by tracer studies, Van Le et al. (2013) recently demonstrated that neurons in both the medial and lateral pulvinar nuclei respond to threatening stimuli with very short latencies. Pictures of snakes elicited neuronal response latencies of less than 60ms. Furthermore, Maior, Hori, Tomaz, Ono, and Nishijo (2010) recently reported that single cells in the pulvinar of macaque monkeys respond differentially to human facial expressions. Similarly, Nguyen et al. (2014) demonstrated that the SC responds to faces and face-like stimuli.

Aggleton, Friedman and Mishkin (1987) also demonstrated that the medial pulvinar was slightly labelled after injections in the lateral amygdala using retrograde horseradish peroxide tracers in rhesus macaque monkeys. Furthermore, Jones and Burton (1976) reported the existence of efferents from the medial pulvinar that project collaterals to the anterior, lateral amygdala in both macaques and squirrel monkeys. However they did not report whether this region of the pulvinar received afferents from the SC. Furthermore, DTI tractography of connections between the SC and amygdala via the pulvinar reported in the published version of this paper demonstrated anatomy similar to that in humans. However,

comparison of this data with that reported by Jones and Burton (1976) is difficult since a reconstruction of tracer tractography in only one squirrel monkey was presented in a figure in their paper (Fig. 1). In their figure they presented an injection site close to the border between the lateral and medial pulvinar, however did not show the number of slices between the injection site and the pulvinar and amygdala. In addition to demonstrating fibres entering the lateral amygdala from the external capsule, it demonstrated tracers above the temporal horn, medial to the tail of the caudate nucleus.

Probabilistic DTI tractography is used to infer the path of axons through a reflection of continuity of anisotropic diffusion. However, it does not provide information regarding the direction of axonal transmission or the presence of synapses. Therefore, the findings reported here do not provide insight into the specific neuronal circuitry. They are equally consistent with a monosynaptic pathway between the SC and the amygdala connecting in the medial pulvinar, as well as a multisynaptic pathway that might include one or more additional synapse in the pulvinar. Indeed, probabilistic tractography cannot be taken as definitive evidence for either pathway.

It is important to consider that while both the current study and that of Tamietto et al. (2012) show connections between the pulvinar and the amygdala, and connections between the SC and voxels within the pulvinar through which a streamline passes to the amygdala, it is not possible with tractography to show that there are connections between the retino-recipient superficial layers of the superior colliculus and pulvinar neurons that then project to the amygdala. Therefore, the streamlines demonstrated in this study represents a topography that traverses the medial and lateral pulvinar and may consist of voxels containing both axons from the superficial layers of the SC projecting to the lateral pulvinar. Likewise, it is not currently possible to define homology between the dorsal pulvinar nucleus of the tree shrew that receives afferents from the retino-recipient SC and projects to the amygdala, with any corresponding pulvinar nuclei in macaques.

Therefore, confirming that the virtual dissections reported here relate to a functional anatomical pathway that transmits visual information that signal threat will need further investigation. DTI tractography can however provide a valuable tool for testing this hypothesis through converging studies in humans and monkeys.

As mentioned in the Introduction, this study aimed to clear up one area of controversy regarding a subcortical connection between the SC-amygdala, which has been a lack of anatomical evidence in primates. The current findings have provided anatomical evidence for a subcortical connection between the SC and amygdala that is potentially involved in threat

processing. However, our data does not suggest a conclusion that this subcortical pathway is 'faster' than the geniculo-striate route. However, it is likely that activation of the amygdala will jointly reflect the input of cortical and subcortical routes. Therefore, a disruption in this subcortical route would likely result in deficits such as slowed or degraded amygdala activation in comparison to fully intact SC-amygdala connections. The published version of the current study included preliminary evidence that tractography can be a useful tool in analysing lesions in future neurophysiological investigations of this subcortical threat mediating pathway for transmission of visual threat. This preliminary analyses also showed how neuropsychological results can address the functional role of pathways found through tractography. Tractographic analysis in two patients with lesions in the pulvinar who also demonstrated deficits in fear and threat processing were retrospectively found that the lesions disrupted the putative pathway. In contrast, the streamline in three other patients with similar pulvinar lesions who did not demonstrate fear deficits, was not disrupted by their lesions.

Such preliminary observations in patients with pulvinar lesions converge with neuropsychological evidence blindsight patients, thereby supporting the case for a subcortical SC-amygdala connection that processes emotional salience. However, while evidence in blindsight patients demonstrate that emotionally valenced visual stimuli can activate the amygdala in absence of the primary visual cortex, whether activation of the pulvinar transmits to the amygdala via a subcortical pathway has not been shown. It is possible that some of the pulvinar connections to cortical areas could in fact transmit signals to the amygdala (McDonald, 1998). Rafal et al.'s (2015) demonstration in patients with pulvinar lesions provides evidence that a subcortical pathway that traverses above the temporal horn likely connects with the area of pulvinar that processes emotionally valenced stimuli. However, such demonstration does not provide direct evidence that SC-pulvinar connections receive visual afferents from retino-recipient SC layers en route to the amygdala. Indeed, Tamietto et al. (2012) showed stronger connectivity between the pulvinar and the amygdala in the lesioned hemisphere of hemianopic patient GY, compared to controls, which was not the case for connections between the SC and the pulvinar.

In order to establish whether such subcortical connections function in transmitting emotion signals to the amygdala will require more definitive evidence, perhaps employing direct physiological studies to target the anatomy of the subcortical pathway at different stages. This could best be achieved with anatomical tracer studies or sophisticated electrophysiological recordings, only invasively possible in monkeys. Results reported here could be used as evidence to extend an anatomical homologue back to the human brain.

As expected, the anatomical results in all participants demonstrated a connection between the bed nucleus of the stria terminalis and the amygdala; a trajectory that emerged from the amygdala, traversing above the temporal horn of the lateral ventricle before tracing along the lateral border of the tail of the caudate nucleus and the border of the anterior thalamic nucleus, prior to descending through the diencephalon to the region of the bed nucleus of the stria terminalis.

However, it is emphasised that a number of precautions should be taken into account when interpreting anatomical connections demonstrated via the technique of DTI tractography. In comparison with the gold standard method of studying brain anatomy in animals, the viral tracer technique where tracers are injected into one part of the brain, and animals are sacrificed sequentially, DTI is non-invasive and there are no ethical concerns regarding its use. However, unlike tracer techniques that yield more robust pathway trajectories as tracers are constrained via white matter axon walls, DTI tractography provides a computerised reconstructed model of white matter, solely based on the movement of water diffusion inside the axon walls, with no information regarding constriction of axon wall boundaries. This may be problematic in cases where virtually dissected brain pathways are claimed to be novel, or exclusive to the human brain. For example, using DTI techniques Krüger et al. (2015) presented a novel anterior connection between BNST and orbitofrontal cortex and Avery et al. (2014) reported a novel structural connection between the BNST and the temporal pole. Although informative presentations of anatomy, it is difficult to interpret such novel connections as being authentic based solely on *in vivo* tractography. When it is possible to link a pathway in the human brain that has been virtually dissected with DTI tractography with behaviour, it provides more convincing evidence that the structure of the pathway that has been found is veridical, since it is related to a function.

The anatomical evidence from this study compares well with that of previous DTI studies in humans. We demonstrate a connection between the BNST and the amygdala via the stria terminalis, connections that are consistent with previous reports (Avery et al., 2014; Krüger et al., 2015). In contrast however, the aim of our study was to specifically restrict connection from the BNST and the rest of the brain in order to dissect only the stria terminalis, rather than exploring all connections between BNST and the rest of the brain. Therefore, we included exclusion masks of the anterior part of the brain and the potential connection between the BNST and the amygdala that bypasses the stria terminalis via the ansa peduncularis. The inclusion of exclusion masks further minimised the likelihood of finding spurious connections. The anatomy of the stria terminalis demonstrated by

tractography is consistent with animal studies, presenting a similar trajectory from the amygdala, traversing above the temporal horn of the lateral ventricle before tracing along the lateral border of the tail of the caudate nucleus and the border of the anterior thalamic nucleus, prior to descending through the diencephalon to the region of the bed nucleus of the stria terminalis (De Olmos & Ingram, 1972).

CHAPTER 5

STRUCTURAL CONNECTIVITY OF CONNECTION BETWEEN THE SUPERIOR COLLICULUS AND AMYGDALA IN HUMANS PREDICTS BIAS IN ORIENTING TOWARD THREAT

Structural connectivity of connection between the superior colliculus and amygdala in humans predicts bias in orienting toward threat

Lesion studies in monkeys and humans advocate the existence of a phylogenetically conserved subcortical pathway projecting from the superior colliculus to the amygdala via the pulvinar thalamus that mediates orienting of attention toward threat. The existence of this pathway is controversial since sufficient evidence associating structural connectivity with behaviour in healthy primates has not been demonstrated. This study demonstrates for the first time that connectivity strength of virtual dissections of this putative pathway using DTI tractography predicts orienting to threat in a saccade decision task.

Blindsight patients with lesions in the visual cortex demonstrate above chance discrimination of threatening stimuli such as threatening facial expressions, despite reporting being unaware of their content (de Gelder, Morris, & Dolan, 2005). Such findings strongly argue for an alternative, geniculo-striate independent visual route that prioritises rapid orienting of attention towards specific types of stimuli for survival, such as threat. A connection between the superior colliculus and the amygdala via the pulvinar nucleus of the thalamus has been proposed as a candidate pathway to mediate an attention orienting bias to threat (de Gelder et al., 2005; Morris, Ohman, & Dolan, 1999). Recent anatomical demonstrations with the use of Diffusion Tensor Imaging (DTI) tractography have provided evidence for connections between the SC and amygdala in one human hemianopic patient and healthy human controls (Tamietto, Pullens, De Gelder, Weiskrantz, & Goebel, 2012) and in both healthy humans, patients with pulvinar lesions and macaque monkeys (Rafal et al., 2015).

In healthy humans, non-conscious perception of fearful masked faces have demonstrated increased fMRI BOLD activation in the right amygdala (Morris et al., 1999). Eye movement studies have provided evidence for a behavioural bias to threat demonstrated in both saccade latency (Bannerman et al., 2009) and attention orienting (Bannerman, Milders, & Sahraie, 2010; Fecica & Stolz, 2008; West, Anderson, & Pratt, 2009). However, an association between structural connectivity and behaviour as evidence for a functional role of a putative, subcortical threat-processing pathway connecting the superior colliculus (SC), pulvinar and amygdala has not yet been reported. The current study employed probabilistic DTI to virtually dissect connections between the SC and the amygdala in healthy human participants. This study is the first to report evidence to support a functional role of the SC-

amygdala connection by demonstrating that strength in connectivity of SC-amygdala connections predicted a bias to orient to threat on a saccade decision paradigm.

Methods

Nineteen neurologically healthy humans (9 male, age range: 18-47yr) participated. All participants were neurologically healthy and screened for high levels of anxiety on psychometric measures of anxiety measured by the State-Trait Anxiety Inventory (STAI range: 23-59, Spielberger, Gorsuch, Lushene, Vagg, & Jacobs, 1983). An attentional bias to threat has been demonstrated with temporal order judgment paradigms (Fecica & Stolz, 2008; West et al., 2009). The current study employed a novel temporal order saccade decision task where on each trial, a threatening and a non-threatening visual stimulus were presented at the same eccentricity in opposite visual fields. The threatening stimulus appeared 53 ms before the non-threatening stimulus on 33% of the trials, 53ms after the non-threatening stimulus on 33% of the trials and simultaneously on the remainder of the trials. Methods and results for the temporal order decision task has been previously reported in Chapter 3. Stimulus picture pairs matched for luminance (e.g. a cobra preparing to strike paired with a puppy, see Figure 3.8 Chapter 3) were selected from International Affective Picture Scale (IAPS: Lang, Bradley & Cuthbert, 1997). Participants were instructed that one stimulus always appeared first, to ignore the picture content and to saccade from central fixation toward whichever stimulus appeared first (Figure 3.2 Chapter 3). An Eyelink1000® device recorded saccade latency and direction under monocular viewing conditions. Critical trials were those with simultaneous onset of the threatening and non-threatening stimuli (see Chapter 3 for full Methods). Each participants' bias towards threat was computed as the percentage of saccadic choices toward threat made on simultaneous onset trials, regressed against connectivity strength measures of SC-Amygdala (FA) analysed using a binomial regression model with participant entered as random effect.

SC-amygdala virtual dissection with probabilistic DTI tractography was achieved as previously described (Rafal et al., 2015, Chapter 4). Two streamlines were generated in each hemisphere: from a seed mask in the amygdala with a target mask in the SC; and from a seed mask in the SC with a target mask in the amygdala (Chapter 4, Fig. 4.2). A composite streamline was generated from the voxels overlapping on these two streamlines. Composite streamlines for all participants were registered to the same brain space and added together to create one pathway demonstrating the common overlap within the sample. This pathway was thresholded at 100% to include only the voxels that included streamlines common to all 19

participants in the sample. A mask of these voxels was created for both left and right hemispheres. This mask was then registered to each individual participant's diffusion space and was used for computation of mean FA for voxels in the residual streamline (Figure 5.1). As previously mentioned in Chapter 2, the justification for using the 100% common overlap amongst participants, rather than individual trajectories for each participant was to exclude potential noise or spurious fibres that may have been included in certain participants' analyses. Given the possibility of inclusion of spurious connectivity when using DTI, using the common overlap of all participants ensured a higher accuracy in the dissection of pathways, whilst still allowing individual variability to be reflected through the measure of FA.

Results

The SC-amygdala streamline was demonstrated successfully in all 19 participants bilaterally. Figure 5.1 presents a composite streamline of virtual dissections of the SC-amygdala streamline in all participants with a composite streamline of the voxels of SC-amygdala that overlapped in 100% of participants. Since the 100% overlapped SC-amygdala connection did not result in a continuous streamline, it was dilated by 2mm for visual purposes.

As described in Chapter 4 the streamline initially ascended dorsally from the SC, continuing to ascend postero-laterally to the pole of the medial pulvinar. The pathway then curved ventro-laterally to a position above the temporal horn of the lateral ventricle proceeding rostrally above the temporal horn, crossing from the medial to the lateral terminal, turning medially thereby connecting with the lateral amygdala.

Critical simultaneous onset trials on the saccade decision task were isolated for statistical analyses. Binomial regression analyses were carried out which tested for random and fixed effects as predictors of a bias to threat. Random intercepts were fitted for each participant (no random slopes). Fixed effects included fractional anisotropy (FA) of pathways and random effects included location of threat (temporal versus nasal) and the mixed random and fixed effects of interactions between FA and threat location as predictor of threat bias. Binomial regression analyses demonstrated no interaction between left and right SC-Amygdala streamline FA and no laterality differences as predictors of orienting toward threat (see Table 5.1).

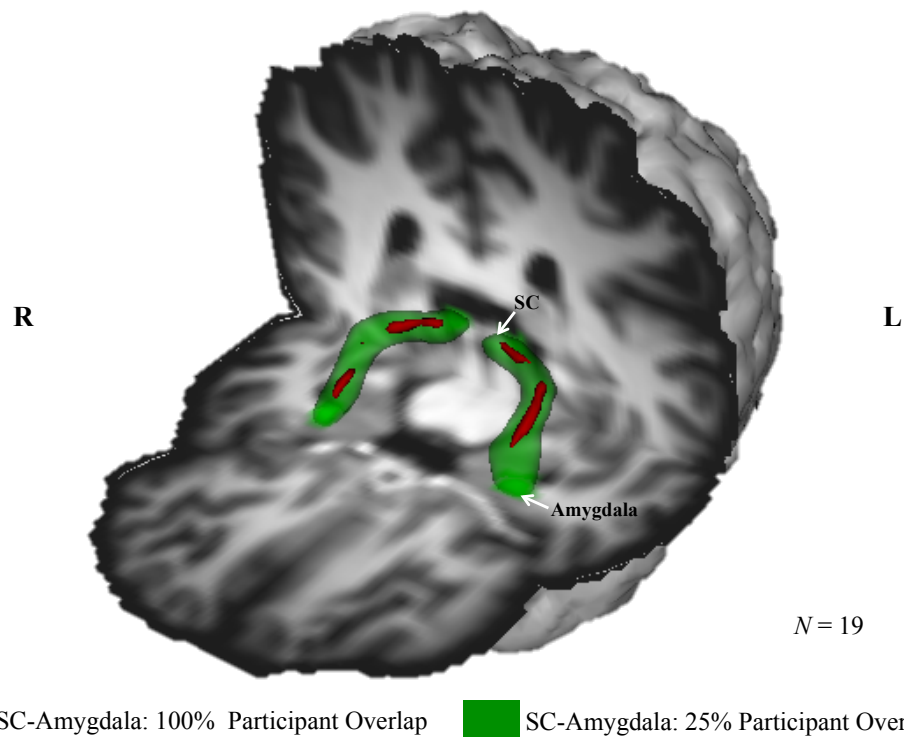


Figure 5.1. Virtual dissection with DTI tractography of connections between the superior colliculus and amygdala in 19 healthy humans. Each streamline for each participant was registered to common brain space and added to create a composite streamline common to all participants (green). The composite streamline includes voxels in which streamlines overlapped between participants in at least 25% of participants. A low threshold was selected to demonstrate variability in common anatomical overlap between participants. The composite pathway was thresholded at 100% to include only the voxels that included streamlines common to all 19 participants in the sample (red). A mask including only voxels in which streamlines were present in all participants was created and registered to individual participant's diffusion space and was used for computation of FA. The SC-Amygdala 100% overlap mask in this figure (red) was dilated by 2mm for visual purposes since the resulting streamline was not continuous.

Mean SC-amygdala FA was collapsed across left and right hemispheres for each participant. Individual bias towards threat stimuli was strongly associated with mean higher SC-amygdala FA across individuals (see Table 5.2). Figure 5.2 demonstrates the effect of SC-amygdala FA as predictor of threat bias.

Table 5.1. SC-amygdala in left and right hemispheres as predictors of threat bias. Binomial regression model with random intercepts fitted for each participant showing effects of connectivity (FA) between the superior colliculus and amygdala in the left and right hemispheres as predictors of threat bias.

	<i>B</i>	<i>SE</i>	<i>p</i>
<i>Step 1</i>			
Threat Bias	0.07	0.37	0.05
<i>Step 2</i>			
Threat Bias	-0.48	0.39	0.22
Left SC-Amygdala FA	1.80	1.28	0.16
<i>Step 3</i>			
Threat Bias	-0.71	0.37	0.06
Left SC-Amygdala FA	-0.30	1.46	0.83
Right SC-Amygdala FA	3.07	1.28	0.02*
<i>Step 4</i>			
Threat Bias	-0.68	3.53	0.85
Left SC-Amygdala FA	-0.41	11.87	0.97
Right SC-Amygdala FA	2.96	12.51	0.81
Left * Right SC-Amygdala FA	0.37	41.54	0.99

* Denotes $p < .05$

Table 5.2 SC-amygdala FA as predictor of threat bias. Binomial regression model with random intercepts fitted for each participant showing main effect of strength in connectivity (FA) of superior colliculus - amygdala as predictor of orienting to threat in the temporal/nasal hemifields.

	<i>B</i>	<i>SE</i>	<i>p</i>
<i>Step 1</i>			
Threat Bias	0.07	0.37	0.05
<i>Step 2</i>			
Threat Bias	-0.83	0.36	0.02*
Mean SC-Amygdala FA	3.05	1.22	0.01*
<i>Step 3</i>			
Threat Bias	-0.97	0.36	<0.008*
Mean SC-Amygdala FA	3.06	1.22	0.01*
Threat Temporal	0.28	0.07	<0.001*
<i>Step 4</i>			
Threat Bias	-1.92	0.51	<0.001*
Mean SC-Amygdala FA	6.29	1.74	<0.001*
Threat Temporal	2.18	0.73	<0.001*
Mean SC-Amygdala FA *Threat Temporal	-6.47	2.45	<0.009*

* Denotes $p < .05$

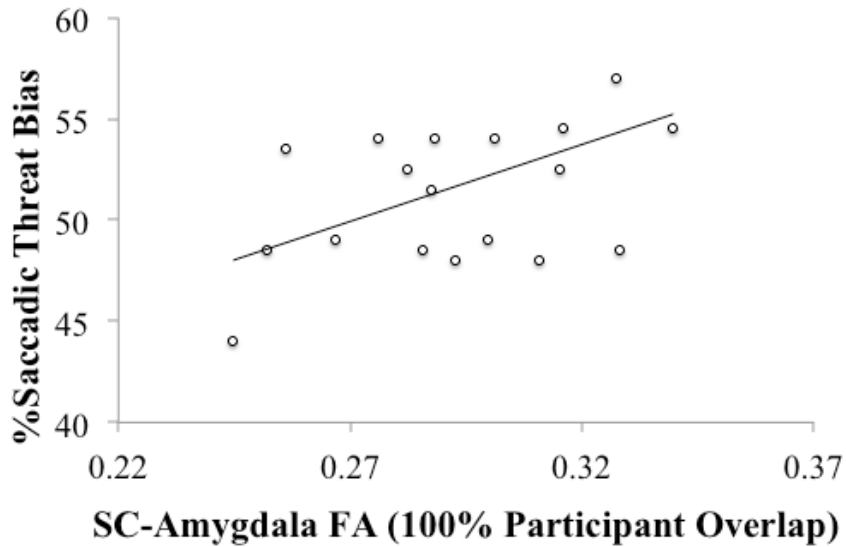


Figure 5.2. SC-Amygdala as predictor of threat bias. SC-Amygdala FA averaged across left and right hemispheres predicted a bias to saccade to threat on a saccade decision paradigm demonstrated with a binomial regression model with participant entered as random effect ($\beta = 3.05, p = <.01$).

An advantage to orient toward stimuli in the temporal rather than nasal visual hemifield has been attributed to extrageniculate visual processing by way of the retinotectal pathway (Sylvester, Josephs, Driver, & Rees, 2007; Tomalski, Johnson, & Csibra, 2009). A bias to orient to threat was exclusive to the temporal visual hemifield as reported in Chapter 3. Therefore, it was expected that the SC-amygdala pathway would be a stronger predictor of threat bias for targets appearing in the temporal compared to nasal visual hemifield. However, an interaction was observed between visual hemifield (temporal versus nasal) and SC-amygdala FA as predictor of threat bias in the opposite direction as opposed to what was predicted: SC-amygdala FA predicted threat bias in the nasal visual hemifield. Figure 5.3 demonstrates strength in connectivity of SC-amygdala FA as predictors of threat bias in the temporal and nasal visual hemifields.

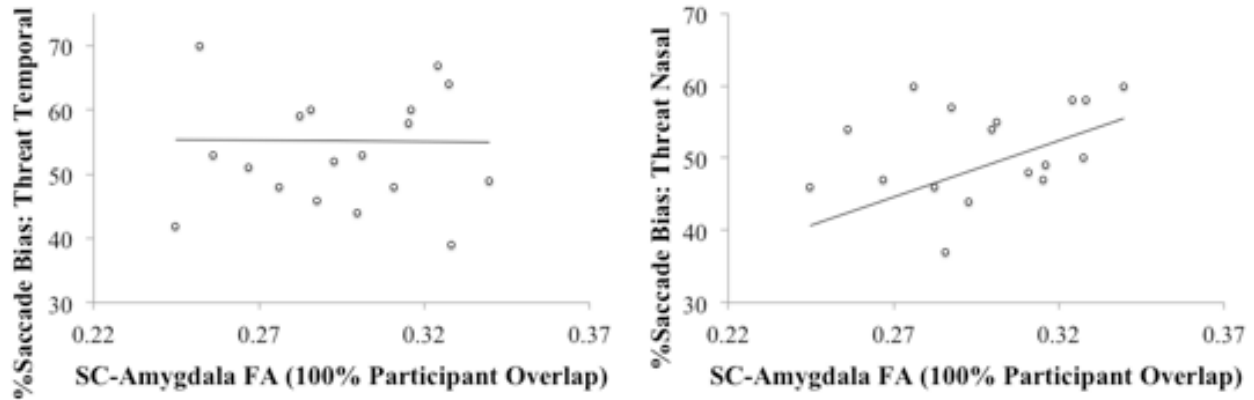


Figure 5.3. Strength in connectivity of SC-Amygdala as predictors of threat bias in temporal and nasal visual hemifields. Binomial regression with participant entered as random effect demonstrated an interaction between SC-amygdala FA and hemifield showing an effect of SC-amygdala FA to predict threat bias in the nasal rather than the temporal hemifield (right, $\beta = -6.47$, $p = <.009$).

Considering similar observations of connectivity strength (FA) of the brachium of the superior colliculus including voxels of the retinotectal tract (RTT, described in Chapter 3) in predicting overall threat bias and predicting a trend to threat in the nasal visual hemifield, it was important to compare the anatomical relationship between the 100% participant overlap of both the SC-amygdala and the isolated retinotectal tract (RTT). Figure 5.4 presents the anatomical relation between the isolated RTT and the SC-amygdala pathway. Anatomical streamlines demonstrated a trajectory of the RTT medial and inferior to the SC-amygdala route. This demonstrates a small number of RTT streamlines sharing voxels with the SC-amygdala tract. Therefore, it is unlikely that the strength in connectivity of the brachium of the superior colliculus and the RTT was driving the effect of SC-amygdala FA as predictor of threat bias. In contrast, a large number of SC-amygdala streamlines also passed through the RTT, suggesting that the bias to threat demonstrated by the RTT may have resulted from contributions from the SC-amygdala FA.

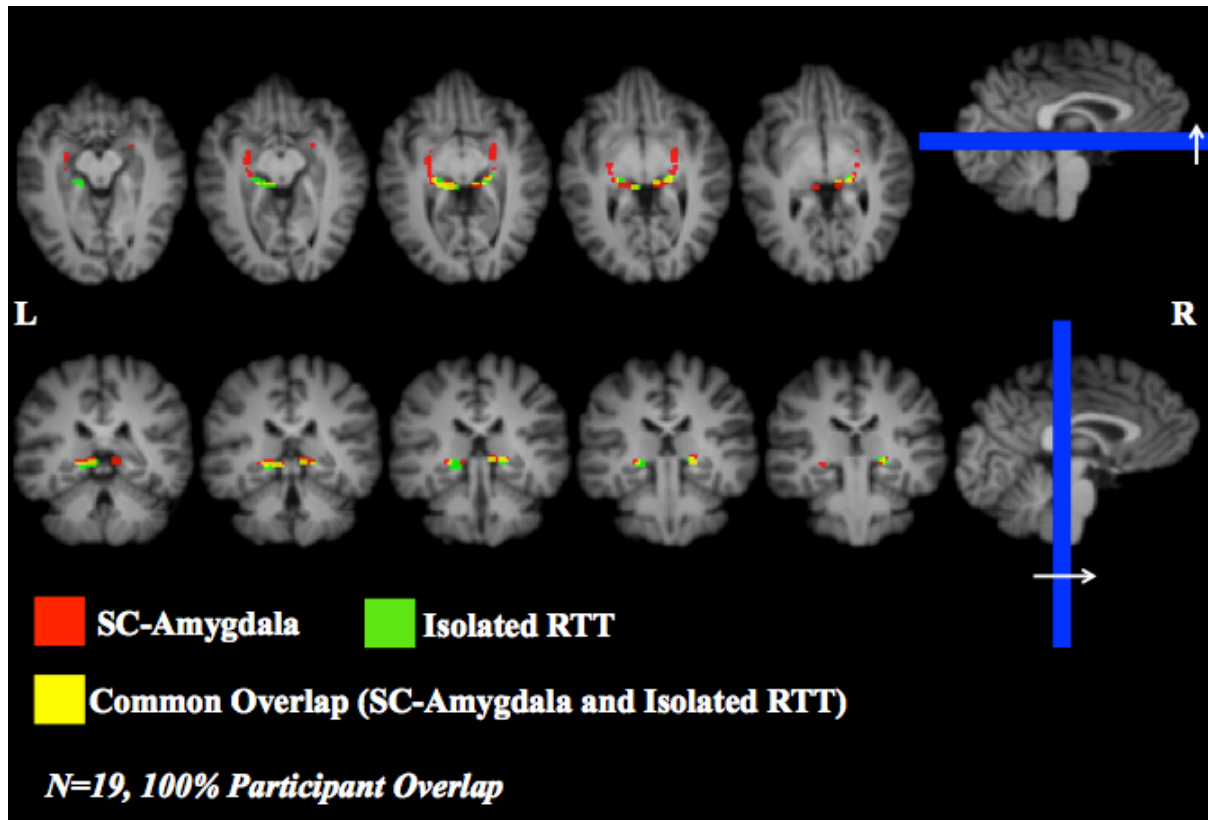


Figure 5.4. Anatomical relation between SC-amygdala and RTT pathways. The RTT (green), which also shared voxels with the brachium of the superior colliculus, followed a trajectory medial and inferior to the SC-amygdala pathway (red). Shared voxels between the two streamlines (yellow) demonstrated a small contribution of RTT fibres to the SC-amygdala streamline, and a large contribution of SC-amygdala streamlines to the RTT.

Discussion

Results from this study demonstrated that strength in pathway connectivity (FA) between the SC and the amygdala virtually dissected with DTI tractography predicted a bias to orient to threat in a saccade decision task. This finding corresponded with that of connectivity between the retinotectal tract (RTT) as predictor of threat bias previously reported in Chapter 3. The anatomical relationship between the two pathways demonstrated a route for the RTT that is medial and inferior to the SC-amygdala streamline, with only few RTT voxels shared with the SC-amygdala, militating against the potential that the threat bias predicted by SC-amygdala FA was due to contribution from the RTT.

Although no interaction was demonstrated between left and right hemisphere SC-amygdala FA, it is important to note that when considered individually (Table 5.1), SC-amygdala FA in the right hemisphere only demonstrated a statistically reliable effect to predict a threat bias. This corresponds with evidence in the literature suggesting that the right

rather than the left amygdala relates to emotion processing (e.g. Morris, Öhman & Dolan, 1999). However, since no interaction between left and right SC-amygdala FA was observed, an exclusive contribution of the right SC-amygdala to predict threat bias cannot reliably be concluded. The lack of interaction between left and right hemisphere SC-amygdala FA may have represented a Type II error, demonstrating a false negative interaction due to small sample size. Alternatively, a false negative effect of the left hemisphere SC-amygdala FA may have been demonstrated due to a higher number of shared voxels with the RTT and the left SC-amygdala tracts compared to the right, as shown in Figure 5.4.

In conclusion, this experiment provides the first evidence that strength in connectivity of connections between the amygdala and the SC through the pulvinar support the processing of individual fear-evoking stimuli.

CHAPTER 6

STRIA TERMINALIS STRUCTURAL CONNECTIVITY IN HUMANS PREDICTS BIAS IN ORIENTING TOWARD THREAT

Stria terminalis structural connectivity in humans predicts bias in orienting toward threat

Kristin Koller¹, Christopher M. Hatton¹, Robert D. Rogers¹ & Robert D. Rafal¹

¹ Wolfson Centre for Clinical and Cognitive Neuroscience, School of Psychology, Bangor University, Bangor, Gwynedd, United Kingdom

Abstract

Current concepts of the extended amygdala posit that basolateral to central amygdala projections mediate fear-conditioned autonomic alerting, whereas projections to the stria terminalis' bed nucleus mediate sustained anxiety. Using DTI tractography in humans, we show that connectivity strength of the stria terminali, correlates with an orienting bias toward threat in a saccade decision task, providing the first evidence that this circuit supports decisions guiding evaluation of threatening stimuli.

A putative threat mediating pathway connecting the superior colliculus with the amygdala was shown to predict a bias to threatening stimuli in Chapter 5, consistent with previous work suggesting that subcortical connections between the superior colliculus (SC), pulvinar and amygdala mediate orienting of attention to threat (de Gelder, Morris, & Dolan, 2005; Morris, Ohman, & Dolan, 1999; Ward, Danziger & Bamford, 2005). Converging evidence in rodent and non-human primate studies has shown two major outputs of the basolateral amygdala, and suggest that they serve different functions in transmitting information about threatening stimuli: (i) a projection to the central nucleus of the amygdala, critical in linking aversive cues to phasic fear-conditioned arousal mediated by the autonomic nervous system; and (ii) a projection to the bed nucleus of the stria terminalis (BNST) via the stria terminalis, mediating tonic states manifest as anxiety (Fox, Oler, Tromp, Fudge, & Kalin, 2015; Walker, Toufexis, & Davis, 2003). Anatomy of the SC and the amygdala connection previously reported (Rafal, Koller, Bultitude, Mullins, Ward, Mitchell, & Bell, 2015; Chapter 4) demonstrated a projection from the pulvinar to the lateral amygdala. This study investigated the role of the the outflow of the amygdala to the BNST after receiving SC-amygdala afferents.

In humans, Kim and Whalen (2009) performed voxelwise regression analyses showing that amygdala BOLD activation elicited by fearful faces regressed against fractional anisotropy (FA) images derived from DTI predicted an axonal connection between the amygdala and the ventromedial prefrontal cortex. By contrast, their data neither demonstrated any association between the integrity of projections between the amygdala and BNST via the stria terminalis, or with amygdala BOLD responses to fearful expressions. Their findings are consistent with animal models (Fox et al., 2015; Walker et al., 2003), suggesting that the bed nucleus of the stria terminalis (BNST) is not involved in eliciting fear in response to threat.

Most experimental models typically involve either a threatening or non-threatening stimulus presented on each trial, and evocation of fear is inferred from phasic, automatic responses by the autonomic system (Bar-Haim, Pergamin, Bakermans-Kranenburg, & Van Ijzendoorn, 2007; Walker, et al., 2003). Here, the current DTI study provides the first evidence that amygdala projections to the BNST via the stria terminalis are involved in orienting to threat. Our starting point is a framework advanced originally by Posner and Boise (1971) who posited two separate, isolable components of attentional orienting: alertness, and selectivity. We tested the hypothesis that projections from the amygdala to BNST via the stria terminalis convey information that influence selective responses to potential threat mediating flee or fight; approach or withdraw responses. We used probabilistic DTI to 'virtually' dissect amygdala innervation via the stria terminalis to the

BNST in humans. We then tested associations between the strength of these connections and a bias to orient toward threat in a novel saccade decision task.

Methods and Results

Nineteen neurologically healthy humans (9 male, age range 18-25yr) participated. All participants were screened for high trait anxiety measured by the State-Trait Anxiety Inventory (Spielberger, 1983, trait anxiety scores ranged between 23-59). On each trial, a threatening and a non-threatening visual stimulus was presented at the same eccentricity in opposite visual fields. The threatening stimulus appeared 53 ms before the non-threatening stimulus on 33% of the trials, 53ms after the non-threatening stimulus on 33% of the trials and simultaneously on the remainder of the trials. Stimulus picture pairs matched for luminance (e.g. a snake preparing to strike paired with a bunny) were selected from the International Affective Picture Scale (Lang, Bradley, & Cuthbert, 2008; supplementary Fig. 6.2). Participants were instructed that one stimulus always appeared first, to ignore the picture content and to saccade from central fixation toward whichever stimulus appeared first (supplementary Fig. 6.3). An Eyelink1000® device recorded saccade latency and direction under monocular viewing conditions. Critical trials for testing our hypothesis were those with simultaneous onset of the threatening and non-threatening stimuli.

Participants' bias towards threat was tested as the percentage of saccadic choices toward threat made on simultaneous onset trials, regressed against connectivity strength measures of stria terminalis (FA) (analysed as a multilevel binomial model).

Stria terminalis virtual dissection with probabilistic DTI tractography was completed as previously described (Rafal et al., 2015). Streamlines were generated in each hemisphere from a seed mask in the amygdala and a target mask in the BNST (supplementary Fig. 6.1). Additionally a waypoint mask was drawn on the stria terminalis along its trajectory adjacent to the lateral ventricle between the body of the caudate and the anterior nucleus of the thalamus. Streamlines in each participant were used for computation of mean fractional anisotropy (FA) values.

The stria terminalis was demonstrated successfully in 19 humans (bilaterally in 18 subjects, unilaterally in the right hemisphere of 1 subject). Consistent with previous DTI findings (Avery et al., 2014; Krüger, Shiozawa, Kreifelts, Scheffler, & Ethofer, 2015; Rafal et al., 2015), the stria terminalis emerged from the amygdala, traversing above the lateral ventricle's temporal horn before running along the lateral border of the caudate nucleus tail to

the border of the anterior thalamic nucleus and the body of the caudate nucleus, and then descended through the diencephalon to enter the BNST (Fig. 6.1A).

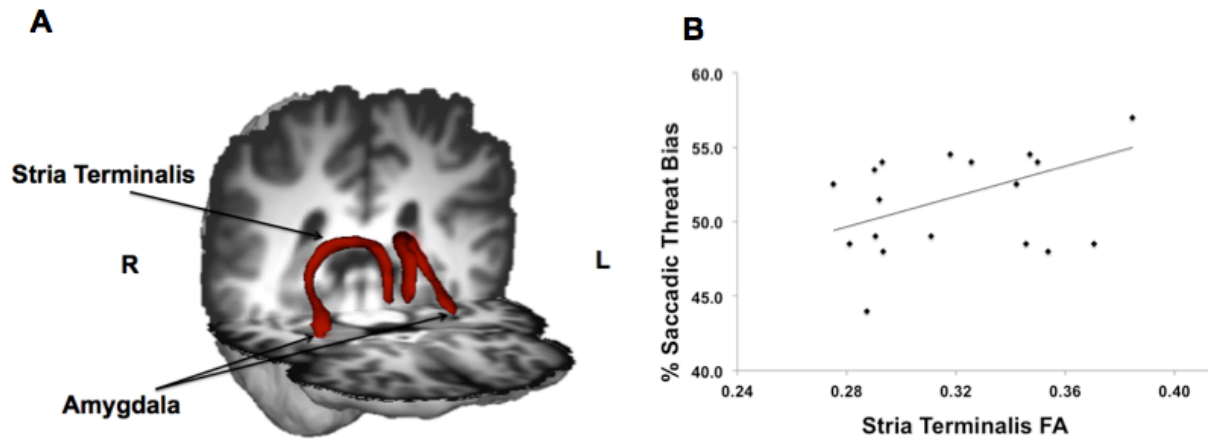


Figure 6.1. Stria terminalis FA as predictor of threat bias. 6.1A: Bilateral stria terminalis composite tracts (in red) of all participants' tracts registered to common space. Tracts represent the composite of common anatomical overlap across participants in left and right hemispheres, showing voxels with streamlines present in at least 67% of participants. DTI data collection, analyses and tractography methods have been reported elsewhere (Rafal et al., 2015: Chapter 4). 6.1B: Figure 6.1B presents scatter plot of main effect of averaged left and right stria terminalis FA as predictor of percentage saccadic choices towards threatening stimuli (supplementary Table 6.1).

Critical simultaneous onset trials were isolated for statistical analyses and the mean stria terminalis FA was collapsed across left and right hemispheres for each participant. Binomial regression analyses with random intercepts fitted for each participant (no random slopes) tested for the fixed effects of fractional anisotropy (FA) as predictor of threat bias. The analyses demonstrated that individuals' bias towards threat stimuli was strongly associated with mean higher stria terminalis FA across individuals (see Table 6.1). Figure 6.1B presents the main effect of stria terminalis FA averaged across left and right hemispheres on orienting bias toward threat.

Table 6.1. *Stria terminalis as predictor of threat bias. Binomial regression model with random intercepts fitted for each participant showing main effect of averaged stria terminalis FA across left and right hemispheres as predictor of orienting bias.*

	<i>B</i>	<i>SE</i>	<i>p</i>
<i>Step 1</i>			
Threat Bias	0.07	0.37	0.05
<i>Step 2</i>			
Threat Bias	-0.59	0.32	0.07
Mean Stria Terminalis FA	2.05	1.00	0.04*

* Denotes $p < .05$

Conclusion

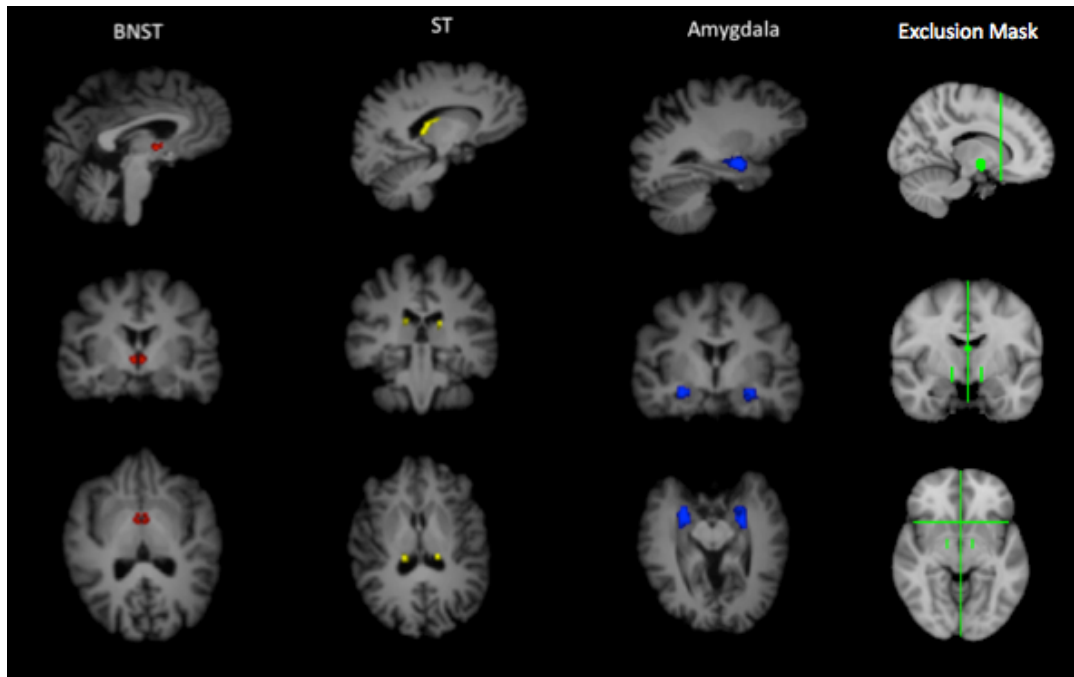
In conclusion, we provide the first evidence that projections from the amygdala to the BNST support the processing of individual fear-evoking stimuli. These findings suggest that, while this limbic pathway may not be involved in evoking of the phenomenal experience of fear, it may instead be part of an attentional network for selective orienting to potentially threatening stimuli.

Supplementary Information

Supplementary Table 6.1. Individual participant stria terminalis FA and threat bias scores.

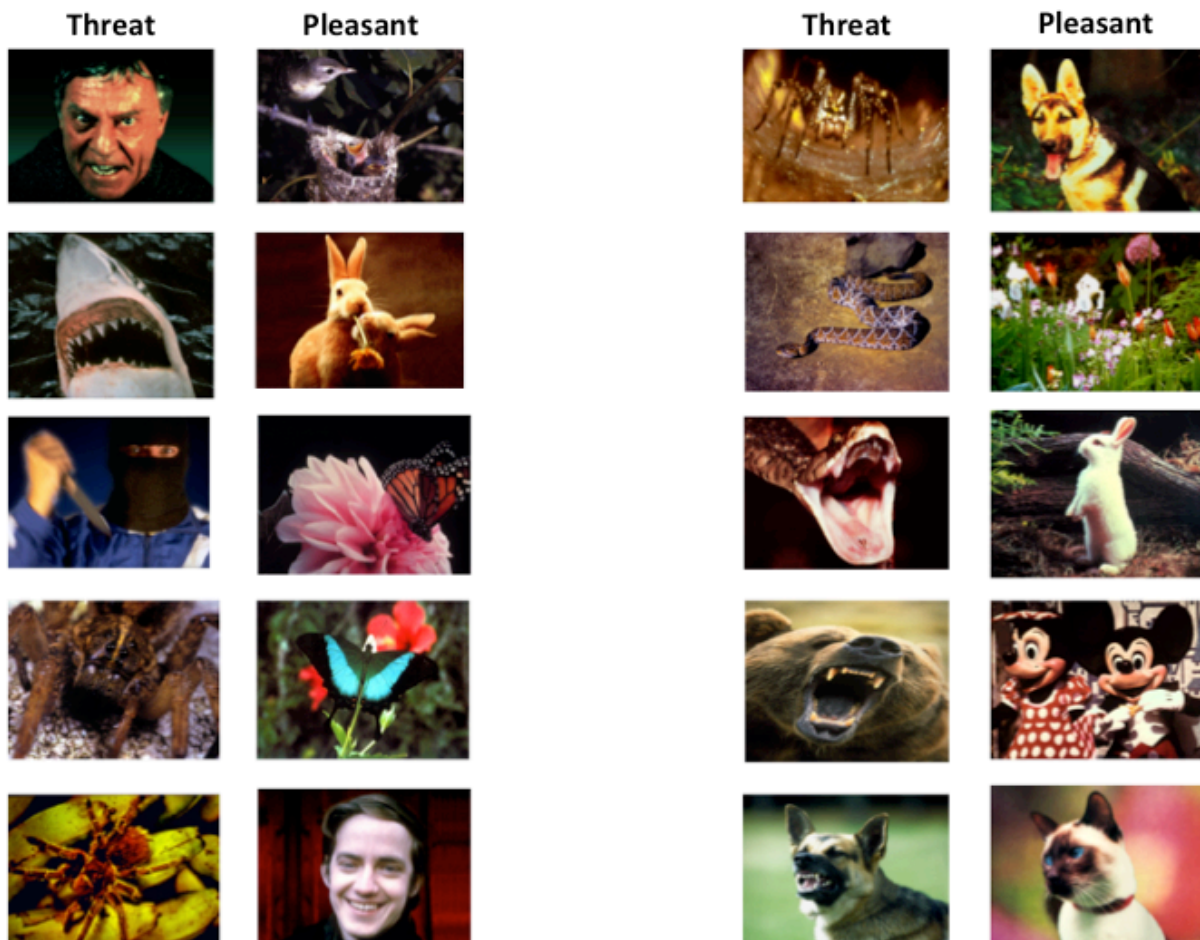
Individual participants' data for percentage saccades made towards threat versus pleasant pictures during simultaneous onset trials, the fractional anisotropy measures (FA) for each participant's stria terminalis (ST) dissection in the left and right hemispheres, and the individual average FA between left and right hemisphere tracts. The stria terminalis was successfully dissected in 18 participants bilaterally, and unilaterally in one participant. Hence, participant 16's right hemisphere FA value was used as the overall average FA value for that participant.

Participant	% Saccades to threat	Left ST FA	Right ST FA	Average ST FA
9	62.5	0.38	0.36	0.37
19	57.0	0.40	0.37	0.38
1	54.5	0.34	0.30	0.32
6	54.5	0.35	0.35	0.35
3	54.0	0.33	0.32	0.33
8	54.0	0.30	0.29	0.29
16	54.0	.	0.35	0.35
4	53.5	0.24	0.34	0.29
7	52.5	0.28	0.27	0.28
11	52.5	0.33	0.36	0.34
15	51.5	0.31	0.27	0.29
2	49.0	0.34	0.24	0.29
17	49.0	0.31	0.32	0.31
5	48.5	0.36	0.33	0.35
10	48.5	0.29	0.27	0.28
14	48.5	0.37	0.38	0.37
12	48.0	0.32	0.27	0.29
13	48.0	0.37	0.34	0.35
18	44.0	0.29	0.28	0.29

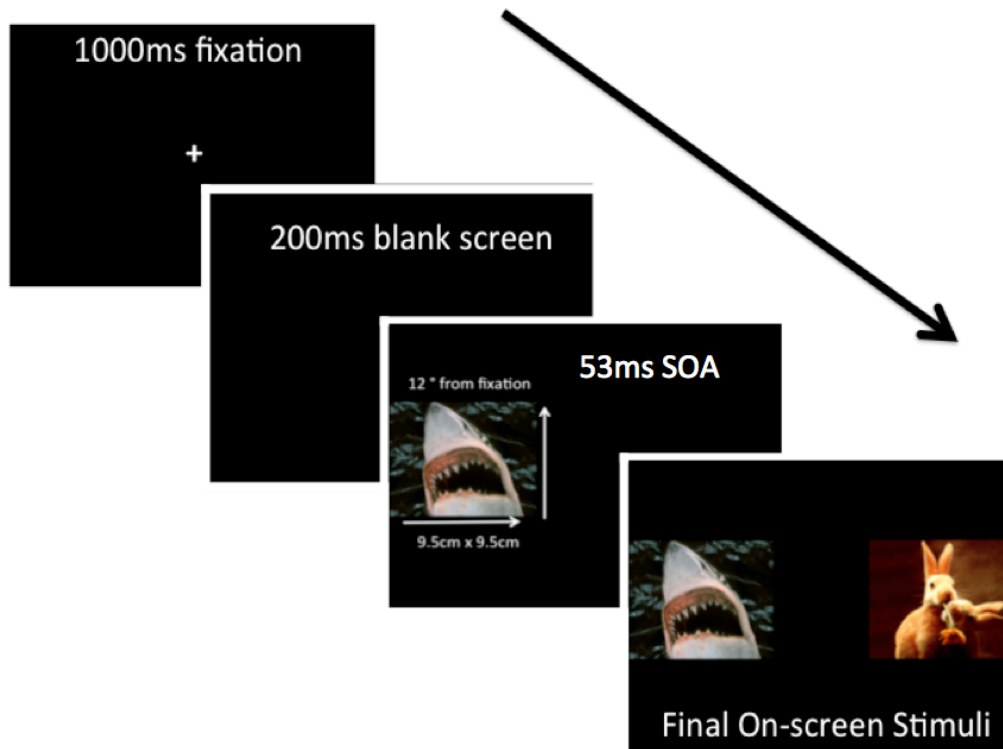


Supplementary Figure 6.1. Masks employed for virtual dissection with DTI tractography of the stria terminalis implemented using the FSL-FDT toolbox (Behrens et al., 2007). Tracts were generated from an amygdala seed mask (shown in blue) with the use of a waypoint mask drawn on the stria terminalis along its trajectory adjacent to the lateral ventricle between the body of the caudate and the anterior nucleus of the thalamus (shown in yellow), and with the use of a target and termination mask in the bed nucleus of the stria terminalis (shown in red). Masks are presented in the sagittal (top row), coronal (middle row) and axial (bottom row) views. A total of 19 subjects took part in the current experiment (including the human subjects previously reported as the “Second Group” (Rafal et al., 2015). In some participants, (eight) small exclusions were required to prevent streamlines reaching regions that do not form connections between the BNST and the amygdala via the stria terminalis. Regions included parts of the fornix, a mid sagittal slice, part of the frontal lobe and a small anterior region between amygdala and BNST. All voxels of resultant tracts were thresholded so that only voxels containing at least 10% of the maximum number of traces were included in the final tract for each participant. In the majority of participants (17 participants in left and right hemispheres), stria terminalis dissections that were achieved with the amygdala as the seed, the stria terminalis mask as the mid-waypoint mask, the BNST as the final waypoint and termination mask demonstrated the most consistent stria terminalis streamlines. In some cases where streamlines consistent with the known topography of the stria terminalis tracts were not obtained via the above-mentioned dissection order, the tract was traced in both directions (BNST as seed mask and amygdala as seed mask), and the resultant

overlapping voxels between the two tracts were used for calculation of fractional anisotropy values (left hemisphere of 2 participants, and the right hemisphere of 2 participants). In one participant in the right hemisphere, the dissection in the opposite order (BNST as seed, stria terminalis and amygdala as waypoints and amygdala as termination mask) produced a streamline most consistent with the known anatomy of the stria terminalis, and was used for FA calculation.



Supplementary Figure 6.2. Threatening and pleasant stimulus pairs selected from IAPS (Lang, Bradley & Cuthbert, 1997) employed during the saccade decision task.



Supplementary Figure 6.3. Stimulus presentation sequence during saccade decision task. Threat-related and unrelated (i.e. pleasant) stimuli appeared randomly on-screen in three conditions: simultaneous onset, right target appeared 53ms before left target, or vice versa. Stimulus types (pleasant vs. threatening) appeared randomly to the left/right, and pictures remained visible until response. Threatening and a non-threatening stimuli were presented at the same eccentricity in opposite visual fields. The threatening stimulus appeared 53 ms before the non-threatening stimulus on 33% of the trials, 53ms after the non-threatening stimulus on 33% of the trials and simultaneously on the remainder of the trials. Participants were instructed that one stimulus always appeared first, to ignore the picture content and to saccade from central fixation toward whichever stimulus appeared first. An EyeLink1000® device recorded saccade latency and direction under monocular viewing conditions. Critical trials for testing our hypothesis were those with simultaneous onset of the threatening and non-threatening stimuli.

CHAPTER 7

GENERAL DISCUSSION

General Discussion

The aim of this thesis was to establish functional evidence for the anatomy of subcortical non-image forming white matter connections in the healthy human brain that mediate reflexive responses to visual stimuli. Strength in connectivity measures (fractional anisotropy) of pathways virtually dissected with diffusion tensor imaging (DTI) tractography was correlated with choice and latency of eye movement responses to two types of salient stimuli that summon visual attention: abrupt onsets and emotionally valenced pictures. Reflexive saccades to peripheral targets on a temporal ‘gap’ paradigm were expected to demonstrate shorter latencies to targets in the temporal compared to nasal visual hemifield, a reflection of mediation by the retinotectal tract (RTT). A temporal hemifield advantage for visual targets was expected to correlate with connection strength of the RTT, projecting afferents from the retina to the superior colliculus (SC). Saccadic response bias to threatening stimuli measured on a temporal order saccade decision task was similarly expected to demonstrate an advantage to orient to threat in the temporal hemifield, reflecting processing by subcortical circuits via retinal projections to the SC via RTT. These predictions were based on demonstrations of preserved responses to threat stimuli in patients with lesions to the striate cortex, presumed to depend instead on a subcortical, rapid fear-processing route involving the superior colliculus, pulvinar and amygdala. Saccadic threat bias measures were correlated with the strength in connectivity of three pathways; the RTT, a connection between the SC and amygdala, and a connection between the amygdala and bed nucleus of the stria terminalis (BNST) via the stria terminalis. Table 7.1 demonstrates a summary of the main findings.

Role of retinal projections to SC in mediation of reflexive saccades

In Chapter 2 I aimed to provide evidence for a functional role of the retinotectal tract’s (RTT) direct projection to the superficial layers of the superior colliculus in mediating reflexive saccades. A saccade ‘gap’ experiment, which included a temporal gap of 200ms after fixation offset prior to target onset, was selected as the paradigm of choice since it optimises the conditions necessary to measure reflexive, express saccades. The goal was not to measure the gap effect *per se*, which measures a difference in response latency to targets preceded by a temporal gap compared to no-gap trials, but instead to take advantage of the fixation offset component of the gap paradigm to encourage generation of a population of short latency, express saccades. Ultimately, the goal was to obtain a measure of express saccades that could

be used to test for the ability of RTT strength in connectivity (FA) to predict reflexive saccade response latency in healthy participants.

Table 7.1. Summary of main findings. *RTT = Retinotectal Tract, SC = Superior Colliculus, FA = Fractional Anisotropy, N/A = Not Applicable*

Chapter	Behaviourial Measure	Anatomical measure	Main Findings	Conclusion
2	Latency of reflexive saccades to peripheral targets on 'gap' paradigm.	RTT (Optic tract - SC)	Shorter saccade latencies to visual targets in the temporal hemifield for potential express but not regular saccades. RTT FA did not predict saccade latency.	Retinal afferents to SC mediate reflexive saccades in temporal hemifield.
3	Choice and latency of saccadic threat bias on temporal order saccade decision paradigm.	RTT (Optic tract - SC)	Threat choice bias in temporal hemifield on simultaneous SOA trials. RTT FA predicted threat bias. RTT ascended from optic tract connecting SC laterally via posterior ventrolateral diencephalon.	Retinal afferents to SC contribute to mediation of threat in temporal hemifield.
4	N/A	SC-amygdala pathway Stria terminalis	Centre of gravity analyses demonstrated SC-amygdala connections distinct from stria terminalis connections. Amygdala-SC pathway ascended dorsally from SC, connecting postero-laterally via medial pulvinar to lateral amygdala. Stria terminalis emerged from amygdala, traversing above temporal horn along caudate nucleus tail and body, descending via diencephalon to BNST.	SC-amygdala and stria terminalis demonstrate anatomically distinct trajectories.
5	Saccade bias to threat on temporal order saccade decision task.	SC-amygdala pathway	SC-amygdala FA predicted overall threat bias.	SC-amygdala plays role in selective orienting to threat.
6	Saccade bias to threat on temporal order saccade decision task.	Stria terminalis	Stria terminalis FA predicted overall threat bias.	Stria terminalis plays role in rapid selective orienting to threat, and not only in mediating slow sustained anxiety as previously suggested.

An advantage for short latency saccades was demonstrated in the temporal hemifield, measured as shorter latencies to peripheral targets in temporal compared to nasal hemifield targets, providing evidence in support of the prediction that reflexive saccades are mediated by retinal input to the superior colliculus via the RTT. Typically, express saccades are

demonstrated as a separate population of saccades within the range of 80-100 ms (Fischer & Weber, 1993; Fischer and Ramsperger, 1986; Wenban-Smith & Finlay, 1991; Reuter-Lorenz et al. 1991), often demonstrated as bimodal distribution peaks of express and regular saccades of 180-250ms (Carpenter, 1977; Wheelless, Boynton & Cohen, 1966). Distributions of express saccades often vary considerably among participants, with mixed reports of unimodal or bimodal distribution peaks at 100ms (Reuter-Lorenz, 1991; Fischer et al., 1993). In appreciation of the considerable variability in saccade frequency distribution observed among participants on the gap task in this thesis, a measure of express saccades in the strict traditional sense was not isolated in a majority of participants. Instead, a more liberal threshold of 70-150ms was chosen to isolate a population of saccades likely to include mostly, but not exclusively, reflexive ‘short’ latency saccades. The temporal hemifields advantage in saccade latency was observed only for the short latency saccades, and was not evident in the analysis of saccade latencies across the whole range. Thus, the temporal hemifields advantage seems to be selective for reflexive saccades and not for saccades with latencies that were chiefly dependent on voluntary control.

Virtual dissections of the RTT with DTI tractography ascended dorsally from the optic tract and entered the superior colliculus (SC) laterally curving around the posterior ventrolateral diencephalon, corresponding to reported anatomy in animal studies (Leventhal et al., 1981; Perry & Cowey, 1984). However, visual inspection of RTT demonstrated considerable overlap of the dissected RTT with other fibres that also pass *via* pass through the brachium of the SC. Subtraction of the retino-geniculo-striate dissections from the RTT eliminated shared voxels with retino-geniculate but could not exclude striato-collicular fibres. For most individuals, most of the voxels in the ‘isolated’ RTT corresponded to the brachium of the SC. Since the brachium also contains projections from visual cortex to the SC, which greatly outnumber those of the RTT (Altman, 1962). I did not, therefore, succeed in isolating voxels that dominantly contained RTT fibres. The lack of correlation of the connectivity strength of the ‘isolated RTT’ with a temporal hemifields advantage for reflexive saccades was, in retrospect, not surprising.

Role of SC in predicting saccade bias to threat

Chapter 3 demonstrated a saccadic threat bias toward threat in the temporal visual hemifield, providing supporting evidence for a subcortical visual route that receives retinal input to SC via RTT to mediate threat processing. The rationale for this prediction was based on evidence in blindsight patients with striate lesions who demonstrate preserved ability to discriminate threatening stimuli (e.g. faces) in the absence of visual awareness. Instead, a phylogenetically conserved subcortical circuit involving the SC, pulvinar thalamus and amygdala has been proposed to process rapid orienting to environmental threat critical for survival, thereby accounting for blindsight phenomena.

On a temporal order saccade decision task participants chose whether a threatening or non-threatening image appeared first, when presentations of the images in the pair was separated by stimulus onset asynchrony (SOA). Unbeknownst to participants, presentation of stimuli occurred simultaneously on a third of the trials, thereby offering a critical measurement of bias to the image attended to first. Isolation of saccadic responses on critical simultaneous SOA trials provided a measure of threat bias, as was demonstrated in the temporal hemifield.

Strength in connectivity (FA) of RTT dissections was expected to predict threat bias on the temporal order saccade decision task and, since it was posited that orienting of attention to threat is mediated by afferents from the retina to the SC via RTT, it was further expected that the correlation of threat bias with connectivity strength would be stronger for trials in which the threat stimulus was presented in the temporal hemifields. Connectivity strength of the isolated brachium did predict a bias to saccade toward threat, but this was not contingent on threat presentation in the temporal hemifield. A possible explanation for this lack of support of RTT FA as predictor of threat bias specific to the temporal hemifield, is that the brachium of the SC, included in virtual dissections of RTT was, as mentioned above, not a pure isolate of RTT fibres. It is thus possible that visual information resulting in the threat bias was transmitted through both the retino-tectal tract and also afferents to the SC from visual cortex. On this account, the behavioural threat bias measured in this experiment may have had contributions from both: 1) visual signals transmitted to the superficial layers of the SC *via* the RTT that activated reflexive (unconscious) orienting mechanisms and that resulted in a temporo-nasal behavioural asymmetry and: 2) visual signals to the SC from visual cortex that mediated an additional contribution of voluntary (conscious) orienting.

Using a temporal order judgment task similar to that used in this thesis, Song, Rafal and McPeck (2011) demonstrated a muscimol inactivation study in rhesus monkeys, showing

that the SC plays a role in the voluntary selection of orienting responses (reaching movements). Target selection was biased towards targets ipsilateral to the inactivated colliculus. This was true for a monkey trained to reach toward the target that appeared *second*. These results demonstrate that the bias was not due to slowed perceptual processing, was not specific to oculomotor responses, and was manifest when target selection was based on a voluntary (non- reflexive) choice.

Therefore, it is feasible that strength in connectivity (FA) of the numerically dominant projections from V1 to SC via the brachium of SC, accounted for most of the correlation with threat bias. On this account bottom-up reflexive orienting toward threat mediated through retinal afferents to SC via RTT, while sufficient to produce a measurable temporo-nasal asymmetry, contributed little to the correlation of brachium connectivity with overall threat bias.

As is evident from inspection of the stimulus pairs shown in Figure 3.8 (Chapter 3), some of the threatening stimuli that elicited the strongest threat bias did so based on features that would likely require some conscious processing of the meaning of the pictures, and could not have been dependent upon simple features that could have been extracted at the level of the colliculus itself. This will be discussed further below.

Anatomical relationship between SC-amygdala and BNST-amygdala connections

Chapter 4 presented probabilistic DTI tractography of two connections with the amygdala; a connection with the SC proposed to mediate rapid orienting to threat (de Gelder, Morris, & Dolan, 2005; Morris, Ohman, & Dolan, 1999), and a projection to the bed nucleus of the stria terminalis (BNST) via the stria terminalis, which plays a role in mediating tonic states that manifest as anxiety (Fox, Oler, Tromp, Fudge, & Kalin, 2015; Walker, Toufexis, & Davis, 2003). Anatomical data in humans presented in Chapter 4 has been published (see Rafal, Koller, Bultitude, Mullins, Ward, Mitchell & Bell, 2015). Additionally, Chapter 5 included unpublished data from 7 additional participants.

Topography of virtual dissections of the SC-amygdala tract demonstrated a projection from the SC that passed through the pole of the pulvinar by first entering through the medial pulvinar. The trajectory then descended and turned laterally, passing rostrally through the lateral pulvinar, prior to exiting the pulvinar traversing above the temporal horn of the lateral ventricle, positioned dorsal and medial relative to the position of the stria terminalis, connecting to the lateral amygdala at the stria terminalis terminal. Anatomical observations of SC-amygdala streamlines are consistent with a previous report of SC-connections

demonstrated with deterministic DTI tractography (Tamietto et al., 2012). Virtual dissections of the stria terminalis demonstrated a trajectory emerging from the amygdala that traversed above the temporal horn of the lateral ventricle prior to tracking along the caudate nucleus tail and in the wall of the lateral ventricle between the body of the caudate anterior thalamic nucleus and finally descending through the diencephalon to the region of the BNST, consistent with recent imaging reports in humans (Avery et al., 2014; Krüger, Shiozawa, Kreifelts, Scheffler & Ethofer, 2015) and anatomy reported in animal studies (De Olmos & Ingram, 1972).

Probabilistic DTI tractography infers the anatomy of an axonal connection based on the degree of anisotropy of the diffusion in the same direction in each voxel of a given streamline. However it is not able to provide information on origin of projections, or the termination of synapses, for example whether SC projects to amygdala, or *vice versa*. Furthermore, in comparison with gold standard tracer techniques that yield tracer tracks constrained within axon walls, only possible in animal studies, DTI tractography provides computerised white matter reconstructions based on only on the diffusion inside the cells, unbounded by cell walls. Therefore, it was important to consider anatomical relationships of the SC-amygdala pathway with neighbouring pathways such as the stria terminalis in order to avoid inclusion of streamlines from other routes that may also pass through the same voxels through which SC-amygdala streamlines pass. Previous reports have not specifically addressed the anatomical relationship between the SC-amygdala pathway and potential neighbouring pathways such as the stria terminalis. Therefore the stria terminalis was virtually dissected to offer anatomical comparison between the two tracts. Chapter 5 presented a novel approach that considered the anatomical position based on axial, coronal and sagittal coordinates, in addition to the spatial resolution of voxels occupying each tract to demonstrate statistically distinct centres of gravity between the SC-amygdala tract and the stria terminalis in the portion of their trajectories that traversed above the temporal horn. Accordingly, Chapter 5 provided a unique contribution to the understanding of the anatomical trajectories demonstrating that the SC-amygdala streamline traversed above the temporal horn just medial to the stria terminalis, following a course dorsal to the stria terminalis, and highlighted the potential spatial resolution of tractography derived from diffusion imaging.

Ward, Danziger and Bamford (2005) demonstrated a critical contribution of the pulvinar in mediating responses to visual threat. In contrast to controls, who had longer mean reaction times to single targets that immediately followed threatening compared to pleasant

image primes demonstrated by healthy controls, a patient with destruction of the medial pulvinar on the left, did not demonstrate such attention to threat in the contralesional field. Instead, a delay in interference of threat was demonstrated, with interference from threat at longer, rather than short, prime-target SOAs. Additionally, Ward, Calder, Parker and Arend (2007) demonstrated impaired discrimination of fearful faces in the contralesional field in one patient with unilateral pulvinar damage. Three other patients with pulvinar lesions did not show deficits in emotion recognition. Motivated by findings of Ward and colleagues, Rafal et al. (2015) reconstructed the topography of the SC-pulvinar-amygdala streamline from healthy controls co-registered to the MRIs of two patients and demonstrated that the lesion of both patients would have interrupted the pathway. In contrast the pathway was not interrupted in the three patients who did not show a contralesional deficit in fearful face discrimination. Figure 7.1 presents the SC-amygdala reconstructed streamline in one patient who demonstrated preserved emotion recognition post lesion to the pulvinar.

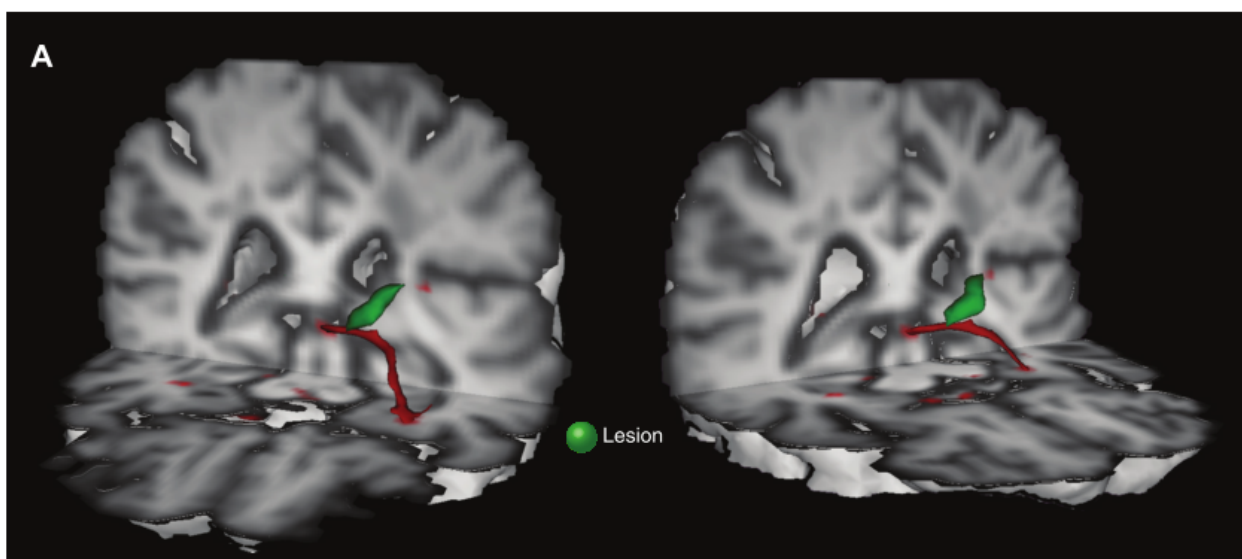


Figure 7.1. Virtual dissection with probabilistic DTI tractography between SC-pulvinar-amygdala in left hemisphere of patient DG (Rafal et al., 2015, p.1959, Fig. 10A). A 3D reconstruction of the pathway is shown in red, relative to the location of the pulvinar lesion, shown in green. DG did not demonstrate a deficit in responding to threat in the contralesional field (Ward et al., 2007), corresponding with the intact streamline demonstrating no interruption by the pulvinar lesion.

These findings provide strong evidence that the virtually dissected streamline connecting pulvinar to amygdala described in this thesis is a functional anatomical pathway transmitting

threat signals. They do not, however, directly confirm that the visual afferents to the part of the pulvinar projecting to amygdala arise from the retino-recipient layers of the superior colliculus. This is a question that cannot be resolved with DTI tractography, which is why the naso-temporal manipulation was employed in my experiments, and why I attempted to determine whether the connectivity strength of the RTT also correlated with threat bias in the saccade decision task.

Associations between function and anatomy in the healthy human brain with the use of DTI dissections alone, and without guidance from lesion sites, can only be indirectly inferred. Therefore, one goal of this thesis was to test the prediction that the SC-amygdala pathway mediates responses to threat in the healthy human brain, as shown in Chapter 5.

Linking SC-amygdala pathway function with anatomy in the healthy brain

Chapter 6 attempted to provide evidence in support of a functional role in threat processing for a putative, phylogenetically conserved subcortical connection between the SC and amygdala via the pulvinar nucleus of the thalamus. Behavioural measures of threat bias, demonstrated on the temporal order saccade decision task in Chapter 3, and virtual dissections of the proposed threat-mediating pathway demonstrated in Chapter 4 were combined to show that SC-amygdala strength in pathway connectivity (FA) predicted a bias to orient to threat across individuals. The effect of SC-amygdala strength in connectivity to predict a bias to threat stimuli corresponded with that presented in Chapter 3, showing a similar effect of RTT FA to predict threat bias. Anatomical comparison of the two pathways demonstrated a trajectory of the RTT medial and inferior to the SC-amygdala tract, with only a small number of RTT containing voxel overlapping with those containing the SC-amygdala streamline. Therefore, it is unlikely that the RTT was contributing to predicting of threat bias. In contrast, a larger number of SC-amygdala voxels overlapped with the RTT, therefore it cannot be ruled out that the SC-amygdala pathway FA potentially was a confound in the correlation between RTT FA and threat bias in Chapter 3.

Contrary to the prediction that the stronger threat bias observed for threat stimuli in the temporal hemifields would be reflected also in a correlation between RTT FA and temporal hemifields threat bias, SC-amygdala FA did not predict threat bias specific to the temporal hemifield. Instead, SC-amygdala FA predicted a threat bias in the nasal visual hemifield. This effect does not correspond with previous reports demonstrating that temporal hemifield advantages reflect SC function via the RTT (Tomalski, Johnson & Csibra, 2009; Sylvester, Josephs, Driver & Rees, 2007). Although this finding was not evidence of

subcortical threat processing *per se*, it still provides novel evidence that the SC-amygdala connections mediate threat. However, the behavioural evidence of a bias in the temporal visual hemifield provided strong support for contribution from retinal afferents to SC via RTT, reflecting subcortical processing. Furthermore, it may be that the supraliminal stimuli employed during the saccade decision task presumably elicited both cortical and subcortical processing, and that subcortical threat processing reflected through the behavioural results demonstrating a temporal hemifield advantage, and that cortical processing was reflected via anatomical results, demonstrating a correlation between SC-amygdala and threat bias. This does not necessarily rule out the dissected SC-amygdala's role in mediating subliminal responses to threat, but instead suggests that perhaps on this paradigm, cortical afferents may have contributed more strongly to threat processing. Consideration of stimuli used during the saccade decision task is discussed in greater detail below.

Consideration of stimuli used in saccade decision task

In the interpretation of findings from this thesis, it was important to consider the stimuli that were used during the temporal order saccade task in Chapter 3. The stimuli were presented to participants unmasked. The aim was to measure SC function by creating conditions optimal to elicit reflexive saccades (via inclusion of a 200ms gap) and by manipulating the viewing field with patching of the eye to create monocular viewing conditions. However, compared to previous demonstrations of responses to unseen threat with the use of masked stimuli, responses on simultaneous trials of the saccade decision task were selected under conditions where the emotional valence of the competing stimuli was consciously available to the participants. Therefore, the possibility that these stimuli were processed via the visual cortex, in addition to the subcortical SC-amygdala route, might reasonably be assumed.

The superior colliculus is biased to stimuli with special (low spatial frequency) features such as faces including stimuli with features that could be perceived as two eyes and a mouth, for example an inverted triangle inside an oval (Johnson, 1990; Tomalski, Johnson & Csibra, 2009). Therefore, consideration of stimuli pairs that elicited a bias to threat in this study was carried out by visually inspecting the order of stimulus pairs that elicited the highest to lowest percentage bias to threat. The stimulus pair that elicited the highest percentage threat bias (pair 2, Figure 3.8, Chapter 3) was a picture of a great white shark paired with a bunny; however some pairs of stimuli that included threatening faces also elicited high percentages of threat bias. Stimulus pair 1, an angry face paired with a bird and nest, elicited the third highest percentage of threat bias. Furthermore, the pair that elicited the

least percentage threat bias was pair 5, a pleasant face paired with a tarantula. Additionally, stimuli that elicited a bias to non-threat pictures may have been biased towards the face-like aspect portrayed in the picture, such as a Mickey Mouse character in stimulus pair 9, the face of a pleasant dog in pair 6 and the cat in pair 10.

Although the second highest percentage of threat bias was elicited in response to stimulus pair 3, a picture of a man brandishing a knife and wearing a balaclava mask paired with a butterfly, it is more likely that the bias in this stimulus pair was towards the threatening aspect of the picture, rather than the face-like aspect, since characteristics of a typical face (inverted triangle) is not present. This perhaps presents an example of a learned response bias, for example learning that a knife pointed towards you is a threat, compared to hard-wired automatic responses to threatening face-like stimuli. Such learned fear could not be processed by the superior colliculus, instead highlighting the possibility that cortical processing rather than subcortical processing elicited a bias to threat for at least some of the stimulus pairs. Furthermore, individual differences in threat bias could have introduced variability in responses measured, since some individuals may find some stimuli pleasant, for example a dog, whereas others may perceive the same friendly dog as a threat. Stimuli used in this experiment provided a useful indication of optimal stimuli to include in future work, discussed in more detail below.

A novel role of the stria terminalis in selective orienting to threat

Evidence in rodent and non-human primate research has shown two major outputs of the basolateral amygdala, serving different functions in transmitting information about threatening stimuli. One output projects to the central nucleus of the amygdala, critical in linking aversive cues to phasic fear-conditioned arousal mediated by the autonomic nervous system. A second output projects to the bed nucleus of the stria terminalis (BNST) via the stria terminalis, and mediates tonic states manifest as anxiety (Walker and Davis, 1997). To date, the stria terminalis – BNST circuit has not been shown to be involved in rapid responding to fear-evoking stimuli.

Typically, experimental paradigms measuring threat processing involve either a threatening or non-threatening stimulus presented on each trial; inferring the evocation of fear from phasic, automatic responses by the autonomic system (Fox, et al., 2015). The data presented in Chapter 6 provides the first evidence that amygdala projections to the BNST via the stria terminalis are involved in orienting to threat. This data showed that the connectivity of the stria terminalis predicts a selective orienting bias toward threat. This effect was similar

to strength in connectivity of connections between the superior colliculus (SC) and the amygdala that also predicted a saccadic bias to threat, demonstrated in Chapter 5.

Chapter 4 demonstrated that the stria terminalis and the SC-amygdala connections are anatomically separate. However based on the findings from Chapters 5 and 6, the functional independence of each pathway in selective orienting of attention to threat could not be determined. Future suggestions for isolating the functional role of the SC-amygdala pathway from that of the stria terminalis pathway in mediating threat processing are discussed below.

Directions for future research

The separation of the small number of RTT voxels, mediating reflexive saccades, from a large number of brachium of superior colliculus voxels, that may contribute to the selection of voluntary saccades, could be investigated in future research. One approach is to virtually dissect cortico-collicular afferents from the visual cortex to the superior colliculus, which forms the majority of fibres passing through the brachium of the superior colliculus, and to subtract these voxels from the RTT dissection. However, this is likely to remove most, if not all of the voxels that form part of the RTT. Therefore, it may not be possible to completely isolate a pathway that includes pure RTT voxels. Another possible way to infer whether the responses measured on the gap paradigm in Chapter 2 were likely mediated by cortical rather than RTT function is by correlating either the geniculo-striate and/or the cortico-collicular pathways with saccadic responses on the gap paradigm. If strength in connectivity of such cortical circuits predicts overall saccade latency on the gap paradigm, it may suggest that cortical processes via V1 contributed to saccade mediation, and that the failure of connectivity strength of brachium SC voxels dissected in Chapter 2 to predict saccade latency may be due to mixed RTT and brachium SC voxels that are not isolable. Furthermore, this would suggest that responses on the gap task were mostly voluntary, rather than reflexive, further explaining a failure of RTT to predict reflexive saccade latency. Alternatively, if no correlation is demonstrated, it could suggest that cortical mediation did not predict saccadic responses on the gap paradigm, supporting a role for the RTT in mediating reflexive saccades.

Isolating RTT fibres from a considerable number of voxels that form part of the SC-amygdala pathway could also be important to verify that the correlation between the FA of the RTT that shared voxels with the brachium of the SC and threat bias on the saccade decision task was not driven by FA of the SC-amygdala pathway.

An important consideration for future research is the stimuli to employ in future experiments in order to create optimal conditions to measure a bias to threat. Stimuli that elicited the highest percentage of threat bias may be isolated and analysed separately to investigate whether they correlate more strongly with strength in connectivity of the RTT, SC-amygdala and stria terminalis pathway. Furthermore, more careful screening for individual differences in perception of certain images as threatening may reduce variability in responses and provide a more accurate measure of threat bias. Furthermore, future experiments may benefit from using threatening faces as a measure of SC function to correlate with threat mediating circuitry, since the SC is biased to facial configurations. Alternatively, to measure a threat bias independent of the influence of faces on SC, facial configurations of animals or characters should be avoided.

Future work could further investigate the function of stria terminalis as predictor of autonomic responses to threat as is measurable on the dot probe task or by pupil responses. Stria terminalis connectivity may be expected to predict selective responses to threat through involvement of the basolateral amygdala, as demonstrated in Chapter 6, but not to autonomic responses, mediated by the central nucleus of the amygdala.

Concluding remarks

This thesis provided novel evidence supporting the function of subcortical non-image forming visual circuits in the healthy human brain. Measures of reflexive saccades and a saccade bias to threatening stimuli demonstrated a temporal hemifield bias, reflecting mediation via the retinotectal pathway. Strength in connectivity (FA) of a putative, subcortical threat-mediating pathway predicted a bias to saccade to threat. Stria terminalis strength in connectivity predicted a bias to saccade to threat, proposing a novel role for the stria terminalis in selective orienting to salient stimuli.

References

- Adolphs, R. (2008). Fear, faces, and the human amygdala. *Current Opinion in Neurobiology*, 18, 166–172. <http://doi.org/10.1016/j.conb.2008.06.006>
- Adolphs, R., & Spezio, M. (n.d.). Role of the amygdala in processing visual social stimuli. *Progress in Brain Research*, 156. [http://doi.org/10.1016/S0079-6123\(06\)56020-0](http://doi.org/10.1016/S0079-6123(06)56020-0)
- Algom, D., Chajut, E., & Lev, S. (2004). A rational look at the emotional Stroop phenomenon: A generic slowdown, not a Stroop effect. *Journal of Experimental Psychology: General*, 133, 323–338.
- Aggleton, J. P., Friedman, D. P., & Mishkin, M. (1987). A comparison between the connections of the amygdala and hippocampus with the basal forebrain in the macaque. *Experimental Brain Research*, 67, 556–568.
- Aggleton, J. P., & Mishkin, M. (1984). Projections of the amygdala to the thalamus in the cynomolgus monkey. *Journal of comparative neurology*, 222(1), 56-68.
- Altman, J. (1962). Some fiber projections to the superior colliculus in the cat. *Journal of Comparative Neurology*, 119(1), 77-95.
- Andersson, J. L., Skare, S., & Ashburner, J. (2003). How to correct susceptibility distortions in spin-echo echo-planar images: application to diffusion tensor imaging. *Neuroimage*, 20(2), 870-888.
- Anderson, A. K., Christoff, K., Panitz, D., De Rosa, E., and Gabrieli, J. D. (2003). Neural correlates of the automatic processing of threat facial signals. *Journal of Neuroscience*. 23, 5627–5633.
- Andino, S. L. G., de Peralta Menendez, R. G., Khateb, A., Landis, T., & Pegna, A. J. (2009). Electrophysiological correlates of affective blindsight. *NeuroImage*, 44(2), 581-589.
- Astruc, J. (1971) Corticofugal connections of area 8 (frontal eye field) in *Macaca mulatto*. *Brain Research*, 33:241-56.
- Assaf, Y., & Pasternak, O. (2008). Diffusion tensor imaging (DTI)-based white matter mapping in brain research: A review. *Journal of Molecular Neuroscience*, 34(1), 51–61. <http://doi.org/10.1007/s12031-007-0029-0>
- Avery, S. N., Clauss, J. a., Winder, D. G., Woodward, N., Heckers, S., & Blackford, J. U. (2014). *NeuroImage*, 91, 311–323.
- Azadbakht, H., Parkes, L. M., Haroon, H. A., Augath, M., Logothetis, N. K., de Crespigny, A. & Parker, G. J. (2015). Validation of high-resolution tractography against in vivo tracing in the macaque visual cortex. *Cerebral Cortex*, bhu326.
- Bannerman, R. L., Milders, M., & Sahraie, A. (2009). Processing emotional stimuli: Comparison of saccadic and manual choice-reaction times. *Cognition & Emotion*, 23(5), 930–954. <http://doi.org/10.1080/02699930802243303>
- Bannerman, R. L., Milders, M., & Sahraie, A. (2010). Attentional bias to brief threat-related faces revealed by saccadic eye movements. *Emotion (Washington, D.C.)*, 10(5), 733–738. <http://doi.org/10.1037/a0019354>
- Bannerman, R. L., Milders, M., Sahraie, A., Calvo, M. G., Lang, P. J., de Gelder, B., ... Pratt, J. (2013). Pulvinar neurons reveal neurobiological evidence of past selection for rapid detection of snakes. *Proceedings of the National Academy of Sciences of the United States of America*, 124(5), 513–531. <http://doi.org/10.1027/1618-3169.55.1.3>

- Barbur, J. L., Watson, J. D., Frackowiak, R. S., & Zeki, S. (1993). Conscious visual perception without V1. *Brain*, *116* (Pt 6, 1293–1302. <http://doi.org/10.1093/brain/116.6.1293>
- Barbur, J., Ruddock, K. H., & Waterfield, V. a. (1980). Human visual responses in the absence of the geniculo-calcarine projection. *Brain : A Journal of Neurology*, *103*(4), 905–928. <http://doi.org/10.1093/brain/103.4.905>
- Bar-Haim, Y., Lamy, D., Pergamin, L., Bakermans-Kranenburg, M. J., & Van Ijzendoorn, M. H. (2007). Threat-related attentional bias in anxious and nonanxious individuals: a meta-analytic study. *Psychological Bulletin*, *133*(1), 1.
- Barbas, H. & Mesulam, M.-M. (1980) Differential afferent input to subdivisions within the frontal eye fields (area 8) of macaque. *Neuroscienc Abstracts*, *114.4*(6):316
- Basser, P.J., Matiello, J., Le Bihan, D., 1994. Estimation of the effective self- diffusion tensor from the NMR spin echo. *Journal of Magnetic Resonance, Series B*, *103*, 247–254.
- Basser, P. J., & Pierpaoli, C. (1996). Microstructural and physiological features of tissues elucidated by quantitative-diffusion-tensor MRI.
- Basser, P. J., Pajevic, S., Pierpaoli, C., Duda, J., & Aldroubi, A. (2000). In vivo fiber tractography using DT-MRI data. *Magnetic Resonance in Medicine*, *44*, 625–632.
- Beck, D. M., Rees, G., Frith, C. D., and Lavie, N. (2001). Neural correlates of change detection and change blindness. *Nat. Neurosci.* *4*, 645–650. doi: 10.1038/88477.
- Behrens, T. E. J., Woolrich, M. W., Jenkinson, M., Johansen- Berg, H., Nunes, R. G., Clare, S., ... & Smith, S. M. (2003). Characterization and propagation of uncertainty in diffusion- weighted MR imaging. *Magnetic Resonance in Medicine*, *50*(5), 1077-1088.
- Behrens, T. E. J., Berg, H. J., Jbabdi, S., Rushworth, M. F. S., & Woolrich, M. W. (2007). Probabilistic diffusion tractography with multiple fibre orientations: What can we gain?. *Neuroimage*, *34*(1), 144-155.
- Benevento, L. A., & Standage, G. P. (1983). The organization of projections of the retinorecipient and nonretinorecipient nuclei of the pretectal complex and layers of the superior colliculus to the lateral pulvinar and medial pulvinar in the macaque monkey. *Journal of Comparative Neurology*, *217*(3), 307-336.
- Bishop, S. J., Duncan, J., and Lawrence, A. D. (2004). State anxiety modulation of the amygdala response to unattended threat-related stimuli. *Journal of Neuroscience*. *24*, 10364–10368. doi: 10.1523/JNEUROSCI.2550-04.2004
- Blythe, I. M., Kennard, C., & Ruddock, K. H. (1987). Residual vision in patients with retrogeniculate lesions of the visual pathways. *Brain*, *110*, 887–905.
- Boch, R. (1989) Saccadic reaction times after chemical lesions in striate and prestriate cortex of the rhesus monkey. *Investigations in Ophthalmology and Visual Science*, *30*:184.
- Bompas, A., Sterling, T., Rafal, R. D., & Sumner, P. (2008). Naso-temporal asymmetry for signals invisible to the retinotectal pathway. *Journal of Neurophysiology*, *100*(1), 412-421.
- Braddick, O. J., Atkinson, J., Hood, B., Harkness, W., Jackson, G., Vargha- Khadem, F. (1992) Possible blindsight in infants lacking one cerebral hemisphere. *Nature*, *360*:461–463

- Breiter, H. C., Etcoff, N. L., & Whalen, P. J. (1996). Response and Habituation of the Human Amygdala during Visual Processing of Facial Expression. *Neuron*, *17*, 875–887.
- Bridge, H., Thomas, O., Jbabdi, S., Cowey, A., Andrews, T., Halpern, S., ... Ffytche, D. (2008). Changes in connectivity after visual cortical brain damage underlie altered visual function. *Brain : A Journal of Neurology*, *131*(Pt 6), 1433–44. <http://doi.org/10.1093/brain/awn063>
- Brindley, G. S., Gautier-Smith, P. C., & Lewin, W. (1969). Cortical blindness and the functions of the non-geniculate fibres of the optic tracts. *Journal of Neurology, Neurosurgery, and Psychiatry*, *32*(4), 259–264. <http://doi.org/10.1136/jnnp.32.4.259>
- Ter Braak, J. W. G., Schenk, V. W. D., & Vliet, A. G. M. Van. (1971). Visual reactions in a case of long-lasting cortical blindness. *Journal of Neurology, Neurosurgery & Psychiatry*, *34*, 140–147.
- Campion, J., Latto, R., & Smith, Y. M. (1983). Is blindsight an effect of scattered light, spared cortex, and near-threshold vision? *Behavioral and Brain Sciences*, *6*(03), 423. <http://doi.org/10.1017/S0140525X00016861>
- Carpenter, R. H. S. (1977). *Movements of the eyes*. New York: Methuen.
- Chelazzi, L., Duncan, J., Miller, E.K., and Desimone, R. (1998). Responses of neurons in inferior temporal cortex during memory-guided visual search. *Journal of Neurophysiology* *80*, 2918–2940. Clark,
- Cohen, J. (1988). *Statistical power analysis for the behavioral sciences* Lawrence Erlbaum Associates. Hillsdale, NJ, 20-26.
- Corbetta, M., Marzi, C. A., Tassinari, G., & Aglioti, S. (1990). Effectiveness of different task paradigms in revealing blindsight. *Brain*, *113*, 603–616.
- Cowey, A. (2010). The blindsight saga. *Experimental Brain Research*, *200*(1), 3–24. <http://doi.org/10.1007/s00221-009-1914-2>
- Cowey, A. (2016). The Quarterly Journal of Experimental Psychology Section A The 30th Sir Frederick Bartlett lecture Fact, artefact, and myth about blindsight. <http://doi.org/10.1080/02724980343000882>
- Cowey, A., & Weiskrantz, L. (1963). Quarterly Journal of Experimental Psychology A perimetric study of visual field defects in monkeys a perimetric study of visual field defects in monkeys. *Quarterly Journal of Experimental Psychology*, *15*(2), 91–115. <http://doi.org/10.1080/17470216308416561>
- Cowey, A., Stoerig, P., Le Mare, C. (1998) Effects of unseen stimuli on reaction times to seen stimuli in monkeys with blindsight. *Conscious Cognition*, *7*:312–323
- Cowey, A., & Stoerig, P. (1999) Spectral sensitivity in hemianopic macaque monkeys. *European Journal of Neuroscience*, *11*:2114–2120
- Czeisler, C. A., Shanahan, T. L., Klerman, E. B., Martens, H., Brotman, D. J., Emens, J. S., ... & Rizzo, J. F. (1995). Suppression of melatonin secretion in some blind patients by exposure to bright light. *New England Journal of Medicine*, *332*(1), 6-11.
- Day-Brown, J. D., Wei, H., Chomsung, R. D., Petry, H. M., & Bickford, M. E. (2010). Pulvinal projections to the striatum and amygdala in the tree shrew. *Frontiers in Neuroanatomy*, *4*, 143.

- De Gelder, B., Morris, J. S., & Dolan, R. J. (2005). Unconscious fear influences emotional awareness of faces and voices. *Proceedings of the National Academy of Sciences of the United States of America*, *102*(51), 18682–7.
<http://doi.org/10.1073/pnas.0509179102>
- De Gelder, B., van Honk, J., & Tamietto, M. (2011). Emotion in the brain: of low roads, high roads and roads less travelled. *Nature Publishing Group*.
<http://doi.org/10.1038/nrn2920-c1>
- De Gelder, B., Vroomen, J., Pourtois, G., & Weiskrantz, L. (1999) Non-conscious recognition of affect in the absence of striate cortex. *Neuroreport* *10*:3759–3763
- De Gelder, B., and Hadjikhani, N. (2006). Non-conscious recognition of emotional body language. *Neuroreport*, *17*, 583–586.
- De Gelder, B., Morris, J. S., & Dolan, R. J. (2005). Unconscious fear influences emotional awareness of faces and voices. *Proceedings of the National Academy of Sciences of the United States of America*, *102*(51), 18682-18687.
- De Olmos, J. S., & Ingram, W. R. (1972). The projection field of the stria terminalis in the rat brain. An experimental study. *The Journal of Comparative Neurology*, *146*(3), 303–334. <http://doi.org/10.1002/cne.901460303>
- De Ruiter, C., & Brosschot, J. F. (1994). The emotional Stroop interference effect in anxiety: Attentional bias or cognitive avoidance? *Behaviour Research and Therapy*, *32*, 315–319.
- Dineen J & Keating eg (1981) The primate visual system after bilateral removal of striate cortex: survival of complex pattern vision. *Experimental Brain Research*, *41*, 338-345.
- Diano, M., Celeghin, A., Bagnis, A., & Tamietto, M. (2016). Amygdala response to emotional stimuli without awareness: facts and interpretations. *Frontiers in Psychology*, *7*, 2029.
- Dodds, C., Machado, L., Rafal, R., & Ro, T. (2002). A temporal/nasal asymmetry for blindsight in a localisation task: evidence for extrageniculate mediation. *Neuroreport*, *13*(5), 655-658.
- Dolan, R. J., Morris, J. S., & de Gelder, B. (2001). Crossmodal binding of fear in voice and face. *Proceedings of the National Academy of Sciences*, *98*(17), 10006-10010.
- Duncan, S., and Barrett, L. F. (2007). The role of the amygdala in visual awareness. *Trends Cogn. Sci.* *11*, 190–192. doi: 10.1016/j.tics.2007.01.007
- Eastwood, J. D., Smilek, D., & Merikle, P. M. (2001). Differential attentional guidance by unattended faces expressing positive and negative emotion. *Perception and Psychophysics*, *63*, 1004-1013.
- Fan, Y., Huang, Z.-Y., Cao, C.-C., Chen, C.-S., Chen, Y.-X., Fan, D.-D., ... Yao. (2013). Genome of the Chinese tree shrew. *Nature Communications*, *4*.
<http://doi.org/10.1038/ncomms2416>
- Fecica, A. M., & Stolz, J. A. (2008). Facial affect and temporal order judgments: Emotions turn back the clock. *Experimental Psychology*, *55*(1), 3–8.
<http://doi.org/10.1027/1618-3169.55.1.3>
- Fendrich, R., Wessinger, C. M., & Gazzaniga, M. S. (1992). Residual vision in a scotoma: implications for blindsight. *Science-New York Then Washington-*, *258*, 1489-1489.

- Fendrich, R., Demirel, S., & Danziger, S. (1999). The oculomotor gap effect without a foveal fixation point. *Vision Research*, 39(4), 833-841.
- Fischer, B., & Ramsperger, E. (1986). Human express-saccades: Effects of randomization and daily practice. *Experimental Brain Research*, 64, 569-578
- Fischer (1987). The preparation of visually guided saccades. *Reviews in Physiology, Biochemistry and Pharmacology*, 106:1-35.
- Fischer & Boch (1990) Cerebral cortex. In: Vision and visual dysfunction, vol. 9: Eye movements, ed. R. Carpenter. Macmillan.
- Fischer, B. & Weber, H. 1993 Express saccades and visual attention. *Behavioural Brain Science*, 16, 533–610
- Folk, C. L., Remington, R. W., & Johnston, J. C. (1992). Involuntary covert orienting is contingent on attentional control settings. *Journal of Experimental Psychology: Human Perception and Performance*, 18, 1030–1044. <http://dx.doi.org/10.1037/0096-1523.18.4.1030>
- Fox, E., Russo, R., Bowles, R., & Dutton, K. (2001). Do threatening stimuli draw or hold visual attention in subclinical anxiety? *Journal of Experimental Psychology. General*, 130(4), 681–700. Retrieved from <http://www.ncbi.nlm.nih.gov/pubmed/11757875>
- Fox, A. S., Oler, J. a., Tromp, D. P. M., Fudge, J. L., & Kalin, N. H. (2015). *Trends in Neurosciences*, 38(5), 319–329.
- Fox, E., Russo, R., & Dutton, K. (2002). Attentional bias for threat: Evidence for delayed disengagement from emotional faces. *Cognition and Emotion*, 16, 355–379. <http://dx.doi.org/10.1080/02699930143000527>
- Glickstein, M., May, J. G. & Mercier, B. E. (1985) Corticopontine projection in the macaque: The distribution of labelled cortical cells after large injections of horseradish peroxidase in the pontine nuclei. *Journal of Comparative Neurology*, 235:343-59.
- Globisch, J., Hamm, A.O., Esteves, F., and Ohman, A. (1999). Fear appears fast: temporal course of startle reflex potentiation in animal fearful subjects. *Psychophysiology*, 36, 66–75.
- Gonzalez-Andino, S. L., Grave de Peralta Menendez, R., Khateb, A., Landis, T., Pegna, A. J. (2009). Electrophysiological correlates of affective blindsight. *NeuroImage*, 44:581–589.
- Green, D. M., & Swets, J. A. (1966). Signal detection theory and psychophysics. 1966. *New York*, 888, 889.
- Hadwin, J. A., Donnelly, N., French, C. C., Richards, A., Watts, A., & Daley, D. (2003). The influence of children's self-report trait anxiety and depression on visual search for emotional faces. *Journal of Child Psychology and Psychiatry and Allied Disciplines*, 44, 432–444.
- Haxby, J. V., Horwitz, B., Ungerleider, L. G., Maisog, J. M., Pietrini, P., & Grady, C. L. (1994). The functional organization of human extrastriate cortex: a PET-rCBF study of selective attention to faces and locations. *The Journal of Neuroscience*, 14(11), 6336-6353.
- Heide, W., Koenig, E., Dichgans, J. (1990) Optokinetic nystagmus, self motion sensation and their after effects in patients with occipito- parietal lesions. *Clinical Vision Science*, 5:145–156

- Hendry, S. H., & Reid, R. C. (2000). The koniocellular pathway in primate vision. *Annual Review of Neuroscience*, 23(1), 127-153.
- Henderson, J. M. (2003). Human gaze control during real-world scene perception. *Trends in Cognitive Sciences*, 7, 498-504.
- Hesse, E., Mikulan, E., Decety, J., Sigman, M., Garcia, M., Silva, W., et al. (2016). Early detection of intentional harm in the human amygdala. *Brain* 139, 54–61. doi: 10.1093/brain/awv336
- Holmes, G. (1918). Disturbances of vision by cerebral lesions. *British Journal of Ophthalmology*, 2:353-84.
- Huettel, S. A., Song, A. W., & McCarthy, G. (2004). *Functional magnetic resonance imaging* (Vol. 1). Sunderland: Sinauer Associates.
- Humphrey, N. K. (1974). Vision in a monkey without striate cortex: a case study. *Perception*, 3(3), 241-255.
- Hunt, A. R., Cooper, R. M., Hung, C., & Kingstone, A. (2007). The effect of emotional faces on eye movements and attention. *Visual Cognition*, 15(5), 513–531. <http://doi.org/10.1080/13506280600843346>
- Inouye, T. (1909). Die Störungen bei Schussverletzungen der kortikalen Sehphäre nach Beobachtungen an Verwundeten der letzten Japanischen Kriege. W. Engelmann, Leipzig.
- Inouye, T. (2000). Visual disturbances following gunshot wounds of the cortical visual area. Translated by Glickstein M and Fahle M. Oxford University Press, Oxford.
- Jolij, J., & Lamme, V. A. (2005). Repression of unconscious information by conscious processing: evidence from affective blindsight induced by transcranial magnetic stimulation. *Proceedings of the National Academy of Sciences of the United States of America*, 102(30), 10747-10751.
- Johnson, M. H. (1990) Cortical maturation and the development of visual attention in early infancy. *Journal of Cognitive Neuroscience*, 2:81- 95.
- Jones, E. G., & Burton, H. (1976). A projection from the medial pulvinar to the amygdala in primates. *Brain Research*, 104(1), 142–7. Retrieved from <http://www.ncbi.nlm.nih.gov/pubmed/813820>
- Jones, D. K., Knösche, T. R., & Turner, R. (2013). White matter integrity, fiber count, and other fallacies: the do's and don'ts of diffusion MRI. *Neuroimage*, 73, 239-254.
- Jones, D. K., & Nilsson, M. (2014). Tractometry and the hunt for the missing link: a physicist perspective. *Microstructures Of Learning*, 38.
- Kalesnykas, R. P. & Hallett, P. E. (1987) The differentiation of visually guided and anticipatory saccades in gap and overlap paradigms. *Experimental Brain Research*, 68:115-21.
- Kato, R., Takaura, K., Ikeda, T., Yoshida, M., and Isa, T. (2011). Contribution of the retino-tectal pathway to visually guided saccades after lesion of the primary visual cortex in monkeys. *European Journal of Neuroscience*, 33, 1952–1960. doi: 10.1111/j.1460-9568.2011.07729
- Keating EG (1975) Effects of prestriate and striate lesions on the monkey's ability to locate and discriminate visual forms. *Experimental Neurology*, 47:16-25

- Kingstone, A., & Klein, R. M. (1993). Visual offsets facilitate saccadic latency: does predisengagement of visuospatial attention mediate this gap effect? *Journal of Experimental Psychology: Human Perception and Performance*, 19(6), 1251.
- Kinzle, H., Akert, K. & Wurtz, R. H. (1976) Projection of area 8 (frontal eye field) to superior colliculus in the monkey. An autoradiographic study. *Brain Research*, 117:487-92.
- Kim, M.J., Whalen, P.J. (2009) The structural integrity of an amygdala–prefrontal pathway predicts trait anxiety. *Journal of Neuroscience*, 29(37):11614–11618.
- Klingler, J., & Gloor, P. (1960). The connections of the amygdala and of the anterior temporal cortex in the human brain. *Journal of Comparative Neurology*, 115(3), 333–369. <http://doi.org/10.1002/cne.901150305>
- King SM, Azzopardi P, Cowey A, Oxbury J, Oxbury S (1996) The role of light scatter in the residual visual sensitivity of patients with complete cerebral hemispherectomy. *Visual Neuroscience*, 13:1–13
- Kirchner, H. & Thorpe, S. J. 2006 Ultra-rapid object detection with saccadic eye movements: visual processing speed revisited. *Vision Research*, 46, 1762–1776. (doi:10.1016/j.visres.2005.10.002)
- Kissler, J., & Keil, A. (2008). Look–don’t look! How emotional pictures affect pro- and anti-saccades. *Experimental Brain Research*, 188(2), 215–222. <http://doi.org/10.1007/s00221-008-1358-0>
- Koster, E. H. W., Crombez, G., Verschuere, B., Van Damme, S., & Wiersema, J. R. (2006). Components of attentional bias to threat in high trait anxiety: Facilitated engagement, impaired disengagement, and attentional avoidance. *Behaviour Research and Therapy*, 44, 1757–1771.
- Koster, E. H. W., Crombez, G., Verschuere, B., & De Houwer, J. (2004). Selective attention to threat in the dot probe paradigm: Differentiating vigilance and difficulty to disengage. *Behaviour Research and Therapy*, 42, 1183–1192. <http://dx.doi.org/10.1016/j.brat.2003.08.001>
- Klüver H (1941) Visual functions after removal of the occipital lobes. *Journal of Psychology*, 11:23–45
- Krüger, O., Shiozawa, T., Kreifelts, B., Scheffler, K., & Ethofer, T. (2015). Three distinct fiber pathways of the bed nucleus of the stria terminalis to the amygdala and prefrontal cortex. *Cortex*, 66, 60–68. <http://doi.org/10.1016/j.cortex.2015.02.007>
- Künzle, H., Akert, K. & Wurtz, R. H. (1976) Projection of area 8 (frontal eye field) to superior colliculus in the monkey. An autoradiographic study. *Brain Research*, 117:487-92.
- Kwon, H. G., Byun, W. M., Ahn, S. H., Son, S. M., & Jang, S. H. (2011). The anatomical characteristics of the stria terminalis in the human brain: a diffusion tensor tractography study. *Neuroscience Letters*, 500(2), 99-102.
- Lang, P.J., Bradley, M.M., & Cuthbert, B.N. (2008). International affective picture System (IAPS): Affective ratings of pictures and instruction manual. Technical Report A-8. University of Florida, Gainesville, FL.
- LeDoux, J. E. (1996). The emotional brain. New York: Simon & Schuster.

- Leventhal, A. G., Rodieck, R. W., & Dreher, B. (1981) Retinal ganglion cell classes in the Old World monkey: morphology and central projections. *Science*, 213, 1139–1142.
- Lepore, F., Cardu, B., Rasmussen, T., & Malmø, R. B. (1975) Rod and cone sensitivity in destriate monkeys. *Brain Research*, Amsterdam, 93, 203-221.
- LeVay, S., Hubel, D. H., & Wiesel, T. N. (1975). The pattern of ocular dominance columns in macaque visual cortex revealed by a reduced silver stain. *Journal of Comparative Neurology*, 159(4), 559-575.
- Linden, R., Perry, V. H. (1983). Massive retinotectal projection in rats. *Brain Research*, 272:145–149.
- Linke, R., De Lima, A. D., Schwegler, H., & Pape, H. C. (1999). Direct synaptic connections of axons from superior colliculus with identified thalamo- amygdaloid projection neurons in the rat: Possible substrates of a subcortical visual pathway to the amygdala. *Journal of Comparative Neurology*, 403(2), 158-170.
- Lucas, R. J., Douglas, R. H. & Foster, R. G. (2001). Characterization of an ocular photopigment capable of driving pupillary constriction in mice. *Nature Neuroscience*, 4:621-626.
- Lundqvist, D. & Ohman, A. (2005). Emotion regulates attention: the relation between facial configurations, facial emotion and visual attention. *Vision Cognition*. 12, 51–84. (doi:10.1080/13506280444000085)
- Luo, Q., Holroyd, T., Jones, M., Hendler, T., and Blair, J. (2007). Neural dynamics for facial threat processing as revealed by gamma band synchronization using MEG. *Neuroimage* 34, 839–847. doi: 10.1016/j.neuroimage.2006.09.023
- Luo, Q., Holroyd, T., Majestic, C., Cheng, X., Schechter, J., and Blair, R. J. (2010). Emotional automaticity is a matter of timing. *Journal of Neuroscience*. 30, 5825–5829. doi: 10.1523/JNEUROSCI.BC-5668-09.2010
- Mack, A., & Rock, I. (1998). Inattentional Blindness (Cambridge, MA: MIT Press).
Markowitsch
- Macknik, S. L., and Livingstone, M. S. (1998). Neuronal correlates of visibility and invisibility in the primate visual system. *Nature Neuroscience*, 1, 144–149. doi: 10.1038/393
- MacLeod, C., Mathews, A., & Tata, P. (1986). Attentional Bias in Emotional Disorders. *Journal of Abnormal Psychology*, 95(1), 15–20. <http://doi.org/10.1037/0021-843X.95.1.15>
- MacLeod, C. M. (1991). Half a century of research on the Stroop effect: an integrative review. *Psychological Bulletin*, 109(2), 163.
- MacLeod, C., Mathews, A., & Tata, P. (1986). Attentional bias in emotional disorders. *Journal of Abnormal Psychology*, 95, 15–20.
- Macmillan, N. A. (2002). Signal detection theory. *Stevens' handbook of experimental psychology*.
- Mars, R. B., Jbabdi, S., Sallet, J., O'Reilly, J. X., Crosson, P. L., Olivier, E., ... & Behrens, T. E. (2011). Diffusion-weighted imaging tractography-based parcellation of the human

- parietal cortex and comparison with human and macaque resting-state functional connectivity. *The Journal of Neuroscience*, 31(11), 4087-4100.
- McDonald, A. J. (1998). Cortical pathways to the mammalian amygdala. *Progress in Neurobiology*, 55(3), 257-332.
- Mendez-Bertolo, C., Moratti, S., Toledano, R., Lopez-Sosa, F., Martinez- Alvarez, R., Mah, Y. H., et al. (2016). A fast pathway for fear in human amygdala. *Nature Neuroscience*, 19, 1041–1049. doi: 10.1038/nn.4324
- Morris, J. S., Ohman, A., & Dolan, R. J. (1999). A subcortical pathway to the right amygdala mediating “unseen” fear. *Proceedings of the National Academy of Sciences of the United States of America*, 96(4), 1680–5. <http://doi.org/10.1073/pnas.96.4.1680>
- Maior, R. S., Hori, E., Tomaz, C., Ono, T., & Nishijo, H. (2010). The monkey pulvinar neurons differentially respond to emotional expressions of human faces. *Behavioural Brain Research*, 215, 129–135. <http://doi.org/10.1016/j.bbr.2010.07.009>
- Malmö RB (1966) Effects of striate cortex ablation of intensity discrimination and spectral intensity distribution in the rhesus monkey. *Neuropsychologia*, 4, 9–26.
- Magnussen, S., & Mathiesen, T. (1989). Detection of moving and stationary gratings in the absence of striate cortex. *Neuropsychologia*, 27(5), 725–8. Retrieved from <http://www.ncbi.nlm.nih.gov/pubmed/2739894>
- Magoun, H. W. (1935). The central path of the light reflex. *Archives of Ophthalmology*, 13(5), 791. <http://doi.org/10.1001/archopht.1935.00840050069006>
- Marcel, A. J. (1998). Blindsight and shape perception: Deficit of visual consciousness or of visual function? *Brain*, 121(8), 1565–1588. <http://doi.org/10.1093/brain/121.8.1565>
- Marzi, C. A., Tassinari, G., Aglioti, S., & Lutzemberger, L. (1986). Spatial summation across the vertical meridian in hemianopsics: A test of blindsight. *Neuropsychologia*, 24(6), 749–758. [http://doi.org/10.1016/0028-3932\(86\)90074-6](http://doi.org/10.1016/0028-3932(86)90074-6)
- May, P. J. (2006). The mammalian superior colliculus: laminar structure and connections. *Progress in Brain Research*, 151, 321-378.
- Machado, H., & Robert, D. Rafal. (2000). Strategic control over saccadic eye movements: studies of the fixation offset effect. *Perception & Psychophysics*, 62.6: 1236-1242.
- McDonald, A. J. (1998). Cortical pathways to the mammalian amygdala. *Progress in Neurobiology*, 55(3), 257–332. [http://doi.org/10.1016/S0301-0082\(98\)00003-3](http://doi.org/10.1016/S0301-0082(98)00003-3)
- Morin, L. P., Blanchard, J. H. & Provencio, I. (2003). Retinal ganglion cell projections to the hamster suprachiasmatic nucleus, intergeniculate leaflet, and visual midbrain: bifurcation and melanopsin immunoreactivity. *Journal of Comparative Neurology*, 465: 401-416.
- Moore, R. Y., Speh, J. C., & Patrick Card, J. (1995). The retinohypothalamic tract originates from a distinct subset of retinal ganglion cells. *The Journal of Comparative Neurology*, 352(3), 351–366. <http://doi.org/10.1002/cne.903520304>
- Morris, J. S., DeGelder, B., Weiskrantz, L., & Dolan, R. J. (2001). Differential extrageniculostriate and amygdala responses to presentation of emotional faces in a cortically blind field. *Brain*, 124, 1241–1252. <http://doi.org/10.1093/brain/124.6.1241>
- Morris, J. S., Friston, K. J., Büchel, C., Frith, C. D., Young, A. W., Calder, A. J., & Dolan, R. J. (1998). A neuromodulatory role for the human amygdala in processing emotional facial expressions. *Brain*, 121, 47–57.
- Morris, J. S., Ohman, A., & Dolan, R. J. (1999). A subcortical pathway to the right amygdala

mediating “unseen” fear. *Proceedings of the National Academy of Sciences of the United States of America*, 96(4), 1680–5. <http://doi.org/10.1073/pnas.96.4.1680>

- Nguyen, M. N., Matsumoto, J., Hori, E., Maior, R. S., Tomaz, C., Tran, A. H., ... De Gelder, B. (2014). Neuronal responses to face-like and facial stimuli in the monkey superior colliculus. *Frontiers in Behavioral Neuroscience*, 8, 85.
- Nieuwenhuys, R., Voogd, J., & Van Huijzen, C. (2007). *The human central nervous system: a synopsis and atlas*. Springer Science & Business Media.
- Öhman, A. (1993). Fear and anxiety as emotional phenomenon: Clinical phenomenology, evolutionary perspectives, and information-processing mechanism. In M. Lewis & J.M. Haviland (Eds.), *Handbook of emotions* (pp. 511–536). New York: Guilford.
- Öhman, A., Flykt, A., & Esteves, F. (2001). Emotion drives attention: Detecting the snake in the grass. *Journal of Personality and Social Psychology*, 130, 466–478.
- Öhman, A., Lundqvist, D., & Esteves, F. (2001). The face in the crowd revisited: A threat advantage with schematic stimuli. *Journal of Personality and Social Psychology*, 80, 381–396.
- Purcell, D.G., Stewart, A.L., & Skov, R.B. (1996).
- Pasik P, Pasik T (1982) Visual functions in monkeys after total removal of visual cerebral cortex. In: Neff WD (ed) *Contributions to sensory physiology*, Vol 7. Academic Press, New York London, pp 147-200
- Pasik, p., pasik, t. And schilder, p. (1969). Extrageniculostriate vision in the monkey: discrimination of luminous flux-equated figures. *Experimental Neurology*, 24, 421-437.
- Pegna, A. J., Khateb, A., Lazeyras, F., & Seghier, M. L. (2005). Discriminating emotional faces without primary visual cortices involves the right amygdala. *Nature Neuroscience*, 8(1), 24-25. <http://doi.org/10.1038/nn1364>
- Pessoa, L. (2005). To what extent are emotional visual stimuli processed without attention and awareness? *Current Opinion in Neurobiology*, 15, 188–196. doi: 10.1016/j.conb.2005.03.002
- Pessoa, L., and Adolphs, R. (2010). Emotion processing and the amygdala: from a ‘low road’ to ‘many roads’ of evaluating biological significance. *Nature Reviews Neuroscience*, 11, 773–783. doi: 10.1038/nrn2920
- Pessoa, L., Japee, S., Sturman, D., and Ungerleider, L. G. (2006). Target visibility and visual awareness modulate amygdala responses to fearful faces. *Cerebral Cortex*, 16, 366–375. doi: 10.1093/cercor/bhi115
- Pessoa, L., McKenna, M., Gutierrez, E., and Ungerleider, L. G. (2002). Neural processing of emotional faces requires attention. *Proceedings of the National Academy of Sciences of the United States of America*, 99, 11458–11463. doi: 10.1073/pnas.172403899
- Pessoa, L., Padmala, S., and Morland, T. (2005). Fate of unattended fearful faces in the amygdala is determined by both attentional resources and cognitive modulation. *Neuroimage* 28, 249–255. doi: 10.1016/j.neuroimage.2005.05.048
- Perenin, M. T., & Jeannerod, M. (1975). Residual vision in cortically blind hemiphields, *Neuropsychologia*, 13(1), 1-7.
- Perenin, M.-T. (1991). Discrimination of motion direction in perimetrically blind fields. *NeuroReport*, 2(7), 397–400. <http://doi.org/10.1097/00001756-199107000-00011>
- Perenin MT, Ruel J, Hecaen H (1980) Residual visual capacities in a case of cortical

- blindness. *Cortex* 16:605–612
- Perenin, M. T., & Rossetti, Y. (1996). Grasping without form discrimination in a hemianopic field. *Neuroreport*, 7(3), 793-797.
- Perenin, M. T., & Jeannerod, M. (1975) Residual vision in cortically blind hemifields. *Neuropsychologia*, 13, 1 -7 .
- Perenin M. T., & Jeannerod, M. (1978) Visual function within the hemianopic field following early cerebral hemidecortication in man. I. Spatial localization. *Neuropsychologia*, 16, 1 — 13
- Perry, V. H., Oehler, R., & Cowey, A. (1984). Retinal ganglion cells that project to the dorsal lateral geniculate nucleus in the macaque monkey. *Neuroscience*, 12(4), 1101-1123.
- Pool, E., Brosch, T., Delplanque, S., & Sander, D. (2015). Attentional Bias for Positive Emotional Stimuli: A Meta-Analytic Investigation. <http://doi.org/10.1037/bul0000026>
- Pöppel, E. (1986). Long-range colour-generating interactions across the retina. *Nature*, 320(6062), 523–525. <http://doi.org/10.1038/320523a0>
- Pöppel, E., Held, R., & Frost, D. (1973). Residual Visual Function after Brain Wounds involving the Central Visual Pathways in Man. *Nature*, 243, 295–296. <http://doi.org/10.1038/243295a0>
- Pourtois, G., Schettino, A., and Vuilleumier, P. (2013). Brain mechanisms for emotional influences on perception and attention: what is magic and what is not. *Biological Psychology*, 92, 492–512. doi: 10.1016/j.biopsycho.2012.02.007
- Posner, M. I. (1980). Orienting of attention. *Quarterly journal of experimental psychology*, 32(1), 3-25.
- Posner, M. I., & Boies, S. J. (1971). Components of attention. *Psychological review*, 78(5), 391.
- Rafal, R. D., Koller, K., Bultitude, J. H., Mullins, P., Ward, R., Mitchell, A. S., & Bell, A. H. (2015). Connectivity between the superior colliculus and the amygdala in humans and macaque monkeys: virtual dissection with probabilistic DTI tractography. *Journal of Neurophysiology*, 114(3), 1947–62. <http://doi.org/10.1152/jn.01016.2014>
- Rafal, R., Smith, J., Krantz, J., Cohen, A. , & Brennan. (1990). Extrageniculate Vision in Hemianopic Humans: Saccade Inhibition by Signals in the Blind Field. *Science*, 250(4977).
- Rafal, R., McGrath, M., Machado, L., & Hindle, J. (2004). Effects of lesions of the human posterior thalamus on ocular fixation during voluntary and visually triggered saccades. *Journal of Neurology, Neurosurgery & Psychiatry*, 75(11), 1602-1606.
- Rasbash, J., Charlton, C., Browne, W. J., Healy, M., & Cameron, B. (2009). MLwiN Version 2.1. *Centre for multilevel modelling, University of Bristol*.
- Reuter-Lorenz, P. A., Hughes, H. C., & Fendrich, R. (1991). The reduction of saccadic latency by prior offset of the fixation point: an analysis of the gap effect. *Perception & Psychophysics*, 49(2), 167-175.
- Rees, G., Russell, C., Frith, C.D., and Driver, J. (1999). Inattention blindness versus inattention amnesia for fixated but ignored words. *Science*, 286, 2504–2507.
- Reulen, J. P. H. (1984) Latency of visually evoked saccadic eye movements. I. Saccadic latency and the facilitation model. *Biological Cybernetics*, 50:251-62.

- Riddoch, G. (1917) Dissociation of visual perceptions due to occipital injuries, with especial reference to appreciation of movement. *Brain* 40:15-57.
- Rinck, M., Becker, E. S., Kellermann, J., & Roth, W. T. (2003). Selective attention in anxiety: Distraction and enhancement in visual search? *Depression and Anxiety*, 18, 18–28.
- Richards, W. (1973). Visual processing in scotomata. *Experimental Brain Research. Experimentelle Hirnforschung. Experimentation Cerebrale*, 17(4), 333–347. <http://doi.org/10.1007/BF00234098>
- Ro, T., Shelton, D., Lee, O. L., & Chang, E. (2004). Extrageniculate mediation of unconscious vision in transcranial magnetic stimulation-induced blindsight. *Proceedings of the National Academy of Sciences of the United States of America*, 101(26), 9933-9935.
- Romanski, L.M., Giguere, M., Bates, J.F. and Goldman-Rakic, P.S. (1997) Topographic organization of medial pulvinar connections with the prefrontal cortex in the rhesus monkey. *Journal of Comparative Neurology*, 379: 313–332.
- Ross, L. E. & Ross, S. M. (1980) Saccadic latency and warning signals: Stimulus onset, offset, and change as warning events. *Perception & Psychophysics*, 27:251-57.
- Rothstein, P., Richardson, M. P., Winston, J. S., Kiebel, S. J., Vuilleumier, P., Eimer, M., et al. (2010). Amygdala damage affects event-related potentials for fearful faces at specific time windows. *Human Brain Mapping*, 31, 1089–1105. doi: 10.1002/hbm.20921
- Saleem, K. S., & Logothetis, N. K. (2012). *A combined MRI and histology atlas of the rhesus monkey brain in stereotaxic coordinates*. Academic Press.
- Sanders, M. D., Warrington, E., Marshall, J., & Wieskrantz, L. (1974). “Blindsight”: vision in a field defect. *The Lancet*, 303(7860), 707–708. [http://doi.org/10.1016/S0140-6736\(74\)92907-9](http://doi.org/10.1016/S0140-6736(74)92907-9)
- Schilder, P., Pasik, P., & Pasik, T. (1971) Extrageniculostriate vision in the monkey. II. Demonstration of brightness discrimination. *Brain Research*, 32:383–389
- Schilder P, Pasik P, Pasik T (1972) Extrageniculostriate vision in the monkey. III. Circle vs triangle and ‘red vs green’ discrimination. *Experimental Brain Research*, 14:436–448
- Schiller, P. H. (1984). The superior colliculus and visual function. In I. Darian-Smith (ed.), *Handbook of physiology, Section 1, The nervous system, Vol3(1), Sensory processes* (pp. 457-505). New York: Oxford University Press.
- Schiller, P. H., and Stryker, M. (1972). Single-unit recording and stimulation in superior colliculus of the alert rhesus monkey. *Journal of Neurophysiology*, 35, 915–924.
- Schiller, P. H., & Logothetis, N. K. (1987). The effect of frontal eye field and superior colliculus lesions on saccadic and pursuit eye-movement initiation. ARVO Abstract #303.11.
- Schiller, P. H., Sandell, J. H. & Maunsell, J. H. R. (1987) The effect of frontal eye field and superior colliculus lesions on saecadic latencies in the rhesus monkey. *Journal of Neurophysiology*, 57:1033—49.
- Saslow, M. G. (1967). Latency for saccadic eye movement. *Journal of Optical Society of America*, 57(8), 1030-1033.

- Schiller, P. H., Sandell, J. H., & Maunsell, J. H. R. (1987). The effect of frontal eye field and superior colliculus lesions on saccadic latencies in the rhesus monkey. *Journal of Neurophysiology*, *57*, 1033-1049.
- Schiller (1998). The neural control of visually guided eye movements. In J. E. Richards (Ed.), *Cognitive neuroscience of attention; a developmental perspective* (pp. 3-50). Mahwah, New Jersey: Lawrence Erlbaum Associates.
- Schneider, K.A., & Bavelier, D. (2003). Components of visual prior entry. *Cognitive Psychology*, *47*, 333–336. Schneider, W. (1988).
- Shang, C., Liu, Z., Chen, Z., Shi, Y., Wang, Q., Liu, S., et al. (2015). BRAIN CIRCUITS. A parvalbumin-positive excitatory visual pathway to trigger fear responses in mice. *Science*, *348*, 1472–1477. doi: 10.1126/science.aaa8694
- Silvert, L., Lepsien, J., Fragopanagos, N., Goolsby, B., Kiss, M., Taylor, J. G., et al. (2007). Influence of attentional demands on the processing of emotional facial expressions in the amygdala. *Neuroimage*, *38*, 357–366. doi: 10.1016/j. neuroimage.2007.07.023
- Tamietto,
- Smith, S. M., Jenkinson, M., Woolrich, M. W., Beckmann, C. F., Behrens, T. E., Johansen-Berg, H., ... & Niazy, R. K. (2004). Advances in functional and structural MR image analysis and implementation as FSL. *Neuroimage*, *23*, S208-S219.
- Song, J. H., Rafal, R. D., & McPeck, R. M. (2011). Deficits in reach target selection during inactivation of the midbrain superior colliculus. *Proceedings of the National Academy of Sciences*, *108*(51), E1433-E1440.
- Sparks, D. L. (1986). Translation of sensory signals into commands for control of saccadic eye movements: Role of primate superior colliculus. *Physiological Review*, *66*, 118–171.
- Spielberger, C. D., Gorsuch, R. L., Lushene, P. R., Vagg, P. R., & Jacobs, A. G. (1983). *Manual for the State-Trait Anxiety Inventory (Form Y). Manual for the state-trait anxiety inventory STAI*.
- Stoerig, P. (1987). Chromaticity and achromaticity. *Brain*, *110*, 869–886.
- Stoerig, P., & Cowey, A. (1997). Blindsight in man and monkey. *Brain*, *120*(Pt 3), 535–559.
- Stoerig, P., & Cowey, A. (1992). Wavelength discrimination in blindsight. *Brain: A Journal of Neurology*, *115* (Pt 2, 425–444. <http://doi.org/10.1093/brain/115.2.425>
- Stoerig, P., & Cowey, A. (1989). Wavelength sensitivity in blindsight. *Nature*, *342*(6252), 916–918. <http://doi.org/10.1038/342916a0>
- Stoerig, P., Hübner, M., & Pöppel, E. (1985). Signal detection analysis of residual vision in a field defect due to a post-geniculate lesion. *Neuropsychologia*, *23*(5), 589–599. [http://doi.org/10.1016/0028-3932\(85\)90061-2](http://doi.org/10.1016/0028-3932(85)90061-2)
- Stoerig, P., & Pöppel, E. (1986). Eccentricity-dependent residual target detection in visual field defects. *Experimental Brain Research*, *64*(3), 469–475. <http://doi.org/10.1007/BF00340483>
- Stormark, K. M., Nordby, H., & Hugdahl, K. (1995). Attentional shifts to emotionally charged cues: Behavioural and ERP data. *Cognition & Emotion*, *9*, 507–523. Tipples, J., & Sharma, D. (2000).
- Sylvester, R., Josephs, O., Driver, J., & Rees, G. (2007). Visual fMRI Responses in Human Superior Colliculus Show a Temporal – Nasal Asymmetry That Is Absent in Lateral

Geniculate and Visual Cortex. *Journal of Neurophysiology*, 1495–1502.
<http://doi.org/10.1152/jn.00835.2006>

- Tamietto, M., & De Gelder, B. (2010). Neural bases of the non-conscious perception of emotional signals. *Nature Reviews Neuroscience*, 11(10), 697–709.
<http://doi.org/10.1038/nrn2889>
- Tamietto, M., Pullens, P., De Gelder, B., Weiskrantz, L., & Goebel, R. (2012). Report Subcortical Connections to Human Amygdala and Changes following Destruction of the Visual Cortex. *Current Biology*, 22, 1449–1455.
<http://doi.org/10.1016/j.cub.2012.06.006>
- Tamietto, M., and Morrone, M. C. (2016). Visual plasticity: blindsight bridges anatomy and function in the visual system. *Current Biology*, 26, R70–R73. doi: 10.1016/j.cub.2015.11.026
- Teuber H-L, Battersby WS, Bender MB (1960) Visual field defects after penetrating missile wounds of the brain. Harvard University Press, Harvard.
- Thorpe, S. J., Fize, D., & Marlot, C. (1996). Speed of processing in the human visual system. *Nature*, 381, 520–522. (doi:10.1038/381520a0)
- Titchener, E.B. (1908). Lectures on the elementary psychology of feeling and attention. New York: MacMillan Co.
- Theeuwes, J. (2010). Top-down and bottom-up control of visual selection. *Acta Psychologica*, 135(2), 77–99. <http://doi.org/10.1016/j.actpsy.2010.02.006>
- Theeuwes, J., & Belopolsky, A. V. (2012). Reward grabs the eye: Oculomotor capture by rewarding stimuli. *Vision Research*, 74, 80–85.
<http://doi.org/10.1016/j.visres.2012.07.024>
- Tomalski, P., Johnson, M. H., & Csibra, G. (2009). Temporal-nasal asymmetry of rapid orienting to face-like stimuli. *Neuroreport*, 20(15), 1309–1312.
<http://doi.org/10.1097/WNR.0b013e32832f0acd>
- Tootell, R. B., Hamilton, S. L. & Switkes, E. (1988) Functional anatomy of macaque striate cortex. IV. Contrast and magno-parvo streams. *Journal of Neuroscience*, 8:1594-1609.
- Tong, F., Meng, M., and Blake, R. (2006). Neural bases of binocular rivalry. *Trends Cogn. Sci.* 10, 502–511. doi: 10.1016/j.tics.2006.09.003
- Treisman, A. M., & Gelade, G. (1980). A feature-integration theory of attention. *Cognitive Psychology*, 12(1), 97–136.
- Van de Moortele, P. F., Auerbach, E. J., Olman, C., Yacoub, E., Uğurbil, K., & Moeller, S. (2009). T1 weighted brain images at 7 Tesla unbiased for Proton Density, T2* contrast and RF coil receive B1 sensitivity with simultaneous vessel visualization. *Neuroimage*, 46(2), 432-446.
- Valenza, E., Simion, F., Cassia, V. M., & Umiltà, C. (1996). Face preference at birth. *Journal of experimental psychology: Human Perception and Performance*, 22(4), 892.
- Van Essen, D. C., Newsome, W. T. & Maunsell, J. H. (1984). The visual field representation in striate cortex of the Macaque monkey: assymetries, anisotropies, and individual variability. *Vision Research*, 24:429-448.

- Van Essen, D. C. (2004). Organisation of visual areas in macaque and human cerebral cortex. In: Chalupa, L. C., Werner, J. S. (Eds) *The visual neurosciences*. MIT Press, Cambridge MA, pp 507-521.
- Van Le, Q., Isbell, L. A., Matsumoto, J., Nguyen, M., Hori, E., Maior, R. S., ... & Nishijo, H. (2013). Pulvinar neurons reveal neurobiological evidence of past selection for rapid detection of snakes. *Proceedings of the National Academy of Sciences*, *110*(47), 19000-19005.
- Van Hof-Van Duin, J., & Mohn, G. (1983). Optokinetic and spontaneous nystagmus in children with neurological disorders. *Behavioural Brain Research*, *10*(1), 163–175. [http://doi.org/10.1016/0166-4328\(83\)90162-6](http://doi.org/10.1016/0166-4328(83)90162-6)
- Vaney D. I., Peichl L., Wässle H. & Illing R. B. (1981) Almost all ganglion cells in the rabbit retina project to the superior colliculus. *Brain Research*, *212*, 447453. 27
- Vuilleumier, P. (2005). Cognitive science: staring fear in the face. *Nature* *433*, 22–23. doi: 10.1038/433022a
- Vuilleumier, P. (2005). How brains beware: neural mechanisms of emotional attention. *Trends in Cognitive Science*, *9*, 585–594. doi: 10.1016/j.tics.2005.10.011
- Vuilleumier, P., & Brosch, T. (2009). Interactions of emotion and attention in perception. In M. S. Gazzaniga (Ed.), *The cognitive neurosciences IV* (pp. 925–934). Cambridge, MA: MIT Press.
- Vuilleumier, P., Armony, J. L., Driver, J., & Dolan, R. J. (2001). Effects of Attention and Emotion on Face Processing in the Human Brain: An Event-Related fMRI Study. *Neuron*, *30*, 829–841.
- Walker, D. L., Toufexis, D. J., & Davis, M. (2003). Role of the bed nucleus of the stria terminalis versus the amygdala in fear, stress, and anxiety. *European journal of pharmacology*, *463*(1), 199-216.
- Walker, R., Mannan, S., Maurer, D., Pambakian, A. L. M., & Kennard, C. (2000). The oculomotor distractor effect in normal and hemianopic vision. *Proceedings of the Royal Society of London B: Biological Sciences*, *267*(1442), 431-438.
- Ward, R., Danziger, S., & Bamford, S. (2005). Response to visual threat following damage to the pulvinar. *Current Biology*, *15*(6), 571-573.
- Ward, R., Calder, A. J., Parker, M., & Arend, I. (2007). Emotion recognition following human pulvinar damage. *Neuropsychologia*, *45*(8), 1973-1978.
- Wei, P., Liu, N., Zhang, Z., Liu, X., Tang, Y., He, X., et al. (2015). Processing of visually evoked innate fear by a non-canonical thalamic pathway. *Nature Communications*, *6*:6756. doi: 10.1038/ncomms7756
- Weiskrantz, L. (1963). Contour discrimination in a young monkey with striate cortex ablation. *Neuropsychologia*, *1*(2), 145-164.
- Weiskrantz, L. (1987). Residual vision in a scotoma. *Brain*, *110*(1), 77-92.
- Weiskrantz, L., Warrington, E. K., Sanders, M. D., & Marshall, J. (1974). Visual Capacity in the Hemianopic Field Following a Restricted Occipital Ablation. *Brain*, *97*(1), 709–728. <http://doi.org/10.1093/brain/97.1.709>
- Weiskrantz L, Barbur JL, Sahraie A (1995) Parameters affecting conscious versus unconscious visual discrimination in a patient with damage to the visual cortex (V1).

- Proceedings of the National Academy of Science*, USA 92:6122–6126
- Wenban-Smith, M. G. & Findlay, J. M. (1991) Express saccades: Is there a separate population in humans? *Experimental Brain Research*, 87:218- 22.
- West, G. L., Anderson, A. A. K., & Pratt, J. (2009). Motivationally significant stimuli show visual prior entry: Evidence for attentional capture. *Journal of Experimental Psychology: Human Perception and Performance*, 35(4), 1032–1042.
<http://doi.org/10.1037/a0014493>
- Whalen, P. J., Rauch, S. L., Etcoff, N. L., McInerney, S. C., Lee, M. B., & Jenike, M. A. (1998). Masked Presentations of Emotional Facial Expressions Modulate Amygdala Activity without Explicit Knowledge. *Journal of Neuroscience*, 18(1), 411–418.
Retrieved from <http://www.jneurosci.org/content/18/1/411.short>
- Wheless, L. L., Boynton, R. M., & Cohen, G. H. (1966). Eye movement response to step and pulse-step stimuli. *Journal of the Optical Society of America*, 57, 396-400.
- Williams, C., Azzopardi, P., & Cowey, A. (1995). Nasal and temporal retinal ganglion cells projecting to the midbrain: Implications for “blindsight.” *Neuroscience*, 65(2), 577–586. [http://doi.org/10.1016/0306-4522\(94\)00489-R](http://doi.org/10.1016/0306-4522(94)00489-R)
- Williams, M. A., Morris, A. P., Mcglone, F., Abbott, D. F., & Mattingley, J. B. (2004). Amygdala Responses to Fearful and Happy Facial Expressions under Conditions of Binocular Suppression. *Journal of Neuroscience*, 24(12).
<http://doi.org/10.1523/JNEUROSCI.4977-03.2004>
- Williams, M. A., and Mattingley, J. B. (2004). Unconscious perception of non- threatening facial emotion in parietal extinction. *Experimental Brain Research*, 154, 403–406.
doi: 10.1007/s00221-003-1740-x
- Williams, M. A., McGlone, F., Abbott, D. F., and Mattingley, J. B. (2005). Differential amygdala responses to happy and fearful facial expressions depend on selective attention. *Neuroimage*, 24, 417–425. doi: 10.1016/j.neuroimage.2004.08.017
- Wilson, M. E., & Toyne, M. J. (1970). Retino-tectal and cortico-tectal projections in Macaca mulatta. *Brain research*, 24(3), 395-406.
- Woolrich, M. W., Jbabdi, S., Patenaude, B., Chappell, M., Makni, S., Behrens, T., ... & Smith, S. M. (2009). Bayesian analysis of neuroimaging data in FSL. *Neuroimage*, 45(1), S173-S186.
- Wurtz, r.h. & Albano, J.E. (1980). Visual-motor function of the pri- mate superior colliculus. *Annual Review of Neuroscience*, 3, 189-226.
- Yiend, J., & Mathews, A. (2010). The Quarterly Journal of Experimental Psychology Section A Anxiety and attention to threatening pictures Anxiety and attention to threatening pictures. <http://doi.org/10.1080/713755991>

Appendix A. Participant study information sheet



BANGOR BRAIN IMAGING UNIT Participant Information Sheet

School of Psychology: Bangor University
Information Sheet for Participating in a Research Project



You are being invited to take part in a research study. Before you decide whether to participate, it is important for you to understand why the research is being done and what it will involve. Please take time to read the following information carefully and discuss it with others if you wish. Ask us if there is anything that is not clear or if you would like more information. Take time to decide whether or not you wish to take part.

TITLE OF STUDY: Anatomical confirmation of a subcortical visual detection pathway in the human brain with in vivo tractography.

INVESTIGATORS:

Prof. Bob Rafal – Project Supervisor
Kristin Koller – PhD Student

WHAT IS THE PURPOSE OF THE STUDY?

You have been asked to participate in a research study using magnetic resonance imaging (MRI). This study will investigate pathways in the brain, which have been identified using MRI scanning methods called diffusion tensor imaging tractography. We are interested in identifying the pathways in the brain that are involved with mediating fast and non-conscious responses to visual targets.

WHAT ARE THE PROCEDURES?

Prior to participation, you will be required to complete a written consent form after having read through the information sheet and safety screening questions. When we have checked that you qualify the necessary safety requirements, you may proceed to the next part of the experiment. Following the safety screening procedure, you will be scanned in the MRI scanner for approximately 30 – 40 minutes. You will not be required to do any task during the scanning session. In addition, you will be asked to participate in brief reaction time tasks (outside the scanner) to visual targets, by responding with an eye movement or key-press (researcher will assign which method participant should use to respond. Please see behavioural testing instruction sheet).

Additionally, you will be asked to complete a short questionnaire which will ask you questions on how often you experience different emotions.

MRI procedures

During this study, you will be required to lie still in the scanner while images are being obtained. The MRI scanner uses a magnetic field, which can be potentially dangerous if you have a pacemaker or any metal in your body. However, the scan is not painful in any way, no radiation is involved and no dye needs to be injected. The scanner does however make a loud noise, so we will give you ear plugs as well as headphones to reduce this noise.

You will be able to see outside the scanner during the scan and will be able to communicate with the operator. If you find the scan to be uncomfortable in any way, the operator will

immediately stop the scan. This study will include MR measurements of static brain anatomy; these require nothing on your part except that you remain still in the scanner.

Other parts of the experiment will involve measurements of functional brain anatomy, where you will be asked to look at visual targets appearing on a computer screen. Your task will be to fixate on the central fixation cross, and press a button when the fixation cross turns red.

Because a magnetic field is involved, you cannot be scanned if you have a pacemaker, or metal in your body. We will go through a list of relevant items with you before scanning. Because the scanner is configured as a narrow tube, some individuals with claustrophobia (fear of confined spaces) may find the procedure uncomfortable or intolerable. So, you should not be scanned if you have a history of claustrophobia. The scanning session will take about 30 – 40 minutes.

WHAT IS THE DEVICE INVOLVED?

We measure brain structure using images taken with a magnetic resonance imaging scanner. This scanner uses a strong magnetic field to create detailed images of brain structure. The scan does not involve any injections or X-rays. For this experiment, you will not be required to carry out a task.

ARE THERE ANY RISKS?

The scanner can be loud when it takes images, and you will be given earplugs and ear defenders to block out some of the sound. Also, the MR environment is quite confined, and people who are uncomfortable in small or confined spaces may not be able to participate. If this should be you, remember that you may withdraw from the study at any time without explaining why. You will have an alarm button that you can press and will be removed from the scanner immediately if you experience any distress whatsoever. Otherwise, given that the procedure involves a non-invasive imaging technique it is not painful or dangerous in any way. There are no known risks or side effects.

WHAT ARE THE BENEFITS?

You will have made a contribution to our understanding of the relationship between brain and behavior. However, there are no direct benefits to you of your participation in the study.

WHAT IF NEW INFORMATION BECOMES AVAILABLE?

If the new information pertains specifically to the health of the volunteer, the volunteer will be informed. Otherwise, new information will be disseminated through traditional scientific channels (e.g. journal articles, conference presentations).

HOW IS CONFIDENTIALITY ENSURED?

The information obtained from the assessments may be published in scientific journals, but your name will not appear in any public document, nor will the results be published in a form which would make it possible for you to be identified.

WHO WILL HAVE ACCESS TO THE DATA?

Members of the BANGOR BRAIN IMAGING UNIT will have access to the data. It is possible that the data may be used by researchers working with the BANGOR BRAIN IMAGING UNIT for other similar ethically approved research protocols, where the same standards of confidentiality will apply. The BANGOR BRAIN IMAGING UNIT complies with the requirements of the Data Protection Act 1998 with regard to the collection, storage,

processing, and disclosure of personal information. All enquiries concerning access to the data held by the BANGOR BRAIN IMAGING UNIT should be addressed to the Freedom of Information Liaison Officer at the Unit in the first instance. If you wish, we can provide you images of your brain.

DO I HAVE A RIGHT TO REFUSE OR WITHDRAW?

You may refuse to participate at any time. You may change your mind about being in the study and quit after the study has started, and if you feel, for any reason, uncomfortable, the study will be discontinued.

WILL MY GP BE INFORMED?

Your GP will not be routinely informed if your participation in this study has been as a normal volunteer.

What if there is something wrong with my brain, would it show up on my images?

This is an important question, and one that can't be answered with a straight yes or no answer. The information below hopes to provide an answer. If you still have questions, please ask the researcher for more information. There is the potential that an unexpected abnormality will be found in your scan. The likely hood of such an abnormality being found in a normal volunteer's scan is estimated to be between 2-10%, so you should be aware that such a possibility exists. The MRI scans being done as part of the study you are participating in are designed to answer research questions and not to provide a medical diagnosis. They may not show problems that a ordinary clinical scan would, and since the scientists reviewing the scans are generally not medical doctors, they may fail to notice such abnormalities. However if something out of the ordinary is suspected in one of your scans, we will ask a neurologist, who is a medical doctor with experience interpreting brain MRI scans and treating brain disorders, to review the images with us. The neurologist will not be told your name, although they may be told your age and gender. If they think there may be a problem, we will then contact you. You will be offered the opportunity to meet and have a discussion with the neurologist about the findings and your options. If you have a GP and you agree, we will contact her/him and pass the scans along with the recommendation from the neurologist. We will only contact your GP with your permission and if your brain scans show something of potential medical concern. These scans do not routinely become a part of a medical record, however, if a problem is detected and with your permission the images are sent to a medic involved in caring for you, they may become part of your medical record. There is also the possibility that you may be unduly worried if a problem is suspected, but is not actually found. If in the future symptoms do arise, do not assume that because your brain has been scanned and we haven't contacted you that there is not a problem. Please take any future concerns to your GP, we can make the images available if required.

WHAT WILL HAPPEN TO THE STUDY RESULTS?

They will be kept securely for a minimum of 10 years and possibly indefinitely in the BANGOR BRAIN IMAGING UNIT data archive in accordance with good research practice. Results of the study may be published in a scientific journal or other public format. In this case your data will either be included as part of a group average, or will be anonymised so that no identifying information is given. You

WHAT IF I HAVE FURTHER QUESTIONS?

We welcome the opportunity to answer any question you may have about any aspect of this study or your participation in it. Please contact Kristin Koller (pspe60@bangor.ac.uk) or Bob Rafal

(r.rafal@bangor.ac.uk) at the School of Psychology, Bangor University, Gwynedd, LL57 2AS, phone 01248 383885.

ARE THERE COMPENSATION ARRANGEMENTS IF SOMETHING GOES WRONG?

In the unlikely event of anything untoward happening, the University's insurer provides insurance for negligent harm. It does not provide insurance for non-negligent harm but does take a sympathetic view should a claim be made.

WHAT IF I HAVE COMPLAINTS?

This research study has been approved by the School of Psychology Research Ethics and Governance Committee. In the case of any complaints concerning the conduct of research, please address these to In the case of any complaints regarding the conduct of research, these should be addressed to Mr Hefin Francis, School Manager, School of Psychology, Bangor University, Bangor, Gwynedd, LL57 2AS. Thank you for considering taking part in this study. Our research depends entirely on the goodwill of potential volunteers such as you. If you require further information, we will be pleased to help you in any way we can.

Appendix B. Participant consent form

**BANGOR BRAIN IMAGING UNIT
Participant Consent Form
CONSENT TO PARTICIPATE IN A RESEARCH STUDY**

TITLE OF STUDY: Anatomical confirmation of a subcortical visual attention detection pathway in the human brain

INVESTIGATORS:

Prof. Bob Rafal - Project Supervisor

Kristin Koller – PhD Student

The volunteer should complete this entire sheet himself/herself.

Please circle as appropriate:

Have you read the participant information sheet? YES / NO

Have you had the opportunity to ask questions and discuss this study? YES / NO

Have you received enough information about the study? YES / NO

Do you understand that your participation is voluntary and that you are free to withdraw from the study,
- At any time
- Without having to give a reason
- And without affecting your future medical care? YES / NO

Do you understand that these are not diagnostic scans? YES/NO

Do you understand that Bangor University provides insurance for negligent harm but that it does not provide insurance for non-negligent harm? YES/NO

Do you understand that the research data may be accessed by researchers working at or in collaboration with the BANGOR BRAIN IMAGING UNIT in similar ethically approved studies, but that at all times your personal data will be kept confidential in accordance with data protection guidelines? YES/NO

Do you agree to take part in this study? YES / NO

Date

Signature of
Participant

Name in block letters

Date

Signature of
Investigator

Name in block letters

Appendix C. Bangor Imaging Unit MR safety screening questionnaire

BANGOR BRAIN IMAGING UNIT MR Safety Screening Questionnaire

To be completed by ANYONE entering the Magnet Room.
Shaded boxes need to be filled in by participants undergoing a scan only.

Name	BANGOR BRAIN IMAGING UNIT no. (Staff Use Only)
Phone number	Date of Birth
Email address	Weight (kg)

MR scanning uses strong magnetic fields. For your own safety and the safety of others it is **very important** that you do not go into the Scanner Room with any metal in or on your body or clothing.

Please answer the following questions carefully and ask if anything is not clear.

All information is held in the strictest confidence.

Circle one answer for each question.

1. Do you have a pacemaker or artificial heart valve?
Y/N
2. Do you have aneurysm clips (clips put around blood vessels during surgery)?
Y/N
3. Do you have any implants in your body? (e.g., replacement joints, drug pumps, metal pins, plates, coronary stents, breast implants etc.)
Y/N
4. Have you ever had any metal fragments in your eyes?
Y/N
5. Have you ever worked with metal (e.g., grinding, machining, welding) without eye protection?
Y/N
6. Do you have any metal or shrapnel fragments anywhere in your body?
Y/N
7. Do have an indwelling catheter in your body?
Y/N
8. Have you ever had an operation on your head, spine, or chest?
Y/N
9. Have you ever had any surgery (if yes, please give brief details)?
Y/N
Details _____
10. Do you have any implanted electrical devices (e.g., hearing aid, cochlea implant, nerve stimulator)?
Y/N
11. Have you ever had an MRI scan before?
Y/N

12. Do you wear dentures, a dental plate, or a brace (not fillings)?
Y/N
13. Do you have any transdermal patches? (skin patches)
Y/N
14. Do you have any tattoos or body piercings?
Y/N
15. Is there any possibility that you could be pregnant?
Y/N
16. Are you susceptible to claustrophobia?
Y/N
17. Do you have hypertension (high blood pressure) sufficient to require medication?
Y/N
18. If Yes to 17 above, has your hypertension been adequately treated by medication?
Y/N
19. Have you had or do you have any heart problems?
Y/N
20. Do you have an impaired ability to perspire?
Y/N
21. Do you have reduced thermal regulatory capabilities or an increased sensitivity to raised body temperature?
Y/N
22. Do you suffer from any other medical condition that might be relevant? (e.g., epilepsy, diabetes, asthma)?
Y/N

Details _____

I confirm that before entering the Magnet Room, I will:

- remove all metal including coins, keys, lighters, body-piercings, jewellery, watches, wigs/hairpieces, clothing with zips and/or metal buttons, false teeth, hearing aids etc.;
 - remove all cosmetics;
 - remove all prostheses (e.g., prosthetic limbs);
 - turn off and remove mobile phones;
 - ensure that I am not wearing damp clothing
 - conform with the operator's instructions in regard to the above
- I confirm that the above information is accurate to the best of my knowledge. I have read and understood this form and the information sheet and have had the opportunity to ask questions regarding their contents and the MRI procedure that I am about to undergo.
 - I acknowledge that BANGOR BRAIN IMAGING UNIT has taken reasonable precautions to screen for potential difficulties and is not liable for any event that might result from incorrect answers to the above.

Signature	Date
Verified by (BANGOR BRAIN IMAGING UNIT Staff Member)	Date
Name	Signature

Appendix D. State-Trait Anxiety Inventory (STAI)

SELF-EVALUATION QUESTIONNAIRE

STAI Form Y-2

Name _____ Date _____

DIRECTIONS

A number of statements which people have used to describe themselves are given below. Read each statement and then circle the appropriate number to the right of the statement to indicate how you generally feel.

ALMOST NEVER
SOMETIMES
OFTEN
ALMOST ALWAYS

- | | | | | |
|---|---|---|---|---|
| 21. I feel pleasant | 1 | 2 | 3 | 4 |
| 22. I feel nervous and restless | 1 | 2 | 3 | 4 |
| 23. I feel satisfied with myself | 1 | 2 | 3 | 4 |
| 24. I wish I could be as happy as others seem to be | 1 | 2 | 3 | 4 |
| 25. I feel like a failure | 1 | 2 | 3 | 4 |
| 26. I feel rested | 1 | 2 | 3 | 4 |
| 27. I am "calm, cool, and collected" | 1 | 2 | 3 | 4 |
| 28. I feel that difficulties are piling up so that I cannot overcome them..... | 1 | 2 | 3 | 4 |
| 29. I worry too much over something that really doesn't matter | 1 | 2 | 3 | 4 |
| 30. I am happy | 1 | 2 | 3 | 4 |
| 31. I have disturbing thoughts | 1 | 2 | 3 | 4 |
| 32. I lack self-confidence | 1 | 2 | 3 | 4 |
| 33. I feel secure | 1 | 2 | 3 | 4 |
| 34. I make decisions easily | 1 | 2 | 3 | 4 |
| 35. I feel inadequate | 1 | 2 | 3 | 4 |
| 36. I am content | 1 | 2 | 3 | 4 |
| 37. Some unimportant thought runs through my mind and bothers me | 1 | 2 | 3 | 4 |
| 38. I take disappointments so keenly that I can't put them out of my mind..... | 1 | 2 | 3 | 4 |
| 39. I am a steady person | 1 | 2 | 3 | 4 |
| 40. I get in a state of tension or turmoil as I think over my recent concerns and interests | 1 | 2 | 3 | 4 |